



University  
of Glasgow

Basile, Francesco (1999) *Non-linear analysis of pile groups under general loading conditions*.

PhD thesis

<http://theses.gla.ac.uk/4315/>

Copyright and moral rights for this thesis are retained by the author

A copy can be downloaded for personal non-commercial research or study, without prior permission or charge

This thesis cannot be reproduced or quoted extensively from without first obtaining permission in writing from the Author

The content must not be changed in any way or sold commercially in any format or medium without the formal permission of the Author

When referring to this work, full bibliographic details including the author, title, awarding institution and date of the thesis must be given



**UNIVERSITY**  
*of*  
**GLASGOW**

**Non-linear Analysis of Pile Groups**  
**under**  
**General Loading Conditions**

*To Teresa*

**Francesco Basile, MEng**

*A thesis submitted for the degree of  
Doctor of Philosophy at the University of Glasgow*

**Department of Civil Engineering**  
**University of Glasgow**  
**February, 1999**

© Francesco Basile, 1999



(1) (1999) 74211

**To Teresa**



# Acknowledgements

I am greatly indebted to Prof. S. J. Wheeler who willingly undertook the supervision of this work. His constructive criticism and guidance have greatly contributed to the standard of this thesis.

My sincere gratitude is to Dr. W. G. K. Fleming of Kvaerner Cementation Foundations for his invaluable advice, concern and support throughout this project. I have derived great benefit from his inspiring discussions and suggestions during the period of preparation of this dissertation.

I would like to express my gratitude to Prof. N. Bicanic, Head of the Civil Engineering Department. Without his help and encouragement, this thesis would never have been completed. Special thanks are due to Dr. T. G. Davies for his initial supervision in this project. Thanks are extended to Dr. W. M. Stewart for the value in his discussions.

I am grateful to Prof. M. Jamiolkowski, Polytechnical University of Torino, for his keen interest in my research, and Prof. Y. K. Chow, National University of Singapore, for some useful suggestions. Appreciation goes to Prof. D. Muir Wood, University of Bristol, for his teaching and initial advice. I am also indebted to Prof. M. Maugeri and Dr. E. Motta, University of Catania, for their constant support and guidance during my extended studies.

Further thanks are extended to Prof. N. Bicanic, Dr. J. G. Herbertson, former Head of the Civil Engineering Department, and Prof. D. R. Green, Vice Principal of Glasgow University, for providing excellent facilities to carry out this research. The financial support given by the Faculty of Engineering, Glasgow University, is gratefully acknowledged. The technical assistance of Mr. K. McColl, Computer Manager, and the kind help and support of Mrs. T. Bryden, Mrs. E. Davies and Miss B. Grant are also deeply appreciated.

My special gratitude is to my friends and colleagues for their consistent encouragement and warm friendship which make particularly enjoyable my stay in Glasgow. In particular, my thanks go to Alessandra, Andy, Barbara, Breac, Dan, Domenico, Federico, Gao, Giovanni, Hamid, Jason, Jayne, Laurence, Lee, Lim, Lisa, Marc, Morna, Nicoletta, Pasquale, Rino, Roberto, Sabina, Zoltan and all the BDD Club. My friendship with them will forever be maintained.

Finally, I am most grateful to my parents, my grandparents, my sisters and Elaine for their sincere love and deep understanding which have always been supporting me throughout the years.

# Abstract

A computer program (called PGROUPN) has been developed for the non-linear analysis of pile groups subjected to any combination of vertical loads, horizontal loads and moments. The code is based on a complete boundary element approach and may be regarded as a generic descendant of the program PGROUP (Banerjee & Driscoll, 1976) which has been extended in order to make the analysis numerically efficient for practical problems and to include the effects of soil nonlinearity by means of a stepwise linear incremental procedure.

One of the main advantages of a non-linear analysis system over a linear elastic approach is that it has the desirable effect of demonstrating a reduction of the corner loads in large groups in both the vertical and horizontal senses. This observation is of basic importance in practice because it offers the prospect of tangible improvements in design procedures and potential saving of materials.

The non-linear analysis put forward in this thesis may be applied to large pile groups embedded in cohesive soil, specifically fully saturated clay under undrained conditions. The soil is modelled as an elastic-perfectly plastic material, which is assumed to behave linearly elastic at small strain levels, but fails when the stresses at the pile-soil interface reach certain limiting values. The analysis only requires the definition of three soil parameters whose physical meanings are clear, ie the (initial tangent) Young's modulus  $E_s$ , the Poisson's ratio  $\nu_s$  and the undrained shear strength  $C_u$ . This represents a significant advantage over more common load-transfer approaches which are based on either empirical parameters or the results of full-scale pile load tests.

The validity and accuracy of the proposed PGROUPN solution have been verified by comparison with alternative numerical analyses for single piles and pile groups subjected to axial and lateral loads. Benchmark solutions in the linear and non-linear range are presented, and the critical question of estimation of soil parameters is addressed. Finally, two published case histories are described which demonstrate the applicability of the method to practical problems.

# Contents

<b>Acknowledgements</b>	<b>i</b>
<b>Abstract</b>	<b>ii</b>
<b>Contents</b>	<b>iii</b>
<b>Notation</b>	<b>viii</b>

<b>CHAPTER 1</b>	<b>Introduction</b>	
1.1	General remarks	1
1.2	Scope of thesis	2
1.3	A review of pile group behaviour	3
1.3.1	Capacity of pile groups	3
1.3.1.1	Axial capacity	5
1.3.1.2	Lateral capacity	5
1.3.2	Deformation of pile groups	5
1.3.2.1	Axial loading	8
1.3.2.2	Lateral loading	11
1.3.3	Effects of pile cap	12
1.4	A review of methods of pile group analysis	14
1.4.1	Load-transfer method	15
1.4.1.1	Load-transfer analysis for axially loaded piles	16
1.4.1.2	Load-transfer analysis for laterally loaded piles	18
1.4.1.3	Extension to pile groups	19
1.4.2	Finite element method	21
1.4.3	Boundary element method	23
1.5	Computer programs for pile group analysis	28
1.6	Concluding remarks	31
	<b>FIGURES</b>	<b>32</b>

<b>CHAPTER 2</b>	<b>Formulation of the non-linear BEM analysis</b>	
2.1	Summary	37
2.2	Introduction	37

2.3	Soil model	39
2.4	Method of analysis	40
2.4.1	Soil domain	41
2.4.2	Pile domain	44
2.4.3	Solution of the pile-soil system	44
2.4.4	Limit stresses	52
2.4.5	Extension to non-linear soil behaviour	53
2.4.5.1	Current analysis	53
2.4.5.2	Approach by Davies & Budhu (1986)	60
2.4.5.3	Modification of the Davies & Budhu approach	64
2.5	Concluding remarks	65
Appendix 2.1	Analytical integration of singular Mindlin's solution	67
Appendix 2.2	Bernoulli-Euler beam theory	76
FIGURES		79

### **CHAPTER 3 Numerical implementation**

3.1	Summary	83
3.2	Introduction	83
3.3	General description of the computer program PGROUPN	84
3.3.1	Scope of the program	84
3.3.2	Computational procedure	84
3.3.2.1	Soil domain	86
3.3.2.2	Pile domain	86
3.3.2.3	Unit boundary conditions	86
3.3.2.4	Solution of the pile-soil system	87
3.3.3	Structure of the program	94
3.3.4	Limitations imposed by the method used	96
3.3.5	Maximum problem size	97
3.4	Input	98
3.4.1	General description	98
3.4.2	System of units adopted	98
3.4.3	Type of analysis	98
3.4.4	Pile group configuration	99
3.4.5	Geometry of the piles	99

3.4.6	Identification of pile types	100
3.4.7	Loading	100
3.4.8	Soil layer	100
3.5	Output	101
3.6	Typical illustrative results	102
3.7	Concluding remarks	103
Appendix 3.1	Inaccuracies in the numerical code PGROUP 2.0	104
TABLES		106
FIGURES		109

## **CHAPTER 4 Numerical results — single piles**

4.1	Summary	118
4.2	Introduction	118
4.3	Piles under axial loading	119
4.3.1	Linear solution	119
4.3.1.1	Convergence of numerical solution	120
4.3.1.2	Pile settlement	122
4.3.1.3	Load transfer	124
4.3.1.4	Finite-layer depth	125
4.3.1.5	Critical length	125
4.3.1.6	Raking piles	126
4.3.1.7	Under-reamed piles	128
4.3.2	Non-linear solution	128
4.3.2.1	Comparison with FEM and BEM analyses	129
4.4	Piles under lateral loading	130
4.4.1	Linear solution	131
4.4.1.1	Convergence of numerical solution	131
4.4.1.2	Pile deflection	132
4.4.1.3	Load transfer	134
4.4.1.4	Critical length	134
4.4.1.5	Raking piles	135
4.4.1.6	Rigid piles	136
4.4.2	Non-linear solution	137
4.4.2.1	Comparison with a BEM analysis	137

4.5	Concluding remarks	138
	TABLES	140
	FIGURES	144

**CHAPTER 5 Numerical results — pile groups**

5.1	Summary	160
5.2	Introduction	160
5.3	Pile groups under axial loading	161
5.3.1	Two-pile interaction analysis	162
5.3.2	Pile group settlement	164
5.3.3	Load distribution	167
5.4	Pile groups under lateral loading	170
5.4.1	Two-pile interaction analysis	171
5.4.2	Pile group deflection	172
5.4.3	Load distribution	173
5.5	Pile groups under general loading conditions	175
5.6	Concluding remarks	176
	TABLES	178
	FIGURES	179

**CHAPTER 6 Comparisons with field test data**

6.1	Summary	199
6.2	Introduction	199
6.3	Selection of soil parameters	200
6.3.1	Young's modulus ( $E_s$ )	200
6.3.2	Poisson's ratio ( $\nu_s$ )	204
6.3.3	Undrained shear strength ( $C_u$ ) and adhesion factor ( $\alpha$ )	204
6.4	Comparison with O'Neill <i>et al.</i> (1982)	206
6.4.1	Current analysis	207
6.4.2	Prediction by previous workers	209
6.4.3	Application of empirical correlations for determining $E_s$	211
6.5	Comparison with Matlock <i>et al.</i> (1980)	212
6.6	Concluding remarks	215
	TABLES	217

<b>FIGURES</b>		<b>218</b>
<b>CHAPTER 7</b>	<b>Conclusions</b>	
7.1	Summary and concluding remarks	232
7.2	Recommendations for future work	234
<b>References</b>		<b>236</b>
<b>Appendix A</b>	<b>Published papers</b>	<b>249</b>

# Notation

The following is a list of main symbols used in this thesis. Other symbols are defined locally in the text.

$A_p$	cross sectional area of pile
$A_{ai}$	shaft area of the pile element $i$
$A_b$	pile base area
$A_s$	pile shaft area
$A_{ti}$	transverse area of the pile element $i$
$B$	pile displacement due to unit boundary conditions
$C_u$	undrained shear strength
$C_{uo}$	undrained shear strength at ground level
$E_p$	pile Young's modulus
$E_s$	soil Young's modulus
$E_{sL}$	soil Young's modulus at the level of the pile base
$E_{so}$	soil Young's modulus at ground level
$F_a^k$	pile head axial force due to unit boundary conditions
$F_a^i$	axial forces acting at the top of pile element $i$
$F_t^k$	pile head shear force due to unit boundary conditions
$F_t^i$	shear forces acting at the top of pile element $i$
$G_s$	soil shear modulus
$G_{sL}$	soil shear modulus at the level of the pile base
$G_o$	soil shear modulus
$H$	applied horizontal load on the cap
$H$	depth of soil layer
$H_{av}$	average lateral load acting on each pile head
$H_g$	total lateral load acting on the group
$H^k$	horizontal load acting on the cap due to unit boundary conditions
$H_u$	ultimate lateral load capacity (if failure occurs by failure of the soil)
$I_p$	second moment of area of pile section

$K$	relative pile-soil stiffness
$K_R$	stiffness ratio
$L$	pile length
$L_c$	pile critical length
$M$	applied moment on the cap
$M$	= $(2N+1)$ total number of pile elements (per pile)
$M^k$	moment acting on the cap due to unit boundary conditions
$M_i^k$	pile head moment due to unit boundary conditions
$M_i^i$	bending moments acting at the top of pile element $i$
$N$	SPT value
$N$	number of pile shaft elements (per pile)
$N_c$	bearing capacity factor
$NINC$	number of equal load increments
$P$	applied axial load
$P_{av}$	average axial load acting on each pile head
$P_b$	load carried by the pile base
$P_g$	total axial load acting on the group
$P_u$	ultimate axial load capacity
$R_s$	group settlement ratio
$R_u$	group deflection ratio
$V$	applied vertical load on the cap
$V^k$	vertical load acting on the cap due to unit boundary conditions
$[F]$	global flexibility matrix of the pile group system
$[G_s]$	soil flexibility matrix obtained from Mindlin's solution
$[G_{s,*}]$	non-linear soil flexibility matrix
$[G_p]$	pile flexibility matrix obtained from Bernoulli-Euler beam theory
$[K_s]$	soil stiffness matrix
$[S]$	global stiffness matrix of the pile group system

$c$	rate of increase of undrained shear strength with depth
$c$	horizontal distance of the pile head from the vertical axis of symmetry of the cap
$d$	pile external diameter
$d_b$	pile base diameter
$d_i$	pile internal diameter
$g$	depth of overhang of the pile cap
$h$	height of the pile shaft element
$k_p$	ratio of applied vertical load to the average settlement of the group
$m$	rate of increase of soil Young's modulus with depth
$m$	number of piles in the group
$n$	number of pile types in the group
$p$	lateral load transfer
$q_b$	end-bearing pressure
$q_c$	cone resistance
$r_o$	pile radius
$s$	pile spacing
$s_{max}$	maximum interaction spacing
$t$	axial load transfer
$t_{ai}^k$	pile axial tractions acting on element $i$ due to unit boundary conditions
$t_p$	pile traction
$t_s$	soil traction
$t_{sc}$	limiting bearing stress
$t_{ss}$	limiting shear stress
$t_{ti}^k$	pile transverse tractions acting on element $i$ due to unit boundary conditions
$u$	horizontal displacement of the cap
$u_p$	pile displacement
$u_s$	soil displacement
$w$	vertical displacement of the cap
$y$	lateral pile displacement
$z$	axial pile displacement
$z$	depth coordinate

$\alpha$	adhesion factor
$\alpha$	two-pile interaction factor
$\beta$	direction of horizontal loading
$\phi$	angle of rake of the pile
$\lambda$	relative pile-soil stiffness
$\theta$	rotation of the cap
$\sigma'_v$	effective overburden stress
$\tau_s$	shear stress
$\nu_s$	soil Poisson's ratio

### *Superscripts*

$aa$	axial-axial interaction
$at$	axial-transverse interaction
$k$	= 1, 2, 3 (it represents the three unit boundary conditions)
$ta$	transverse-axial interaction
$tt$	transverse-transverse interaction
$e$	linear elastic conditions
$n$	non-linear conditions

### *Subscripts*

$a$	axial
$i$	pile element
$p$	pile
$s$	soil
$t$	transverse

# CHAPTER 1

## Introduction

### 1.1 General remarks

Despite the pessimistic statement of Terzaghi & Peck (1967), '*...theoretical refinements in dealing with pile problems ... are completely out of place and can be safely ignored*', the past three decades have seen major advances in understanding the manner in which piled foundations interact with the surrounding soil.

For many years, the design practices of piled foundation have been based on empirical rules which are implicitly conservative and, in many cases, may turn out to be inadequate. Today, the development of numerical approaches such as the finite element method (FEM) and the boundary element method (BEM), in conjunction with the wide availability of desktop computers, has put many powerful methods of analysis at the disposal of the pile designer. The influence of battered piles, different pile sizes, enlarged base diameters, soil nonlinearity and inhomogeneity, as well as pile-soil-pile interaction, can now be examined with different degrees of rigour, depending on the approximations incorporated in the method of analysis. Such methods allow exhaustive estimates of pile group response to loading which even two decades ago would not have been considered practical for foundation design. This advance has resulted in a better understanding of pile group behaviour and tangible improvements in design practice (Poulos, 1989; Fleming *et al.*, 1992).

The analysis and design of a pile group imply the consideration of three main categories of parameters, namely, material properties, geometrical characteristics and loading conditions. Material properties encompass both the mechanical characteristics of the soil, which can include consideration of such factors as nonlinearity, inhomogeneity and anisotropy, and the stiffnesses of the structural members, ie the piles and the pile cap. Geometrical characteristics include the specification of pile group configuration, the geometry of the cap and the individual piles, ie lengths,

diameters and the angles of rake. Loading conditions may include any combination of vertical loads, horizontal loads and moments. Vertical loads are mainly due to the self-weight of the superstructure, while horizontal loads are relevant in stadia, bridges, harbours, pipelines and in structures subjected to wind and wave action, earth pressure and ground movements (ie earthquakes). In this thesis, attention will be confined to problems involving static loading.

## 1.2 Scope of thesis

Present practice in evaluating the load-deformation response of pile groups is to adopt linear elastic approaches, but these ignore the non-linear load-deformation characteristics of soil and hence misrepresent the forces in piles, specifically by giving higher stresses in group corners. The cost of this in practice is high and there is an urgent need in industry for practical non-linear analysis methods. In addition, current numerical approaches suffer from restrictions imposed by the number of piles in the group which make such analyses computationally inefficient.

For this purpose, the present research aims to develop a numerical procedure, implemented in a computer program called PGROUPN, by which realistic pile groups embedded in cohesive soils (specifically fully saturated clay under undrained conditions) and subjected to any combination of vertical loads, horizontal loads and moments may be investigated by means of a non-linear analysis. The main feature of PGROUPN lies in its capability to adopt a complete BEM approach while retaining a computationally efficient code which runs on an ordinary desktop computer. The various strategies adopted for achieving efficiency gains result in an economically viable analysis even if nonlinearity effects are simulated in large pile groups.

In Chapter 2, the complete BEM approach, as proposed by Banerjee & Driscoll (1976), is further developed in order to make the analysis more numerically efficient and to include the effect of soil nonlinearity by means of a stepwise linear incremental procedure. Chapter 3 depicts the numerical implementation of the non-linear BEM formulation, together with a general description of the PGROUPN program. Comparison of the results with some published numerical solutions is undertaken in Chapters 4 and 5 for single piles and pile groups, respectively. In addition, Chapters 4 and 5 present parametric studies in

the linear and non-linear range to illustrate the influence of the relevant parameters on the behaviour of single piles and pile groups. Finally, in order to demonstrate the applicability of the method to practical problems, Chapter 6 presents some comparisons with published field test data.

### **1.3 A review of pile group behaviour**

Piled foundations have the dual purpose of strengthening the soil and also of transferring the applied loads to deeper and stiffer soil strata. In most cases, piled foundations consist of a group of piles installed fairly close together (typically the centre-to-centre pile spacing is about 4 to 6 pile diameters) and joined by a cap cast on the top of the piles.

The pile cap can be in contact with the ground, in which case part of the applied load is carried directly on the soil immediately below the surface. If the cap is not in direct contact with the soil, as in the case of offshore platforms, the piles in the group are referred to as free-standing. However, in most practical situations, it is customary to ignore the resistance offered by the top layer of soil because of fill or other soft or variable ground, and hence the contact between cap and soil may be considered ineffective.

#### **1.3.1 Capacity of pile groups**

Failure of a group of piles may occur either by failure of the individual piles or as failure of the overall block of soil enclosing the piles. If block failure occurs, soil between the piles may move with the piles resulting in failure planes which follow the periphery of the group or parts of the group (Fleming *et al.*, 1992).

When investigating failure mechanism of the individual piles, it is necessary to take into consideration the effects of interaction between neighbouring piles so that the capacity of each pile may be altered. The beneficial effects of installing neighbouring driven piles may be relevant in cohesionless soils, where the soil between the piles becomes highly compacted leading to higher shaft capacities than for single piles. This has been proved experimentally by Vesic (1969), who showed that the shaft capacities of piles driven into loose and medium sand could increase by a factor of 2. A similar

effect has been observed by Van Weele (1993) for free-draining soils, where the increased effective stress level due to an external load applied to neighbouring piles will enhance the capacity of each pile within the group.

In other cases, the capacity of a pile within a group may be reduced by comparison with a single pile. For example, groups of piles driven into sensitive clays cause extensive remoulding of the surrounding soil and thus a heave of the ground surface occurs. Once the soil reconsolidates, this produces a drag-down on the pile shaft and hence a lower shaft capacity than for individual piles.

As discussed by Van Impe (1991) and Fleming *et al.* (1992), the method of pile construction can have a critical influence on the capacity of a pile foundation. For instance, for a displacement (generally driven) pile, lateral stresses are increased as the pile shaft enters the ground and hence the soil stiffness may be expected to be higher in the zone immediately around the pile. In contrast, in a non-displacement (generally bored) pile, lateral stresses in the ground are reduced during excavation and hence the soil stiffness is likely to be reduced.

Conceptually, the effect of pile installation may be modelled by 'softening' the value of soil stiffness in a zone near the pile face. Away from the pile, the soil stiffness may revert to the in-situ value because of the reduced effects of disturbance and also the reduced level of shear strain. Recent attempts have been made to incorporate this effect into pile group analysis: Poulos (1988) assumed a simplified form of soil modulus variation to assess the single pile behaviour and the interaction effects between piles, as indicated in Fig. 1.1; Hirayama (1991) assumed a hyperbolic variation of soil modulus with strain, while Chow (1991) considered a weakened zone near the piles.

The significant effect of time since installation, particularly for displacement piles installed in soils of low permeability, has been discussed by Fleming *et al.* (1992). After a pile is driven into cohesive soil, the excess pore pressures will dissipate, mainly by radial flow of pore water away from the pile, and the soil will consolidate. Because of this consolidation process, the shear strength of the soil may increase by between 30 and 100% close to the pile. This amount is governed by the coefficient of consolidation in a horizontal plane, the time since installation of the pile and the pile radius

(Randolph *et al.*, 1979; Randolph & Wroth, 1979). In general, the effects of pile installation will not extend beyond 10 to 15 pile diameters (Fleming *et al.*, 1992).

#### 1.3.1.1 Axial capacity

For pile groups with an effective ground-contacting cap, it is likely that axial failure occurs as failure of the overall block of soil rather than failure of the individual piles. Model tests by Whitaker (1957) show that this situation can also occur in free-standing groups of piles with a centre-to-centre spacing less than about 2 pile diameters. In these circumstances, the pile group capacity corresponds to that of the block enclosing the piles. The analysis of the failing block is exactly the same as the analysis of a single pile but now taking the base area as the total base area of the block enclosing the piles and by evaluating the total skin friction on the basis of the perimeter area of the entire block.

Modern trends in pile group design tend to favour the use of fewer, more widely spaced piles. In these circumstances, it is common practice to estimate the failure load of the group as the sum of the failure loads calculated for the piles acting individually. This has been confirmed by full-scale tests on pile groups in stiff clay (see, for example, O'Neill *et al.*, 1982).

#### 1.3.1.2 Lateral capacity

A pile group under lateral loading will be subjected to lateral deformation as well as rotation and hence piles at the edge of the group will be loaded in compression and tension. As a consequence, the lateral response of the group will depend on both the axial capacity and the lateral capacity of the piles. In practice, the lateral capacity of a group of piles will rarely be critical in design and the only requirement is to ensure that the maximum bending moment in the piles will not lead to overstressing the piles (Fleming *et al.*, 1992).

### 1.3.2 Deformation of pile groups

Burland *et al.* (1977) pointed out that the primary purpose of most pile groups is to satisfy a serviceability limit on deformations — nevertheless, traditionally pile

designers have asked themselves how many piles are needed to carry the weight of the building rather than asking themselves the question of how many piles are needed to reduce settlements to an acceptable level.

In spite of this primary purpose of piles, twenty years later, common practice in pile group design philosophy still concentrates on providing suitable capacity from the piles to carry the structural load, and estimation of the settlement is generally treated as a secondary issue. The dominance of capacity-based design, which is evident in current revisions of national and regional design codes, may be partially attributed to the common belief that predicting deformations is more difficult and less reliable than predicting capacity. In reality, however, the reverse is often true for pile foundations (Randolph, 1994).

Thus, provided there is a minimum factor of safety, which may be as low as 1.5, pile group design should be approached in terms of satisfying the settlement criterion, rather than be based on a crude notional factoring of the ultimate state of each pile (Fleming *et al.*, 1992). If this design philosophy is adopted, and hence low safety factors are employed, consideration of non-linear soil deformations becomes mandatory. This approach would result in tangible improvements in design practice and worthwhile savings in construction costs.

A variety of techniques are used in practice to predict the settlement of pile groups. These techniques fall into three main categories (Poulos, 1993):

- a) purely empirical techniques which relate the deformation of a group to that of a single pile (Skempton, 1953; Meyerhof, 1959);
- b) simplified approaches which reduce the pile group to an equivalent simpler form of foundation, ie a pier or raft (Bjerrum *et al.*, 1957; Wood, 1978; Poulos & Davis, 1980; Tomlinson, 1994; Randolph, 1994);
- c) analytical methods which consider pile-soil-pile interaction (Poulos, 1968; Butterfield & Banerjee, 1971a; Randolph & Wroth, 1979; Poulos & Davis, 1980; Fleming *et al.*, 1992).

Recently, with the development of numerical techniques such as FEM and BEM, there has been significant development of the third category and hence many aspects of pile group behaviour may be modelled with different degrees of rigour.

One of the most useful concepts in the analysis of pile group behaviour is the use of interaction factors to represent the influence of a pile on the displacement of another pile. An interaction factor,  $\alpha$ , may be defined as the additional deformation (that is settlement, deflection or rotation at the pile head) of a pile due to an equally loaded identical adjacent pile:

$$\alpha = \frac{\text{additional deformation due to adjacent pile}}{\text{deformation of pile under its own load}} \quad (1.1)$$

As first suggested by Poulos (1968), superposition of the two-pile interaction factors may be employed to analyse the deformation behaviour of a pile group.

The value of the interaction factor depends on several features, including type of loading (axial or lateral), spacing between piles, relative pile-soil stiffness, length-diameter ratio of the piles, nature of the bearing stratum and the distribution of soil modulus with depth. Interaction factors for a wide range of situations are presented by Randolph & Wroth (1979), Poulos & Davis (1980), Randolph (1981) and Fleming *et al.* (1992).

The use of interaction factors has been justified experimentally from field tests on axially loaded piles in London Clay (Cooke *et al.*, 1980). The authors show that, at loads up to one half of the ultimate load, the overall deformation of the pile group may be determined by superposition of the separate deformation fields of each pile. Thus, the deformation of one pile may be thought of as made up of the sum of the deformation due to its own loading (without the presence of the neighbouring piles) and the deformations due to each of the other pile displacement fields. It should be emphasised that the experimental results of Cooke and colleagues are restricted to a purely elastic analysis, which is appropriate for working loads of the order of less than one half of the ultimate load. However, as the loading increases, the divergence from

elastic conditions becomes more marked and nonlinearity effects have considerable influence on pile behaviour.

### 1.3.2.1 Axial loading

An approach by Randolph & Wroth (1979), in which theoretical interaction factors are deduced from the deformation field around a single pile, shows the transfer of a higher percentage of load to the bases of piles within a group than for isolated piles. This phenomenon has been confirmed experimentally by model tests (eg Ghosh, 1975).

When calculating interaction effects between piles in a group, care must be taken over the choice of the maximum interaction spacing. Randolph & Wroth (1979) showed theoretically that interaction effects between piles in a group become insignificant for pile spacing (centre-to-centre) greater than a limiting value  $s_{max}$ , which is defined as:

$$s_{max} = 2.5L\rho(1 - \nu_s) + r_g \quad (1.2)$$

where

$L$  is the pile length,

$\rho$  is the inhomogeneity factor — its value is 1 for a homogeneous soil, while for a non-homogeneous soil it is the ratio of the soil modulus at pile mid-depth to that at the pile base,

$\nu_s$  is the soil Poisson's ratio,

$r_g$  may be taken, for rectangular groups, as the radius of the circle of equivalent area to that covered by the pile group; Mandolini (1994) provides values of  $r_g$  for groups of any shape.

Chin & Poulos (1991) have calculated the value of  $s_{max}$  for the particular cases of two-layered soil and Gibson soil, ie a soil with stiffness linearly proportional to depth (Gibson, 1974).

However, a field investigation on the behaviour of a row of piles at close spacings in London Clay by Cooke *et al.* (1980) shows that the interaction factor approach considerably overestimates interaction between piles. Observed values of the interaction factors indicate that the interaction is practically zero at a pile spacing of 12 pile diameters.

From a practical viewpoint, in order to estimate the settlement of a pile group (with a rigid pile cap), it may be convenient to relate the settlement of the group to the settlement of an isolated single pile, as follows:

$$R_s = \frac{w_g}{w_1} \quad (1.3)$$

where

$R_s$  = group settlement ratio,

$w_g$  = settlement of group,

$w_1$  = settlement of single pile carrying the same average load as a pile in the group.

Some values of  $R_s$  are calculated by Poulos (1979) by means of the interaction factor approach. Fleming *et al.* (1992) present an useful approximation for the value of  $R_s$  in large pile groups:

$$R_s = n^\omega \quad (1.4)$$

where

$n$  = number of piles in the group,

$\omega$  = exponent which lies between 0.4 and 0.6 for most pile groups (tabulated in Fleming *et al.*, 1992).

**Load distribution.** A consequence of the interaction between piles is that, in a pile group with a rigid cap (a reasonable assumption in most practical cases), the

distribution of load among the piles is generally non-uniform. This is because neighbouring piles will be within each others' displacement fields and hence the load per pile to generate a given displacement will be reduced for the central piles and increased for the outer ones. Therefore, in a square pile group, the corner piles carry the greatest proportion of load, while those near the centre carry least.

Typical load distributions calculated for small pile groups (Poulos & Davis, 1980) show that corner piles may take up to 3 to 4 times as much load as piles near the centre. This trend has been confirmed experimentally for a group of 9 piles by Koizumi & Ito (1967), who show that, at working load, the corner piles carry about three times the centre pile load and the centre side piles carry about 1.5 times the centre pile load. Further, carefully conducted tests on a group of 351 piles (Cooke *et al.*, 1981) show that piles at the corner take more than twice the mean centre pile load and piles around the edge carry about 1.5 times the mean centre pile load.

*Short-term and long-term settlements.* There appear to be no theoretical solutions available in the literature for the rate of consolidation settlement of pile groups. As discussed by Poulos (1993), finite element analyses of an equivalent impermeable block representing the pile group indicate that the rate of consolidation decreases as the length-to-diameter ratio of the equivalent block increases. For a relatively deep homogeneous layer, the time for 50% consolidation of a block having a length-to-diameter ratio of 5 is about 9 times that for a corresponding impermeable surface footing of the same diameter.

Fleming *et al.* (1992) state that the immediate settlement of a pile group is a smaller fraction of the corresponding long-term settlement than is the case for a single pile (where the immediate settlement is generally 80 to 90% of the long-term settlement). This is confirmed by Poulos & Davis (1980), by means of an elastic analysis which uses drained and undrained parameters, and by Fathallah (1978) using FEM. Field tests by Cooke *et al.* (1981) on a group of 351 piles in London Clay (which is consolidating) show that the observed settlement was 10 mm at the completion of construction, 25 mm after 5 years and it was continuing at the rate of less than 1 mm per year.

### 1.3.2.2 Lateral loading

A finite element study carried out by Randolph (1981) showed that interaction under lateral loading decreases much more rapidly with pile spacing than for axial loading. It is also shown that interaction of piles normal to the applied load is half that for piles in line with the lateral load.

However, it must be observed that it is not possible to separate the lateral load deformation characteristics of a pile group from the axial characteristics. In fact, as the laterally loaded pile group tries to rotate, piles at the edges of the group will be loaded axially in tension and compression, providing significant rotational stiffness to the group.

As discussed by Fleming *et al.* (1992), if pile cap rotation is prevented, it is possible to define a deflection ratio  $R_u$ , which is similar to the settlement ratio  $R$ , for axial loading, ie:

$$R_u = \frac{u_g}{u_1} \quad (1.5)$$

where

$R_u$  = group deflection ratio,

$u_g$  = group deflection (under conditions of zero rotation of the pile cap),

$u_1$  = deflection of single pile carrying the same average load as a pile in the group (under conditions of zero rotation of the pile cap).

Some values of  $R_u$  for square fixed-head pile groups in homogeneous and Gibson soils are presented by Fleming and colleagues. These charts show that interaction effects between piles in a Gibson soil are less marked than for piles in a homogeneous soil.

A significant influence on the response of closely spaced pile groups (ie spacings less than 5 pile diameters) subjected to lateral loading is represented by a 'shadowing' effect. This effect is thought to be related to the influence of the leading row of piles on the yield zones developed in the soil ahead of the trailing row of piles, as shown in Fig. 1.2. Because of this overlapping of failure zones, the front row will be

pushing into virgin soil while the trailing row will consist of piles pushing into soil which is in the shadow of the front row piles. A consequence of this loss of soil resistance for piles in a trailing row is that the leading piles in a group will carry a higher proportion of the overall applied load than the trailing piles. This effect also results in gap formation behind the closely spaced piles and an increase in group deflection.

This feature of behaviour has been observed in finite element analyses (Brown & Shie, 1990b), model tests (Barton, 1982; Cox *et al.*, 1984) and full-scale tests (Brown *et al.*, 1987; Rollins *et al.*, 1998), for pile spacings of 2 to 3 pile diameters. However, Brown & Shie and Cox *et al.* show that the shadowing effect rapidly decreases as the spacing between piles increases and becomes insignificant for spacing greater than 6 pile diameters.

### 1.3.3 Effects of pile cap

In his Rankine Lecture, Poulos (1989) stated that the effect on group settlement of the pile cap being in contact with the soil is relatively small unless the pile spacing is large and the group is relatively small. It has been shown that, even for piles at an unusually large centre-to-centre spacing of 10 diameters, the reduction in settlement due to cap contact is only about 5%. Therefore, for practical purposes and at working loads, the influence of pile cap contact can be ignored.

A rigorous boundary element analysis of a compressible pile group including a rigid smooth ground contacting cap (Butterfield & Banerjee, 1971b) shows that the load displacement characteristics of similar pile groups with floating or contacting caps are slightly different, resulting in an increase of the system stiffness of only 5-15%. Although significant load may be carried by the cap (up to 30 - 50% depending on the group size and pile spacing), there is a corresponding decrease in load transfer in the upper region of each pile. The two effects compensate, giving only marginally greater stiffness of the overall foundation compared with a pile group with a free-standing pile cap.

This finding has been subsequently validated by model tests (Ghosh, 1975; Abdrabbo, 1976) and field tests on large buildings in London Clay (Cooke *et al.*, 1981). The field tests in London Clay show that the increase in load to settlement stiffness of a pile

raft foundation over the corresponding group of free-standing piles is less than the increase in ultimate bearing capacity and is unlikely to be greater than 30%, irrespective of the pile spacing. Further, it is shown that the proportion of load carried by the pile cap drops from an initial value of about 50% down to a long-term value of 23%.

Several methods of analysis are available to give an estimate of the bearing contribution of the cap. An approximate method, widely used in practice due to its simplicity, has been proposed by Randolph (1983a), in which the separate stiffnesses of the raft and the pile group are combined. The method is based on the use of average interaction factors between the pile and pile cap and takes no account of the detailed load distribution under the cap or the precise pattern of loads carried by the piles. The stiffness of the piles can be easily combined to give estimates of the overall stiffness and the proportion of load carried by each component. Comparison of the approach with more rigorous solutions shows good agreement for a 9-pile group. One disadvantage of the method is that it only gives total settlement, no attempt being made to assess differential settlements or bending moments in the raft.

In order to estimate the overall raft stiffness, pile group efficiency charts have been presented by Butterfield & Douglas (1981) and Fleming *et al.* (1992), while closed-form analytical solutions for circular or rectangular rafts have been introduced by Poulos & Davis (1974).

Poulos & Davis (1980) proposed an 'equivalent pier approach' which allows the analysis of large pile groups by replacing the full number of piles by a small number of equivalent piers. Such an approach allows an estimate of differential settlements, which are often critical to design and therefore need to be reduced to an acceptable level. A more rigorous approach proposed by Randolph & Clancy (1993) provides a method of calculating the differential settlements of a piled raft from an analysis of the raft alone and a subsequent factorisation to account for the overall reduction in settlements due to the presence of the piles. This method has been termed the 'combined pile group and raft' approach.

A recent study of Clancy & Randolph (1996) presents two approximate methods for the analysis of piled raft foundations: the first method combines the separate responses of the piles and raft in isolation; the second uses an equivalent-piered raft approach to

reduce greatly the number of piles analysed. Both methods provide good predictions of overall piled raft stiffness and load-sharing between the piles while differential settlements are underestimated. Although these approximate methods are computationally efficient and simple to use, a full piled raft analysis is suggested to ensure the accuracy of the results.

One of the first attempts to analyse rigorously the problem of pile group-pile cap interaction was presented by Ottaviani (1975) using three-dimensional finite elements, but this was restricted to a maximum of 15 piles because of enormous computational cost.

In order to reduce computational resources, several hybrid approaches have been proposed, for instance the combination of BEM and FEM proposed by Hain & Lee (1978) and El-Mossallamy & Franke (1997).

A hybrid finite element-elastic continuum-load transfer approach including allowance for bending of the raft has been proposed by Griffiths *et al.* (1991). In this approach, the piles are modelled with one-dimensional rod finite elements, the pile-soil contact is represented at node points by linear load-transfer springs and the raft is subdivided into two-dimensional 'thin' plate elements. The three kinds of interactions, namely, pile-soil-pile, pile-soil-raft and raft-soil-raft are accounted for using the elastic theory of Mindlin (1936). The results from the analysis compared with the approximate method proposed by Randolph (1983a) show correct trends in terms of foundation stiffness, but a tendency for the approximate analysis to underpredict the amount of load carried by the raft by up to 30%, especially for low values of the pile-soil stiffness ratio.

However, even with the development of hybrid methods which include allowance for bending of the pile cap, the applicability of complete numerical analyses to practical problems remains deficient, due to the considerable computer resources required for large piled foundations. It is therefore essential to employ approximate methods that represent extrapolation of more rigorous analyses.

## **1.4 A review of methods of pile group analysis**

The complexity of the problem of pile-soil interaction has meant that generally some form of numerical method of analysis has to be resorted to. This section attempts to present a classification of these methods and examine similarities and differences among them.

Numerical techniques for estimating the performance of piled foundations fall into two main categories: continuum based approaches, such as FEM and BEM, and load-transfer approaches. The second category encompasses methods which are phenomenological by nature. The soil is treated not as a continuum but merely as a source of resistance to deformation of the pile. These methods, which are based on the so-called Winkler (1867) idealization of the soil, employ load-transfer functions to represent the relationship between the load at any point along the pile shaft and the corresponding deformation of the soil at that point.

This category is attractive in its flexibility, enabling non-linear and inhomogeneous soil conditions to be incorporated easily (ie the  $t$ - $z$  or  $p$ - $y$  curve methods of analysis). The main drawback to this approach is that no direct tests can be conducted to establish force-displacement relationships along the pile-soil interface for that particular pile and soil type — these curves must be back calculated from the data obtained by conducting pile load tests. Thus, a significant amount of engineering judgement is needed when formulating these curves for site conditions which differ markedly from the recorded field tests. In addition, disregard of continuity through the soil oversimplifies the problem and makes it impossible to find a rational way to quantify the interaction effects between piles in a group.

In order to overcome these limitations, solutions based on finite element (Ottaviani, 1975; Randolph, 1977) and boundary element (Poulos, 1968; Butterfield & Banerjee, 1971a) modelling of the soil continuum have been proposed. These solutions provide an efficient means of retaining the essential aspects of pile interaction through the soil continuum and hence a more realistic representation of the problem. Further, the mechanical characteristics to be introduced into the model have now a clear physical meaning and they can be measured directly.

#### **1.4.1 Load-transfer method**

The load-transfer or modulus of subgrade reaction method has been probably the most widely adopted technique for the analysis and design of single piles, especially where non-linear soil behaviour has to be considered and/or soil stratification is complicated. The approach is unable to deal with pile groups and recourse has to be made to 'hybrid'

methods in which a continuum model is adopted to evaluate interaction effects between piles.

The approach models the soil behaviour using load-transfer functions which relate the load per unit length of pile which is transferred to the soil at any depth along the pile, to the displacement of the pile at that depth. Thus, a load-transfer function is not a soil property but instead gives the overall effect of the soil continuum as seen by the pile at a specific depth, and hence this function will depend on the pile properties and loading conditions as well as the soil properties.

#### 1.4.1.1 Load-transfer analysis for axially loaded piles

The use of the load-transfer method for the analysis of axially loaded single piles is based on an idea first proposed by Coyle & Reese (1966). Currently, several procedures are available to generate the relationship between shear stress at the pile shaft (load transfer,  $t$ ) and pile displacement,  $z$ , along the pile shaft and at the tip.

In the load-transfer method the pile is modelled as a system of one-dimensional rigid elements, connected by linear springs to represent pile shortening. Castelli *et al.* (1992) showed that inclusion of non-linear springs to account for pile shortening does not produce significant differences. However, use of non-linear springs is critical to model the soil resistance in skin friction and end-bearing, as indicated in Fig. 1.3.

The governing differential equation for the axial displacement of a single pile may be written as:

$$-E_p A_p \frac{d^2 w}{dz^2} + k_v w = 0 \quad (1.6)$$

where

$E_p$  = Young's modulus of pile,

$A_p$  = cross sectional area of pile,

$w$  = axial displacement,

$z$  = depth coordinate,

$k_v$  = modulus of subgrade reaction of soil for vertical loading in units of force/length<sup>2</sup>.

The governing differential equation may be solved by means of a finite difference approximation to obtain the relevant stiffness matrices for the pile and the soil (Meyer *et al.*, 1975). Although a consistent formulation of soil element matrix is more accurate, a lumped equivalent formulation in which the soil stiffness is lumped at the nodal points of the elements, will be adequate in most practical problems. Effects of soil nonlinearity may be simulated by using non-linear springs at the pile nodes. In order to represent different sizes of pile element and varying pile properties, a finite element representation of the pile may be more convenient (Smith, 1982).

The approximate solution to Equation (1.6) is then solved using the incremental tangent stiffness approach by inputting lumped values of soil spring tangential reaction modulus  $k_v$  at each node for each pile-head load or displacement increments. The modulus  $k_v$ , which is a function of the load level, may be evaluated using  $t$ - $z$  curves from a field test on an instrumented pile. However, such a test is expensive and 'standard'  $t$ - $z$  curves are usually employed in practice.

Work by Kraft *et al.* (1981) indicates that load-transfer curves may be constructed following the theoretical work of Randolph & Wroth (1978), in which the influence of pile shaft and pile base is considered separately. An empirical approach by Vijayvergiya (1977) proposes a form of  $t$ - $z$  curve applicable to both side and end springs. A comparison of normalized theoretical and empirical curves (Ha & O'Neill, 1983) shows that the theoretical curve agrees well with the curve proposed by Coyle & Reese (1966), but differs markedly from the empirical curve by Vijayvergiya. This difference is mainly due to the higher  $z_c$  (the critical displacement required to mobilize the maximum shaft resistance) in the empirical curve.

An efficient approach is outlined by Fleming (1992). This work, which is an extension of an idea first developed by Chin (1970), proposes a load-transfer method based on the use of linear-fractional (hyperbolic) functions to describe individual shaft and base performance. By a simple method of linkage, based on the fact that a linear-fractional function requires only definition of its origin, its asymptote and either its initial slope or a single point on the function, conventional elastic soil parameters and ultimate loads may be used to describe total performance. However, it has recently been recognised (England,

1993; Fleming, 1997) that a double linear-fractional function (one related to shaft friction and another to end-bearing) would prove much more successful, as shown by analysis of over a thousand pile tests.

#### 1.4.1.2 Load-transfer analysis for laterally loaded piles

The load-transfer approach for the analysis of laterally loaded single piles, known as the  $p$ - $y$  curve method (where  $p$  is the lateral soil resistance and  $y$  the lateral pile displacement), is similar to the axially loaded case. The principles of the technique were established during the 1960's (Reese & Matlock, 1960; Matlock & Haliburton, 1964) and it has been used extensively since then, mainly to meet the demands of the oil industry for the design of offshore pile foundations.

This technique models the pile as a vertical beam supported on horizontal (generally non-linear) springs representing the soil resistance, as indicated in Fig. 1.4. The governing differential equation for the deflection  $u$  of a laterally loaded pile is given by:

$$E_p I_p \frac{d^4 u}{dz^4} + k_h u d = 0 \quad (1.7)$$

where

$E_p$  = Young's modulus of pile,

$I_p$  = second moment of area of pile section,

$u$  = lateral displacement,

$z$  = depth coordinate,

$k_h$  = modulus of subgrade reaction of soil for horizontal loading in units of force/length<sup>2</sup>,

$d$  = width or diameter of pile.

The approximate solution to Equation (1.7) is then solved using the incremental tangent stiffness approach, in the same way as for the axially loaded case. The modulus  $k_h$ , which varies at different load levels, may be evaluated using  $p$ - $y$  curves obtained from back-analysis of a field test or empirical  $p$ - $y$  curves. Procedures for the construction of these

empirical  $p$ - $y$  curves have been presented by Reese *et al.* (1974) for piles in sand and by Matlock (1970) and Sullivan *et al.* (1979) for piles in clay.

This technique is widely used and it is recommended by the American Petroleum Institute (API) Code RP 2A (1984) for the design of pile foundations for offshore platforms, mainly with a view to assessing the effects of cyclic loading. However, such analyses are relatively complicated and time-consuming, and are rarely justifiable for onshore applications.

#### 1.4.1.3 Extension to pile groups

In addition to the empiricism of load-transfer approaches, another major limitation of representing the soil by an equivalent spring is that no information is available from the analysis regarding the deformation pattern around the pile. Thus, it is not possible to evaluate the interaction between neighbouring piles in a group. In order to overcome this limitation, hybrid methods have been proposed, in which the use of elasticity to estimate interaction effects is combined with a load-transfer approach to determine single pile behaviour.

One of the first attempts to solve the problem was developed by Focht & Koch (1973) who used the  $p$ - $y$  approach for single piles, but considered pile-soil-pile interaction using a modification of the interaction factor approach proposed by Poulos (1971b). They suggested the following equation to obtain the deflection of each pile of the group, assuming the soil to act elastically:

$$\rho_k = \bar{\rho}_F \left( \sum_{\substack{j=1 \\ j \neq k}}^n H_j \alpha_{\rho F k j} + R H_k \right) \quad (1.8)$$

where

$\rho_k$  = deflection of the  $k$ -th pile,

$\bar{\rho}_F$  = the unit reference displacement of a single pile under a unit horizontal load, computed by using the elastic theory,

$H_j$  = lateral load on pile  $j$ ,

- $\alpha_{\rho Fkj}$  = interaction factor between pile  $j$  and  $k$  (fixed-head condition), as suggested by Poulos (1971b),
- $R$  = relative stiffness factor,
- $H_k$  = the lateral load on pile  $k$ ,
- $n$  = number of piles in the group.

The relative stiffness factor  $R$  is the ratio of the groundline deflection of a single pile computed by the  $p$ - $y$  approach to the deflection computed by the Poulos method. In both instances, the lateral load on the single pile is the total lateral load acting on the pile group divided by the number of piles. It may be observed that, in the outlined approach, nonlinearity in the group response is only related to the behaviour of the pile head, and is thus not consistent with the stress level in the soil along the piles. Furthermore, the interaction factor approach only gives the loads and bending moments at the pile heads but not their variations along the piles. These variations need to be approximated by using single pile solutions with the corresponding pile head loads and bending moments.

An improved method of analysis, including extension of the analysis to axially loaded pile groups, has been suggested by O'Neill *et al.* (1977), in which the soil response at the individual piles is modelled using load transfer curves ( $t$ - $z$  or  $p$ - $y$  curves), while pile-soil-pile interaction is approximated by 'softening' the stiffnesses of the load-transfer curves with an empirical factor based on added soil displacements obtained from single pile solutions. Thus, an iterative procedure is required whereby the single pile load-transfer curves are continuously softened as a result of group effects.

A refinement of this approach has been presented by Chow (1986a) and Leung & Chow (1987) in which the individual pile response is obtained by a load-transfer technique while pile-soil-pile interaction is considered directly using Mindlin's solution. It may be noted that by taking small load/displacement increments, the accuracy of the solutions is adequate for practical purposes without the need to iterate. Good agreement is observed when comparing this method with the commonly used interaction factor approaches for the computation of pile groups embedded in a homogeneous, isotropic half space.

A simplified hybrid load-transfer approach for the analysis of linear and non-linear responses of axially loaded pile groups has been presented by Lee (1993). In this approach,

the non-linear single pile response is represented by a simple hyperbolic pile-soil model. The shaft and base flexibility coefficients are considered separately, and semi-analytical closed-form solutions are derived to calculate these flexibility coefficients. The interaction between piles is evaluated explicitly by calculating, for pairs of identical piles, the average shaft and base flexibility coefficients.

An alternative method for closely spaced pile groups subjected to lateral loading has been proposed by Brown *et al.* (1987) who apply  $p$ - $y$  multipliers to account for group shadowing effects. This method represents a convenient way of predicting the loss of soil resistance in piles within trailing rows. Thus, it is possible to reduce the computed load-carrying capacity of the piles in a group relative to the single pile capacity, as observed in load test results.

In conclusion, the load-transfer approach may be regarded as a link between the interpretation of full-scale pile tests and the design of similar piles rather than a general design tool for 'class A' (Lambe, 1973) predictions. In fact, more general use of the method is restricted by the difficulty of evaluating suitable values of the coefficient of subgrade reaction from intrinsic soil properties.

#### 1.4.2 Finite element method

The finite element method (Zienkiewicz, 1971) is theoretically the most powerful tool available to the pile designer, in which a variety of constitutive soil models can be employed and such aspects as soil inhomogeneity and anisotropy can be considered. In addition, the complete history of the pile may be simulated, ie the processes of installation, reconsolidation of the soil following installation, and subsequent loading of the pile (eg Nystrom, 1984).

One of the first attempts to use three-dimensional finite elements for the analysis of a pile group under vertical loading was presented by Ottaviani (1975), but this was limited to a group of 15 piles embedded in a linear elastic homogeneous soil by the enormous computer cost due the complexity of the single element stiffness computation and to the large number of elements needed to represent realistically a three-dimensional structure, as indicated in Fig. 1.5. The method has been used with some success for the analysis of a vertically loaded symmetrical pile group by idealising a ring of piles as a continuous annulus

of equivalent stiffness and the same total surface area as the piles which it replaces (Naylor & Hooper, 1974).

However, the most useful and economically viable application of FEM is in the analysis of an axisymmetric pile foundation, ie a single cylindrical pile. In fact, the cost of a finite element analysis increases sharply as the transition is made from a two-dimensional to a three-dimensional problem. As a result, most finite element analyses of piles have been of vertically loaded cylindrical piles (see, for example, Ottaviani, 1972; Lee, 1973; Poulos, 1979; Jardine *et al.*, 1986). Brown & Shie (1990a, 1990b) presented analyses of laterally loaded single piles and small pile groups and proposed constitutive models for soil which include two types of plasticity models to represent either undrained loading of saturated clay or drained loading of sands. In addition, frictional interface elements are used to provide for slippage and gapping at the pile-soil interface. The three-dimensional nature of the problem and the high degree of nonlinearity which is present require an enormous computational effort (eg a mesh with 10,000 degrees of freedom has been used for the single pile) and preclude the routine use of such techniques in design.

Zienkiewicz (1971) proposed to analyse the effect of non-axisymmetric loading of an axisymmetric structure, without the expense of a full three-dimensional treatment, by using techniques of Fourier analysis.

Combined finite element and theoretical solutions have also been applied to piles and pile groups by the extensive work of Randolph and his associates (Randolph, 1977, 1981, 1983a, 1983b, 1987, 1994; Randolph & Wroth, 1978, 1979, 1982; Clancy & Randolph, 1996; Guo & Randolph, 1997). Approximate analytical solutions for the axial and torsional response of single piles are based on the assumption that the load transfer down the pile shaft may be treated separately from that at the pile base. The load-settlement response for the pile base is obtained directly from the Boussinesq's (1885) solution for a point load acting on the surface of an elastic half-space. The pile shaft response is determined by considerations of vertical equilibrium (Cooke, 1974; Frank, 1974; Baguelin *et al.*, 1975). To evaluate the response of piles to lateral loading, Randolph has fitted the results of a parametric study using FEM by simple algebraic expressions giving the ground level deflection and rotation due to applied lateral load and moment. In order to extend such analyses to deal with pile groups, theoretical interaction factors are deduced from the

results of finite element analyses and expressed in terms of simplified expressions. By evaluating the interaction factors for all the possible pairs of piles in the group and by superimposing the effects, it is possible to yield the overall stiffness of the group.

Although the outlined approach of Randolph and associates is confined to the assumption of linear elastic soil behaviour, it is widely used in practice due to its economy and simplicity. Instead, a complete FEM solution of the pile group problem is not possible in practice because of enormous computational cost and complexity. It may be concluded that FEM is essential for clarifying the mechanism of load transfer from the pile to the surrounding soil but, especially for pile groups, is not readily applicable to practical problems. The considerable effort of data preparation and the enormous computational effort (especially if non-linear soil behaviour is to be considered) make the cost of analysing realistic pile groups using FEM prohibitively expensive and restrict its applications to single piles.

### **1.4.3 Boundary element method**

A reasonable compromise between the inadmissible simplicity of load-transfer approaches and the disproportionate complexity of FEM is provided by boundary element methods, in which the characteristics of the soil response are represented in a lumped form by ascribing the behavioural features of the soil to the pile-soil interface elements. This approach, based on a surface discretization scheme, provides a complete problem solution in terms of boundary values only (specifically at the pile-soil interface), with substantial savings in computing time and data preparation effort. Thus, for three-dimensional problems involving low surface area to volume ratios, such as those found in pile foundation problems, BEM represents a simpler and more efficient approach than FEM. Indeed, most of the existing formulations for pile analysis are of the boundary element type and hence the approach is widely used in practice.

In FEM the differential equation governing the behaviour of an elastic medium are solved by discretizing the continuum into a number of elements or node modules. By contrast, BEM relies on one or more particular, exact solutions of the whole continuum. By superposing a number of these particular solutions, distributed over the surface of the

elastic body (ie the pile-soil interface), the boundary conditions may be satisfied and an exact solution generated.

Most of BEM analyses are based on the consideration of the pile and the surrounding soil domains separately and then compatibility and equilibrium conditions are imposed at the interface. The elastic solution of Mindlin (1936) is often employed to relate the stress and displacements fields due to a point load acting in the interior of a homogeneous elastic half-space. This solution is particularly convenient for analysing the pile problem since the boundary conditions along the (unloaded) ground surface are automatically satisfied. This has led to its widespread use in the analysis of piles and pile groups since 1970's, mainly due to the work of Poulos and Banerjee with respective associates. It should be emphasised that Mindlin's solution is strictly valid for a homogeneous soil. However, in practice, the influence of soil inhomogeneity is often approximated using some averaging of the soil moduli (Banerjee, 1978; Poulos, 1979; Chow, 1986a, 1987a; Yamashita *et al.*, 1987).

There are other known solutions of an elastic continuum, besides that developed by Mindlin. Chan *et al.* (1974) formulated, by the technique of integral transforms, the solution of a layered half space subjected to a concentrated force acting in the interior of the system. This solution has been applied to pile problems by Banerjee (1978), Banerjee & Davies (1978), Chin (1988), Chin & Poulos (1991) and Chow *et al.* (1990). Banerjee (1976) outlined a method based on Kelvin's (1848) solution for a point load acting in the interior of an infinite elastic continuum, which enables the analysis of piles embedded in a layered soil. Using this method, it is possible to analyse the problem of a pile in a Gibson soil by treating the soil as a number of homogeneous layers (Banerjee & Davies, 1977). The main drawback to this approach is that the stress resultants are distributed over each interface between the layers and so the total number of equations to be solved is considerably greater than for the case of a pile in a homogeneous soil. Thus, the analysis is very expensive in terms of computational cost.

An outline of the principles involved in the BEM analysis of axially and laterally loaded piles is given below.

*Axially loaded piles.* It is assumed that the pile and the soil are initially stress-free and that no residual stresses exist in the pile resulting from its installation. As regards the soil domain, a set of distributed stress resultants acting at the boundary of the pile is considered, as indicated in Fig. 1.6a. These stress resultants, which may be regarded as shear stresses down the pile shaft and normal stresses at the pile base, are assumed to be symmetric about the pile vertical axis and are constant over each element of the pile-soil interface. The greater the number of these elements, ie the finer the discretization of the pile-soil interface, the more accurate the final solution will be. Making use of the Mindlin's solution, the vertical displacement of the mid-point of each pile element may be calculated by integrating the effects of all the stress resultants.

The pile, at present regarded as a free-standing cylindrical pile, is subjected to equal and opposite stress resultants along its boundary, balanced by the applied axial load, as shown in Fig. 1.6b. In addition, from elasticity, compression of the pile under this axial loading may be calculated at the same points as the displacements were calculated in the soil.

If conditions at the pile-soil interface remain elastic and no slip or local yield occurs at any of the elements, it is possible to match these two displacement fields and satisfy overall equilibrium and hence values of the unknown stress resultants may be calculated. The final step replaces the soil from within the pile-soil boundary with the actual pile. The key-point of the method is that, if tractions are applied at the interface so that the deformation is compatible with that of the free-standing pile under equal and opposite tractions, then it is immaterial whether there is pile or soil inside the shaded region of Fig. 1.6c.

*Laterally loaded piles.* The approach to laterally loaded piles is similar to that for axially loaded piles except that an equivalent pile is considered, as proposed by Poulos (1971a). Referring to Fig. 1.7, the pile is idealized as an infinitely thin strip of the same diameter (or width) and bending rigidity as the prototype pile. Normal stress intensities are assumed to act on both faces of the strip pile and, if purely elastic conditions prevail, compatibility of the horizontal displacement fields is considered. It is also assumed that the soil at the back of the pile near the ground surface adheres to the pile.

An approximate method of allowing for pile-soil separation is outlined by Poulos & Davis (1980).

The earliest contribution to the analysis of pile behaviour by BEM is due to Poulos and his associates (Poulos, 1968, 1971a, 1971b, 1973, 1974, 1975, 1976, 1977, 1979, 1980a, 1980b, 1982, 1988, 1989, 1990, 1993, 1994; Poulos & Davis, 1968, 1974, 1980; Poulos & Mattes, 1969, 1971; Poulos & Hewitt, 1986; Mattes & Poulos, 1969). This work has resulted in a wealth of information on the response characteristics of pile foundations. The approach, based on Mindlin's solution, adopts the procedure outlined above to evaluate the axial and lateral response of single piles and also to calculate interaction factors between pairs of adjacent, identical piles. A method has also been developed by Poulos & Hewitt (1986) to evaluate axial interaction between dissimilar piles in a group.

Poulos & Davis (1980), for pairs of identical piles embedded in a homogeneous elastic soil, provide useful design charts for the calculation of the interaction factors as a function of the pile spacing, the relative pile-soil stiffness and the geometric characteristics of the piles. Allowance is also made for the effects of a finite base layer, enlarged pile bases and variation of the Poisson's ratio.

For a group of piles, the interaction factors calculated for all the possible pairs of piles in the group may be superimposed and used together with the single pile stiffnesses to yield an overall stiffness of the group. This approach, termed 'the interaction factor method', is widely used in practice due to its relative simplicity and economy compared with the complete BEM approach of Banerjee and associates (the latter approach is discussed below).

A modified form of the interaction approach has been described by Poulos (1988). This approach considers that, in reality, the soil between piles undergoes smaller strains and is likely to be stiffer than near the pile-soil interface, and hence interaction between the piles will consequently be reduced. In order to take into account these effects, different horizontal values of soil Young's modulus are used to determine the single pile behaviour and the interaction factors. This approach allows a better agreement between measured and calculated group settlements (Poulos, 1989).

Poulos (1980b, 1990) presented an extension of the outlined linear elastic approach to include soil nonlinearity, in an approximate manner, by limiting the stresses at the pile-soil interface, specifically shear stresses for axial loading and normal stresses for lateral loading. However, the analysis is limited to groups of 25 piles due to enormous computational resources needed to analyse larger groups (Poulos, 1993).

It should be emphasised that the interaction factor approach is a fairly approximate procedure because the interaction coefficients of each pair of piles do not take into account the simultaneous presence of all the piles in the group. In order to overcome this limitation, the work of Banerjee and his associates solves the problem of pile-soil-pile interaction by taking into account the simultaneous interaction of all the piles of the group with the surrounding soil. In this category of methods, termed 'complete' analysis methods, the behaviour of each pile is considered in detail by evaluating, by means of Mindlin's solution, its displacement from the stress resultants on all the piles of the group. Thus, piles of different length, diameter and/or stiffness within a group may be easily incorporated. The analysis is generally based on the assumption that all piles are connected by a rigid cap which imposes the same head deformations and prevents differential head rotation.

For axially loaded piles and pile groups, a rigorous (linear elastic) analysis has been proposed by Mattes (1969, 1972) and Butterfield & Banerjee (1970, 1971a, 1971b), in which both vertical and radial displacement compatibility are considered, and a normal stress system should also then be imposed on the pile elements. Thus, the contribution to vertical displacements from the radial stress resultants and vice versa must be considered too. However, Mattes (1972) and Poulos (1977) showed that this more sophisticated analysis produces a load-deformation behaviour and distribution of shear stress along the pile that are almost identical with those from a simpler analysis that considers only vertical displacement compatibility. Only for relatively short piles (length to diameter ratio less than 25) does the inclusion of radial displacement compatibility have any effect on the solutions, and even in such cases the effect is unimportant from a practical point of view. Therefore, in subsequent work, the contribution of radial resultant stress has been ignored.

Banerjee & Driscoll (1975, 1976, 1977) presented a complete analysis of a pile group under general loading conditions (ie vertical loads, horizontal loads and moments) in the assumption of linear elastic soil behaviour. The analysis of raked piles is carried out by considering two sets of stress resultants, one parallel to the sides of the pile and the other normal to the pile, and then the horizontal and vertical components of these stresses are taken; this enables Mindlin's solution to be applied in order to produce horizontal and vertical displacement fields. For a single raking pile, the horizontal displacements due to vertical stress components and vice versa are assumed to be negligible (Banerjee & Driscoll, 1974).

Banerjee & Davies (1980) have also described an approximate non-linear method of analysis in which, by means of an incremental and iterative procedure, the effects of yielding and slipping are introduced by distributing initial stresses over volume cells and distributing initial surface tractions over slip-surfaces, respectively. However, the method is restricted to small pile groups due to enormous computational resources required to analyse the response of large groups of piles.

In conclusion, even in linear elastic hypothesis of soil behaviour, the computational resources required to perform the complete analysis described above become excessive for all but the simplest foundation systems.

## **1.5 Computer programs for pile group analysis**

The complexity and magnitude of pile group problems have necessitated the use of computer programs based on the methods outlined in the previous sections. Currently, a number of computer programs are available, by which pile groups under general loading conditions (ie vertical loads, horizontal loads and moments) may be analysed in order to give estimates of the deformations and load distributions among the piles. Such programs have led to a much better understanding of the factors which affect the performance of a pile group and have enabled parametric studies (in the linear elastic range) to be undertaken.

Computer programs for the analysis of pile groups vary in the type of approach used and in the sophistication of treatment of different aspects of group behaviour. A brief

description of some of the programs which are currently widely available, and for which some comparison of results has been undertaken, is given below.

- **PGROUP** (Banerjee & Driscoll, 1976) is based on a complete BEM solution of the pile group, ie the simultaneous effect of all elements of all the piles within the group is considered. The soil, which is assumed to behave linearly elastically, may be variously idealised as a homogeneous, Gibson or two-layered material. The effect of a (rigid) cap in contact with the ground may be analysed. Pile group systems of up to 200 piles (vertical or raked), up to 100 cap elements and up to 400 degrees of freedom may be analysed. This program is, in principle, the most rigorous of the programs discussed — in practice, the computational resources required to perform the analysis become excessive for all but the simplest foundation systems, thereby precluding its use for routine design problems.
- **DEFPIG** (Poulos, 1980a) is based on a simplified BEM approach for the analysis of single piles and the use of interaction factors for two equally loaded identical piles. The program is limited to groups of up to 160 identical piles. Initial calculation of the individual pile stiffnesses and interaction factors involves a large amount of computing time, even for a relatively small pile group. The program can handle, in an approximate manner, non-homogeneous soil profiles, by an averaging procedure using Mindlin's solution, and non-linear pile-soil response, by limiting the stresses at the pile-soil interface. However, use of the non-linear option of the code is restricted to groups of 25 piles because it needs enormous computational resources. Pile cap elements may be included for vertical loading.
- **PIGLET** (Randolph, 1987) is based on approximate analytical solutions that are either derived theoretically or fitted to FEM results to give single pile response. Pile-soil-pile interaction is based on interaction factors determined from expressions fitted to the results of finite element analyses. The program can analyse groups of up to 300 vertical or raked piles, which are all of same length. The soil is modelled as an elastic material, with a linear variation of stiffness with depth. Rigid or flexible pile cap (for vertical loading only) may be considered while the effects of pile cap-soil interaction are neglected. Since the program

makes use of previously derived solutions, computing time is reasonable, the main limitation being the assumption of linear elastic soil behaviour.

- **GRUPPALO** (Mandolini & Viggiani, 1997) is based on a hyperbolic load-settlement relationship for the single pile response and the use of interaction factors to evaluate group effects. The soil is modelled as a horizontally stratified elastic medium. The non-linear behaviour of the single pile is simply obtained by fitting the results of loading tests with a hyperbolic function (Chin, 1970), while the interaction between pairs of piles is evaluated by means of a linear elastic BEM model. The code is restricted to axially loaded pile groups.

It is worth noting that the interaction factor approach (employed in DEFPIG, PIGLET and GRUPPALO) produces the following limitations:

- (a) The superposition of the two-pile interaction factors to determine the pile group response is approximate only, as the reinforcing effect of intervening piles in a group is ignored; such an approach leads to an overestimation of interaction between piles;
- (b) The use of interaction factors becomes questionable for cases in which not all the piles are identical;
- (c) The interaction factor approach only gives the loads and bending moments at the pile heads, but not their distributions along the piles; these may only be approximated utilising the single pile solutions with the corresponding pile head loads and bending moments.

These limitations can be removed by adopting a complete BEM or FEM analysis of the group (for example, that employed in PGROUP).

Other computer codes, such as PILGP1 (O'Neill *et al.*, 1977) and the ones developed by Chow (1987b, 1987c), propose a hybrid approach in which load-transfer non-linear springs are used to obtain the response of the individual piles and a continuum model

is used to determine the effects of interaction between the piles. Their main disadvantages lie in the assessment of the value of the modulus of subgrade reaction from intrinsic soil properties and the computational effort required to analyse large groups.

## **1.6 Concluding remarks**

Application of available numerical methods to realistic pile group problems is deficient because these are mainly restricted to linear elastic analyses and relatively small groups of piles. With respect to the first limitation, it should be emphasised that the assumption of a linear elastic soil model is unrealistic for most soils and the choice of a suitable secant soil modulus is by no means straightforward. In addition, for pile group systems designed according to the deformation-based approach, and hence characterised by a low safety factor, consideration of soil nonlinearity becomes compulsory. Further, current methods suffer from limitations imposed by the number of piles in the group and the global dimension of the problem which render such analyses computationally inefficient.

It is expected that the numerical method developed in this thesis will remove these restrictions, thereby leading to an improved understanding of pile group behaviour and considerable savings in construction costs.

### FIGURES CHAPTER 1

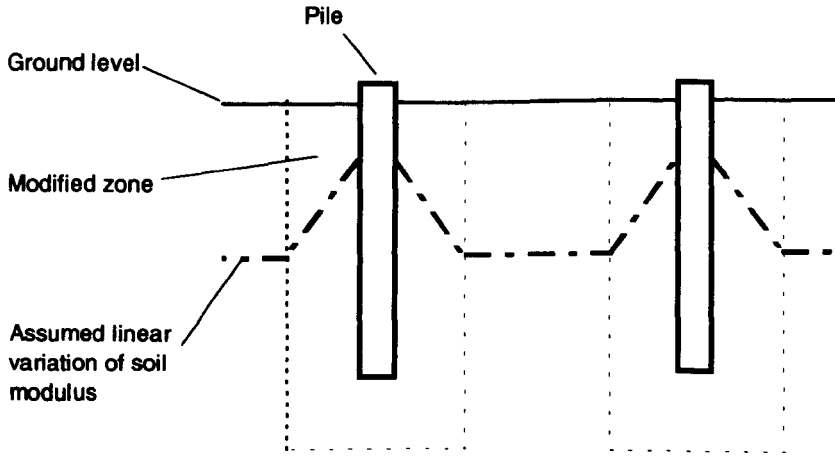


Fig. 1.1 Assumed soil modulus variation by Poulos (1988).

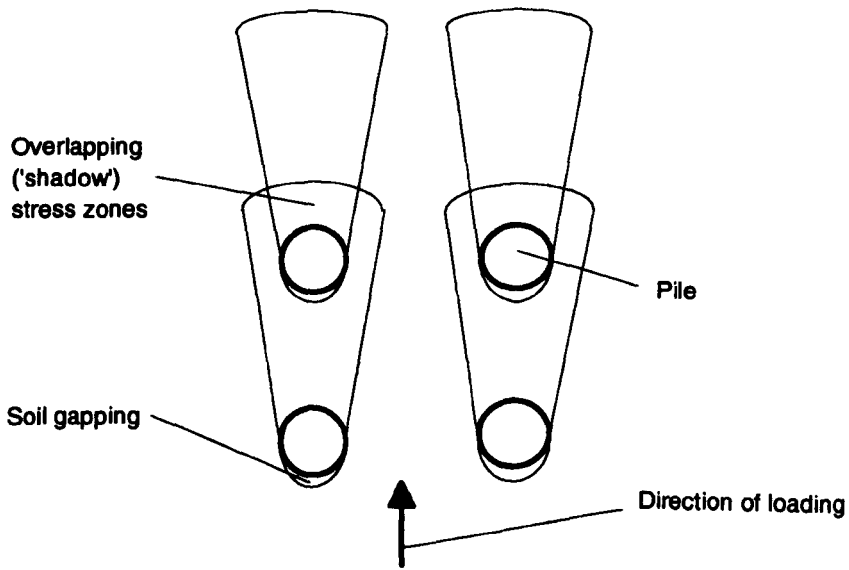


Fig. 1.2 Schematic drawing illustrating overlapping of failure zones ('shadowing') and gap formation behind closely spaced piles under lateral loading.

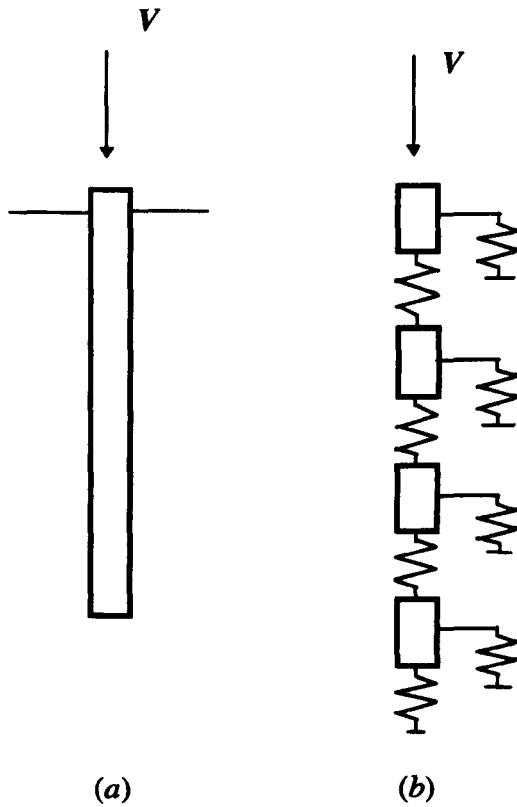


Fig. 1.3 Load-transfer analysis of pile under axial loading  $V$ . (a) Actual pile. (b) Pile modelled as a system of rigid elements connected by springs. Soil resistance modelled as external springs.

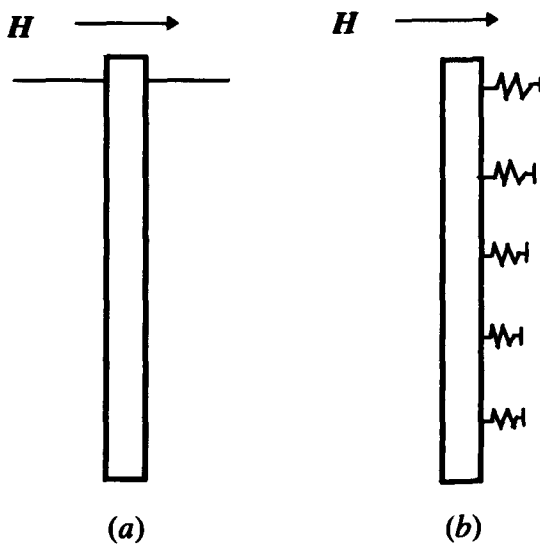


Fig. 1.4 Load-transfer analysis of pile under lateral loading  $H$ . (a) Actual pile. (b) Pile modelled as a vertical beam supported on horizontal springs.

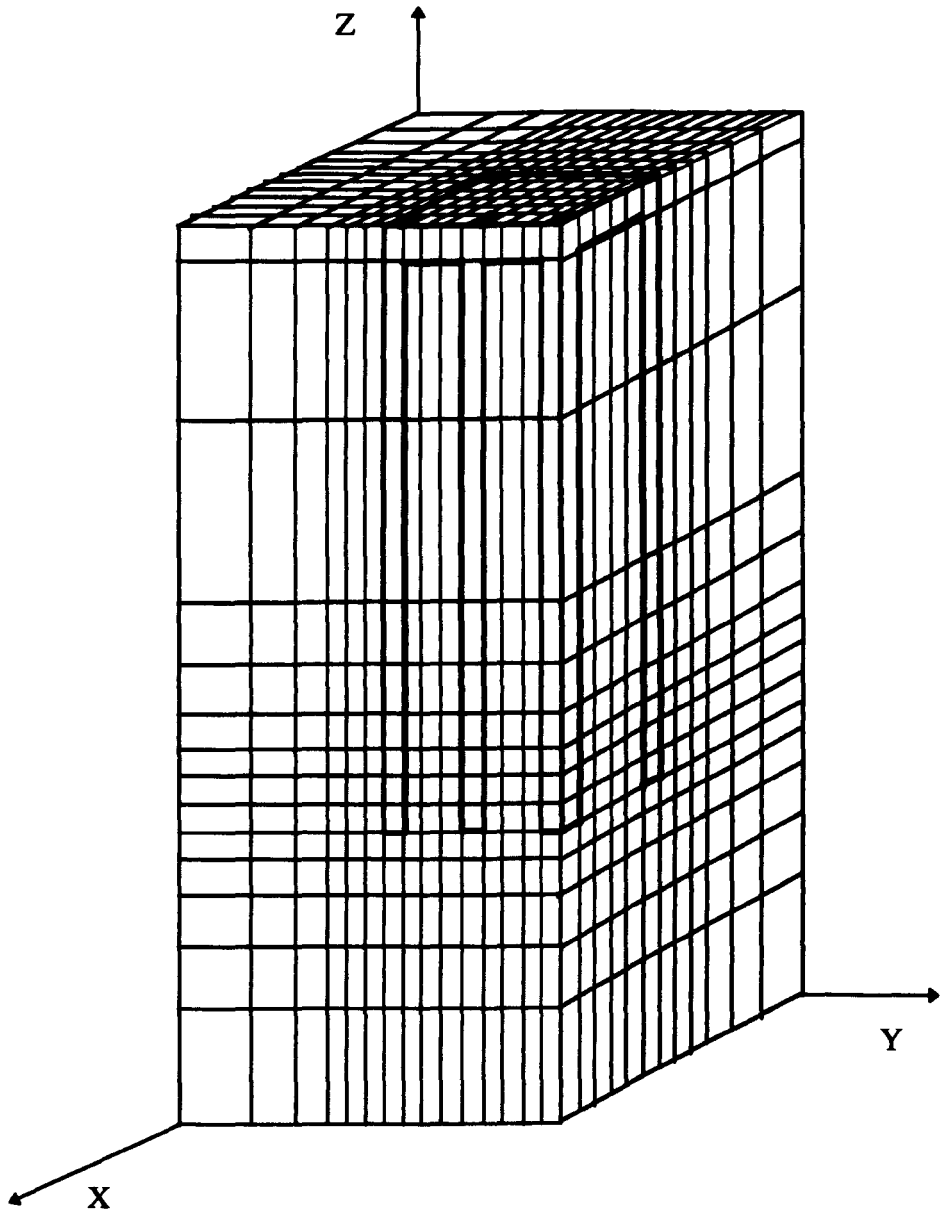


Fig. 1.5 Three-dimensional finite element mesh for a vertically loaded  $3 \times 2$  pile group (after Ottaviani, 1975).

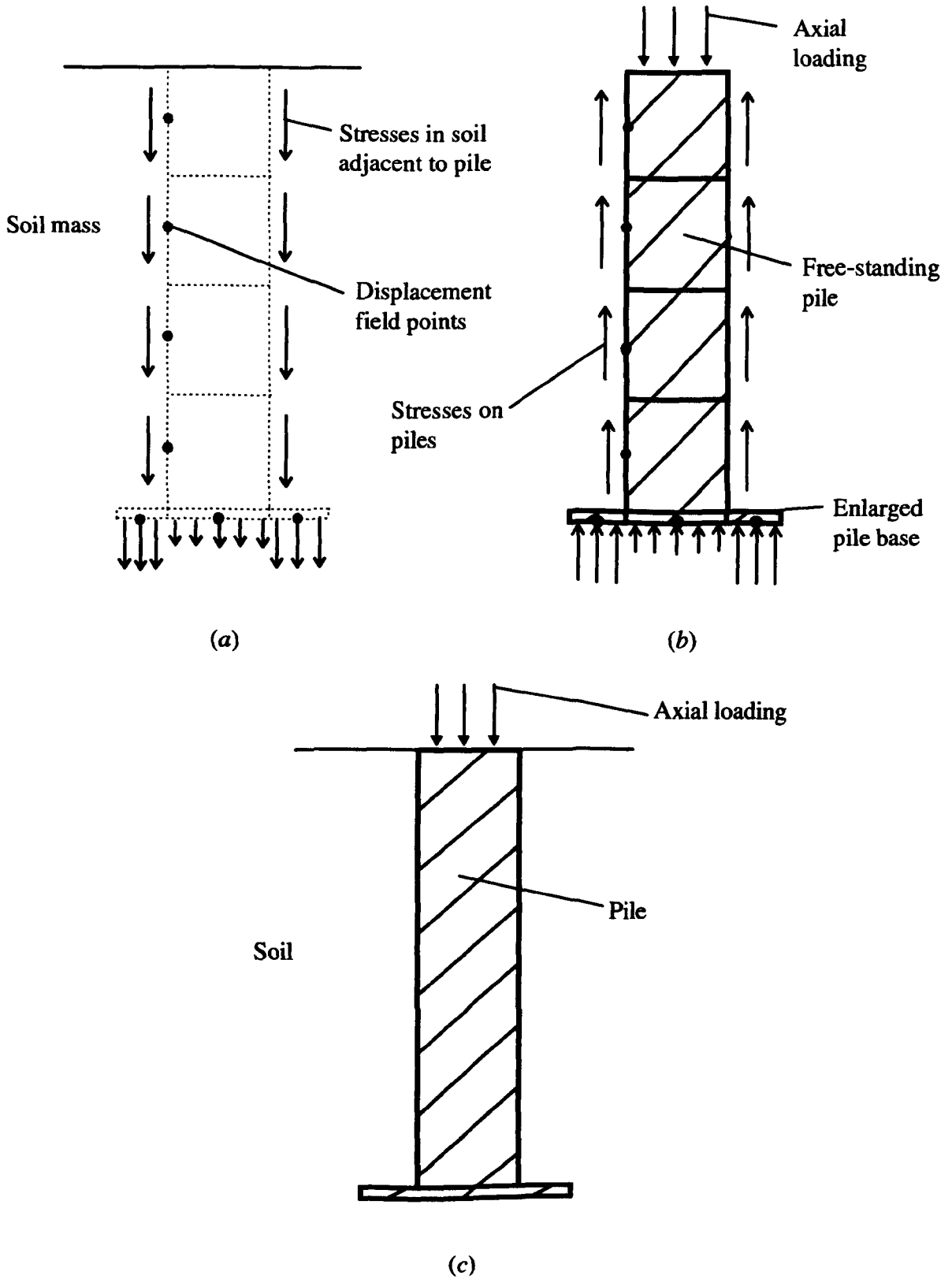


Fig. 1.6 Schematic diagram of boundary element approach for an axially loaded pile. (a) Soil domain. (b) Pile domain. (c) Coupled pile and soil domains.

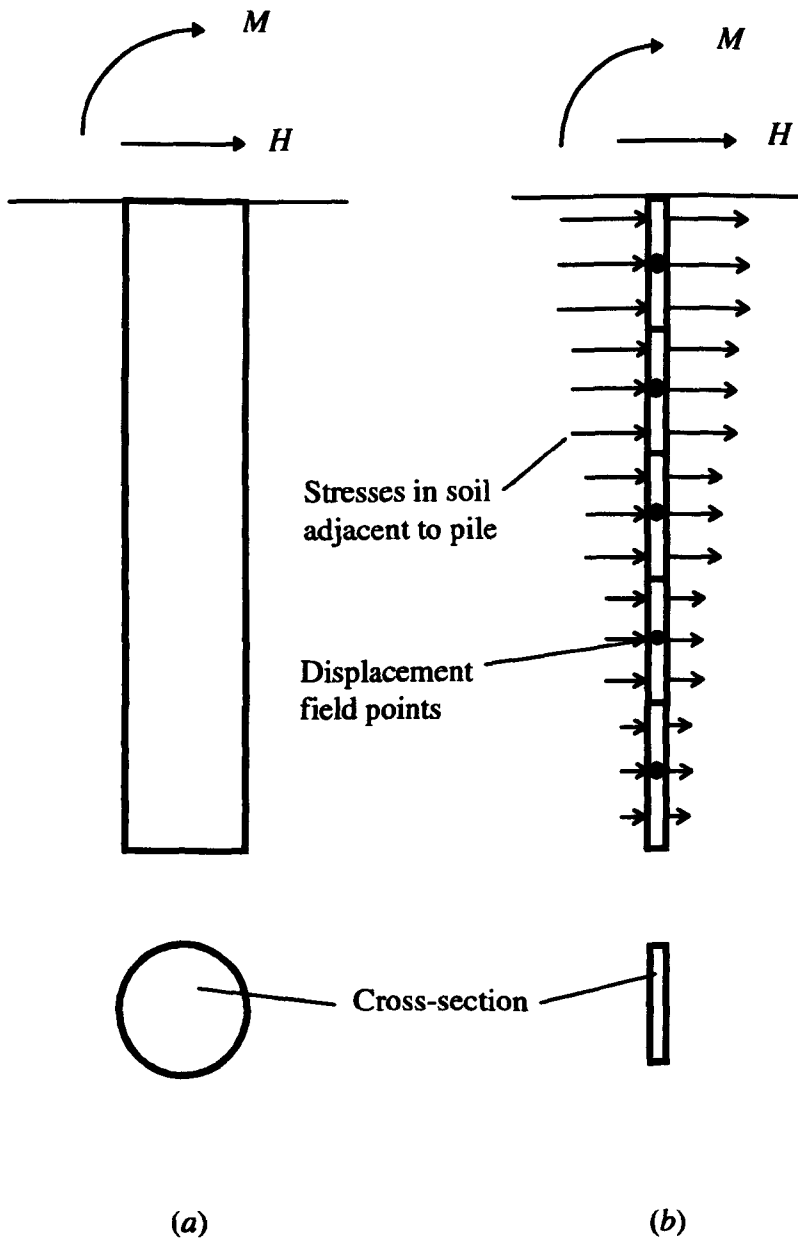


Fig. 1.7 Boundary element analysis of a pile under horizontal loading  $H$  and moment  $M$ .  
 (a) Actual pile. (b) Pile idealised as a thin strip.

# CHAPTER 2

## Formulation of the non-linear BEM analysis

### 2.1 Summary

This Chapter describes the proposed boundary element method formulation for the non-linear analysis of pile groups embedded in cohesive soils and subjected to general loading conditions (ie vertical and horizontal loads and moments). This formulation has been implemented in a computer program called PGROUPN. The analysis is capable of determining the load-displacement and rotation response of the pile cap and the loads and moments carried by the individual piles of the group. Soil inhomogeneity and nonlinearity are accounted for in the analysis, in an approximate manner.

### 2.2 Introduction

A complete boundary element approach, implemented in the computer program PGROUPN, is presented for the non-linear analysis of realistic pile groups embedded in cohesive soils (specifically fully saturated clay under undrained conditions) and subjected to any combination of vertical loads, horizontal loads and moments. The program, given the geometry of the piles, their stiffness and the soil stiffness profile, computes the pile cap load-displacement and rotation response and the distribution of stresses, loads and moments in the individual piles of the group. The soil may be idealized as a homogenous or a Gibson soil which, optionally, may be underlaid by a rigid base. The piles are assumed to be rigidly connected by a rigid cap (a reasonable assumption in most cases) which imposes the same horizontal head displacements and head rotations for all piles, while differential vertical head displacements are solely due to rotation of the rigid cap. The pile cap is assumed to be clear of the soil (the so-called 'free-

standing cap'), ie the effects of interaction between cap and soil are neglected. This is a plausible assumption in most practical situations where it is customary to ignore the resistance offered by the superficial soil layers. For this purpose, it is possible to specify a gap between the pile cap and the effective ground surface. Piles may have different geometries (length, external and internal diameter, base diameter) and may be inclined in the direction of horizontal loading.

The analysis is based on the indirect formulation of BEM, as first proposed for pile group analysis by Butterfield & Banerjee (1971a). The approach employed in this thesis may be regarded as an extremely efficient extension of the complete BEM algorithm proposed by Banerjee & Driscoll (1976), and implemented in the computer program PGROUP.

It has been shown that application of the complete BEM solution to large pile groups is uneconomical due to enormous computational resources. This restricts its use in normal design (Butterfield & Douglas, 1981; Randolph, 1994; Mandolini & Viggiani, 1997). By contrast, one of the main features of the proposed analysis lies in its capability to adopt a complete BEM approach while retaining a highly computationally efficient code, and this renders the analysis of large groups economically viable with an ordinary desktop computer.

The other innovative aspect of the proposed analysis is the inclusion of the non-linear continuum response of the surrounding soil by means of a stepwise linear incremental procedure. A significant simplification of the method is that, although assumed limit stress conditions at the pile-soil interface are satisfied, the yield conditions within the soil continuum are not explicitly satisfied. However, previous work on BEM analysis of pile foundations (Poulos & Davis, 1968; Poulos, 1980b; Chow, 1986a; Davies & Budhu, 1986; Lee, 1997) indicates that the errors engendered by this approach are slight and the method is capable of capturing all of the essential features of the problem. The non-linear analysis is based on an elastic-perfectly plastic model for the soil, which is assumed to behave linearly elastic at small strain levels, but fails when the stresses at the pile-soil interface reach certain limiting values, namely, bearing failure in the compression zone (ie the base for the axial response and the shaft for the lateral response) and shear failure in the slip zone (ie the shaft for the axial response).

The main modifications to the BEM algorithm developed by Banerjee & Driscoll (1976) may be summarised as follows:

- 1) Various strategies adopted for achieving efficiency gains: (a) the pile base is represented by one (circular) element only; (b) the diagonal soil flexibility terms are calculated via analytical integration of the singular Mindlin functions; (c) the off-diagonal soil flexibility terms are evaluated by approximating the continuously distributed loads by equivalent point loads acting at the pile nodes; (d) use of Bernoulli-Euler beam theory for pile domain discretization and analytical integration of the singular functions; (e) exploitation of similarities in forming single-pile flexibility matrices; (f) more efficient calculation of the unit boundary condition vector; (g) pile-soil system solved via LU decomposition;
- 2) Inclusion of non-linear soil response.

### 2.3 Soil model

It is assumed, for simplicity, that the soil behaves as an elastic-perfectly plastic material. While such a simple model cannot fully describe the behaviour of soils, it is sufficiently accurate for most practical boundary-value problems.

The soil parameters required in the analysis are the profiles of the undrained shear strength ( $C_u$ ) and the Young's modulus ( $E_s$ ), while the Poisson's ratio ( $\nu_s$ ) is assumed to be constant throughout the pile depth. Two possibilities are included: homogeneous soil, with  $C_u$  and  $E_s$  assumed constant throughout the pile depth, or a Gibson soil, with  $C_u$  and  $E_s$  assumed to vary linearly with the depth ( $z$ ) below ground level:

$$C_u = C_{u0} + cz \quad (2.1)$$

$$E_s = E_{s0} + mz \quad (2.2)$$

where  $C_{uo}$  and  $E_{10}$  are the undrained shear strength and Young's modulus at the ground surface, respectively, and  $c$  and  $m$  are constants. The Gibson soil would typically be representative of a normally consolidated or lightly overconsolidated clay, whereas the uniform soil might be more representative of a heavily overconsolidated clay.

## 2.4 Method of analysis

The basic requirements for developing a boundary element formulation for elastostatics are a reciprocal identity between two elastic states, such as the reciprocal work theorem, and a fundamental point force solution of the governing differential equation of the problem (for statics it may be readily obtained from the Navier-Cauchy equation as a special case). The synthesis of the reciprocal identity and the point force solution may be accomplished in two separate ways, namely, the direct and the indirect BEM methods. The direct method (Rizzo, 1967; Cruse 1969, 1973, 1974; Lachat & Watson, 1976) is formulated in terms of physical quantities such as displacements and tractions, while the indirect method (Massonet, 1965; Butterfield & Banerjee, 1970, 1971a, 1971b; Banerjee & Driscoll, 1976) is based on 'fictitious' quantities as source densities (eg displacement gradients). However, the formal equivalence of the two methods can be established quite easily using the reciprocal work theorem.

The approach presented in this thesis, based on the indirect formulation of BEM, involves the selection of an elementary singular solution of the governing differential equation of the problem. Then, by distributing this singular solution in terms of an arbitrary density function (traction vectors) over the surface of a given domain, a general solution in terms of the arbitrary function is developed. These point force solutions can be conceived as influence coefficients which express the displacement at any point (field point) in the solid due to a point load acting at any other point (load point), in terms of the coordinates of the load and field points and the elastic properties of the solid. With reference to the present problem, which involves an unloaded ground surface, it is convenient to adopt the solution of Mindlin (1936) for a point load within a semi-infinite medium, whose elastic properties are defined by the shear modulus  $G$ , and the Poisson's ratio  $\nu_s$ .

The proposed approach is based on a linear elastic analysis which is then extended to allow approximately for soil nonlinearity by means of an incremental

procedure. The method involves discretization of the pile-soil interface into a number of surface elements — this number must be the same for each pile in the group, irrespective of pile length (refer to Fig. 2.1). The behaviour of each element is considered at a node which is located at the mid-height of the element on the centre line of the pile. The stress on each element is assumed to be constant, as shown in Fig. 2.2. According to widely accepted methods of pile group analysis (Banerjee & Driscoll, 1976; Poulos, 1980a; Randolph, 1987), it is assumed that there is no coupling between axial and lateral response of each pile element. As regards the axial response of the single pile, the pile-soil interface is discretized into a number  $N$  of shaft cylindrical elements over which axial shear stresses are applied, while the base is represented by a circular (disc) element over which normal stresses are acting. This is a first simplification of the analysis of Banerjee & Driscoll (1976) in which the base may also be subdivided into a number of elements. As regards the lateral response, the pile is assumed to be a thin rectangular strip which is subdivided into a number  $N$  of rectangular elements. Only normal stresses on the compressive face are considered. Further, if the pile base is assumed to be smooth, the effects of the tangential components of stresses over the base area can be ignored. Thus, each pile is characterised by  $(2N+1)$  surface elements.

In the proposed analysis, the soil and pile compliance equations are evaluated separately and then compatibility and equilibrium are imposed at the interface. Given unit boundary conditions, ie unit value of vertical displacement, horizontal displacement or rotation of the pile cap, these equations are solved, thereby leading to the distribution of stresses, loads and moments in the piles for any loading condition.

### 2.4.1 Soil domain

Assuming purely linear elastic soil behaviour, the soil deformations at the pile-soil interface nodes can be related to the soil tractions via integration of the Mindlin's kernel (Mindlin, 1936), yielding (eg Banerjee & Driscoll, 1976):

$$\{u_i\} = [G_i] \{t_i\} \quad (2.3)$$

where

$\{u_s\}$  = column vector of soil displacements of size  $(2N+1)$ ,

$\{t_s\}$  = column vector of soil tractions of size  $(2N+1)$ ,

$[G_s]$  = square matrix, of size  $(2N+1) \times (2N+1)$ , of soil flexibility coefficients  
obtained via integration of the Mindlin's kernel for the axial and lateral  
response (for further details see Appendix 2.1),

$N$  = number of pile shaft elements per pile.

The off-diagonal flexibility coefficients of  $[G_s]$  are evaluated by approximating the influence of the continuously distributed loads by discrete point loads applied at the nodal points along the centerline of the piles; the rationale being that, at some distance, their effects on the soil displacements are indistinguishable. The accuracy of this assumption has been verified for pile groups by Chow (1986a) and Leung & Chow (1987). Instead, the approach of Banerjee & Driscoll (1976) considers distributed stresses over the pile-soil interface.

The diagonal terms of the flexibility matrix  $[G_s]$  are calculated via analytical integration of the singular Mindlin functions (see Appendix 2.1), which has yielded very accurate results with considerable saving of computing time. This is one of the innovative features of the proposed analysis and represents a significant advance over previous work where these have been integrated numerically (ie Butterfield & Banerjee, 1971a; Banerjee & Driscoll, 1976), since these singular integrals require considerable computing resources, especially for large pile groups.

It is worth noting that the soil flexibility matrix  $[G_s]$  obtained from Mindlin's solution is fully populated (in the initial stage of elastic loading) in contrast with the load-transfer methods which suppose a diagonal flexibility matrix.

*Approximate treatment for non-homogeneous soil.* Mindlin's solution is strictly applicable to homogeneous soil conditions. However, in practice, this limitation is not strictly adhered to, and the influence of soil non-homogeneity is often approximated using some averaging of the soil moduli. In this thesis, non-homogeneity of the soil is taken into account in the manner proposed by Poulos (1979). In the evaluation of the influence of one loaded element on another, the value of soil modulus is taken as the mean of the values at the two

elements. This approximation is particularly adequate in problems where the soil stiffness increases linearly with depth (Gibson soil) and it is widely accepted to analyse pile groups under general loading conditions (see, for example, Poulos, 1980a; Leung & Chow, 1987; Chow, 1986a, 1986c, 1987b). It should be emphasised that this approximate solution becomes inaccurate if large differences in soil modulus exist between adjacent elements or if a soil layer is overlain by a much stiffer layer (Poulos, 1989).

*Approximate treatment for layer of finite depth.* The elements of the soil flexibility matrix  $[G_s]$  calculated as previously described (refer to Equation (2.3)) apply only for a soil mass of infinite depth. However, Mindlin's solution may be used to obtain approximate solutions for a layer of finite thickness by employing the Steinbrenner approximation (Steinbrenner, 1934) to allow for the effect of the underlying rigid base in reducing the soil displacements (Poulos, 1968, 1977, 1980a, 1989; Poulos & Davis, 1968). From this approximation, the flexibility coefficient ( $G_s^{ij(H)}$ ) relating axial displacement for a nodal point  $i$  in a layer of depth  $H$  due to axial stress on element  $j$  is given by:

$$G_s^{ij(H)} = G_s^{ij(\infty)} - G_s^{Hj(\infty)} \quad (2.4)$$

where

$G_s^{ij(\infty)}$  is the flexibility coefficient relating axial displacement for a nodal point  $i$  due to axial stress on element  $j$  in a semi-infinite mass;

$G_s^{Hj(\infty)}$  is the flexibility coefficient relating axial displacement for a point within the semi-infinite mass directly beneath  $i$  at a depth  $H$  below the surface due to axial stress on element  $j$ .

Thus, the adjusted coefficients of  $[G_s]$  are introduced into Equation (2.3). It should be emphasised that for piles bearing directly on a stiffer stratum, ie  $H = L$  (where  $L$  is the pile length), this approximation becomes less reliable (Poulos & Davis, 1968; Poulos, 1977), and alternative approaches have to be employed (eg the 'mirror-image' technique described by Poulos & Davis, 1980).

### 2.4.2 Pile domain

If the displacements of the pile-soil interface are known, then Equation (2.3) can be solved directly. But these displacements can be specified only for perfectly rigid piles — for most practical situations, piles cannot be considered as rigid and hence we must couple Equation (2.3) with a corresponding set obtained from the considerations of the axial and flexural rigidity of the pile domain (Banerjee & Driscoll, 1976).

This can be accomplished by considering the piles as simple beam-columns rigidly fixed at their heads to the pile cap. Following the subdivision of the pile shaft into  $N$  number of elements, the displacements and tractions at the pile-soil interface nodes can be related to each other via the Bernoulli-Euler beam theory (eg Ahmad *et al.*, 1985), yielding:

$$\{u_p\} = [G_p]\{t_p\} + \{B\} \quad (2.5)$$

where

$\{u_p\}$  = column vector of pile displacements of size  $(2N+1)$ ,

$\{t_p\}$  = column vector of pile tractions of size  $(2N+1)$ ,

$[G_p]$  = square matrix, of size  $(2N+1) \times (2N+1)$ , of flexibility coefficients obtained via integration of the Bernoulli-Euler kernel for the axial and flexural response of the pile (for further details see Appendix 2.2),

$\{B\}$  = column vector, of size  $(2N+1)$ , of pile displacements due to unit boundary displacements and rotation of the pile cap (see Section 2.4.3).

The coefficients of the pile flexibility matrix  $[G_p]$  are calculated via analytical integration of the Bernoulli-Euler kernel. It is worth noting that use of the elementary (Bernoulli-Euler) beam theory for pile domain discretization is computationally more efficient than the finite difference approximation adopted in the analysis of Banerjee & Driscoll (1976).

### 2.4.3 Solution of the pile-soil system

In order to couple these equations for the pile domain (2.5) with those for the soil domain (2.3), compatibility and equilibrium at the pile-soil interface must be invoked. The equilibrium condition implies that the tractions acting on the soil are equal and opposite to the tractions acting on the pile:

$$\{t_s\} = -\{t_p\} \quad (2.6)$$

Compatibility at the pile-soil interface implies that the displacements of the soil are equal to the displacements of the pile:

$$\{u_s\} = \{u_p\} \quad (2.7)$$

If the conditions of equilibrium (2.6) and compatibility (2.7) are substituted into the Equation (2.3) for the soil domain, Equations (2.3) and (2.5) can be combined and the following set of  $m(2N+1)$  simultaneous linear equations can then be written for the group of  $m$  piles:

$$\{t_p\} = -[G_p + G_s]^{-1} \{B\} \quad (2.8)$$

where

$\{t_p\}$  = column vector of pile tractions due to unit boundary conditions of size  $(m \times M)$ ,

$M$  =  $(2N+1)$  is the total number of elements per pile,

$[G_p + G_s]$  = fully populated  $(m \times M) \times (m \times M)$  square flexibility matrix of the group,

$\{B\}$  = column vector of unit boundary conditions of size  $(m \times M)$ .

The assembly of the global flexibility matrix  $[G_p + G_s]$  for a group of  $m = 2$  piles with a number  $N$  of pile shaft elements (per pile) can be described by the following expression:

$$[G_p + G_s] = \begin{bmatrix} (G_p^{aa})_{1,1} + (G_s^{aa})_{1,1} & (G_s^{aa})_{1,1} & (G_s^{aa})_{1,2} & (G_s^{aa})_{1,2} \\ (G_s^{ta})_{1,1} & (G_p^{tt})_{1,1} + (G_s^{tt})_{1,1} & (G_s^{ta})_{1,2} & (G_s^{tt})_{1,2} \\ (G_s^{aa})_{2,1} & (G_s^{aa})_{2,1} & (G_p^{aa})_{2,2} + (G_s^{aa})_{2,2} & (G_s^{aa})_{2,2} \\ (G_s^{ta})_{2,1} & (G_s^{tt})_{2,1} & (G_s^{ta})_{2,2} & (G_p^{tt})_{2,2} + (G_s^{tt})_{2,2} \end{bmatrix} \quad (2.9)$$

where

- $(G_p^{aa})_{1,1}$  = single-pile submatrix, of size  $(N+1) \times (N+1)$ , of flexibility coefficients relating axial displacements and axial tractions of pile 1 for pile domain,
- $(G_s^{aa})_{1,1}$  = single-pile submatrix, of size  $(N+1) \times (N+1)$ , of soil flexibility coefficients relating axial displacements and axial tractions of pile 1,
- $(G_s^{aa})_{1,2}$  = single-pile submatrix, of size  $(N+1) \times N$ , of soil flexibility coefficients relating axial displacements and transverse tractions of pile 1,
- $(G_s^{ta})_{1,1}$  = single-pile submatrix, of size  $N \times (N+1)$ , of soil flexibility coefficients relating transverse displacements and axial tractions of pile 1,
- $(G_p^{tt})_{1,1}$  = single-pile submatrix, of size  $N \times N$ , of flexibility coefficients relating transverse displacements and transverse tractions of pile 1 for pile domain,
- $(G_s^{tt})_{1,1}$  = single-pile submatrix, of size  $N \times N$ , of soil flexibility coefficients relating transverse displacements and transverse tractions of pile 1,
- $(G_s^{aa})_{1,2}$  = interaction submatrix, of size  $(N+1) \times (N+1)$ , of soil flexibility coefficients expressing axial displacements of pile 1 due to axial tractions on pile 2,

- $(G_s^{at})_{1,2}$  = interaction submatrix, of size  $(N+1) \times N$ , of soil flexibility coefficients expressing axial displacements of pile 1 due to transverse tractions on pile 2,
- $(G_s^{ta})_{1,2}$  = interaction submatrix, of size  $N \times (N+1)$ , of soil flexibility coefficients expressing transverse displacements of pile 1 due to axial tractions on pile 2,
- $(G_s^{tt})_{1,2}$  = interaction submatrix, of size  $N \times N$ , of soil flexibility coefficients expressing transverse displacements of pile 1 due to transverse tractions on pile 2.

The average coefficients of the single-pile flexibility submatrices  $(G_s^{at})_{1,1}$ ,  $(G_s^{ta})_{1,1}$ ,  $(G_s^{at})_{2,2}$  and  $(G_s^{tt})_{2,2}$  are of the order of  $10^{-4}$  times the average coefficients of the remaining submatrices (see, for example, Banerjee & Driscoll, 1977). Thus, in the present analysis, these submatrices can be assumed to be zeros without introducing any serious errors. This physically means that, in the evaluation of the single pile response, the contribution of axial displacements due to transverse tractions and transverse displacements due to axial tractions can be ignored.

The analysis described above needs prescribed displacements of the pile cap. However, for most problems, it is the loading that is specified. Therefore we need to establish the relationship between the displacements of the cap and the applied loading. This can be accomplished by successively applying unit vertical displacement  $w$ , unit horizontal displacement  $u$  and unit rotation  $\theta$  to the pile cap with the corresponding rigid body displacements of the pile group  $\{B\}$  as shown in Fig. 2.3, and calculating the vertical load, horizontal load and moments necessary to equilibrate the system of stresses developed. In practice, the unit vertical displacement, the unit horizontal displacement and the unit rotation problems are solved independently, so that  $\{t_p\}$  and  $\{B\}$  are represented by three column vectors (one for each unit boundary condition). Thus, Equation (2.8) can be written as:

$$\{t_p^k\} = -[G_p + G_s]^{-1} \{B^k\} \quad (2.10)$$

where

- $\{t_p^k\}$  = three vectors, each of size  $(m \times M)$ , of unknown pile tractions due to unit vertical displacement, unit horizontal displacement and unit rotation of the pile cap,
- $k$  = 1, 2, 3 (it represents the three unit boundary conditions),
- $[G_p + G_s]$  = fully populated  $(m \times M) \times (m \times M)$  square flexibility matrix of the pile group,
- $\{B^k\}$  = three vectors, each of size  $(m \times M)$ , of unit vertical displacement, unit horizontal displacement and unit rotation of the pile cap.

In order to obtain the pile tractions, the system of Equations (2.10) may be solved using a direct LU decomposition approach. Integrating the axial and transverse tractions, yields the distribution of pile head axial and shear forces and moments (due to unit boundary conditions):

$$\begin{aligned} F_a^k &= \sum_{i=1}^{N+1} A_{ai} t_{ai}^k \\ F_t^k &= \sum_{i=1}^N A_{ti} t_{ti}^k \\ M_t^k &= \sum_{i=1}^N A_{ti} t_{ti}^k z_i \end{aligned} \quad (2.11)$$

where

- $F_a^k$  = pile head axial force due to unit boundary conditions,
- $F_t^k$  = pile head shear force due to unit boundary conditions,
- $M_t^k$  = pile head moment due to unit boundary conditions,
- $N$  = number of pile shaft elements per pile,
- $A_{ai}$  = shaft area of the pile element  $i$ ,

- $t_{ai}^k$  = pile axial tractions acting on element  $i$  due to unit boundary conditions,  
 $A_{ti}$  = transverse area of the pile element  $i$ ,  
 $t_{ti}^k$  = pile transverse tractions acting on element  $i$  due to unit boundary conditions,  
 $z_i$  = depth of the centre of pile element  $i$ .

The set of Equations (2.11) can be written for each pile. Then, in order to obtain the system of vertical loads  $V^k$ , horizontal loads  $H^k$  and moments  $M^k$  acting on the cap that are necessary to equilibrate the stresses developed in the piles, the sum of the vertical and horizontal components of the pile head axial and shear forces and moments of each pile is performed, yielding:

$$\begin{aligned}
 V^k &= \sum_{j=1}^m (F_a^k \cos \phi + F_t^k \sin \phi) = S_{1k} \\
 H^k &= \sum_{j=1}^m (-F_a^k \sin \phi + F_t^k \cos \phi) = S_{2k} \\
 M^k &= \sum_{j=1}^m (M_i^k + V^k \times (c - g \tan \phi) - H^k \times g) = S_{3k}
 \end{aligned} \tag{2.12}$$

where

- $V^k$  = vertical load acting on the cap due to unit boundary conditions,  
 $H^k$  = horizontal load acting on the cap due to unit boundary conditions,  
 $M^k$  = moment acting on the cap due to unit boundary conditions,  
 $\phi$  = angle of rake of the pile,  
 $c$  = horizontal distance of the pile head from the vertical axis of symmetry of the pile cap,  
 $g$  = depth of overhang of the pile cap,  
 $m$  = number of piles in the group.

Thus, if an external loading system  $V$ ,  $H$  and  $M$  is acting on the cap, the corresponding vertical displacement  $w$ , horizontal displacement  $u$  and rotation  $\theta$  of the cap are related via:

$$\begin{Bmatrix} V \\ H \\ M \end{Bmatrix} = \begin{bmatrix} S_{11} & S_{12} & S_{13} \\ S_{21} & S_{22} & S_{23} \\ S_{31} & S_{32} & S_{33} \end{bmatrix} \begin{Bmatrix} w \\ u \\ \theta \end{Bmatrix} \quad (2.13)$$

where the coefficients  $S_{ik}$  of the  $(3 \times 3)$  matrix represent the system of equilibrating forces as discussed previously. The matrix  $[S]$  can be described as the global stiffness matrix of the pile group system which may be used as boundary conditions to the analysis of superstructures. By inverting the  $[S]$  matrix, it is possible to obtain the global flexibility matrix  $[F]$  of the pile group system and hence the vertical displacement, the horizontal displacement and rotation of the pile cap may be obtained for any loading condition:

$$\begin{Bmatrix} w \\ u \\ \theta \end{Bmatrix} = \begin{bmatrix} f_{11} & f_{12} & f_{13} \\ f_{21} & f_{22} & f_{23} \\ f_{31} & f_{32} & f_{33} \end{bmatrix} \begin{Bmatrix} V \\ H \\ M \end{Bmatrix} \quad (2.14)$$

where

$w, u, \theta = (3 \times 1)$  vector of vertical displacement, horizontal displacement and rotation of the pile cap,

$[F] = (3 \times 3)$  global flexibility matrix of the pile group system,

$V, H, M = (3 \times 1)$  vector of external loads and moments acting on the pile cap.

By virtue of Maxwell's reciprocal theorem, the  $(3 \times 3)$  global flexibility matrix  $[F]$  of Equation (2.14) must be symmetric. Also, for symmetrical vertical pile groups, it must be  $f_{12} = f_{21} = f_{31} = f_{13} \cong 0$ , indicating that the interaction between vertical and horizontal loads is negligible. However, for non-symmetrical pile groups, there is considerable interaction between these loadings (Banerjee & Driscoll, 1976).

In order to obtain the real tractions acting on the piles, pile tractions due to unit boundary conditions from Equation (2.10) must be scaled by a factor represented by the vector of vertical displacement  $w$ , horizontal displacement  $u$  and rotation  $\theta$  of the cap

obtained from Equation (2.14). Therefore, for each pile, axial and transverse tractions can be expressed as:

$$\begin{aligned} t_a^i &= t_{ai}^1 w + t_{ai}^2 u + t_{ai}^3 \theta \\ t_t^i &= t_{ti}^1 w + t_{ti}^2 u + t_{ti}^3 \theta \end{aligned} \quad (2.15)$$

where

- $t_a^i$  = pile axial tractions acting on element  $i$ ,
- $t_{ai}^k$  = pile axial tractions acting on element  $i$  due to unit vertical displacement, unit horizontal displacement and unit rotation of the pile cap ( $k = 1, 2, 3$ ),
- $w, u, \theta$  = vertical displacement, horizontal displacement and rotation of the cap,
- $t_t^i$  = pile transverse tractions acting on element  $i$ ,
- $t_{ti}^k$  = pile transverse tractions acting on element  $i$  due to unit vertical displacement, unit horizontal displacement and unit rotation of the pile cap ( $k = 1, 2, 3$ ).

Finally, integrating the axial and transverse tractions acting on the piles, yields the values of the axial forces  $F_a$ , shear forces  $F_t$  and bending moments  $M_t$  acting at the top of each element  $i$  for each pile:

$$\begin{aligned} F_a^i &= F_a^{i+1} + A_a^i t_a^i \\ F_t^i &= F_t^{i+1} + A_t^i t_t^i \\ M_t^i &= M_t^{i+1} - A_t^i t_t^i \times \frac{h^i}{2} - F_t^{i+1} \times h^i \end{aligned} \quad (2.16)$$

where

- $F_a^i$  = axial forces acting at the top of pile element  $i$ ,
- $F_t^i$  = shear forces acting at the top of pile element  $i$ ,

$M_i^i$  = bending moments acting at the top of pile element  $i$ ,

$h^i$  = height of the pile element  $i$  (given by  $L_j$  divided by  $N$ , where  $L_j$  is the length of pile  $j$  and  $N$  is the number of pile shaft elements per pile).

#### 2.4.4 Limit stresses

It is assumed that the elastic equations described above are valid until the tractions on the pile-soil interface reach certain limiting values (Poulos, 1980b; Davies & Budhu, 1986; Lee, 1997). For cohesive soils, the limiting bearing stress on the compressive zone (ie the pile base for the axial response and the pile shaft for the lateral response) can be expressed as:

$$t_{sc} = N_c C_u \quad (2.17)$$

while the limiting shear stress ('skin friction') in the slip zone (ie the pile shaft for the axial response) is taken as:

$$t_{ss} = \alpha C_u \quad (2.18)$$

where

$N_c$  is the bearing capacity factor,

$C_u$  is the undrained shear strength,

$\alpha$  is an empirical adhesion factor.

A distinction should be made about the choice of the appropriate value of the bearing capacity factor ( $N_c$ ). As regards the evaluation of the end-bearing pressure beneath the pile,  $N_c$  may be assumed to be equal to 9 for depths relevant for piles. This value has been confirmed in tests in London Clay (Skempton, 1959) and is widely accepted in practice (eg Fleming *et al.*, 1992; Tomlinson, 1994). In evaluating the limiting lateral pressure, the bearing capacity factor ( $N_c$ ) is assumed to increase linearly from 2 at the surface to a constant value of 9 at a depth of 3 pile diameters and below, much as was originally

suggested by Broms (1964). This assumption is made to avoid the introduction of additional soil parameters which are included in more sophisticated solutions (eg Matlock, 1970; Randolph & Houlsby, 1984). In many cases, however, the suggested values for the limiting lateral pressure lead to a profile of  $N_c$  which corresponds to that adopted in the present analysis (Fleming *et al.*, 1992).

Methods of estimating the adhesion factor ( $\alpha$ ) and the undrained shear strength ( $C_u$ ) for use in Equations (2.17) and (2.18) are discussed in Section 6.3.

#### 2.4.5 Extension to non-linear soil behaviour

The linear elastic analysis described above can be extended to include non-linear effects by generalising an idea first proposed by Poulos & Davis (1968) and applied to pile foundation problems by Poulos (1980b), Chow (1986a), Chow (1987c), Davies & Budhu (1986) and Lee (1997). In the present analysis, the boundary element equations used for the linear response are solved incrementally while enforcing the conditions of yield, equilibrium and compatibility at the pile-soil interface.

##### 2.4.5.1 Current analysis

Since the pile is assumed to remain elastic during loading, the pile flexibility matrix  $[G_p]$  is unaltered. It is possible to incorporate the effects of soil yielding, in an approximate manner, by assuming that the interface behaviour at an element is perfectly linear until the stresses on the pile surface equal certain limiting values (determined from Equations (2.17) and (2.18)). For these elements which have gone plastic, no more increment in tractions is permitted. This can be accomplished by applying the external load incrementally so that the soil flexibility matrix  $[G_s]$  changes as one or more elements reach the yield conditions. The remaining elastic elements are those given by the Mindlin's solution and there is no further interaction through the soil between these elements and the yielded elements in the pile group. It may be noted that the manner in which the non-linear response of the pile group is obtained is approximate. In fact, the yielding of an element introduces a discontinuity in the material property. Thus, the use of Mindlin's solution to determine the remaining elastic flexibility coefficients is only approximate.

It should be emphasised that this method enforces load transfer to the elastic elements in that the element which has failed can take no additional load and the increase in load is thus redistributed between the remaining elastic elements until all elements have failed. This procedure will generate a load-deformation curve to failure as yielding along the pile-soil interface progresses.

Thus, the non-linear (elasto-plastic) response of the group may be obtained by casting the linear equations described in the previous sections in incremental form (as indicated by the superposed dot) and solving using small load increments, as depicted in Fig. 2.4.

### Soil domain

Assuming purely elastic soil behaviour, Equation (2.3) becomes:

$$\left\{ \dot{u}_s \right\} = [G_s] \left\{ \dot{t}_s \right\} \quad (2.19)$$

where

$\left\{ \dot{u}_s \right\}$  = column vector of incremental soil displacements of size  $M$ ,

$\left\{ \dot{t}_s \right\}$  = column vector of incremental soil tractions of size  $M$ ,

$[G_s]$  = elastic soil flexibility matrix, of size  $M \times M$ , obtained from Mindlin's solution,

$M$  =  $(2N+1)$  is the total number of elements per pile,

$N$  = number of pile shaft elements per pile.

As one or more elements at the interface reach the yield conditions at the end of an increment, the elastic soil flexibility matrix  $[G_s]$  will be altered. In this case, there will be no dependence of the soil displacements of the remaining elastic elements  $\left\{ \dot{u}_s^e \right\}$  on the soil tractions of the yielded elements  $\left\{ \dot{t}_s^n \right\}$ , ie  $\left\{ \dot{t}_s^n \right\} = 0$  (where the superposed 'e' and 'n' indicate elastic and non-linear conditions, respectively). In addition, it is assumed that the

elastic soil flexibility submatrix  $[G_s^{ee}]$ , ie the submatrix formed by the remaining elastic coefficients, is unaltered by yielding of other elements (ie these coefficients are still calculated from the elastic solution of Mindlin). Thus, the elastic soil displacements  $\left\{ \dot{u}_s^e \right\}$  may be written as:

$$\left\{ \dot{u}_s^e \right\} = [G_s^{ee}] \left\{ \dot{t}_s^e \right\} \quad (2.20)$$

where

$L$  = number of elements which have yielded in a pile,

$\left\{ \dot{u}_s^e \right\}$  = column vector of incremental elastic soil displacements of size  $(M-L)$ ,

$[G_s^{ee}]$  =  $(M-L) \times (M-L)$  square flexibility submatrix of coefficients corresponding to those soil elements which remain elastic,

$\left\{ \dot{t}_s^e \right\}$  = column vector of incremental elastic soil tractions of size  $(M-L)$ .

### Pile domain

Since the pile is assumed to remain elastic during loading, the pile flexibility matrix of Equation (2.5) is unaltered (ie  $[G_p]$  is an elastic matrix). However, for convenience, in order to relate the soil and the pile matrices,  $[G_p]$  may be partitioned as follows (eg Lee, 1997):

$$\begin{Bmatrix} \dot{u}_p^e \\ \dot{u}_p^n \end{Bmatrix} = \begin{bmatrix} G_p^{ee} & G_p^{en} \\ G_p^{ne} & G_p^{nn} \end{bmatrix} \begin{Bmatrix} \dot{t}_p^e \\ \dot{t}_p^n \end{Bmatrix} + \begin{Bmatrix} \dot{B}^e \\ \dot{B}^n \end{Bmatrix} \quad (2.21)$$

where

$\left\{ \dot{u}_p^e \right\}$  = column vector, of size  $(M-L)$ , of incremental pile displacements

corresponding to the elastic soil elements,

$\left\{ \dot{u}_p^n \right\}$  = column vector, of size  $L$ , of incremental pile displacements corresponding

to the plastic soil elements,

$[G_p^{ee}]$  = pile flexibility submatrix, of size  $(M-L) \times (M-L)$ , of coefficients

corresponding to the elastic soil elements,

$[G_p^{ne}]$  = pile flexibility submatrix, of size  $L \times (M-L)$ , of coefficients corresponding

to the plastic soil elements,

$[G_p^{en}]$  = pile flexibility submatrix, of size  $(M-L) \times L$ , of coefficients corresponding

to the plastic soil elements,

$[G_p^{nn}]$  = pile flexibility submatrix, of size  $L \times L$ , of coefficients corresponding to

the plastic soil elements,

$\left\{ \dot{t}_p^e \right\}$  = column vector, of size  $(M-L)$ , of incremental pile tractions corresponding

to the elastic soil elements,

$\left\{ \dot{t}_p^n \right\}$  = column vector, of size  $L$ , of incremental pile tractions corresponding to

the plastic soil elements,

$\left\{ \dot{B}^e \right\}$  = column vector, of size  $(M-L)$ , of incremental pile displacements (due to

unit boundary displacements and rotation of the cap) corresponding to the elastic soil elements,

$\left\{ \dot{B}^n \right\}$  = column vector, of size  $L$ , of incremental pile displacements (due to unit

boundary displacements and rotation of the cap) corresponding to the plastic soil elements.

### *Solution of the pile-soil system*

The non-linear response of the group may be obtained by coupling the equations describing the non-linear load-displacement behaviour of the soil with the linear elastic equations describing the pile behaviour. In order to couple these equations for the pile domain (2.21) with those for the soil domain (2.20), compatibility and equilibrium at the elastic pile-soil interfaces must be invoked while enforcing the yield conditions.

After each load increment, if the stress state in the soil violates the limiting stresses, then elastic equations are no longer valid and an elasto-plastic solution of the problem has to be formulated. Soil yielding can be reached in one or more elements at the pile-soil interface if, at any increment, the soil tractions equal the limiting values defined in Equations (2.17) and (2.18):

$$t_s = t_{sy} \quad (2.22)$$

where

$t_s$  = soil tractions,

$t_{sy}$  = limiting stresses defined in Equations (2.17) and (2.18).

This check of soil tractions must be done for each element of the pile, and those elements in which the yield criteria are satisfied can be regarded as plastic or yielded.

Equilibrium condition at the pile-soil interface implies that the tractions acting on the soil are equal and opposite to the tractions acting on the pile:

$$\left\{ \dot{t}_p^e \right\} = - \left\{ \dot{t}_s^e \right\} \quad (2.23)$$

$$\left\{ \dot{t}_p^n \right\} = - \left\{ \dot{t}_s^n \right\} = 0 \quad (2.24)$$

where Equation (2.24) shows that, for those elements which have gone plastic, no more increment in tractions is permitted.

Compatibility at the pile-soil interface implies that the soil displacements are equal to the pile displacements:

$$\left\{ \dot{u}_p^e \right\} = \left\{ \dot{u}_s^e \right\} \quad (2.25)$$

$$\left\{ \dot{u}_p^n \right\} \neq \left\{ \dot{u}_s^n \right\} \quad (2.26)$$

where Equation (2.26) shows that compatibility condition for the yielded elements is no longer satisfied as the plastic soil displacements are undetermined (ie there are no unique solutions).

Thus, invoking Equation (2.24), Equation (2.21) may be rewritten as follows:

$$\left\{ \dot{u}_p^e \right\} = [G_p^{ee}] \left\{ \dot{t}_p^e \right\} + \left\{ \dot{B}^e \right\} \quad (2.27)$$

$$\left\{ \dot{u}_p^n \right\} = [G_p^{ne}] \left\{ \dot{t}_p^e \right\} + \left\{ \dot{B}^n \right\} \quad (2.28)$$

If the elastic conditions of equilibrium (2.23) and compatibility (2.25) are substituted into the Equation (2.20) for the soil domain, Equations (2.20) and (2.27) can be combined (in the same way as for the linear elastic analysis), and the following set of simultaneous linear equations can then be written for the group of  $m$  piles:

$$\left\{ \dot{t}_p^e \right\} = -[G_s^{ee} + G_p^{ee}]^{-1} \left\{ \dot{B}^e \right\} \quad (2.29)$$

where  $[G_s^{ee} + G_p^{ee}]$ , which is a square matrix of size  $m(M-L) \times m(M-L)$  (where  $L$  is the number of soil elements which has gone plastic), represents the global flexibility matrix of the pile group. This set of equations may be regarded as the non-linear (elasto-plastic) equivalent of the linear elastic set of Equations (2.8). It is worth noting that, having solved

Equation (2.29) for  $\left\{ \dot{t}_p^e \right\}$ , the pile displacements corresponding to the yielded soil elements  $\left\{ \dot{u}_p^n \right\}$  may be evaluated using Equation (2.28).

In order to keep the size of the global flexibility matrix of the pile group used in Equation (2.29) equal to the full elastic size  $(m \times M) \times (m \times M)$ , the PGROUPN analysis solves the non-linear problem by setting the appropriate rows and columns (ie those corresponding to the soil elements which have yielded) in the elastic global flexibility matrix  $[G_p + G_s]$  (from Equation (2.8)) to zero. This procedure, which results in  $\left\{ \dot{t}_p^n \right\} = 0$ , is the equivalent of solving Equation (2.29).

It should be emphasised that, in the same way as for the elastic analysis, the incremental pile tractions  $\left\{ \dot{t}_p^e \right\}$  from Equation (2.29) are due to unit boundary conditions (ie vertical displacement, horizontal displacement and rotation of the cap), and hence  $\left\{ \dot{t}_p^e \right\}$  and  $\left\{ B^e \right\}$  are represented by 3 column vectors (one for each unit boundary condition).

From Equation (2.29), by following a procedure similar to the elastic algorithm (described in Equations (2.11) to (2.15)), it is possible to calculate the 'real' increment (ie not due to unit boundary conditions) in pile tractions  $\dot{t}_{pi}^j$ . The current (resultant) axial and transverse tractions acting on the element  $i$  of each pile can then be calculated by summation, yielding:

$$t_i = \sum_{j=1}^J \dot{t}_i^j \quad (2.30)$$

where

$t_i$  = current axial and transverse tractions acting on pile element  $i$ ,

$\dot{t}_i^j$  = incremental axial and transverse tractions acting on pile element  $i$  at the

load increment  $j$ ,

$J$  = current total number of load increments ( $J = 1, NINC$ ),

$NINC$  = total number of load increments.

In the same way, at the end of each increment, the current displacements and rotation of the pile cap and the current forces and moments acting on piles are computed by updating these values from the data for the previous increment.

#### 2.4.5.2 Approach by Davies & Budhu (1986)

A similar approach has been applied to single piles under static lateral loading by Davies & Budhu (1986) and then extended to the case of cyclic loading by Lee (1997). The essence of the method is described below.

##### *Soil domain*

As one or more elements at the pile-soil interface reach the yield conditions (ie the limiting stresses) at the end of an increment, the non-linear (elasto-plastic) relationship between soil displacements and soil tractions is written:

$$\begin{Bmatrix} \dot{u}_s^e \\ \dot{u}_s^n \end{Bmatrix} = \begin{bmatrix} G_{s^*}^{ee} & G_{s^*}^{en} \\ G_{s^*}^{ne} & G_{s^*}^{nn} \end{bmatrix} \begin{Bmatrix} \dot{t}_s^e \\ \dot{t}_s^n \end{Bmatrix} \quad (2.31)$$

where

$M$  = total number of elements for a pile,

$L$  = number of elements which have yielded in a pile,

$\begin{Bmatrix} \dot{u}_s^e \end{Bmatrix}$  = column vector of incremental elastic soil displacements of size  $(M-L)$ ,

$\begin{Bmatrix} \dot{u}_s^n \end{Bmatrix}$  = column vector of incremental plastic soil displacements of size  $L$ ,

$[G_{s^*}]$  = non-linear (elasto-plastic) soil flexibility matrix, of size  $M \times M$

(where (\*) denotes that this matrix is different from the elastic soil flexibility matrix  $[G_s]$ ),

$\left\{ \begin{smallmatrix} \bullet \\ t_s^e \end{smallmatrix} \right\}$  = column vector of incremental elastic soil tractions of size  $(M-L)$ ,

$\left\{ \begin{smallmatrix} \bullet \\ t_s^n \end{smallmatrix} \right\}$  = column vector of incremental plastic soil tractions of size  $L$ .

The non-linear soil flexibility matrix  $[G_{s*}]$  may be obtained by means of the procedure outlined below. At each increment, if the current pile tractions reach the limiting values in one or more elements:

a) Invert the elastic soil flexibility matrix  $[G_s]$  in order to obtain the soil stiffness matrix  $[K_s] = [G_s]^{-1}$ ;

b) Set the rows and columns (corresponding to the yielded soil elements) of the soil stiffness matrix  $[K_s]$  to zero. In fact, the matrix  $[K_s]$  may be partitioned as follows:

$$\left\{ \begin{smallmatrix} \bullet \\ t_s^e \\ \bullet \\ t_s^n \end{smallmatrix} \right\} = \begin{bmatrix} K_s^{ee} & K_s^{en} \\ K_s^{ne} & K_s^{nn} \end{bmatrix} \left\{ \begin{smallmatrix} \bullet \\ u_s^e \\ \bullet \\ u_s^n \end{smallmatrix} \right\} \quad (2.32)$$

where  $[K_s]$  is the partitioned soil stiffness matrix of size  $M \times M$ .

Invoking Equation (2.24), noting that the plastic soil displacements are arbitrary, and making the assumption that the (incremental) displacement of any single element does not induce traction change at yielded elements, it is possible to write:

$$\begin{aligned} [K_s^{ne}] &= 0 \\ [K_s^{nn}] &= 0 \end{aligned} \quad (2.33)$$

and, invoking symmetry:

$$[K_s^{en}] = 0 \quad (2.34)$$

c) Invoking Equations (2.33) and (2.34), and making the assumption that the elastic stiffness submatrix  $[K_s^{ee}]$  is unaltered by yielding of other elements (ie these coefficients are still calculated from the elastic solution of Mindlin), Equation (2.32) can be written as:

$$\left\{ \dot{t}_s^e \right\} = [K_s^{ee}] \left\{ \dot{u}_s^e \right\} \quad (2.35)$$

It may be noted that, in Equation (2.20) (used in the current analysis described in Section 2.4.5.1), it is the elastic flexibility submatrix  $[G_s^{ee}]$  which remains unchanged, whereas in the approach by Davies & Budhu it is the elastic stiffness submatrix  $[K_s^{ee}]$  which is unaltered. In addition, the Davies & Budhu approach also requires the assumptions described above in Equations (2.33) and (2.34) which are less satisfactory (physically) than those made to write Equation (2.20).

Inverting Equation (2.35) yields:

$$\left\{ \dot{u}_s^e \right\} = [G_s^{ee}] \left\{ \dot{t}_s^e \right\} \quad (2.36)$$

where  $[G_s^{ee}] = [K_s^{ee}]^{-1}$ . In Equation (2.31), it is worth noting that the flexibility submatrices  $[G_{s,s}^{nn}]$ ,  $[G_{s,s}^{ne}]$  and  $[G_{s,s}^{nn}]$  are undetermined terms, as the inverse of zero terms from Equations (2.33) and (2.34) will be infinity. This suggests that the soil displacements for the yielded elements cannot be determined. However, as discussed above, this is not a major concern as the pile displacements corresponding to the yielded soil elements, ie  $\left\{ \dot{u}_p^n \right\}$ , may still be evaluated using Equation (2.28).

*Pile domain*

In the same way as described in Section 2.4.5.1, Equations (2.27) and (2.28) are obtained.

### *Solution of the pile-soil system*

In the same way as described in Section 2.4.5.1, enforcing compatibility and equilibrium at the elastic pile-soil interfaces via Equations (2.23) and (2.25), Equations (2.27) and (2.36) can be coupled to give:

$$\left\{ \dot{r}_p^e \right\} = -[G_{s^e}^e + G_p^e]^{-1} \left\{ \dot{B}^e \right\} \quad (2.37)$$

where  $[G_{s^e}^e + G_p^e]$ , which is a square matrix of size  $m(M-L) \times m(M-L)$  (where  $L$  is the number of soil elements which has gone plastic), represents the global flexibility matrix of the pile group.

It is worth noting the differences between Equation (2.37) and the formulation adopted in the current analysis (Equation (2.29)), ie  $[G_s^e] \neq [G_{s^e}^e]$ . In fact, the term  $[G_s^e]$  simply represents the elastic flexibility submatrix obtained from Mindlin's solution, whereas, in the approach by Davies & Budhu, the term  $[G_{s^e}^e]$  is obtained by inverting the elastic soil flexibility matrix  $[G_s]$  (thus obtaining the corresponding soil stiffness matrix  $[K_s]$ ), deleting the rows and columns of  $[K_s]$  which correspond to the yielded soil elements, and inverting again to obtain  $[G_{s^e}^e]$  for use in Equation (2.37).

However, if the outlined approach of Davies & Budhu is applied to the present problem, this will result, at some load increments, in an increase of the pile group (or single pile) system stiffness (refer to Equation (2.13)) as yielding along the pile-soil interface progresses. This inconsistent behaviour is observed in most of the numerical simulations carried out on single piles under axial loading and pile groups subjected to either vertical or horizontal loads, whereas the load-deflection curves obtained for laterally loaded single piles show a physically plausible trend. Numerical simulations which show these features of behaviour are presented in Section 3.6.

### 2.4.5.3 Modification of the Davies & Budhu approach

It has been found that the approach proposed by Davies & Budhu (1986) may be slightly modified in order to give physically acceptable results, as described below. In this modified formulation, it is assumed that the soil stiffness submatrix  $[K_s^{en}]$  (refer to Equation (2.32)) is not zero (as proposed by Davies & Budhu), but it is still given by the elastic theory. Physically, in the modified formulation, it is assumed that the traction change at any single elastic element due to the (incremental) displacement of any yielded element is still given by the elastic theory, ie the soil stiffness submatrix  $[K_s^{en}]$  is unaffected by yielding within the soil. This assumption corresponds to setting only the appropriate rows in the stiffness soil matrix  $[K_s]$  (of Equation (2.32)) to zero. Making this hypothesis, and following a procedure similar to that described in Section 2.4.5.2, it is possible to obtain a physically tenable load-deformation response for single piles and pile groups under either vertical or horizontal loads.

By comparison, the original approach by Davies & Budhu assumes that  $[K_s^{en}] = 0$  (Equation (2.34)), and this corresponds to setting the appropriate columns in the soil stiffness matrix  $[K_s]$  (of Equation (2.32)) to zero as well as the corresponding rows. This physically implies that, in a general pile group, the (incremental) traction at any single elastic element ( $t_s^e$ ) induced by the (incremental) displacement of any yielded element ( $u_s^n$ ) is neglected. Therefore, in this case, the stiffness soil matrix  $[K_s]$  is simply formed by the elastic submatrix  $[K_s^{ee}]$ , whereas the other submatrices  $[K_s^{en}]$ ,  $[K_s^{ne}]$  and  $[K_s^{nn}]$  (which express the influence of plastic elements) are all zero.

It should be emphasised that the outlined modification to the Davies & Budhu approach takes into account an interaction effect between elastic and plastic soil elements, ie  $[K_s^{en}] \neq 0$ . This implies that, in order to couple the equations for the pile and soil domains, the compatibility condition between plastic pile and soil displacements has to be invoked, ie:

$$\left\{ \dot{u}_p^n \right\} = \left\{ \dot{u}_s^n \right\} \quad (2.38)$$

Equation (2.38) means that no relative movement of pile and soil in the slip or compression zone at the pile-soil interface takes place once the stress state in the soil violates the limiting stresses. Thus, in the outlined modification to the Davies & Budhu approach, the non-linear response is simply obtained by limiting the soil tractions at the pile-soil interface, and there will be no mismatch in the displacements of the pile and soil elements at interfaces which have reached the limiting stress conditions.

However, as already pointed out by other workers (eg Poulos, 1977; Poulos & Davis, 1980; Chow, 1986a), it is more realistic to assume that the compatibility condition will no longer hold for those soil elements where the yield criteria are satisfied. In addition, as observed above, the formulation depicted in Section 2.4.5.1 requires some physical assumptions which are more satisfactory than those employed in either the Davies & Budhu approach or its modified version. Thus, the formulation outlined in Section 2.4.5.1 will be adopted in this thesis.

A comparison of load-deformation curves obtained by adopting the approach put forward in this thesis, the Davies & Budhu approach and the modified Davies & Budhu approach for single piles and pile groups under either axial or lateral loading is presented in Section 3.6.

## 2.5 Concluding remarks

A formulation of the indirect BEM approach for the linear and non-linear analysis of pile groups under general loading conditions has been presented. The analysis is capable of predicting the load-displacement behaviour of a group of piles (which are assumed to be connected by a rigid free-standing cap), and the distribution of stresses, loads and moments in the individual piles of the group.

The proposed solution, which may be regarded as an extension of the linear elastic analysis of Banerjee & Driscoll (1976), presents an incremental procedure to simulate the effects of soil nonlinearity while retaining continuity within the soil through a complete boundary element analysis of the pile group. The analysis models the soil at the interface as

an elastic-perfectly plastic material — by comparison with a purely linear elastic analysis, the present method requires only one additional soil parameter to be completely defined, ie the undrained shear-strength distribution with depth. This parameter is routinely measured in soils investigation. The pile is assumed to remain elastic during loading.

It is believed that the current analysis will remove the limitations of current solutions, whose application is mainly restricted to linear elastic analysis and relatively small pile groups. Further, the proposed method, taking into account the continuous nature of pile-soil interaction, eliminates the uncertainty of empirical load-transfer approaches and provides a simple design tool based on conventional soil parameters.

## Appendix 2.1

### Analytical integration of singular Mindlin's solution

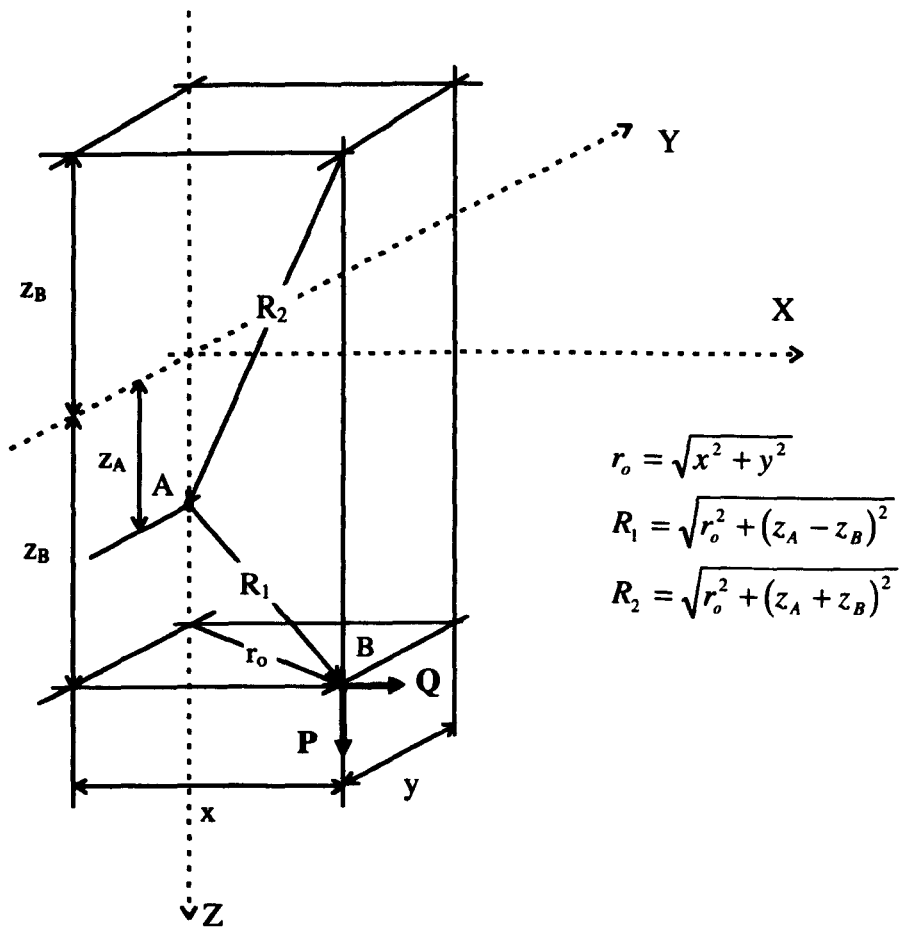


Fig. A2.1-1 Geometry for Mindlin problem.

Mindlin's solution (Mindlin, 1936) is adopted to determine the coefficients of the soil flexibility matrix  $[G_s]$  in Equation (2.3). These flexibility coefficients express the displacement at any point (field point A) within a homogeneous, isotropic elastic half-

space due to a point load acting at any other point (load point  $B$ ), in terms of the coordinates of the load and field points and the elastic properties of the solid, namely, the shear modulus  $G$ , and the Poisson's ratio  $\nu$ , (refer to Fig. A2.1-1).

Mindlin's solution becomes singular whenever the field point  $A$  and the load point  $B$  coincide, ie  $R_1 = 0$ . One of the original features of the analysis put forward in this thesis is the analytical integration of the singular Mindlin functions, which has yielded very accurate results with significant saving of computing time. This represents a significant advance over previous work where these have been integrated numerically (see, for example, Butterfield & Banerjee, 1971a; Banerjee & Driscoll, 1976), since these singular integrals require considerable computing resources, especially for large pile groups.

Integration of Mindlin's equations makes it possible to compute the vertical displacement at the nodal point of each element due to vertical forces distributed uniformly over a cylindrical area (for the pile shaft) and a circular area (for the pile base), and the horizontal displacement at the nodal point of each element due to horizontal forces distributed uniformly over a rectangular area in the  $YZ$  plane. The derivation of these equations, which may have other applications, is presented here in full.

The vertical displacement  $w$  at the nodal point  $A$  caused by a vertical point load  $P$  at  $B$  may be expressed as:

$$w(A) = G(A, B)P(B) \quad (\text{A2.1-1})$$

where  $G(A, B)$  is given by Mindlin's solution:

$$G(A, B) = \frac{1}{16\pi G_s(1-\nu_s)} \left\{ \frac{3-4\nu_s}{R_1} + \frac{8(1-\nu_s)^2 - (3-4\nu_s)}{R_2} + \frac{(z_A - z_B)^2}{R_1^3} \right. \\ \left. + \frac{(3-4\nu_s)(z_A + z_B)^2 - 2z_A z_B}{R_2^3} + \frac{6z_A z_B (z_A + z_B)^2}{R_2^5} \right\} \quad (\text{A2.1-2})$$

For distributed (constant) tractions  $t$  over a surface  $S$ , we obtain:

$$w(A) = t(B) \iint_S G(A, B) dS(B) \quad (\text{A2.1-3})$$

where the axial tractions  $t$  are distributed over a cylindrical shaft area of the pile-soil interface for the pile shaft solution, and over a circular area for the pile base solution.

The singular part  $G^*(A, B)$  of Mindlin's solution may be expressed as:

$$G^*(A, B) = C \left[ \frac{3 - 4\nu_s}{R_1} + \frac{(z_A - z_B)^2}{R_1^3} \right] \quad (\text{A2.1-4})$$

where  $C$  is a constant equal to  $\frac{1}{16\pi G_s(1 - \nu_s)}$ .

#### *Pile shaft solution (vertical response)*

In order to integrate the expression (A2.1-4), it is convenient to choose the origin of coordinates at the nodal point  $A$ , thus:

$$z_A = 0$$

and, for simplicity:

$$z_B = z$$

Thus,  $R_1$  can be expressed as (refer to Fig. (A2.1-1)):

$$R_1 = \sqrt{r_o^2 + z^2}$$

where  $r_o$  represents the pile radius.

Thus, (A2.1-4) becomes:

$$G^*(A, B) = C \left[ \frac{3 - 4\nu_s}{\sqrt{r_o^2 + z^2}} + \frac{z^2}{(r_o^2 + z^2)^{3/2}} \right] \quad (\text{A2.1-5})$$

and the following surface integral has to be evaluated:

$$\iint_S G^*(A, B) dS(B) = C \iint_S \left[ \frac{3 - 4\nu_s}{\sqrt{r_o^2 + z^2}} + \frac{z^2}{(r_o^2 + z^2)^{3/2}} \right] dS(B) \quad (\text{A2.1-6})$$

where  $S$  is the cylindrical surface of the pile shaft element.

The two integrals in (A2.1-6) are evaluated (in polar coordinates) separately.

The first integral yields:

$$\begin{aligned} (3 - 4\nu_s) \iint_S \frac{1}{\sqrt{r_o^2 + z^2}} dS(B) &= (3 - 4\nu_s) \int_0^{2\pi} \int_{-h/2}^{h/2} \frac{1}{\sqrt{r_o^2 + z^2}} r_o dz d\vartheta = \\ &2\pi r_o (3 - 4\nu_s) \left[ \ln \left| z + \sqrt{z^2 + r_o^2} \right| \right]_{-h/2}^{h/2} = \\ &2\pi r_o (3 - 4\nu_s) \left[ \ln \left( \frac{h}{2} + \sqrt{\frac{h^2}{4} + r_o^2} \right) - \ln \left( -\frac{h}{2} + \sqrt{\frac{h^2}{4} + r_o^2} \right) \right] = \\ &2\pi r_o (3 - 4\nu_s) \ln \frac{h + \sqrt{h^2 + 4r_o^2}}{-h + \sqrt{h^2 + 4r_o^2}} = \pi d (3 - 4\nu_s) \ln \frac{h + \sqrt{h^2 + d^2}}{-h + \sqrt{h^2 + d^2}} \end{aligned}$$

where  $h$  is the height of the pile shaft element (which is given by the pile length  $L$  divided by the number of pile shaft elements  $N$ ) and  $d$  is the pile shaft diameter.

The second integral yields:

$$\iint_S \frac{z^2}{(r_o^2 + z^2)^{3/2}} dS(B) = \int_0^{2\pi} \int_{-h/2}^{h/2} \frac{z^2}{(r_o^2 + z^2)^{3/2}} r_o dz d\vartheta = 2\pi r_o \int_{-h/2}^{h/2} \frac{z^2}{(r_o^2 + z^2)^{3/2}} dz$$

This integral can be evaluated by substitution — if we let  $z = r_o \tan \vartheta$ , then:

$$dz = r_o \sec^2 \vartheta d\vartheta$$

Thus:

$$\int_{-h/2}^{h/2} \frac{z^2}{(r_o^2 + z^2)^{3/2}} dz = \int_{-\arctan h/2r_o}^{\arctan h/2r_o} \frac{r_o^2 \tan^2 \vartheta}{(r_o^2 \tan^2 \vartheta + r_o^2)^{3/2}} r_o \sec^2 \vartheta d\vartheta = \int_{-\arctan h/d}^{\arctan h/d} \tan \vartheta \sin \vartheta d\vartheta$$

The above integral can be evaluated by parts — we let:

$$u = \tan \vartheta, \quad dv = \sin \vartheta d\vartheta, \quad du = \sec^2 \vartheta d\vartheta, \quad v = -\cos \vartheta$$

Thus:

$$\begin{aligned} \int_{-\arctan h/d}^{\arctan h/d} \tan \vartheta \sin \vartheta d\vartheta &= [-\cos \vartheta \tan \vartheta]_{-\arctan h/d}^{\arctan h/d} + \int_{-\arctan h/d}^{\arctan h/d} \cos \vartheta \sec^2 \vartheta d\vartheta = \\ &[-\sin \vartheta]_{-\arctan h/d}^{\arctan h/d} + \int_{-\arctan h/d}^{\arctan h/d} \sec \vartheta d\vartheta = -2 \sin \arctan \frac{h}{d} + [\ln |\sec \vartheta + \tan \vartheta|]_{-\arctan h/d}^{\arctan h/d} = \\ &-2 \sin \arctan \frac{h}{d} + \ln \left( \sec \arctan \frac{h}{d} + \frac{h}{d} \right) - \ln \left( \sec \arctan \frac{h}{d} - \frac{h}{d} \right) = \\ &-2 \sin \arctan \frac{h}{d} + \ln \frac{\sec \arctan \frac{h}{d} + \frac{h}{d}}{\sec \arctan \frac{h}{d} - \frac{h}{d}} \end{aligned}$$

It may be observed that there is no need to keep the absolute value as the terms in brackets will be positive.

Thus, the final expression of (A2.1-6) is:

$$\iint_S G^*(A, B) dS(B) = C\pi d \left[ (3 - 4\nu_s) \ln \frac{h + \sqrt{h^2 + d^2}}{-h + \sqrt{h^2 + d^2}} - 2 \sin \arctan \frac{h}{d} + \ln \frac{\sec \arctan \frac{h}{d} + \frac{h}{d}}{\sec \arctan \frac{h}{d} - \frac{h}{d}} \right]$$

### Pile base solution

For a vertical point load acting on the pile base, considering that  $z_A = z_B$ , analytical integration of the singular part  $G^*(A, B)$  of Mindlin's solution (from (A2-1.4)) yields:

$$\iint_S G^*(A, B) dS(B) = C \iint_S \frac{3-4\nu_s}{R_1} dS(B) = C \int_0^{2\pi} \int_0^{r_b} \frac{3-4\nu_s}{R_1} R_1 dR_1 d\vartheta = C\pi d_b (3-4\nu_s)$$

where

$S$  is the circular surface of the pile base element,

$R_1$  is the distance between the field point  $A$  (at the centre of the base element) and the load point  $B$ ,

$r_b$  is the pile base radius,

$d_b$  is the pile base diameter.

### Pile shaft solution (horizontal response)

The horizontal displacement  $u$  at  $A$  caused by a horizontal point load  $Q$  at  $B$  may be expressed as:

$$u(A) = G(A, B)Q(B) \quad (\text{A2.1-7})$$

where  $G(A, B)$  is given by Mindlin's solution:

$$G(A, B) = \frac{1}{16\pi G_s(1-\nu_s)} \left\{ \frac{3-4\nu_s}{R_1} + \frac{1}{R_2} + \frac{x^2}{R_1^3} + \frac{(3-4\nu_s)x^2}{R_2^3} + \frac{2z_A z_B}{R_2^3} \left( 1 - \frac{3x^2}{R_2^2} \right) + \frac{4(1-\nu_s)(1-2\nu_s)}{R_2 + z_A + z_B} \left( 1 - \frac{x^2}{R_2(R_2 + z_A + z_B)} \right) \right\} \quad (\text{A2.1-8})$$

where  $x$  is the distance between  $A$  and  $B$  in the direction of the  $X$  axis.

For distributed (constant) tractions  $t$  over a surface  $S$ , we obtain:

$$u(A) = t(B) \int_S G(A, B) dS(B) \tag{A2.1-9}$$

where the lateral tractions  $t$  are distributed over the idealised rectangular surface on the YZ plane (refer to Fig. A2.1-2).

Considering that on the YZ plane  $x = 0$ , the singular part  $G^*(A, B)$  of Mindlin's solution may be expressed as:

$$G^*(A, B) = C \frac{3 - 4\nu_s}{R_1} \tag{A2.1-10}$$

where  $R_1$  is the distance between the field point  $A$  (at the centre of the rectangular area) and the load point  $B$ . Thus, the following surface integral has to be evaluated:

$$\iint_S G^*(A, B) dS(B) = C(3 - 4\nu_s) \iint_S \frac{1}{R_1} dS(B) \tag{A2.1-11}$$

where  $S$  is the idealised rectangular surface of dimension  $h \times d$ .

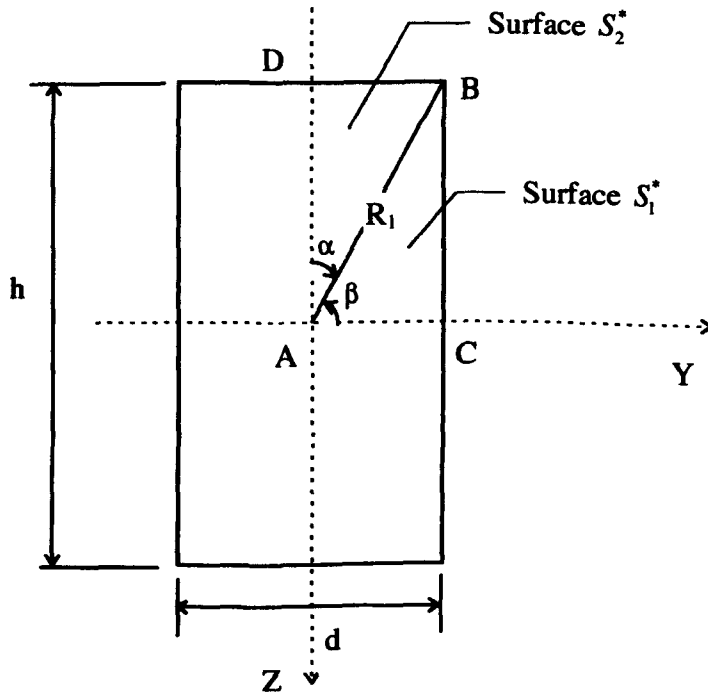


Fig. A2.1-2 Geometry for pile shaft solution (horizontal response).

The integral in (A2.1-11) may be evaluated as the sum of 4 integrals:

$$\iint_S \frac{1}{R_1} dS(B) = 4 \iint_{S^*} \frac{1}{R_1} dS^*(B) \quad (\text{A2.1-12})$$

where  $S^*$  is the rectangular surface ( $ADBC$ ) of dimension  $\frac{h}{2} \times \frac{d}{2}$ .

The integral in (A2.1-12) may be evaluated as the sum of the integrals over the triangular surfaces  $S_1^*$  (the triangle  $ABC$ ) and  $S_2^*$  (the triangle  $ADB$ ), as indicated in Fig. (A2.1-2). Thus, (A2.1-12) becomes:

$$4 \iint_{S^*} \frac{1}{R_1} dS^*(B) = 4 \left[ \iint_{S_1^*} \frac{1}{R_1} dS_1^*(B) + \iint_{S_2^*} \frac{1}{R_1} dS_2^*(B) \right] \quad (\text{A2.1-13})$$

The two integrals in (A2.1-13) are evaluated (in polar coordinates) separately. In the first integral, if we let  $\frac{d}{2} = R_1 \cos \vartheta$  (where  $\vartheta$  varies from zero to  $\beta = \arctan \frac{h}{d}$ ), then:

$$R_1 = \frac{d}{2} \sec \vartheta$$

Thus, the first integral becomes:

$$\begin{aligned} \iint_{S_1^*} \frac{1}{R_1} dS_1^*(B) &= \int_0^\beta \int_0^{R_1(\vartheta)} \frac{1}{R_1} R_1 dR_1 d\vartheta = \int_0^\beta \int_0^{\frac{d}{2} \sec \vartheta} dR_1 d\vartheta = \frac{d}{2} \int_0^\beta \sec \vartheta d\vartheta = \\ &= \frac{d}{2} [\ln |\sec \vartheta + \tan \vartheta|]_0^\beta = \frac{d}{2} \ln (\sec \beta + \tan \beta) = \frac{d}{2} \ln \left( \sec \arctan \frac{h}{d} + \frac{h}{d} \right) \end{aligned}$$

By following a similar procedure, the second integral in (A2.1-13) becomes:

$$\iint_{S_2^*} \frac{1}{R_1} dS_2^*(B) = \frac{h}{2} \ln \left( \sec \arctan \frac{d}{h} + \frac{d}{h} \right)$$

Thus, the final expression of (A2.1-11) is:

$$\iint_S G^*(A, B) dS(B) = 2C(3 - 4\nu_s) \left[ d \ln \left( \sec \arctan \frac{h}{d} + \frac{h}{d} \right) + h \ln \left( \sec \arctan \frac{d}{h} + \frac{d}{h} \right) \right]$$

## Appendix 2.2

### Bernoulli-Euler beam theory

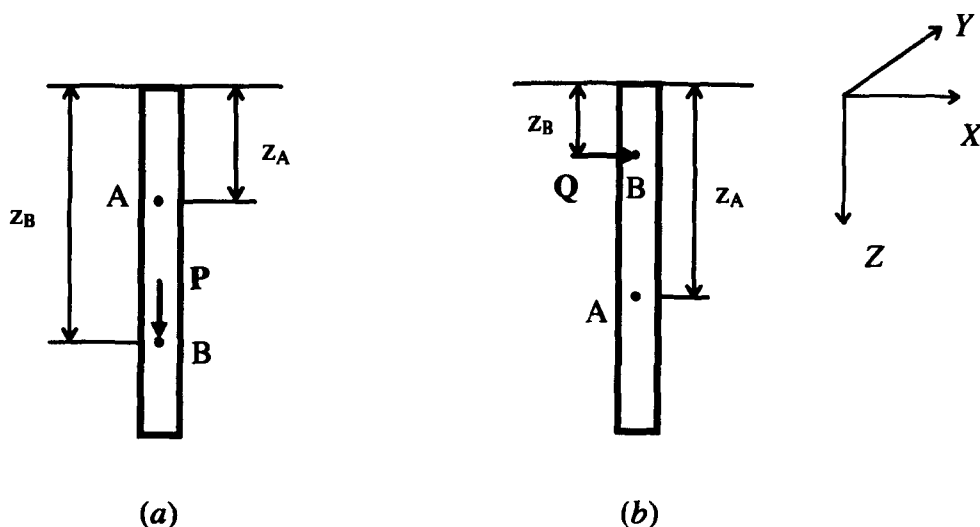


Fig. A2.2-1 Definition of influence function parameters: (a) vertical load, (b) horizontal load.

Bernoulli-Euler beam theory is adopted to determine the pile flexibility matrix  $[G_p]$  (refer to Equation (2.5)) for the axial and flexural response of the pile (see, for example, Ahmad *et al.*, 1985). These flexibility coefficients express the displacement at any point  $A$  due to a point load acting at any other point  $B$ , in terms of the depth coordinates of  $A$  and  $B$  and the Young's modulus  $E_p$  of the pile (refer to Fig. A2.2-1).

Thus, the vertical displacement  $w$  at  $A$  caused by a vertical point load  $P$  at  $B$  may be expressed as:

$$w(A) = G(A, B)P(B) \quad (\text{A2.2-1})$$

where  $G(A, B)$  is an influence function given by the elementary (Bernoulli-Euler) beam theory:

$$G(A, B) = \frac{z_A}{E_p A_p} \quad \text{for } z_A \leq z_B \quad (\text{A2.2-2})$$

$$G(A, B) = \frac{z_B}{E_p A_p} \quad \text{for } z_A \geq z_B \quad (\text{A2.2-3})$$

where  $A_p$  is the cross-sectional area of the pile.

For distributed (constant) tractions  $t$  over a surface  $S$ , we obtain:

$$w(A) = t(B) \int_S G(A, B) dS(B) \quad (\text{A2.2-4})$$

where the axial tractions  $t$  are distributed over a cylindrical shaft element of the pile.

As regards the horizontal response, the horizontal displacement  $u$  at  $A$  caused by a horizontal point load  $Q$  at  $B$  may be expressed as:

$$u(A) = G(A, B)Q(B) \quad (\text{A2.2-5})$$

where  $G(A, B)$  is an influence function given by the elementary (Bernoulli-Euler) beam theory:

$$G(A, B) = \frac{3z_B z_A^2 - z_A^3}{6E_p I_p} \quad \text{for } z_A \leq z_B \quad (\text{A2.2-6})$$

$$G(A, B) = \frac{3z_A z_B^2 - z_B^3}{6E_p I_p} \quad \text{for } z_A \geq z_B \quad (\text{A2.2-7})$$

where  $I_p$  is the second moment of area of the pile.

For distributed (constant) tractions  $t$  over a surface  $S$ , we obtain:

$$u(A) = t(B) \int_S G(A, B) dS(B) \quad (\text{A2.2-8})$$

where the lateral tractions  $t$  are distributed over the idealised rectangular pile element on the YZ plane.

The above integrations are trivial and may be performed analytically.

FIGURES CHAPTER 2

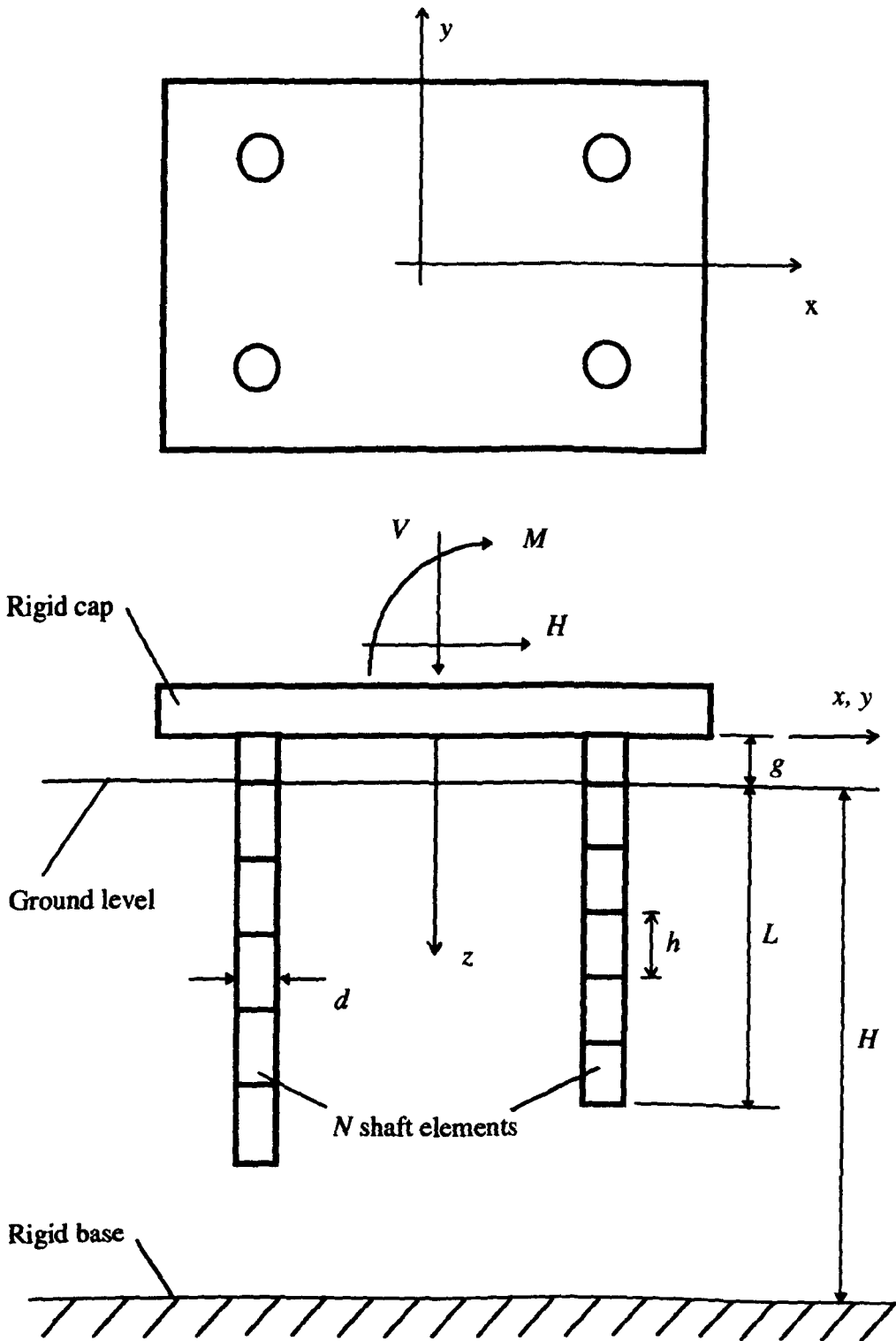


Fig. 2.1 A typical pile group problem.

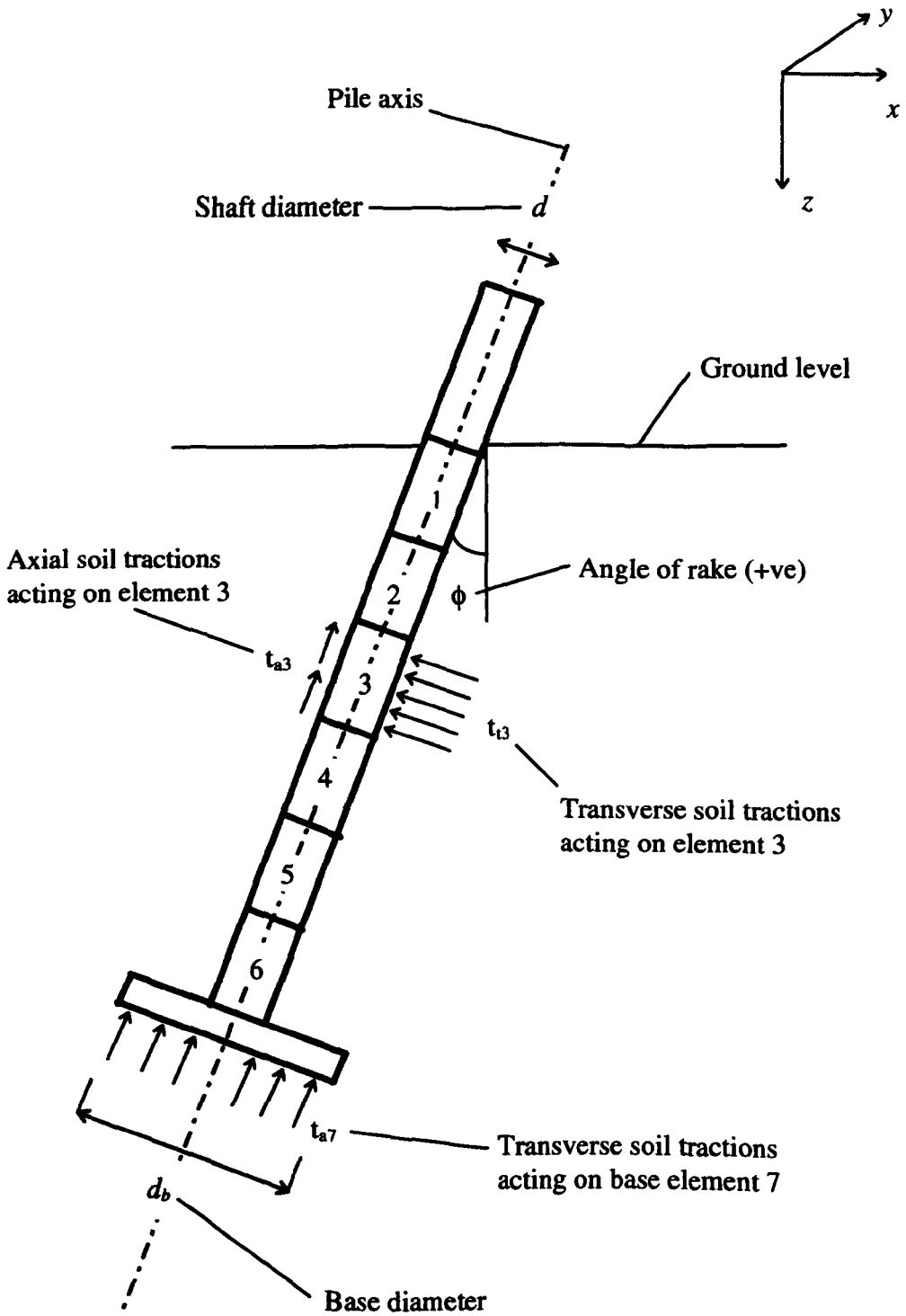


Fig. 2.2 Discretization of the pile-soil interface into  $N = 6$  shaft elements.

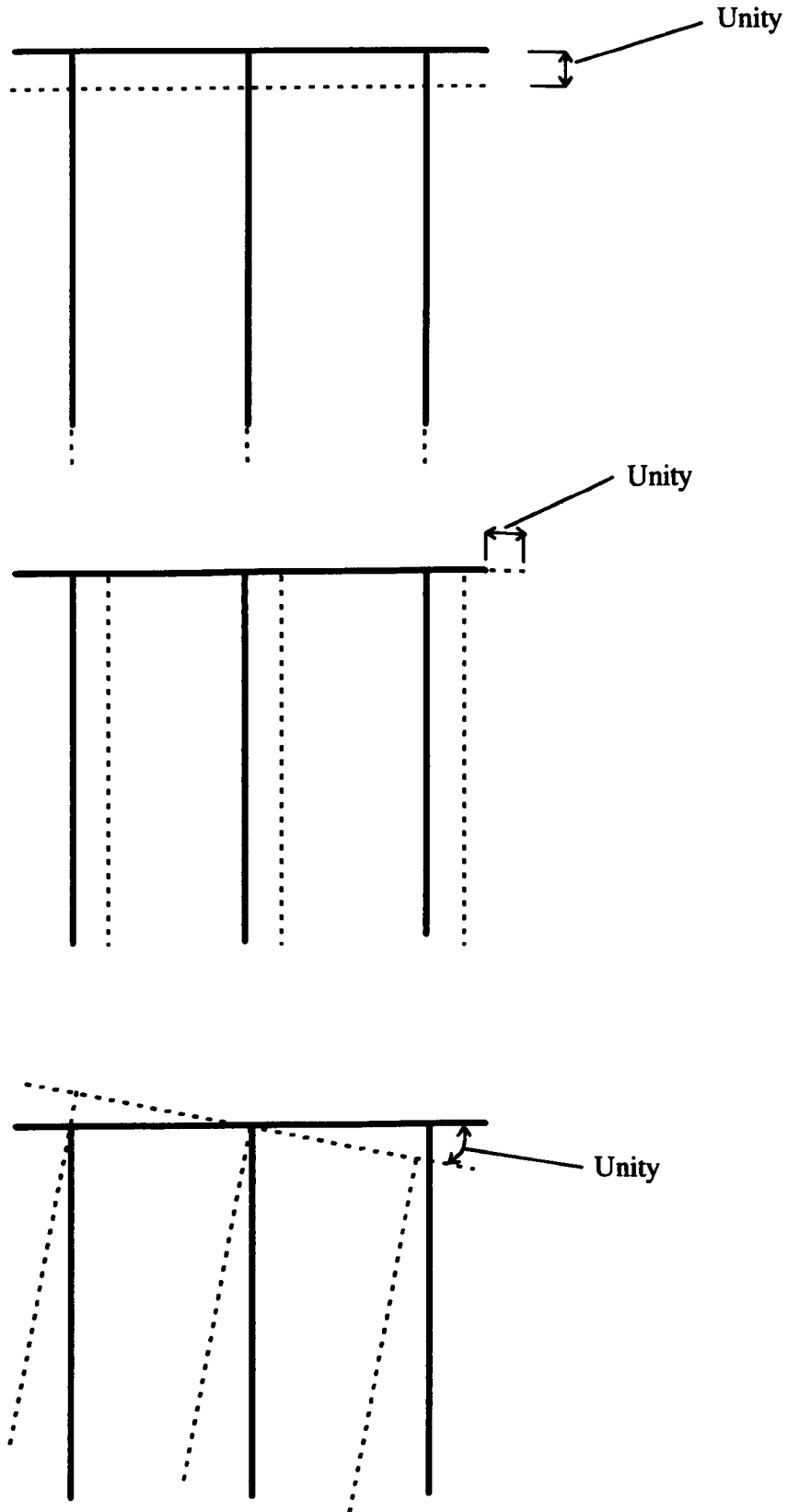


Fig. 2.3 Application of unit boundary displacements and rotation to the pile cap.

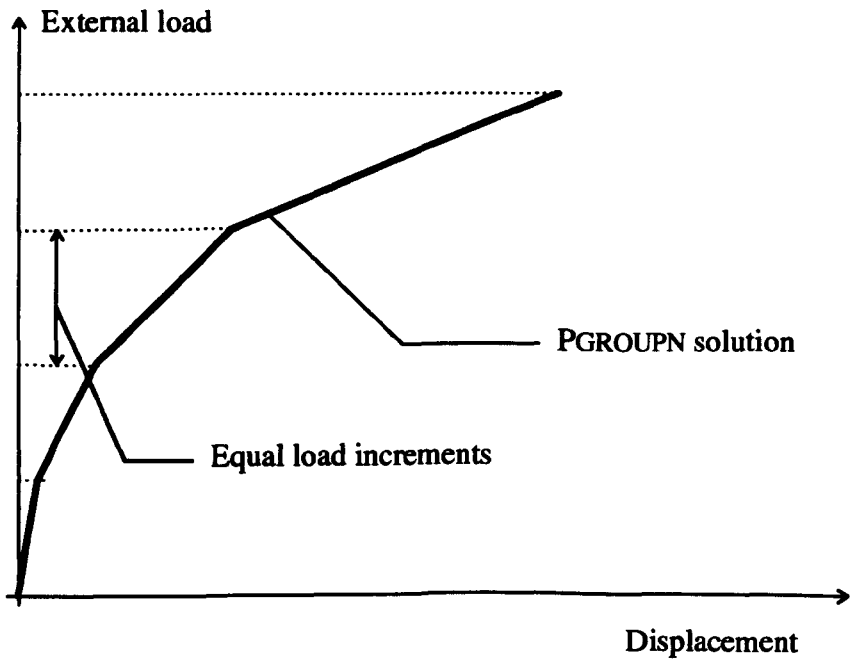


Fig. 2.4 Incremental solution scheme of the PGROUPN analysis.

## CHAPTER 3

### Numerical implementation

#### 3.1 Summary

This Chapter describes the numerical implementation of the non-linear BEM formulation in a computer program called PGROUPN. The computational procedure and the main subroutines involved are presented, together with a description of how to use the program and typical illustrative results.

#### 3.2 Introduction

The incremental BEM solution described in Chapter 2 has been implemented in a numerical code called PGROUPN. The code represents an extension of the computer program PGROUP developed by Banerjee & Driscoll (1976), which has been entirely rewritten in a more efficient way in order to render the analysis of large groups economically viable with an ordinary desktop computer — the main modifications proposed for achieving efficiency gains are summarised in Section 2.2. In addition, non-linear soil response has been introduced by means of a stepwise linear incremental procedure.

The program is intended for the non-linear analysis of pile groups under vertical loads, horizontal loads and moments. The proposed BEM algorithm involves the discretization of the pile-soil interface into elements and the calculation and assembly of the soil and pile flexibility matrices for each pile. By imposing equilibrium and compatibility conditions at the elastic pile-soil interfaces, and checking the state of each element during the loading increment, the stress increments at the pile-soil interface can be determined, and hence the pile displacements, loads and moments can be easily evaluated.

Effects of soil nonlinearity are included, in an approximate manner, by means of a stepwise linear incremental procedure in which the global flexibility matrix  $[G_p + G_s]$

is modified as one or more elements reach the yield conditions. Various strategies are adopted in order to achieve efficiency gains, thereby leading to an economically viable analysis even if nonlinearity effects are simulated in large pile group problems.

### 3.3 General description of the computer program PGROUPN

#### 3.3.1 Scope of the program

The computer program PGROUPN allows for the non-linear analysis of pile groups of large dimensions, embedded in cohesive soils (specifically fully saturated clay under undrained conditions) and subjected to any combination of vertical loads, horizontal loads and moments. The program, given the pile group geometry, the stiffness of the piles, the external loads (ie vertical and horizontal loads and moments) and the surrounding soil conditions (ie the Young's modulus  $E_s$ , the Poisson's ratio  $\nu_s$  and the undrained shear strength  $C_u$ ), will compute the pile head deformations and the distribution of axial force, shear force and bending moment along the individual piles. The program also calculates the overall stiffnesses of the group which can then be used as boundary conditions for the superstructure analysis.

The soil is assumed to behave as an elastic-perfectly plastic material whose stiffness may be constant or may vary linearly with depth (Gibson soil). The influence of a soil layer of finite thickness may be examined. The piles are rigidly fixed to a rigid pile cap (a reasonable assumption in most practical cases) which imposes the same horizontal head displacements and head rotations for all piles, while differential vertical head displacements are solely due to rotation of the rigid cap. Piles may have different geometries (length, external, internal and base diameter) and may be raked in the direction of horizontal loading. Moreover, the pile group may be free-standing, ie an appreciable gap may exist between the pile cap and ground level.

#### 3.3.2 Computational procedure

##### *Sign conventions*

The sign conventions adopted for loads, moments, tractions, displacements and rotations are shown in Fig. 3.1.

### *Procedure*

The computational procedure implemented in the PGROUPN program may be described in terms of the following steps.

#### *Step (1)*

Read all the input data: type of analysis (ie 'Linear' or 'Non-linear'), number  $m$  of piles, number  $n$  of pile types (refer to Section 3.4.6), number  $N$  of pile shaft elements per pile (this must be the same for each pile in the group, irrespective of pile length), number  $NINC$  of equal load increments (only if the type of analysis is 'Non-linear' and hence an incremental procedure is required), pile group geometry, stiffness of the piles, external loads and surrounding soil conditions (refer to Table 3.1).

#### *Step (2)*

If 'Non-linear' analysis is selected, the values of limiting stresses at the nodal points of each element are determined as follows:

*limit bearing stress*

$$t_{sc} = N_c C_u \quad (3.1) \quad (2.17 \text{ bis})$$

*limit shear stress*

$$t_{ss} = \alpha C_u \quad (3.2) \quad (2.18 \text{ bis})$$

where

- $N_c$  is the bearing capacity factor,
- $C_u$  is the undrained shear strength,
- $\alpha$  is an empirical adhesion factor.

### 3.3.2.1 Soil domain

#### *Step (3)*

Set up the fully elastic soil flexibility matrix  $[G_s]$  (see Equation (2.3)) via integration of the Mindlin's solution (Mindlin, 1936). Coefficients of the soil flexibility matrix  $[G_s]$ , which includes the single-pile matrices and the interaction matrices, are calculated for each pile and then assembled in the global soil flexibility matrix of the group. For piles of equal length, diameter and rake, the single-pile soil flexibility matrices need be formed only once and copied into the global soil flexibility matrix corresponding to the identical piles. This reduces the computation time for large groups significantly in that the single-pile flexibility coefficients need not be calculated each time for each of the other identical piles. Further, if a number of piles within a group are identified as behaving in identical fashion (due to symmetries) or approximately identical fashion, then the number  $n$  of pile types can be set at less than the number  $m$  of piles in Step (1) (for further details refer to Section 3.4.6). The size of the global soil flexibility matrix of the group may then be reduced by performing a matrix condensation (as depicted in Fig. 3.2), thereby leading to substantial savings of computing time in the following steps of the analysis (Banerjee & Driscoll, 1976). This will yield a fully populated  $n(2N+1) \times n(2N+1)$  square matrix  $[G_s]$ .

### 3.3.2.2 Pile domain

#### *Step (4)*

Set up the fully populated pile flexibility matrices  $[G_p]$  for each pile type (see Equation (2.5)). Coefficients of  $[G_p]$ , which correspond to the single-pile flexibility matrices, are calculated via integration of the Bernoulli-Euler (beam theory) kernel, with the beam assumed as a circular section, and then assembled in the global pile flexibility matrix of the group. This will yield a  $n(2N+1) \times n(2N+1)$  square matrix  $[G_p]$ . Computation time may be reduced by exploiting similarities in forming the single-pile matrices for piles of equal length and diameter, as described for the soil domain.

### 3.3.2.3 Unit boundary conditions

*Step (5)*

Define the three vectors  $\{B^k\}$ , each of size  $n(2N+1)$ , due to unit vertical displacement, unit horizontal displacement and unit rotation of the pile cap (see Equation (2.10)).

## 3.3.2.4 Solution of the pile-soil system

A stepwise linear incremental procedure (as indicated by the superposed dot) is introduced to simulate the effects of soil nonlinearity. For a purely linear elastic analysis, the number of load increments (*NINC*) is equal to 1.

*Step (6)*

Calculate the incremental pile tractions due to unit boundary conditions by solving the following set of equations via LU decomposition:

$$\left\{ \begin{matrix} \dot{t}_p^k \\ \dot{t}_p^k \end{matrix} \right\} = -[G_p + G_s]^{-1} \left\{ \begin{matrix} \dot{B}^k \\ \dot{B}^k \end{matrix} \right\} \quad (3.3) \quad (2.10 \text{ bis})$$

where

$\left\{ \begin{matrix} \dot{t}_p^k \\ \dot{t}_p^k \end{matrix} \right\}$  = three vectors, each of size  $n(2N+1)$ , of incremental pile tractions due to unit vertical displacement, unit horizontal displacement and unit rotation of the pile cap,

$k$  = 1, 2, 3 (it represents the three unit boundary conditions),

$[G_p + G_s]$  = fully populated  $n(2N+1) \times n(2N+1)$  square flexibility matrix of the pile group,

$\left\{ \begin{matrix} \dot{B}^k \\ \dot{B}^k \end{matrix} \right\}$  = three vectors, each of size  $n(2N+1)$ , of unit vertical displacement, unit horizontal displacement and unit rotation of the pile cap.

It should be emphasised that  $[G_p + G_s]$  is initially a fully populated elastic matrix. The effects of nonlinearity are introduced at Step (16).

*Step (7)*

Separate the incremental pile tractions  $\dot{t}_p^k$  due to unit boundary conditions into axial tractions  $\dot{t}_{ai}^k$  and transverse tractions  $\dot{t}_{ti}^k$ .

*Step (8)*

Integrate the incremental axial/transverse pile tractions obtained from Equation (3.3), thereby leading to the incremental pile head axial/shear forces and moments (due to unit boundary conditions):

$$\begin{aligned}\dot{F}_a^k &= \sum_{i=1}^{N+1} A_{ai} \dot{t}_{ai}^k \\ \dot{F}_t^k &= \sum_{i=1}^N A_{ti} \dot{t}_{ti}^k \\ \dot{M}_t^k &= \sum_{i=1}^N A_{ti} \dot{t}_{ti}^k z_i\end{aligned}\quad (3.4) \quad (2.11 \text{ bis})$$

where

$\dot{F}_a^k$  = three vectors, each of size  $n$ , of incremental pile head axial force due to unit boundary conditions,

$\dot{F}_t^k$  = three vectors, each of size  $n$ , of incremental pile head shear force due to unit boundary conditions,

$\dot{M}_t^k$  = three vectors, each of size  $n$ , of incremental pile head moment due to unit boundary conditions,

$A_{ai}$  = shaft area of the pile element  $i$ ,

$\dot{t}_{ai}^k$  = three vectors, each of size  $n(N+1)$ , of incremental pile axial tractions acting on element  $i$  due to unit boundary conditions,

$A_{ti}$  = transverse area of the pile element  $i$ ,

$\dot{t}_{ti}^k$  = three vectors, each of size  $(n \times N)$ , of incremental pile transverse tractions acting on element  $i$  due to unit boundary conditions,

$z_i$  = depth of the centre of pile element  $i$ .

*Step (9)*

Calculate the system of (incremental) vertical loads  $\dot{V}^k$ , horizontal loads  $\dot{H}^k$  and moments  $\dot{M}^k$  acting on the cap that are necessary to equilibrate the (incremental) stresses developed in the piles. This may be accomplished by summation of the vertical and horizontal components of the pile head axial/shear forces and moments due to unit boundary conditions of each pile:

$$\begin{aligned}\dot{V}^k &= \sum_{j=1}^m (\dot{F}_a^k \cos \phi + \dot{F}_t^k \sin \phi) = \dot{S}_{1k} \\ \dot{H}^k &= \sum_{j=1}^m (-\dot{F}_a^k \sin \phi + \dot{F}_t^k \cos \phi) = \dot{S}_{2k} \\ \dot{M}^k &= \sum_{j=1}^m (\dot{M}_t^k + \dot{V}^k \times (c - g \tan \phi) - \dot{H}^k \times g) = \dot{S}_{3k}\end{aligned}\quad (3.5) \quad (2.12 \text{ bis})$$

where

$\dot{V}^k$  = incremental vertical load acting on the cap due to unit boundary conditions,

$\dot{H}^k$  = incremental horizontal load acting on the cap due to unit boundary conditions,

$\dot{M}^k$  = incremental moment acting on the cap due to unit boundary conditions,

$\phi$  = angle of rake of the pile,

$c$  = horizontal distance of the pile head from the vertical axis of symmetry of the pile cap,

$g$  = depth of overhang of the pile cap (see Fig. 2.1),

$m$  = number of piles in the group.

The coefficients  $\dot{S}_{ik}$  represent the system of (incremental) equilibrating forces discussed above. Therefore, the  $(3 \times 3)$  matrix  $[\dot{S}]$  can be regarded as the (incremental) global stiffness matrix of the pile group system:

$$\begin{Bmatrix} \dot{V} \\ \dot{H} \\ \dot{M} \end{Bmatrix} = \begin{bmatrix} \dot{S}_{11} & \dot{S}_{12} & \dot{S}_{13} \\ \dot{S}_{21} & \dot{S}_{22} & \dot{S}_{23} \\ \dot{S}_{31} & \dot{S}_{32} & \dot{S}_{33} \end{bmatrix} \begin{Bmatrix} \dot{w} \\ \dot{u} \\ \dot{\vartheta} \end{Bmatrix} \quad (3.6) \quad (2.13 \text{ bis})$$

where

$\dot{V}, \dot{H}, \dot{M}$  = incremental external loads and moments acting on the pile cap  
(given by total load/moment divided by number of load increments),

$[\dot{S}]$  =  $(3 \times 3)$  incremental global stiffness matrix of the pile group system,

$\dot{w}, \dot{u}, \dot{\vartheta}$  = incremental vertical displacement, horizontal displacement and rotation of the pile cap.

*Step (10)*

Invert the  $[\dot{S}]$  matrix and calculate the incremental vertical displacement, horizontal displacement and rotation of the pile cap produced by the increments of loading  $\dot{V}$ ,  $\dot{H}$  and  $\dot{M}$ :

$$\begin{Bmatrix} \dot{w} \\ \dot{u} \\ \dot{\vartheta} \end{Bmatrix} = \begin{bmatrix} \dot{f}_{11} & \dot{f}_{12} & \dot{f}_{13} \\ \dot{f}_{21} & \dot{f}_{22} & \dot{f}_{23} \\ \dot{f}_{31} & \dot{f}_{32} & \dot{f}_{33} \end{bmatrix} \begin{Bmatrix} \dot{V} \\ \dot{H} \\ \dot{M} \end{Bmatrix} \quad (3.7) \quad (2.14 \text{ bis})$$

where the matrix in Equation (3.7) is the  $(3 \times 3)$  incremental global flexibility matrix  $\left[ \dot{F} \right]$  of the pile group system.

### Step (11)

In order to calculate the incremental real tractions acting on the piles, the incremental pile tractions due to unit boundary conditions from Equation (3.3) are scaled by a factor represented by the incremental vector of vertical displacement  $\dot{w}$ , horizontal displacement  $\dot{u}$  and rotation  $\dot{\vartheta}$  of the cap obtained from Equation (3.7). Therefore, for each pile type, the incremental axial/transverse tractions can be expressed as:

$$\begin{aligned} \dot{t}_a^i &= \dot{t}_{ai}^1 \dot{w} + \dot{t}_{ai}^2 \dot{u} + \dot{t}_{ai}^3 \dot{\vartheta} \\ \dot{t}_t^i &= \dot{t}_{ti}^1 \dot{w} + \dot{t}_{ti}^2 \dot{u} + \dot{t}_{ti}^3 \dot{\vartheta} \end{aligned} \quad (3.8) \quad (2.15 \text{ bis})$$

where

$\dot{t}_a^i$  = vector, of size  $n(N+1)$ , of incremental axial tractions acting on pile element  $i$ ,

$\dot{t}_{ai}^k$  = three vectors, each of size  $n(N+1)$ , of incremental pile axial tractions acting on element  $i$  due to unit boundary conditions ( $k = 1, 2, 3$ ),

$\dot{w}, \dot{u}, \dot{\vartheta}$  = incremental vertical displacement, horizontal displacement and rotation of the pile cap,

$\dot{t}_t^i$  = vector, of size  $(n \times N)$ , of incremental transverse tractions acting on pile element  $i$ ,

$\dot{t}_{ti}^k$  = three vectors, each of size  $(n \times N)$ , of incremental pile transverse tractions acting on element  $i$  due to unit boundary conditions ( $k = 1, 2, 3$ ).

### Step (12)

Integrate the axial/transverse incremental tractions acting on the piles obtained from Equation (3.8), thereby leading to the (incremental) values of the axial forces  $\dot{F}_a$ , shear forces  $\dot{F}_t$  and bending moments  $\dot{M}_t$  acting at the top of each element  $i$  for each pile type:

$$\begin{aligned}\dot{F}_a^i &= \dot{F}_a^{i+1} + A_a^i \dot{t}_a^i \\ \dot{F}_t^i &= \dot{F}_t^{i+1} + A_t^i \dot{t}_t^i \\ \dot{M}_t^i &= \dot{M}_t^{i+1} - A_t^i \dot{t}_t^i \times \frac{h^i}{2} - \dot{F}_t^{i+1} \times h^i\end{aligned}\quad (3.9) \quad (2.16 \text{ bis})$$

where

$\dot{F}_a^i$  = vector, of size  $n(N+1)$ , of incremental axial forces acting at the top of pile element  $i$ ,

$\dot{F}_t^i$  = vector, of size  $(n \times N)$ , of incremental shear forces acting at the top of pile element  $i$ ,

$\dot{M}_t^i$  = vector, of size  $(n \times N)$ , of incremental bending moments acting at the top of pile element  $i$ ,

$h^i$  = height of the pile element  $i$  (given by  $L_j$  divided by  $N$ , where  $L_j$  is the length of pile  $j$  and  $N$  is the number of pile shaft elements).

*Step (13)*

By summation, calculate the current (resultant) axial/transverse tractions acting on pile element  $i$  for each pile type, yielding:

$$t_i = \sum_{j=1}^J \dot{t}_i^j \quad (3.10) \quad (2.30 \text{ bis})$$

where

$t_i$  = vector, of size  $n(2N+1)$ , of current axial/transverse tractions acting on pile element  $i$ ,

- $\bullet^j$   
 $t_i$  = vector, of size  $n(2N+1)$ , of current axial/transverse tractions acting on pile element  $i$  at the load increment  $j$ ,
- $J$  = current total number of load increments ( $J = 1, NINC$ ),
- $NINC$  = total number of load increments.

In the same way, the current displacements and rotation of the pile cap and the current axial/shear forces and moments acting on piles are calculated by summation of the incremental values.

#### Step (14)

Check that pile cap equilibrium between current applied loads and current total reactions of the piles is satisfied.

#### Step (15)

Test whether an element  $i$  has yielded by introducing a flag  $I_{pi}$  as:

$$I_{pi} = H\left[|t_{si}| - |t_{siy}|\right] \quad (3.11)$$

where

$I_{pi}$  is a flag which determines whether (in the next increment) an element  $i$  should be regarded as elastic or plastic,

$t_{si}$  ( $= -t_{pi}$ ) are the current soil tractions acting on the  $i$ -th element,

$t_{siy}$  are the limiting stresses acting on the  $i$ -th element, as defined in Equations (2.17) and (2.18),

$H[x]$  is the 'Heaviside function' which assumes the following values:

$$\begin{aligned} H[x] &= 0 && \text{if } x < 0 \text{ (ie the element } i \text{ remains elastic),} \\ H[x] &= 1 && \text{if } x > 0 \text{ (ie the element } i \text{ yields).} \end{aligned}$$

*Step (16)*

Set up zero the rows and columns of the global flexibility matrix  $[G_p + G_s]$  (from Equation (3.3)) corresponding to those soil elements which have yielded. The incremental procedure restarts from Step (6).

**3.3.3 Structure of the program**

The computer program PGROUPN is written in Salford Fortran 77 language, containing approximately 4000 lines. The program represents an extension of the numerical code PGROUP by Banerjee & Driscoll (1976), which has been entirely rewritten in order to make it more computationally efficient and to include the effects of soil nonlinearity (these modifications are summarised in Section 2.2). The only subroutines which do not alter the original structure are those labelled SORT, UNLOAD, RGSCAL, GLOAD and EQUIB. Such subroutines have the task of evaluating the actual pile displacements, loads and moments having already obtained the stresses due to unit boundary conditions (Steps (7) to (12)). In addition, various bugs in the version PGROUP 2.0 by Banerjee & Driscoll (1977) have been sorted out (as depicted in Appendix 3.1).

Only a brief description of the main subroutines involved in the PGROUPN algorithm will be given here (see Fig. 3.3).

**Subroutine DRIVER**

- Call for Subroutines INPUT, SVEC, ASSMBI, GDASSI and UNITSC at the start of the analysis;
- Call for Subroutines SOLVER, SORT, UNLOAD, RGSCAL, GLOAD, UPDATE and EQUIB for incremental analysis;
- Call for Subroutines PLOTV and PLOTH to print plots.

**Subroutine INPUT**

- Step (1): reads/writes all input data to a file. A description of required input data is given in Table 3.1.

**Subroutine SVEC**

- Step (2): determine the limiting stresses for the soil elements.

**Subroutine ASSMBI**

- Step (3): set up the single-pile and the interaction soil flexibility matrices  $[G_s]$  for each pile via integration of the Mindlin's kernel (Mindlin, 1936) (via Subroutines HSINGH, VSINGH and APILE), and assemble in the global soil flexibility matrix  $[G_s]$  of the group. If sets of pile types are exploited, a matrix condensation is performed (refer to Fig. 3.2).

**Subroutine GDASSI**

- Step (4): set up the pile flexibility matrix  $[G_p]$  via integration of the Bernoulli-Euler (beam theory) kernel for each pile type (via Subroutine DMATX), and assemble in the global pile flexibility matrix  $[G_p]$  of the group.

**Subroutine UNITSC**

- Step (5): compute the vectors of unit boundary conditions for each pile type.

**Subroutine SOLVER**

- Step (6): compute the incremental pile tractions due to unit boundary conditions for each pile type (for a linear elastic analysis, the number of increments is assumed to be equal to 1).

**Subroutine SORT**

- Step (7): extract the incremental axial/transverse pile tractions due to unit boundary conditions.

**Subroutine UNLOAD**

- Step (8): compute the incremental pile head axial/shear forces and moments due to unit boundary conditions for each pile type.

**Subroutine RGSCAL**

- Step (9): compute the (incremental) global stiffness matrix of the pile group system;
- Step (10): compute the incremental vertical displacement, horizontal displacement and rotation of the pile cap.

**Subroutine GLOAD**

- Step (11): compute the incremental 'real' pile tractions for each pile type;
- Step (12): compute the distribution of the incremental axial/shear forces and moments for each pile type.

**Subroutine UPDATE**

- Step (13): compute the current (resultant) axial/transverse pile tractions, the current displacements and rotation of the pile cap and the distribution of the axial/shear forces and moments for each pile type;
- Call for Subroutine PLAST (see below);
- Write output data to a file.

**Subroutine EQUIB**

- Step (14): check that pile cap equilibrium is satisfied;
- Return back to Subroutine SOLVER for the next increment.

**Subroutine PLAST**

- Step (15): check for yielded soil elements;
- Step (16): set up zero rows and columns of the global flexibility matrix  $[G_p + G_s]$  corresponding to yielded soil elements.

**3.3.4 Limitations imposed by the method used**

The program has the following limitations:

- (a) The non-linear analysis is restricted to pile groups embedded in cohesive soils, specifically fully saturated clay under undrained conditions, which can be defined by the shear strength  $C_u$ , the Young's modulus  $E_s = E_u$  and the Poisson's ratio  $\nu_s$  (this is generally taken as 0.5). The linear elastic analysis can be an undrained analysis of clays or a drained analysis of clays or sands (with suitable choice of  $E_s$  and  $\nu_s$ );
- (b) The piles can be raked in one plane only, namely the XZ plane (refer to Fig. 2.1). Banerjee & Driscoll (1977) suggested that it is possible, in an approximate manner, to analyse pile groups with piles raked in two directions by considering the angle of rake in the plane of the applied horizontal loads and moments and assuming that the angle of rake is equal to the angle between the projection of the piles on to the plane of horizontal loads and moments, and the vertical axis. This will lead to an overestimate of displacements and moments;
- (c) The applied horizontal load and moment must all act in one plane (ie the XZ plane). In order to analyse approximately pile groups subjected to horizontal loads and moments in two directions, Banerjee & Driscoll (1977) suggested separating the problem into two parts and obtaining the final results by applying the principle of superposition;
- (d) The pile slenderness ratios (ie the ratio of pile length to shaft diameter) should not be less than 5 (refer to Butterfield & Banerjee, 1971a);
- (e) In the analysis of single piles under axial loading and pile groups under either axial or lateral loading, the height of the pile shaft element should not be less than twice the shaft diameter (see Sections 4.3.1.1 and 5.2).

### 3.3.5 Maximum problem size

The maximum problem size is governed by the following parameters:

- (a) Maximum number of piles in a group ( $m$ ) = 500

- |  |   |      |
|--|---|------|
| (b) Maximum number of pile types in a group ( $n$ )        | = | 100  |
| (c) Maximum number of pile shaft elements per pile ( $N$ ) | = | 50   |
| (d) Maximum number of degrees of freedom ( $dof$ )         | = | 2000 |
| (e) Maximum number of (equal) load increments ( $NINC$ )   | = | 1000 |

NOTE:  $dof$  is represented by the number of simultaneous linear equations which are to be generated and solved by the program, ie  $n(2N+1)$ .

## 3.4 Input

### 3.4.1 General description

The amount of data input required by the program is minimal. The input data, which include specification of the pile group geometry and properties, loading conditions and soil properties are handled by an interactive set of subroutines specially designed to reduce the effort needed for data preparation. The application offers the possibility of using previous input data which become temporary defaults — thus, if the User wishes to examine the effect of changing only a few input values, he/she does not need to re-enter all of the data. If no previous data are used, then default values are adopted.

### 3.4.2 System of units adopted

The program is independent of units. Any consistent set of units can be chosen by the User. For instance, if the soil and pile moduli are expressed in kPa, the pile geometry must be expressed in metres, the loads in kN and the moments in kNm. The angle of rake of the piles is defined in degrees.

### 3.4.3 Type of analysis

The User may choose between two types of analysis: (a) Linear elastic analysis; (b) Non-linear analysis. If 'Non-linear' analysis is selected, the number of (equal) load increments (*NINC*) needs to be entered.

#### 3.4.4 Pile group configuration

Groups containing up to 500 piles may be analysed. The piles may be arranged in any geometrical configuration, ie in a rectangular grid plan (with the possibility of adding and/or removing piles) or in a random plan, provided that the pile group remains symmetrical about the XZ plane (refer to Fig. 2.1). Although the individual piles may have different diameters and lengths as well as different angles of rake, the resulting arrangement must also be symmetrical about the XZ plane.

The pile coordinates are defined at the intersection of the centre of the pile and the ground level. The piles are rigidly connected to the pile cap which is itself assumed to be rigid. The cap is assumed to be free-standing and non-effective (ie the effects of interaction between pile cap and soil are not considered). A depth of overhang (*g*) of the cap (given by the vertical distance between the underside of the pile cap and the ground level) may be specified where the superficial soil layers are ineffective or where the group loads are applied above ground level.

#### 3.4.5 Geometry of the piles

Piles may have different geometries but all are assumed to be constructed from the same material, ie all piles have the same Young's modulus ( $E_p$ ). The pile length ( $L$ ) is the embedded length of the pile. The base diameter ( $d_b$ ) may be different from the shaft diameter ( $d$ ). An internal diameter ( $d_i$ ) may be specified in order to take into consideration hollow piles (for solid piles the internal diameter is zero). Piles of non-circular cross-sections can also be investigated by representing them as equivalent cylindrical piles. Piles may be vertical or raked in the XZ plane (refer to Fig. 2.2). The angle of rake ( $\phi$ ) is defined in degrees and is deemed to be positive if the rotation of the pile is clockwise, ie if the X-coordinate of the pile head is greater (algebraically) than the X-coordinate of the pile base. Vertical piles have zero rake.

Repeated data, ie pile lengths, base diameters, shaft diameters (internal and external) and pile rake angles, need not be re-submitted, thus greatly facilitating data preparation for large pile groups.

### 3.4.6 Identification of pile types

Computing time may be greatly reduced by exploiting symmetries between piles which are supposed to carry equal loads, a feature which is particularly significant for large pile groups. In most pile groups,  $n$  sets of pile types may be identified whose members carry identical loads to each other under all group loading conditions. Such sets of piles may be identified by an unique number in the input data, ie by the same 'Pile type number'.

An example of correct pile numbering for a  $3 \times 3$  pile group is given in Fig. 3.4a. It is worth noting that although under vertical centroidal loading only three sets of pile types would be required, such a pile numbering (depicted in Fig. 3.4b) is inadequate because, as stated above, the pile numbering must be valid for all loading conditions (in fact, under horizontal loading, the pile group tries to rotate and hence piles at the edges will be loaded in tension and compression).

Frequently, for reasons of economy or of difficulty in identifying piles which act identically, it is possible to identify sets of piles which only carry approximately equal loads. It should be emphasised that the identification of pile types is the key to the efficient application of the program to large pile groups, and hence the User should strive to specify the minimum number of pile types consistent with the required accuracy of the solution.

### 3.4.7 Loading

The group loads are applied to the pile cap and may consist of any combination of vertical load ( $V$ ), horizontal load ( $H$ ) and moment ( $M$ ), all acting in the XZ plane through the group centroid (refer to Fig. 2.1). An eccentric vertical load may be specified by entering the X-coordinate of its location on the cap. A vertical load in the direction of the positive Z-axis, a horizontal load in the direction of the positive X-axis and a clockwise moment in the XZ plane (viewed from 'negative Y') are all assumed to be positive.

### 3.4.8 Soil layer

The soil may be idealised as a homogeneous or non-homogeneous (Gibson type) material. The soil properties are described by the profiles of the Young's modulus ( $E_s$ ) and the undrained shear strength ( $C_u$ ), and by the constant values of the Poisson's ratio ( $\nu_s$ ) and the adhesion factor ( $\alpha$ ). A finite depth ( $H$ ) of soil layer may be specified.

### 3.5 Output

The normal output of the PGROUPN program consists of the following data:

- (a) The input data;
- (b) The resultant global stiffness and flexibility ( $3 \times 3$ ) matrices (described in Equations (3.6) and (3.7), respectively) which may be used for superstructure analysis;
- (c) The resultant displacements and rotation of the pile cap;
- (d) A table with the resultant cap displacements and rotation at each load increment;
- (e) The resultant pile shaft shear/normal stresses of each pile element, starting at the top element, ie at the ground level;
- (f) The final identification state (ie elastic or plastic) of each pile element;
- (g) The resultant axial/shear forces and bending moment acting at the top of each pile element, starting from the top element. In the case of free-standing portions of the piles being specified, the moment at each pile-head cap joint will be given by the moment at the top of the first pile element plus the moment due to the transverse load at the first pile element multiplied by the free-standing height (ie the depth of overhang of the cap);
- (h) The load-displacement curves of the pile cap (using graphics subroutines).

In addition, the User may choose to print the soil limiting stresses (from Equations (3.1) and (3.2)) and the current (resultant) quantities (b), (c), (d), (e), (f) and (g) at each load increment.

### 3.6 Typical illustrative results

In order to show typical results from PGROUPN and, also, to make a comparison between the results obtained by adopting the approach put forward in this thesis, the approach by Davies & Budhu (1986) and the modified Davies & Budhu approach (which are described in Section 2.4.5), the load-deformation curves of single piles and  $2 \times 2$  pile groups in homogeneous soil are presented in Figs. 3.5 to 3.8. The details of the input parameters are as follows:

Pile diameter ( $d$ )	= 1 m
Centre-to-centre pile spacing ( $s$ )	= 3 m
Pile Young's modulus ( $E_p$ )	= 25 GPa
Soil Poisson's ratio ( $\nu_s$ )	= 0.5
$E_p/C_u$	= 100
Adhesion factor ( $\alpha$ )	= 0.5

In order to cover a wide range of pile geometries and pile-soil relative stiffnesses, ratios of  $L/d = 20, 80$ , and  $K = E_p/E_s = 100, 20000$  have been selected. Thus, four cases may be identified, as depicted in Table 3.2.

As regards pile discretization, for single piles under axial loading and pile groups under either axial or lateral loading, the height-to-diameter ratio ( $h/d$ ) of the pile shaft element adopted here is 2, whereas, for laterally loaded single piles,  $h/d = 1$  (as shown later in Sections 4.3.1.1, 4.4.1.1 and 5.2).

In all the numerical simulations presented in this thesis, the computational work is done on a Pentium 133 MHz with 16 Mb RAM, and using the Lahey Fortran 3.0 compiler. It has been found that about 200 load increments ( $NINC$ ) are generally sufficient to achieve convergence of the PGROUPN solution process.

Figures 3.5 to 3.8 show load-deformation curves which are typical of relatively rigid (Cases 1, 2 and 4) and relatively flexible (Case 3) single piles and pile groups. For instance, in an axially loaded flexible pile, high shear stresses occur near the top of the pile, and hence the effects of soil yielding are evident from the start of loading. This results in a markedly non-linear load-settlement response. Instead, in a rigid pile, the distribution of shear stresses is relatively uniform with depth, thereby resulting in a nearly elastic-perfectly plastic load-settlement response.

It is evident that, if the approach proposed by Davies & Budhu (1986) for laterally loaded single piles is applied to the pile group problem, this will result, at some load increments, in an apparent increase of the pile group stiffness as yielding along the pile-soil interface progresses. This inconsistent behaviour has been observed in most of the numerical simulations carried out on single piles under axial loading and pile groups subjected to either vertical or horizontal loads, and it is more evident for relatively rigid piles. Instead, the load-deflection curves of laterally loaded single piles show a plausible trend which is similar to that obtained using the current approach.

It is worth noting that the modified Davies & Budhu approach produces a plausible load-deformation behaviour for all the cases analysed. However, as discussed in Section 2.4.5.3, this approach is discarded as it requires some physical assumptions which are less satisfactory than those employed in the current approach.

### **3.7 Concluding remarks**

The non-linear BEM analysis has been successfully implemented in the computer program PGROUPN using the procedure described above. The boundary element algorithm proposed by Banerjee & Driscoll (1976) has been extended in order to increase computational efficiency and to include the effects of soil nonlinearity by means of a stepwise linear incremental procedure. The structure of the algorithm is outlined, together with a general description of the input data required and the results of the analysis. In the following chapters, the validity and generality of the proposed approach will be examined by comparison with alternative numerical methods and field tests.

## Appendix 3.1

### Inaccuracies in the numerical code PGROUP 2.0

In order to familiarise with the boundary element algorithm for pile group analysis, the computer program PGROUP (version 2.0) by Banerjee & Driscoll (1977) has been carefully examined. A brief description of some inaccuracies found in the algorithm is given below.

(a) In Subroutine GDASSI (which computes the pile flexibility matrix  $[G_p]$ ), the variable  $DEP$  (which is equal to the free-standing length of the pile) should be divided by  $\cos \phi$  in order to take into account the pile rake, ie it should be:

$$DEP = \frac{DEP}{\cos \phi} \quad (\text{A3.1-1})$$

where  $\phi$  is the angle of rake of the pile.

In addition, the columns  $(N-1)$  and  $N$  (where  $N$  corresponds to the number of pile shaft elements per pile) of the pile flexibility matrix  $[G_p]$  are slightly in error and, consequently, the  $[G_p]$  matrix is not symmetric. This error may be due to the finite difference form adopted for the pile domain in PGROUP 2.0.

(b) In Subroutine UNITSC (which defines the unit boundary condition vector), the term  $COX \sin \phi$  has been omitted in the definition of the transverse column vector due to unit rotation of the pile cap. Therefore, the correct expression is:

$$BVEC(N1, 3) = COX \sin \phi - \frac{DEP}{\cos \phi} - AL(NK) \times (FI1 - 0.5) / FN \quad (\text{A3.1-2})$$

where

$BVEC(N1, 3)$  is the transverse column vector due to unit rotation of the cap,  
 $N1, FII$  indicate the appropriate element of the column vector,  
 $COX$  is the horizontal distance of the pile head from the vertical axis of symmetry  
of the pile cap,  
 $DEP$  is the depth of overhang of the pile cap,  
 $AL$  is the pile length,  
 $NK$  indicates the pile number,  
 $FN$  is the number of pile shaft elements per pile.

(c) In subroutine UNLOAD (which computes the pile head axial/shear forces and moments due to unit boundary conditions for each pile type), the term  $(-DEP \tan \phi)$  has been omitted in the calculation of  $COUPLE$ . Therefore, the correct expression is:

$$COUPLE = SUM \times 2A(NK)HOLD + (ALOAD \cos \phi + TLOAD \sin \phi)(COX - DEP \tan \phi) - (TLOAD \cos \phi - ALOAD \sin \phi)DEP \quad (A3.1-3)$$

where

$COUPLE$  is the moment acting on the cap due to unit boundary conditions,  
 $SUM \times 2A(NK)HOLD$  represents the pile head moment due to unit boundary  
conditions,  
 $ALOAD$  are the pile head axial forces due to unit boundary conditions,  
 $TLOAD$  are the pile head shear forces due to unit boundary conditions.

The term  $(-DEP \tan \phi)$  has also been omitted in the analogous calculation of  $COUPLE$  in Subroutine EQUIB.

## TABLES CHAPTER 3

Table 3.1 Input data for the PGROUPN program.

DESCRIPTION	VARIABLE
Number of piles ( $m$ )	$NPILES$
Number of pile types ( $n$ )	$NS$
Number of pile shaft elements per pile ( $N$ )	$N$
Depth of overhang of the pile cap ( $g$ )	$PCXYZ(3)$
Type of analysis: <ul style="list-style-type: none"> <li>• 0 = Linear elastic</li> <li>• 1 = Non-linear</li> </ul>	$LPLAS$
...only if the type of analysis is 'Non linear':	
Number of equal load increments ( $NINC$ )	$NINC$
...for each pile $i$ ( $i = 1, m$ ):	
Pile $i$ type number	$KK(i)$
Pile $i$ embedded length ( $L_i$ )	$PLEN(i)$
Pile $i$ external diameter ( $d_i$ )	$PDIA(i)$
Pile $i$ internal diameter ( $d_{ii}$ )	$PDII(i)$
Pile $i$ base diameter ( $d_{bi}$ )	$PDIB(i)$
Pile $i$ rake ( $\phi_i$ )	$RAKE(i)$
$x$ -coordinate of pile $i$ at ground level	$CORD(i,1)$
$y$ -coordinate of pile $i$ at ground level	$CORD(i,2)$

*continued...*

DESCRIPTION	VARIABLE
Pile Young's modulus ( $E_p$ )	<i>EP</i>
Depth of soil layer ( $H$ )	<i>PLAYER</i>
Soil Young's modulus at ground level ( $E_{so}$ )	<i>ESS</i>
Rate of increase of soil Young's modulus with depth ( $m$ )	<i>ESZ</i>
Soil Poisson's ratio ( $\nu_s$ )	<i>PM</i>
Vertical load on cap ( $V$ )	<i>SCALE(1,1)</i>
Horizontal load on cap ( $H$ )	<i>SCALE(1,2)</i>
Moment on cap ( $M$ )	<i>SCALE(1,3)</i>
$x$ -coordinate of vertical load on cap	<i>SCALE(1,4)</i>
...only if the type of analysis is 'Non-linear':	
Undrained shear strength at ground level ( $C_{uo}$ )	<i>CUS</i>
Rate of increase of undrained shear strength with depth ( $c$ )	<i>CUZ</i>
Adhesion factor ( $\alpha$ )	<i>CUA</i>

Table 3.2 Input data for comparison between approaches.

Case	$L/d$	$K$
1	20	100
2	20	20,000
3	80	100
4	80	20,000

### FIGURES CHAPTER 3

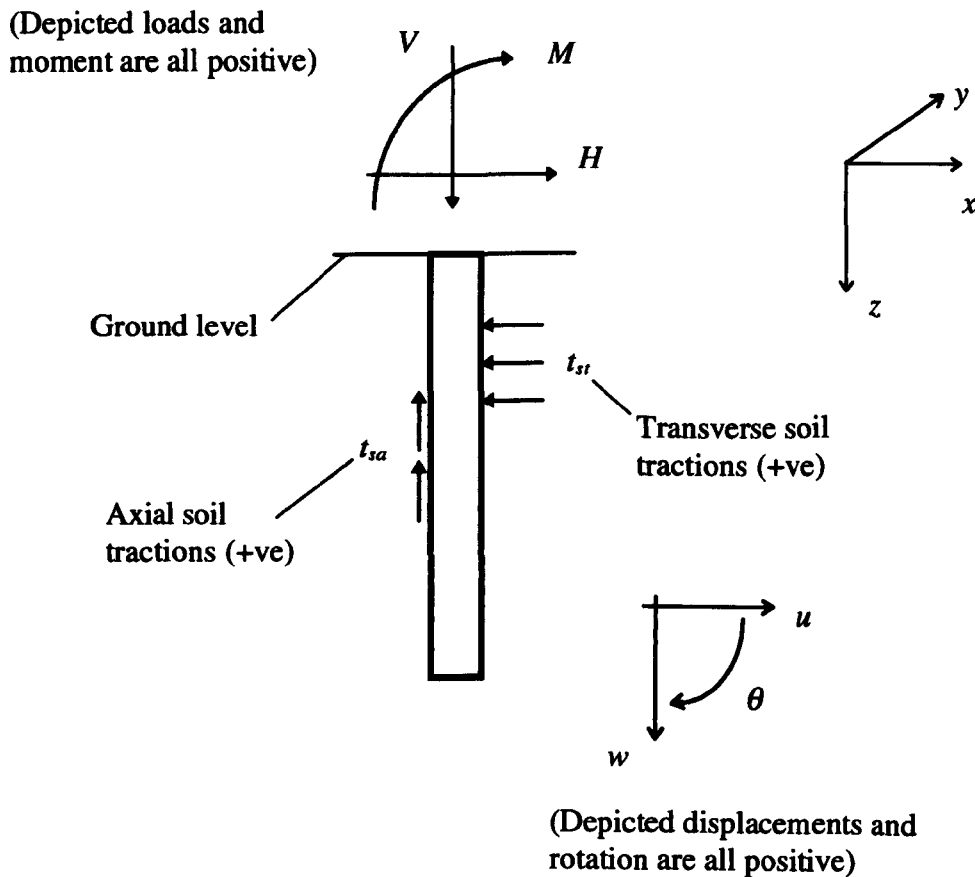
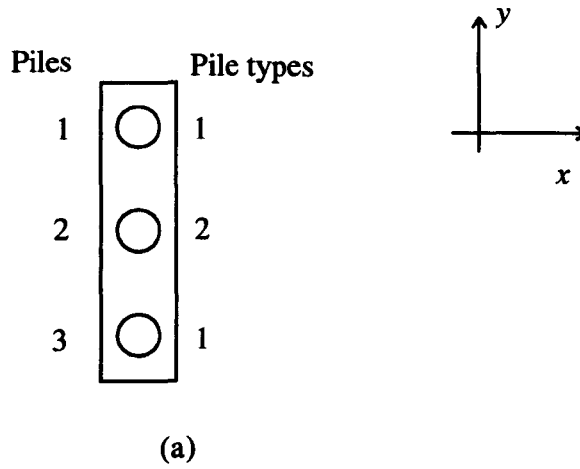


Fig. 3.1 Sign conventions for a pile.



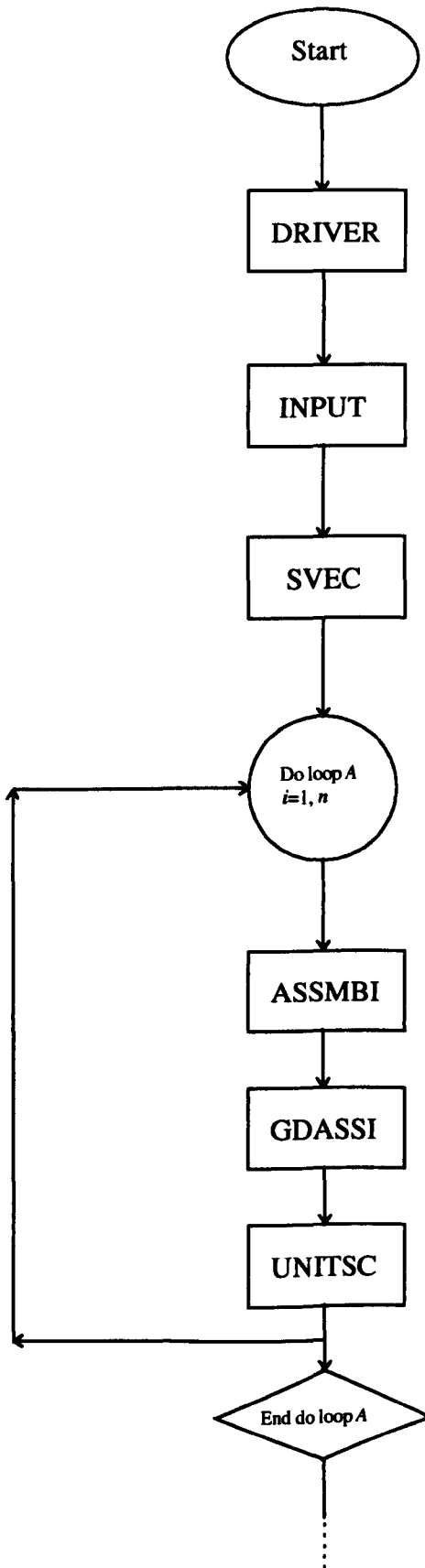
$$[G_s] = \begin{bmatrix} (G_s)^{1,1} & (G_s)^{1,2} & (G_s)^{1,3} \\ (G_s)^{2,1} & (G_s)^{2,2} & (G_s)^{2,3} \\ (G_s)^{3,1} & (G_s)^{3,2} & (G_s)^{3,3} \end{bmatrix}$$

(b)

$$[G_s] = \begin{bmatrix} (G_s)^{1,1} + (G_s)^{1,3} & (G_s)^{1,2} \\ (G_s)^{2,1} + (G_s)^{2,3} & (G_s)^{2,2} \end{bmatrix}$$

(c)

Fig. 3.2 Condensation of the global soil flexibility matrix  $[G_s]$  for a group of  $m = 3$  piles with  $n = 2$  pile types. (a) Pile group geometry. (b) Non-condensed global soil flexibility matrix  $[G_s]$ . (c) Condensed global soil flexibility matrix  $[G_s]$  after exploiting symmetries between piles (NOTE:  $(G_s)^{i,i}$  is the single-pile (pile  $i$ ) soil flexibility matrix of size  $(2N+1) \times (2N+1)$ ;  $(G_s)^{i,j}$  is the interaction (between pile  $i$  and pile  $j$ ) soil flexibility matrix of size  $(2N+1) \times (2N+1)$ ;  $N$  is the number of pile shaft elements per pile).



*...continued*

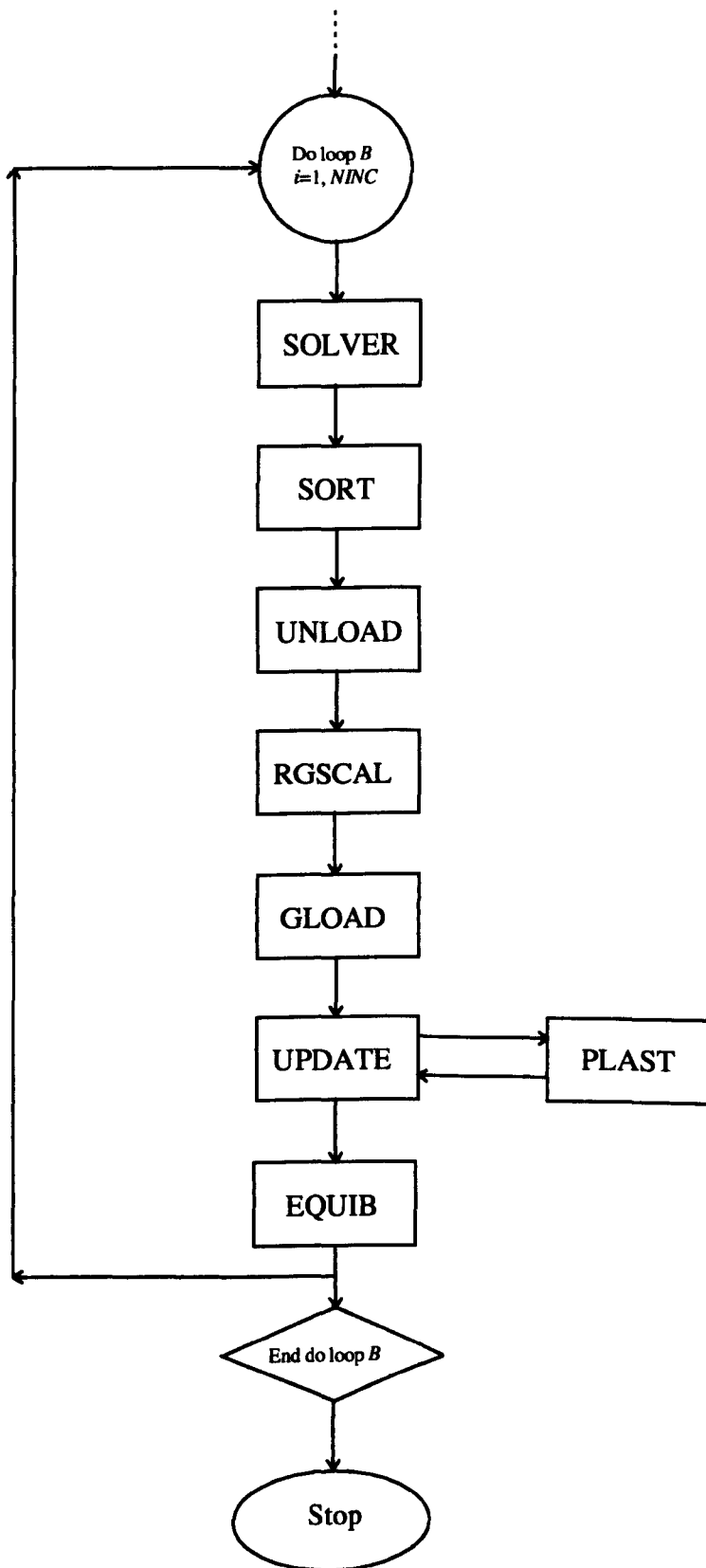


Fig. 3.3 Structure of the PGROUPN program with its subroutines (NOTE:  $n$  = number of pile types,  $NINC$  = number of equal load increments).

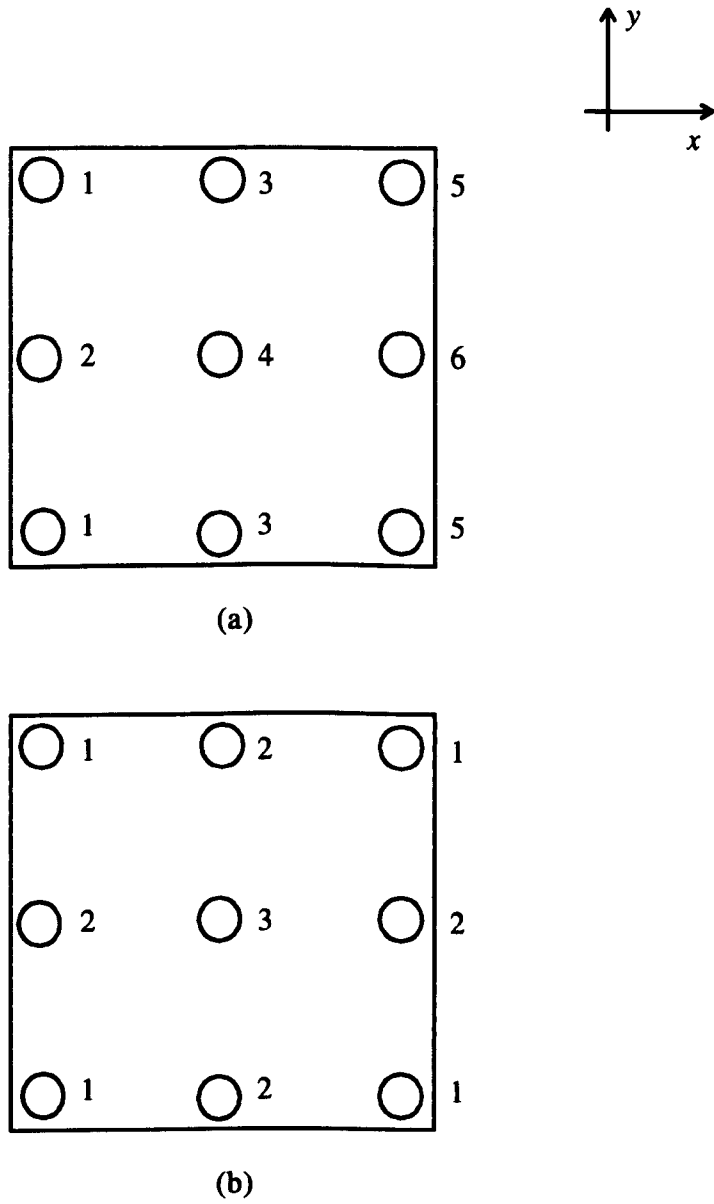


Fig. 3.4 Selection of pile types for a  $3 \times 3$  pile group. (a) Valid numbering. (b) Invalid numbering.

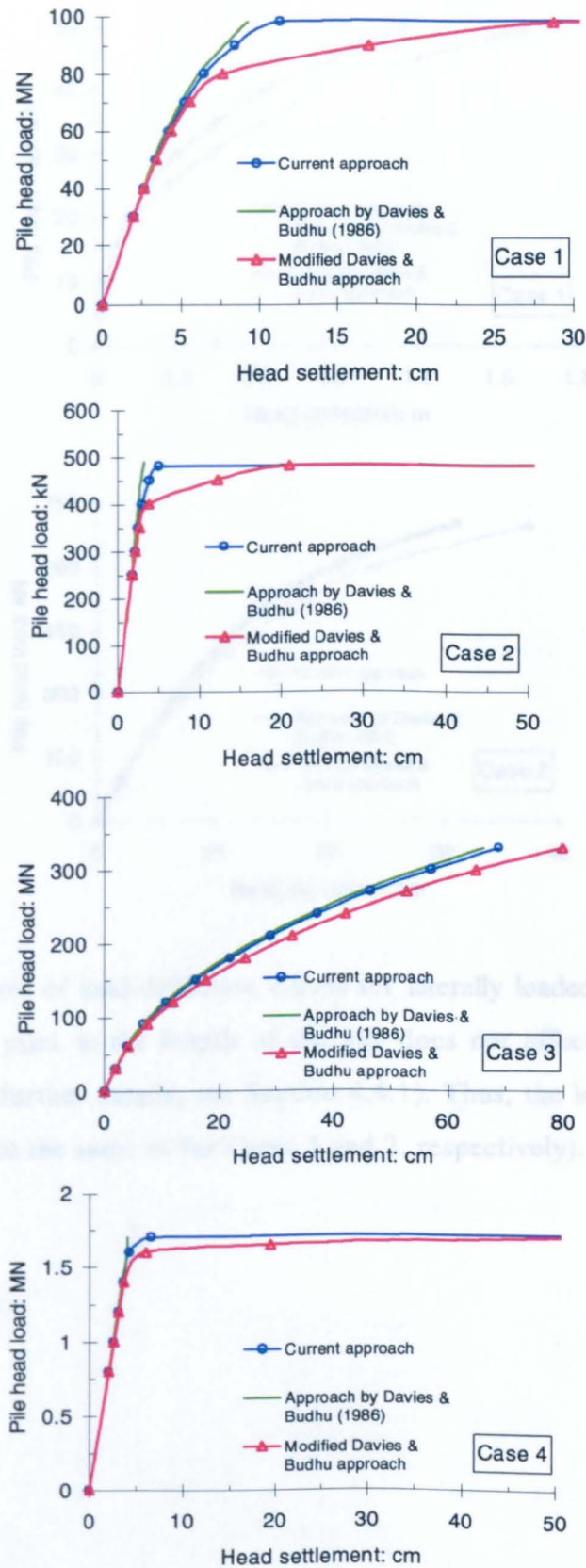


Fig. 3.5 Comparison of load-settlement curves for axially loaded single piles.

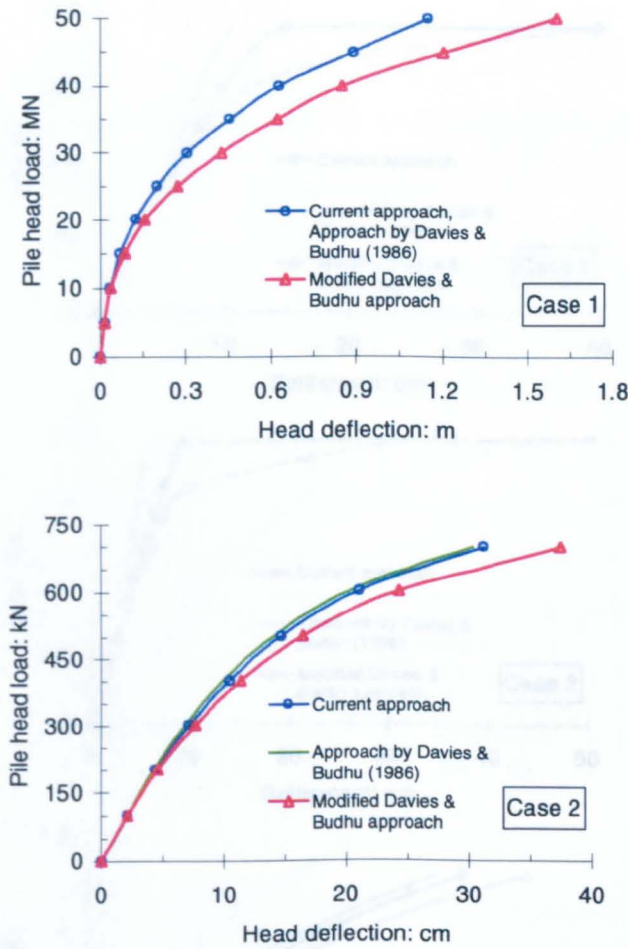


Fig. 3.6 Comparison of load-deflection curves for laterally loaded single piles (NOTE: These are ‘flexible’ piles, ie the length of the pile does not affect the response under lateral loading (for further details, see Section 4.4.1). Thus, the load-deflection curves for Cases 3 and 4 are the same as for Cases 1 and 2, respectively).

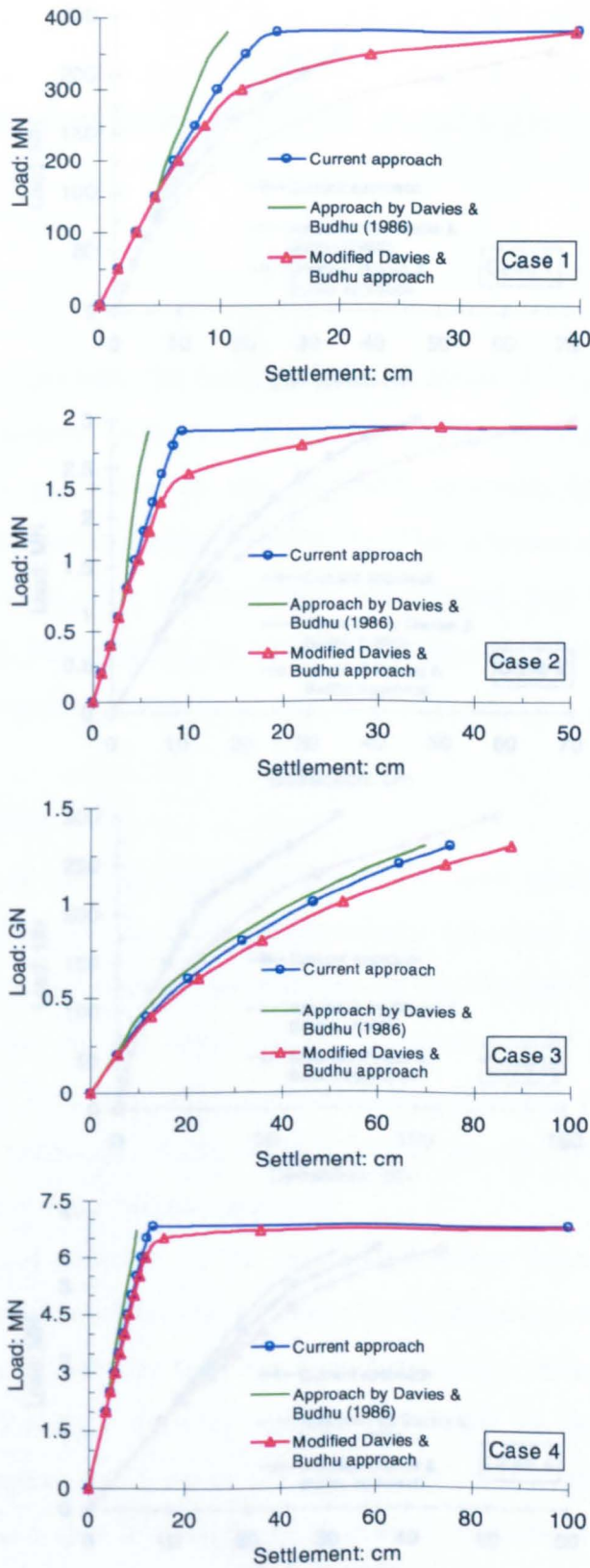


Fig. 3.7 Comparison of load-settlement curves for axially loaded 2 × 2 pile groups.

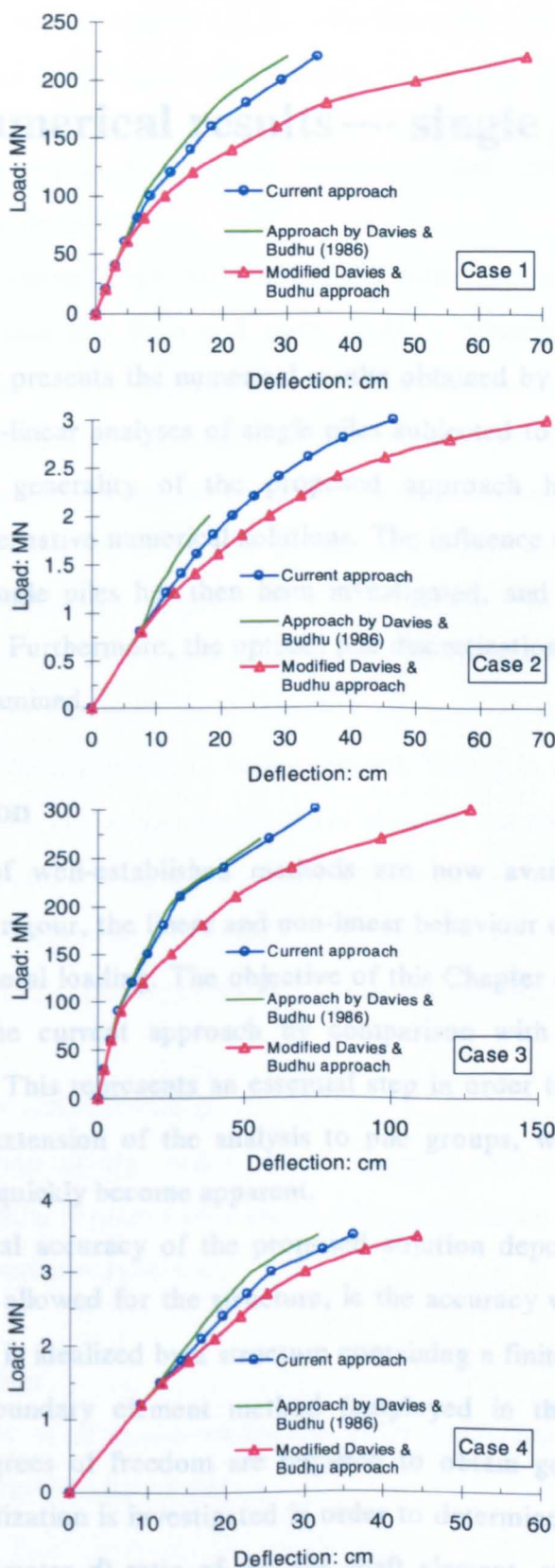


Fig. 3.8 Comparison of load-deflection curves for laterally loaded 2 x 2 pile groups.

## CHAPTER 4

### Numerical results — single piles

#### 4.1 Summary

This Chapter presents the numerical results obtained by the PGROUPN program from linear and non-linear analyses of single piles subjected to axial and lateral loads. The accuracy and generality of the proposed approach have been verified by comparison with alternative numerical solutions. The influence of major parameters on the behaviour of single piles has then been investigated, and a series of parametric studies is presented. Furthermore, the optimal pile discretization under axial and lateral loading has been examined.

#### 4.2 Introduction

A number of well-established methods are now available to analyse, with different degrees of rigour, the linear and non-linear behaviour of single piles subjected to either axial or lateral loading. The objective of this Chapter is to assess the validity and accuracy of the current approach by comparison with some of the existing numerical methods. This represents an essential step in order to proceed with greater confidence to the extension of the analysis to pile groups, where the limitations of current approaches quickly become apparent.

The numerical accuracy of the proposed solution depends on the number of degrees of freedom allowed for the structure, ie the accuracy with which an infinitely redundant structure is idealized by a structure containing a finite number of degrees of freedom. In the boundary element method (employed in the PGROUPN analysis), remarkably few degrees of freedom are required to obtain good accuracy. For this purpose, pile discretization is investigated in order to determine the optimal height ( $h$ ) to width (ie the diameter  $d$ ) ratio of the pile shaft element, such that computational efficiency may be achieved. Thus, the height  $h$  of the pile shaft element is given by:

$$h = \frac{L}{N} \quad (4.1)$$

where  $L$  is the pile length and  $N$  is the number of shaft elements which has been adopted to discretize the pile.

In the linear elastic range, the influence of major parameters, such as enlarged base diameter, pile rake and finite-soil layer depth, is examined, and charts showing how the deformation of a pile depends on the various parameters of pile geometry and pile-soil relative stiffness are presented in non-dimensional form. In the non-linear range, the load-deformation response and load transfer are investigated.

As regards the Poisson's ratio of the soil ( $\nu_s$ ), this is a necessary input parameter into analyses that involve the elastic solution of Mindlin. Its effect is generally quite minor for piles under axial loading as the axial displacement of a pile depends primarily on the soil shear modulus  $G$ , and is relatively unaffected by variations in Poisson's ratio (with  $G$ , held constant). This is in contrast with a laterally loaded pile, where the horizontal displacement depends on the (horizontal) Young's modulus,  $E_s = 2G_s/(1+\nu_s)$ . In this thesis, unless otherwise specified, the value of the soil Poisson's ratio ( $\nu_s$ ) is taken as 0.5, which is the appropriate value for fully saturated clay under undrained conditions (for further details see Section 3.3.4a).

### 4.3 Piles under axial loading

The initial step of the validation of the proposed approach consists of a comparison of the axial response of a single pile predicted by the PGROUPN program against published numerical solutions.

#### 4.3.1 Linear solution

The behaviour of an axially loaded pile in an elastic soil is governed largely by the following dimensionless parameters:

- (a) The length-to-diameter ratio  $L/d$ ;

(b) The relative pile-soil stiffness  $K = E_p/E_s$ , where  $E_p$  is the pile Young's modulus and  $E_s$  is the soil Young's modulus — typical values of the stiffness ratio  $K$ , calculated for various types of pile and soil, are given in Table 4.1 (after Poulos & Davis, 1980). The relative pile-soil stiffness may also be expressed by the ratio  $\lambda = E_p/G_s$ , which is related to  $K$  by the expression  $\lambda = 3K$  (under the assumption that  $\nu_s = 0.5$ ). It may be noted that, in comparing the PGROUPN results with those obtained by other authors, sometimes  $K$  is used whereas at other times  $\lambda$  is used (depending on what the other authors have used).

#### 4.3.1.1 Convergence of numerical solution

One of the key points for the correct application of the PGROUPN analysis is the optimal definition of the number  $N$  of pile shaft elements. This definition is crucial for the efficient application of the method to large pile groups where the requirement of limiting the computational time is preponderant.

In order to investigate the convergence of the numerical solution provided by the PGROUPN program for different values of  $N$ , the head settlements of a floating pile characterised by different values of  $K = E_p/E_s$  and  $L/d$  have been computed with different values of shaft element height-to-diameter ratios  $h/d$ . The pile (0.5 m in diameter) is loaded by an axial force of 10 MN acting at the top and is embedded in a deep homogeneous elastic soil mass with a Young's modulus ( $E_s$ ) of 1 GPa.

The pile-head settlement calculated from PGROUPN are shown in Tables 4.2 and 4.3. The following characteristics of behaviour are observed:

- (a) Settlements decrease with increasing  $h/d$ , ie with decreasing  $N$ ;
- (b) Settlements decrease with increasing the relative pile-soil stiffness  $K$ ;
- (c) Settlements decrease with increasing  $L/d$ .

Tables 4.2 and 4.3 show that, even for  $h/d = 6$ , corresponding to a very coarse discretization of the pile, the results differ very little from those given by a much finer discretization, such as  $h/d = 2$ . In fact, the results for  $h/d = 2$  and those for  $h/d = 6$  differ by only 1.6%.

Moreover, it is critical to observe that values of  $h/d$  ratio less than 2 (the 'shaded' area in Tables 4.2 and 4.3) produce numerical instability, resulting in oscillation of shear stresses along the lower part of the pile, as depicted in Figs. 4.1 and 4.2 for a pile characterised by a  $L/d$  ratio of 25 and for  $K = 100$  (compressible pile) and  $K = 10,000$  (relatively rigid pile), respectively.

Such an unstable profile of shear stress along the pile for  $h/d$  ratios less than 2 is associated with the values of terms in the soil flexibility matrix  $[G_s]$ , obtained from Mindlin's solution (refer to Equation (2.3)). This may be partially attributed to an approximation involved in the PGROUPN analysis: in the application of Mindlin's solution, the field point (ie the point at which the displacement is calculated) should be located at the mid-height of the element along the pile-soil interface but, because the pile is narrow compared with its length, all positions may be referred to the mid-height of the element on the centre line of the pile (eg D'Appolonia & Romualdi, 1963). This approximation is necessary to allow the analytical integration of the singular Mindlin functions, thereby leading to significant savings in computational costs. Instead, if the field point is located along the pile-soil interface, the integration is conveniently evaluated only numerically (Poulos & Davis, 1980). The error generated by this approximation is represented by the pile radius, ie the horizontal distance of the centre line of the pile from the pile shaft surface. Consequently, the effects of this approximation will become less significant for slender pile elements. This is confirmed by the results obtained using a version of PGROUPN which assumes the field point to be located along the pile-soil interface. It has been found that the discrepancies between the two approaches are negligible for  $h/d$  ratios equal or greater than 2. Instead, using the solution with the field point located along the pile-soil interface for  $h/d$  ratios less than 2, the instability of shear stress along the lower part of the pile is greatly reduced.

Based on these observations, it may be concluded that the number  $N$  of shaft elements to discretize a pile subjected to axial loading must be such that:

$$\frac{h}{d} \geq 2 \quad (4.2)$$

where  $h$  is the height of the pile shaft element and  $d$  its diameter.

Another test on accuracy of the solution may be carried out by observing the symmetry of the pile stiffness and flexibility ( $3 \times 3$ ) matrices described in Equations (2.13) and (2.14). In the present test, these matrices have been found to be symmetric to within 3% for  $h/d = 2$  (fine discretization) and to within 10% for  $h/d = 6$  (coarse discretization), over the entire range of  $K$  and  $L/d$  ratios.

From the computational (time) point of view, the required CPU (central processor unit) time is about 1 s for the finest pile discretization adopted (ie  $N = 50$  for the pile with  $L/d = 50$  and  $h/d = 1$ ). Thus, for the linear analysis of single piles, computational costs are negligible.

It may be concluded from this study that the optimal number  $N$  of shaft elements to discretize a single pile under axial loading appears to be:

$$N = \frac{L}{2d} \quad (4.3)$$

#### 4.3.1.2 Pile settlement

Figure 4.3 shows the effect of the stiffness ratio  $\lambda = E_p/G_s$ , on the load-settlement behaviour of plain piles embedded in a deep homogeneous soil mass over a range of  $L/d$  ratios. The normalised load-settlement ratios  $P/G_s dw$  (where  $P$  is the applied axial load and  $w$  is the pile head settlement) calculated by PGROUPN are compared with those predicted by the more rigorous BEM analysis of Butterfield & Banerjee (1971a) (for further details, see Section 1.4.3). It may be noted that the effect of the stiffness ratio  $\lambda$  is negligible for relatively short piles ( $L/d < 20$ ), ie a relatively short pile behaves as a rigid pile, regardless of its relative pile-soil stiffness. The three sets of solutions are in close agreement, the average difference being less than 3%. However, it should be emphasised that, in this thesis, the results from the other methods are taken by measurement from published diagrams. This suggests that inaccuracies of about 2% may be expected.

Figures 4.4 and 4.5 compare the load-settlement ratios of a single pile over a range of slenderness ratios  $L/d$  for homogeneous and Gibson soils, respectively. In the Gibson soil, the shear modulus increases from zero (at the ground surface) to  $G_{sL}$  at the level of the pile base. The Poisson's ratio is taken as 0.3.

Results from PGROUPN are compared with those obtained by the approach of Fleming *et al.* (1992), which is based on the analytical work of Randolph (1977), and the BEM approaches of Poulos (1979) and Poulos & Davis (1980), which may be considered to have approximately the same degree of rigour as PGROUPN for single piles. The agreement between solutions is close, the greatest potential for differences appearing to be for relatively short piles ( $L/d < 20$ ). The higher values of pile stiffness obtained by Poulos (1979) and Poulos & Davis (1980) for long compressible piles may, in part, be attributed to the coarse discretization of the very long piles, leading to numerical inaccuracies. In addition, as observed by Fleming and colleagues, the scope for error when using a number of multiplicative factors taken from charts based on logarithmic scale should be considered.

It is worth noting that there are combinations of slenderness ratio ( $L/d$ ) and stiffness ratio ( $\lambda$ ) beyond which further increase in pile length produces no increase in the load-settlement ratio of the pile, ie the pile starts behaving as if it were infinitely long, with no load reaching the lower region.

An application of the closed-form expression derived from Randolph (1977) to estimate the head settlement of a pile in non-homogeneous elastic soil has been reported by Fleming *et al.* (1992). The details of the input parameters are:

Pile embedded length ( $L$ )	= 14 m
Pile free-standing length ( $g$ )	= 2 m
Pile diameter ( $d$ )	= 0.46 m
Pile Young's modulus ( $E_p$ )	= 25 GPa
Soil Young's modulus at surface ( $E_{s0}$ )	= 25,200 kPa
Rate of increase of soil Young's modulus with depth ( $m$ )	= 3343 kPa
Soil Poisson's ratio ( $\nu_s$ )	= 0.2
Applied axial load ( $P$ )	= 800 kN

The pile-head settlement  $w$  calculated by PGROUPN is:

$$w = 3.51 \text{ mm}$$

which is about 3% more than the value ( $w = 3.40 \text{ mm}$ ) calculated from the closed-form expression developed by Randolph.

Poulos & Davis (1980) have compiled an extensive collection of charts showing how the (elastic) settlement of a pile depends on the various parameters of pile geometry and relative pile-soil stiffness.

The head settlements of a floating pile have been computed as a function of the ratio  $L/d$  and the relative pile-soil stiffness  $K = E_p/E_s$ . The pile (0.5 m in diameter) is loaded by an axial force ( $P$ ) of 10 MN acting at the top and is embedded in a deep homogeneous elastic soil mass with a Young's modulus ( $E_s$ ) of 1 GPa.

Table 4.4 shows the comparison between the pile head settlements predicted by the Poulos & Davis analysis and PGROUPN. It is indicated that the settlement decreases as  $L/d$  and  $K$  increase. Further, as already observed above, the value of  $K$  has greater influence on the pile settlement with increasing  $L/d$ . For the case  $L/d = 25$ , there is an excellent agreement between the two solutions, for both relatively compressible ( $K = 1000$ ) and relatively rigid ( $K = 10,000$ ) pile. For the case  $L/d = 10$  (relatively short pile), the agreement is not as close, even if the predicted settlements from the two solutions are within 3%.

#### 4.3.1.3 Load transfer

For a pile in a deep uniform soil mass, the distributions of shear stress ( $\tau_s$ ) along the shaft predicted by PGROUPN and Butterfield & Banerjee (1971a) are shown in Figs. 4.6 and 4.7 for  $L/d = 20, 80$ , respectively. Again, for the shorter pile ( $L/d = 20$ ), the effect of the stiffness ratio ( $\lambda$ ) is seen to be negligible, and the agreement between solutions is close. Figure 4.7 shows similar curves for a longer pile ( $L/d = 80$ ) with  $\lambda = 60,000$  and  $\lambda = \infty$ , for which the pile is almost incompressible and the shear stresses are relatively uniform. However, for  $\lambda = 6000$ , the longer pile becomes relatively compressible and high shear

stresses occur near the top of the pile. The agreement between the solutions is reasonable, the maximum difference being less than 10%.

Figures 4.8 and 4.9 show the predicted shear stress ( $\tau_s$ ) and axial load ( $P_z$ ) distributions along the shaft of a pile with a  $L/d$  ratio of 25. The results for the homogeneous soil profile are calculated for a relative pile-soil stiffness  $K = E_p/E_s$  of 1000. In the Gibson soil, the soil modulus increases from zero (at the surface) to  $E_{sL} = 2E_s$  at the level of the pile base (where  $E_s$  is the average soil modulus over pile depth). As already observed, for the homogeneous soil, the distribution of shear stress is relatively uniform with depth, whereas for the Gibson soil the shear stresses increase almost linearly with depth. The similarity between the stress distribution and the distribution of soil modulus may justify why load transfer approaches can give good predictions of pile behaviour (Poulos, 1989). An excellent agreement between the two solutions is obtained.

#### 4.3.1.4 Finite-layer depth

The influence of a finite-layer depth ( $H = 2L$ ) on the settlement of a pile in Gibson soil is examined in Fig. 4.10. The pile head settlement ( $w$ ) is expressed in terms of the ratio  $I_p = (wdE_{sL})/P$ , where  $P$  is the applied vertical load and  $E_{sL}$  is the soil modulus at the level of the pile base. The results are calculated for a relative pile-soil stiffness  $K = E_p/E_{sL}$  of 1000, with the soil modulus at the surface assumed to be zero.

Results from the PGROUPN analysis, which is based on the approximate solution of Steinbrenner (1934) (see Section 2.4.1) to allow for the effect of a rigid stratum, are compared with a similar BEM approach proposed by Poulos (1989), a FEM analysis reported by Poulos (1979) and the BEM solution of Banerjee & Davies (1977), which treats the Gibson soil as a series of homogeneous layers — it should be emphasised that the last two solutions are very expensive in terms of computational cost. A good agreement between the solutions is obtained, the greatest potential for differences being for relatively short piles ( $L/d < 20$ ).

#### 4.3.1.5 Critical length

There is a critical length ( $L_c$ ) for a pile subjected to axial loading, beyond which further increase in length produces no further reduction in settlement. This limiting situation

corresponds to the case where the pile starts behaving as if it were infinitely long, with no load reaching the lower region. For a floating pile embedded in a homogeneous soil, the critical length may be given by the approximate expression (Hull, 1987):

$$L_c / d = \left( \frac{\pi K A_p}{d^2} \right)^{0.5} \quad (4.4)$$

where  $A_p$  is the area of pile cross-section and  $K = E_p/E_s$  is the relative pile-soil stiffness.

For circular piles, Equation (4.4) can be written as:

$$L_c / d = 1.57 K^{0.5} \quad (4.5)$$

In order to investigate the agreement between the values of  $L_c$  given by Equation (4.5) and those predicted by PGROUPN, the head settlements of a floating pile in homogeneous soil have been computed as a function of the length-to diameter ratio  $L/d$  and the relative pile-soil stiffness  $K$ .

The head settlements ( $w$ ), as calculated from PGROUPN, are plotted in non-dimensional form in Fig. 4.11 (where  $w_{10}$  is the pile head settlement calculated for  $L/d = 10$ ). From this plot, the values of the pile critical length obtained from the PGROUPN analysis may be extrapolated. These values agree well with the values of  $L_c$  calculated by Hull using Equation (4.5), and reported in Table 4.5.

#### 4.3.1.6 Raking piles

The load-settlement behaviour of a raking pile predicted by the PGROUPN analysis has been compared with that calculated according to the method suggested by Poulos & Davis (1980). The angles of rake employed in the numerical simulation are  $\phi = 15^\circ, 30^\circ$ . The following numerical example has been evaluated:

Pile length ( $L$ )	= 12.5 m
Pile diameter ( $d$ )	= 0.5 m
Pile Young's modulus ( $E_p$ )	= 5000 GPa

Constant soil Young's modulus ( $E_s$ )	= 1 GPa
Applied vertical load ( $P$ )	= 10 MN

Common practice in evaluating the single pile response is to treat the axial and lateral response of the pile separately (Poulos & Davis, 1980; Fleming *et al.*, 1992). Thus, the response of a raking pile to load may be determined by taking the components of load parallel and normal to the pile axis. This approximate procedure is also supported by the analytical work of Evangelista & Viggiani (1976), which shows that the axial and lateral deformation response of a pile is almost independent of the angle that the pile makes with the ground surface, for angles of rake up to about  $30^\circ$ .

Based on these observations, Poulos & Davis derived the following expression to evaluate the vertical head displacement ( $w$ ) of a raking pile under vertical load ( $P$ ):

$$w = \frac{PI_{vV}}{E_s L} \quad (4.6)$$

where:

$$I_{vV} = I_{\rho A} \cos^2 \phi + I_{\rho V} \sin^2 \phi,$$

$$I_{\rho A} = IL/d = 1.975 \quad (\text{from the charts provided by Poulos \& Davis}),$$

$$I_{\rho V} = I_{\rho H} = 8.18 \quad (\text{from the charts provided by Poulos \& Davis}).$$

The values of the pile head settlement ( $w$ ) calculated from Equation (4.6) are reported in Table 4.6. If the same (approximate) procedure of considering the axial and normal components of the applied vertical load is adopted in the PGROUPN analysis, the pile head settlements may be evaluated, as shown in Table 4.6 (refer to PGROUPN (A & N)). In addition, the values obtained from the exact PGROUPN solution are reported.

The three sets of solutions are in excellent agreement for  $\phi = 15^\circ$ , whereas small discrepancies arise from increasing the angle of rake to  $\phi = 30^\circ$ , thereby confirming the observations by Evangelista & Viggiani. It is also of interest to note that the head settlement of the vertical pile ( $\phi = 0$ ) is about one-half of the head settlement of the raking pile with  $\phi = 30^\circ$ .

#### 4.3.1.7 Under-reamed piles

The applicability of the PGROUPN analysis to piles with enlarged bases (under-reamed piles) is examined. In order to analyse the behaviour of an under-reamed pile, the base has been considered as a circular (disc) element of diameter  $d_b$  which can be greater than the shaft diameter ( $d$ ) of the pile. This is an idealisation of a real under-reamed pile, where the effect of friction acting on the surface of the side slope may be significant — usual specifications require that the side slope should make an angle of  $60^\circ$  or more with the under-ream floor (Fleming *et al.*, 1992), as depicted in Fig. 4.12.

Figures 4.13 and 4.14 show the effect of the stiffness ratio ( $\lambda = E_p/G_s$ ) and the slenderness ratio ( $L/d$ ) on the load-settlement behaviour of piles in homogeneous soil over a range of base-to-shaft diameter ratios ( $1 \leq d_b/d \leq 4$ ). The load-settlement ratios calculated by PGROUPN are compared with those predicted by the rigorous analysis of Butterfield & Banerjee (1971a) in which greater accuracy may be achieved by dividing the base into a number of uniformly loaded concentric rings and considering the displacements due to each ring. By comparison, PGROUPN considers a simple circular (disc) element to represent the pile base. In spite of this approximation, the agreement between solutions is close, the maximum difference being about 2% for the relatively long piles ( $L/d = 80$ ). Again, it is worth noting that the effect of  $\lambda$  for the relatively short piles ( $L/d = 20$ ) is negligible.

These differences between solutions are more marked in the prediction of the percentage of the total load carried by the pile base ( $(P_b/P) \times 100$ ), which is slightly underestimated in the more approximate PGROUPN analysis, as depicted in Figs. 4.15 and 4.16 for  $\lambda = 6000$  and  $\lambda = 30,000$ , respectively. However, this divergence becomes less marked for  $L/d$  ratios greater than 20.

#### 4.3.2 Non-linear solution

The numerical experiments undertaken above are valid only for a linear elastic analysis. In reality, at normal working loads (of the order of 40% of the ultimate load), non-linear behaviour of the soil generally does not have considerable influence on single pile (and pile group) settlement. However, as the loading increases, the divergence from elastic conditions becomes more marked and nonlinearity effects result in an increase in the

settlement, especially for relatively compressible piles (Poulos, 1989; Mandolini & Viggiani, 1997).

#### 4.3.2.1 Comparison with FEM and BEM analyses

In comparing non-linear solutions for single pile response to axial loading, the problem examined is that reported by Poulos (1989) in his Rankine Lecture. This numerical example offers an excellent opportunity to validate the PGROUPN approach in the non-linear range and, also, to investigate the influence of soil model.

The test pile is 30 m long, 0.75 m in diameter and is embedded in a homogeneous soil layer 50 m deep. The initial tangent modulus of the soil (for very low strains) is 1056 MPa, Poisson's ratio is assumed to be equal to 0.49, and a constant limiting shaft resistance of 220 kPa is adopted. Two values of pile Young's modulus are considered,  $E_p = 30$  GPa and  $E_p = 30,000$  GPa (the latter would be unrealistically stiff in practice). It has been found that about 200 load increments are sufficient to achieve convergence of the PGROUPN solution process — the resulting CPU time is about 4 s.

Figures 4.17 and 4.18 show the computed pile head load-settlement response, together with the results from a non-linear load-transfer analysis (Guo & Randolph, 1997) and from a FEM analysis (Jardine *et al.*, 1986) involving the use of a non-linear elastic-perfectly plastic soil model, the LPC2 model, in which the Young's modulus decreases markedly from an initial value of 1056 MPa as the axial strain level increases (reaching a value of 83 MPa at an axial strain of 0.2%, at which point the soil yields and then behaves perfectly plastically at a yield stress of 110 kPa). The LPC2 model described by Jardine and colleagues is representative of a stiff low plasticity clay with an overconsolidation ratio of 2. In addition, Figs. 4.17 and 4.18 show the load-settlement curves obtained by Poulos (1989) who performed the following three boundary element analyses: (a) an elastic-perfectly plastic continuum-based interface model (similar to PGROUPN), using a constant soil Young's modulus of 1056 MPa; (b) a hyperbolic non-linear continuum-based interface model, using an initial tangent soil Young's modulus of 1056 MPa and a constant shaft resistance of 220 kPa; (c) a load-transfer approach in which the interface response at each element is elastic-perfectly plastic, the linear portion being derived from the initial tangent soil modulus of 1056 MPa.

It is worth noting that, for the more compressible (and realistic) pile, all the BEM analyses are capable of predicting a very similar load-settlement response to that obtained from the FEM analysis which utilizes a non-linear constitutive model of soil behaviour. For the stiffer pile, the agreement between the curves is not as close, the greatest potential for differences being for loads of more than one-half of the ultimate; in particular, the hyperbolic model (curve (b)) and, to a lesser extent, the FEM model predict larger settlements than the other three solutions. It is clear that, for very stiff piles, the details of the pile-soil interface model have a greater influence on the load-settlement response than for more compressible piles (Poulos, 1989).

It is also of interest to note that PGROUPN calculates a value of the ultimate load ( $P_u$ ) of about 16.6 MN. This value agrees well with that calculated by means of the commonly used formula for ultimate pile capacity:

$$P_u = P_b + P_s = A_b q_b + A_s \bar{\tau}_s = 16.4 \text{ MN} \quad (4.7)$$

where

- $P_b$  = ultimate base capacity,
- $P_s$  = ultimate shaft capacity,
- $A_b$  = area of the pile base,
- $q_b$  = end-bearing pressure,
- $A_s$  = area of the pile shaft,
- $\bar{\tau}_s$  = average limiting shear stress down the pile shaft.

Finally, Fig. 4.19 shows the mobilization of shaft resistance  $\tau_s/C_u$  at a load level  $P/P_u = 0.5$  (where  $P$  is the applied axial load). The results show that the distribution of shear stress predicted by PGROUPN is very consistent with that obtained from the FEM analysis of Jardine and colleagues.

#### 4.4 Piles under lateral loading

For piles subjected to lateral force (and/or moment), the dominant design criteria are the (maximum) pile-head deflection and the maximum bending moment.

The bending moment is required in sizing the pile, and the deflection is important with regard to the serviceability of the supported structure. In addition, the magnitude of the deflection would be instructive in regard to the ability of the soil to respond to somewhat higher loads.

In this section, the validity of the proposed PGROUPN approach for laterally loaded single piles has been verified by comparison with available numerical analyses. First numerical solutions in the linear elastic range are considered, and then the analysis is extended to examine the significant influence of soil nonlinearity.

#### 4.4.1 Linear solution

In practical applications, the deformations and induced bending moments of a pile under lateral load are confined to the upper part of the pile, seldom extending beyond about 10 pile diameters below the ground surface (Randolph, 1981; Fleming *et al.*, 1992). As such, the length of the pile is rarely a relevant parameter when developing solutions for laterally loaded piles, and hence the (linear elastic) behaviour of the pile is mainly governed by the relative stiffness between pile and soil.

In view of this consideration, it should be emphasised that the numerical solutions presented below are valid for all piles which are longer than the critical length ( $L_c$ ) beyond which the pile behaves as if it were infinitely long, ie the pile length no longer affects the response under lateral loading. Such piles are termed 'flexible'.

##### 4.4.1.1 Convergence of numerical solution

In order to investigate the convergence of the numerical solution provided by the PGROUPN program for different values of the number of pile shaft elements ( $N$ ), the head deflection and the maximum bending moment of a free-head floating pile have been calculated over a practical range of pile stiffness ratios, ie  $500 \leq \lambda = E_p/G_s \leq 10^4$  (where  $E_p$  is the pile Young's modulus, which is taken as 25 GPa, and  $G_s$  is the soil shear modulus). The pile (0.5 m in diameter) is loaded by a lateral force of 1 MN acting at the top and is embedded in a deep homogeneous elastic soil mass.

The pile-head deflections and the maximum bending moments calculated from PGROUPN are shown in Tables 4.7 and 4.8, respectively, as a function of  $\lambda$  and  $h/d$  (where

$h$  is the height of the pile shaft element and  $d$  the pile diameter). The following characteristics of behaviour are observed from the PGROUPN analysis:

- (a) Deflections and maximum moments increase with increasing  $h/d$ , ie with decreasing  $N$ ;
- (b) Deflections and maximum moments increase with increasing the pile stiffness ratio  $\lambda$ .

Table 4.7 shows that the pile deflections converge for an aspect ratio of unity ( $h/d = 1$ ). Taking the results for  $h/d = 1$  as the reference solution, Tables 4.7 and 4.8 show that for  $h/d$  ratios of 2, 3 and 4 the pile deflections are overestimated by 4%, 15% and 39%, respectively, and the corresponding maximum moments are overpredicted by 9%, 17% and 25%, respectively. These values refer to the mean of the percentage values over each  $\lambda$ .

It is worth noting that, for the laterally loaded pile, the accuracy of pile discretization has a greater influence on the solution than for the case of an axially loaded pile, especially for more compressible piles.

It may be concluded from this study that the correct number  $N$  of shaft elements to discretize a laterally loaded pile appears to be:

$$N = \frac{L}{d} \quad (4.8)$$

which corresponds to an aspect ratio of unity (ie  $h/d = 1$ ). An aspect ratio of unity has also been employed in a similar work by Davies & Budhu (1986) and Lee (1997).

#### 4.4.1.2 Pile deflection

A parametric study has been performed for laterally loaded free-head piles in homogeneous and Gibson soils. In order to avoid needing different solutions for different values of Poisson's ratio ( $\nu_s$ ), Randolph (1981) introduced a modulus  $G_s^*$  as follows:

$$G_s^* = G_s(1 + 3\nu_s / 4) \quad (4.9)$$

where  $G_s$  is the soil shear modulus. The analogous expression for Gibson soil is:

$$m^* = m(1 + 3\nu_s / 4) \quad (4.10)$$

where  $m$  is the rate of increase of shear modulus with depth. In the solutions presented below, the soil shear modulus at ground level is assumed to be zero for the Gibson soil.

Figure 4.20 shows a comparison of the computed head deflections ( $u$ ) of a pile ( $r_o$  in radius) subjected to lateral force ( $H$ ) and embedded in homogeneous soil. Some discrepancies are observed between the results predicted by PGROUPN and the finite element fitted algebraic expressions of Randolph (1981). This divergence may, in part, be attributed to the different idealization of the pile when considering lateral loads: in the three-dimensional analysis of Randolph, bearing stress on the front face of the pile, shear stress along the sides and tension stress in the soil adjacent to the back face of the pile are all taken into account, whereas in PGROUPN the pile is assumed to be a thin rectangular strip and only the stress on the compressive face is considered. This may partially explain why the pile deflections predicted by PGROUPN are generally greater than those predicted by a three-dimensional analysis. Such an approximation simplifies the analysis and results in significant savings in computational costs, especially if soil nonlinearity is to be considered in pile group problems. Over the range of pile stiffness ratios commonly encountered in practice ( $500 \leq \lambda^* = E_p/G_s^* \leq 10^4$ ), the discrepancies between PGROUPN and Randolph predictions vary from 27% (at  $\lambda^* = 500$ ) to 8% (at  $\lambda^* = 10^4$ ).

Better agreement is found with the BEM analysis of Poulos (1971a), in which the pile is idealized as a rectangular thin strip. It is worth noting that the results of Poulos show some dependence of the predicted pile deflections on the pile length, even for relatively flexible piles where the pile length should not affect the ground level deflections. This divergence may partially be attributed to numerical inaccuracies of the solution due to a coarse discretizing of the longer piles (Randolph, 1981; Evangelista & Viggiani, 1976).

Figure 4.21 shows similar trends for the ground level deformations of laterally loaded piles in Gibson soil. It should be emphasised that in the BEM analysis of Poulos

(1973) the displacement of a point is obtained from the Mindlin solution using the elastic moduli at that point, whereas the BEM analysis of Banerjee & Davies (1978) adopts a more rigorous numerical approach to account for soil inhomogeneity, ie it employs the solution of Chan *et al.* (1974) for a layered half space.

#### 4.4.1.3 Load transfer

Figures 4.22-4.23 (free-head pile) and Fig. 4.24 (fixed-head pile) show typical moment distributions along a pile ( $L/d = 25$ ) subjected to lateral force ( $H$ ) or moment ( $M$ ) and embedded in a homogeneous soil. The profiles of normalized bending moments are evaluated as a function of a stiffness ratio ( $K_R$ ), defined as follows (Poulos, 1971a):

$$K_R = \frac{E_p I_p}{E_s L^4} \quad (4.11)$$

where  $I_p$  is the second moment of area of the pile and  $E_s$  is the soil Young's modulus. The results are plotted for a stiffness ratio  $K_R = 1$ , which corresponds to a very stiff pile, and for  $K_R = 10^{-4}$ , which corresponds to piles commonly encountered in practice, ie flexible piles. It is worth noting the pronounced effects of variation of  $K_R$  on the two sets of solutions. The agreement with the BEM analysis of Poulos & Davis (1980) is close. It should be emphasised that, for a fixed-head pile, the maximum moment occurs at the pile head where the restraint is provided.

#### 4.4.1.4 Critical length

A value of the critical length ( $L_c$ ) for laterally loaded single piles has been deduced from the finite element analyses of Randolph (1981):

$$L_c = 2 r_o (E_p / G_s^*)^{2/7} \quad (\text{Homogeneous soil}) \quad (4.12)$$

$$L_c = 2 r_o (E_p / m * r_o)^{2/9} \quad (\text{Gibson soil}) \quad (4.13)$$

where  $G_s^*$  and  $m^*$  have been defined in Equations (4.9) and (4.10), respectively.

In order to investigate the agreement between these values and those predicted by PGROUPN, the head deflections of a pile in a homogeneous soil have been computed as a function of the length-to diameter ratio  $L/d$  and over a practical range of pile stiffness ratios, ie  $500 \leq \lambda^* = E_p/G_s^* \leq 10^4$ . The pile head deflections ( $u$ ), as calculated from PGROUPN, are plotted in non-dimensional form in Fig. 4.25 (where  $u_d$  is the pile deflection calculated for  $L/d = 4$ ). From this plot, the values of the pile critical length obtained from the PGROUPN analysis may be extrapolated. These values agree well with the values of  $L_c$  calculated by Randolph using Equation (4.12), and reported in Table 4.9.

#### 4.4.1.5 Raking piles

Raking piles are often used to provide the necessary support to structures which are subjected to lateral forces. The load-deflection behaviour of a raking pile predicted by the PGROUPN analysis has been compared with that calculated according to the method suggested by Poulos & Davis (1980), similarly to the vertically loaded case. The angles of rake employed in the numerical simulation are  $\phi = 15^\circ, 30^\circ$ . The following numerical example has been evaluated:

Pile length ( $L$ )	= 12.5 m
Pile diameter ( $d$ )	= 0.5 m
Pile Young's modulus ( $E_p$ )	= 5000 GPa
Constant soil Young's modulus ( $E_s$ )	= 1 GPa
Applied horizontal load ( $H$ )	= 10 MN

By taking the components of load parallel and normal to the pile axis, Poulos & Davis derived the following expression to evaluate the horizontal displacement ( $u$ ) of a raking pile under horizontal load ( $H$ ):

$$u = \frac{HI_{MH}}{E_s L} \quad (4.14)$$

where:

$$I_{hH} = I_{\rho A} \sin^2 \phi + I_{\rho N} \cos^2 \phi,$$

$$I_{\rho A} = IL/d = 1.975 \quad (\text{from the charts provided by Poulos \& Davis}),$$

$$I_{\rho N} = I_{\rho H} = 8.18 \quad (\text{from the charts provided by Poulos \& Davis}).$$

Table 4.10 shows the values of the pile head deflection ( $u$ ) calculated from Equation (4.14). If the same (approximate) procedure of considering the axial and normal components of the applied horizontal load is adopted in the PGROUPN analysis, the pile head deflections may be evaluated, as shown in Table 4.10 (refer to PGROUPN (A & N)). In addition, the values obtained from the exact PGROUPN solution are reported.

The agreement between the three sets solutions is satisfactory for  $\phi = 15^\circ$ , whereas the differences become more significant for  $\phi = 30^\circ$ .

#### 4.4.1.6 Rigid piles

If the pile length is less than its critical length, the pile is termed 'rigid'. The behaviour of a laterally loaded rigid pile embedded in a homogeneous elastic soil has been studied and a comparison between the results predicted by PGROUPN (which is based on an indirect BEM approach) and those obtained by the direct BEM approach of Abedzadeh & Pak (1995) is presented.

For a single pile subjected to lateral loading, the stiffness matrix  $[K]$  can be expressed as:

$$\begin{Bmatrix} H \\ M \end{Bmatrix} = \begin{bmatrix} K_{HH} & K_{HM} \\ K_{MH} & K_{MM} \end{bmatrix} \begin{Bmatrix} u \\ \vartheta \end{Bmatrix}$$

where  $H$ ,  $M$ ,  $u$  and  $\vartheta$  are respectively the lateral load, the applied bending moment, the lateral displacement and the rotation at the top of the pile.

Abedzadeh & Pak have calculated the elements of the  $[K]$  matrix for a rigid short pile embedded in a homogeneous elastic half-space by means of an exact BEM formulation, which involves the solution of three coupled Fredholm integral equations at the pile-soil

interface. These stiffness coefficients are shown in Fig. 4.26 as a function of the  $L/d$  ratio, together with the values obtained from PGROUPN (using a very high value of the pile modulus  $E_p$  to simulate a rigid pile). Consistent with Maxwell's reciprocal theorem, the values of  $K_{HM}$  and  $K_{MH}$  cannot be distinguished graphically at this scale.

It is worth noting that the percentage difference between the two solutions decreases as the  $L/d$  ratio increases. One possible explanation of this divergence for low values of  $L/d$ , which correspond to very short piles, is that the treatment of the base is different: in PGROUPN the base is assumed to be smooth (ie zero tractions), while Abedzadeh & Pak demonstrate that the tractions are infinite at the base. It may be concluded that, for practical pile geometries (typically  $L/d > 20$ ), the results obtained here justify the simplifications arising from the assumption of a smooth base.

#### 4.4.2 Non-linear solution

It is widely recognised that a linear analysis is of limited validity for laterally loaded piles since the actual load-deflection behaviour is markedly non-linear, even at low load levels.

##### 4.4.2.1 Comparison with a BEM analysis

Poulos & Davis (1980) proposed a series of BEM solutions which enable the load-deflection behaviour of a laterally loaded pile to be calculated, assuming the soil to be an elastic-perfectly plastic material (such as in the PGROUPN analysis). The theoretical results are presented as a series of graphs of elastic influence factors (already utilised for some of the comparisons in Section 4.4.1) and modification factors for soil yield. Using these graphs, the non-linear load-deflection behaviour of a relatively rigid ( $K_R = 10^{-2}$ ) and relatively flexible ( $K_R = 10^{-4}$ ) pile in homogeneous soil has been calculated, as shown in Figs. 4.27 and 4.28, respectively. The details of the input parameters are as follows:

Pile length ( $L$ )	= 25 m
Pile diameter ( $d$ )	= 0.5 m
Pile Young's modulus ( $E_p$ )	= 25 GPa

$$E/C_u = 200$$

For the PGROUPN analyses, it has been found that about 100 load increments are sufficient to achieve convergence of the solution process — the resulting CPU time is about 3 s. For consistency with the Poulos & Davis analysis, the PGROUPN program has been modified in order to adopt an uniform profile of the limiting lateral pressure along the whole length of the pile, ie  $t_{sc} = 9C_u$  (refer to Section 2.4.4). In addition, it must be remembered that, in the numerical simulations described in this thesis, the effects of pile yielding are not considered, ie the pile is assumed to remain elastic.

Figures 4.27 and 4.28 show the typical features of behaviour of laterally loaded piles: for relatively rigid piles ( $K_R = 10^2$ ), the effect of soil yielding is relatively unimportant, and an elastic solution may be adequate to predict deflections at ordinary working loads; for relatively flexible piles ( $K_R = 10^4$ ), which are the piles commonly encountered in practice, the consideration of local yield of the soil is essential, even for low load levels. The agreement with the Poulos & Davis analysis is satisfactory, with a general tendency of PGROUPN to predict smaller head deflections.

Figure 4.29 shows the profile of the normalized bending moments along a relatively rigid pile ( $K_R = 10^2$ ) subjected to lateral force ( $H$ ) and embedded in a homogeneous soil. Poulos & Davis presented their results for different load levels  $H/H_u$ , where the ultimate lateral load capacity of the pile  $H_u$  (if failure occurs by failure of the soil) is deduced from statical considerations. For the input parameters described above (with the only difference that the pile length is 12.5 m), the value of  $H_u$  deduced from the graphs by Poulos & Davis is 362 kN. It is worth noting that, at failure, the maximum value of normalized moment ( $M_z/HL$ ) is about twice the elastic value (ie that for  $H/H_u \leq 0.38$ ). A generally good agreement between solutions is observed.

#### 4.5 Concluding remarks

A generally good agreement has been found by comparing the axial and lateral response of single piles obtained from the proposed PGROUPN approach with that derived from available numerical solutions in the linear elastic and non-linear range. Having validated the PGROUPN program for single piles (where existing numerical methods are

successful), it is now possible to proceed with greater confidence to the analysis of pile groups, where current numerical approaches are deficient.

As regards pile discretization, a number of pile shaft elements which corresponds to a height-to-diameter ratio  $h/d$  of 2 has been found to be suitable to evaluate the single-pile axial response, whereas a  $h/d$  ratio of 1 is recommended for the single-pile lateral response, regardless of the total pile length.

In the non-linear analyses, the number of load increments which is necessary to achieve convergence of the solution process is relatively small. In fact, from the numerical simulations described above, it has been found that about 200 load increments are sufficient in the evaluation of the axial response, whereas about 100 load increments are adequate for the lateral response. This results in negligible computational costs for the case of single piles.

## TABLES CHAPTER 4

Table 4.1 Typical values of  $K = E_p/E_s$  for solid piles (after Poulos & Davis, 1980) (NOTE: For hollow or H-piles, multiply these values by the ratio of area of pile section  $A_p$  to area bounded by outer circumference of pile).

Soil type	Pile material	
	Steel	Concrete
Soft clay	60,000	6000
Medium clay	20,000	2000
Stiff clay	3000	300
Loose sand	15,000	1500
Dense sand	5000	500

Table 4.2 Test of convergence for head settlements (in mm) of single pile in homogeneous soil with  $L/d = 25$  (NOTE: The 'shaded' area represents non-admissible values of the  $h/d$  ratio, ie those values which produce oscillations of shear stresses along the pile).

K	h/d							
	1	1.5	1.75	2	2.5	3	4	6
10,000	1.62	1.58	1.54	1.53	1.52	1.51	1.50	1.50
1000	1.83	1.79	1.75	1.74	1.73	1.72	1.71	1.71
100	3.32	3.25	3.22	3.21	3.20	3.19	3.20	3.23

Table 4.3 Test of convergence for head settlements (in mm) of single pile in homogeneous soil with  $K = 1000$  (NOTE: The 'shaded' area represents non-admissible values of the  $h/d$  ratio, ie those values which produce undulations of shear stresses along the pile).

$L/d$	$h/d$							
	1	1.5	1.75	2	2.5	3	4	6
50	1.35	1.31	1.31	1.30	1.30	1.29	1.29	1.29
25	1.83	1.79	1.75	1.74	1.73	1.72	1.71	1.71
10	3.24	3.14	3.04	3.02	2.99	2.96	2.94	2.93

Table 4.7 Test of convergence for head deflections (in cm) of flexible pile in homogeneous soil.

Table 4.4 Comparison between solutions for head settlements (in mm) of single pile in homogeneous soil.

$K$	PGROUPN	Poulos & Davis (1980)	PGROUPN	Poulos & Davis (1980)
	$L/d = 25$	$L/d = 25$	$L/d = 10$	$L/d = 10$
10,000	1.53	1.52	2.93	2.86
5000	1.55	1.54	2.94	2.86
1000	1.74	1.72	3.02	2.93

Table 4.8 Test of convergence for maximum bending moment (in kNm) along a flexible pile in homogeneous soil.

Table 4.5 Values of the critical slenderness ratio ( $L_c/d$ ) proposed by Hull (1987) for piles in homogeneous soil.

$K = E_p/E_s$	100	1000	10,000
$L_c/d$	15.7	49.6	157.2

Table 4.6 Comparison between solutions for head settlements ( $w$ ) of single pile in homogeneous soil as a function of the pile rake ( $\phi$ ).

$\phi$	$w$ (mm)		
	PGROUPN	PGROUPN (A & N)	Poulos & Davis (1980)
0	1.55	1.55	1.58
15°	1.92	1.91	1.91
30°	3.02	2.89	2.82

Table 4.7 Test of convergence for head deflections (in cm) of flexible pile in homogeneous soil.

$\lambda$	$h/d$							
	0.5	1	1.5	2	2.5	3	4	6
500	0.92	0.91	0.94	1.00	1.07	1.23	1.66	3.57
5000	5.88	5.76	5.78	5.85	5.95	6.14	6.61	8.39
10,000	10.2	10.0	10.0	10.1	10.2	10.4	10.9	12.8

Table 4.8 Test of convergence for maximum bending moment (in kNm) along a flexible pile in homogeneous soil.

$\lambda$	$h/d$							
	0.5	1	1.5	2	2.5	3	4	6
500	320	316	355	384	396	409	432	526
5000	608	606	615	595	635	688	737	777
10,000	735	727	724	745	722	779	856	917

Table 4.9 Values of the critical slenderness ratio ( $L_c/d$ ) proposed by Randolph (1981) for piles in homogeneous soil.

$\lambda^* = E_p / G_s^*$	500	5000	10,000
$L_c/d$	5.9	11.4	13.9

Table 4.10 Comparison between solutions for deflections ( $u$ ) of single pile in homogeneous soil as a function of the pile rake ( $\phi$ ).

$\phi$	$u$ (mm)		
	PGROUPN	PGROUPN (A & N)	Poulos & Davis (1980)
0	6.93	6.93	6.54
15°	6.68	6.56	6.21
30°	5.95	5.59	5.30

### FIGURES CHAPTER 4

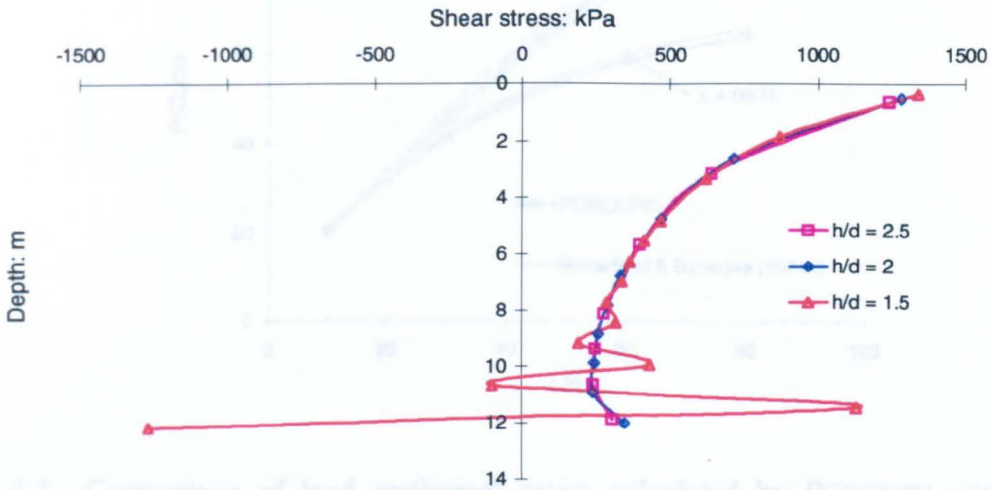


Fig. 4.1 Distribution of shear stress along an axially loaded pile ( $K = 100$ ) in homogeneous soil.

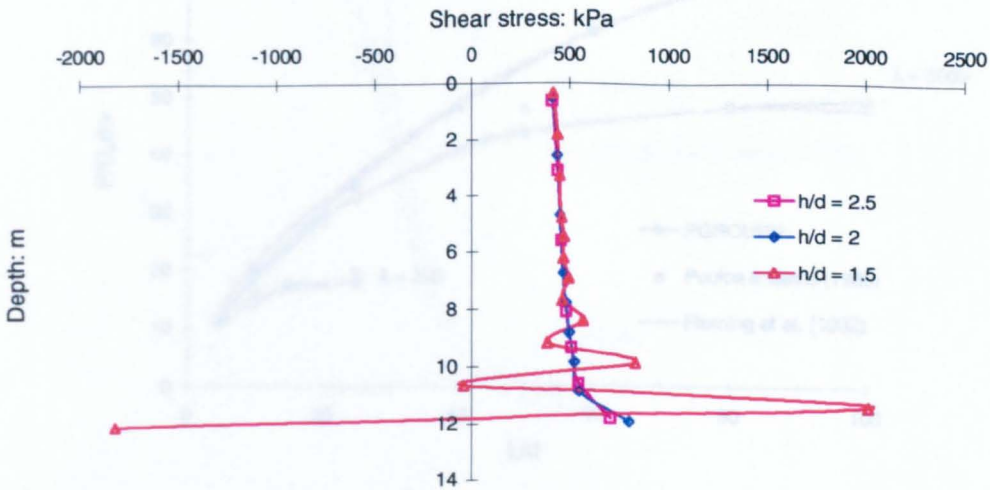


Fig. 4.2 Distribution of shear stress along an axially loaded pile ( $K = 10,000$ ) in homogeneous soil.

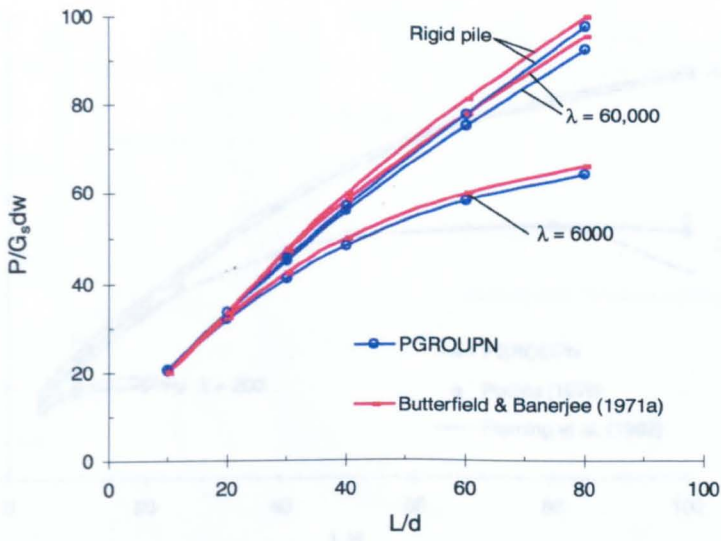


Fig. 4.3 Comparison of load settlement ratios calculated by PGROUPN with that of Butterfield & Banerjee (1971a) for single pile in homogeneous soil.

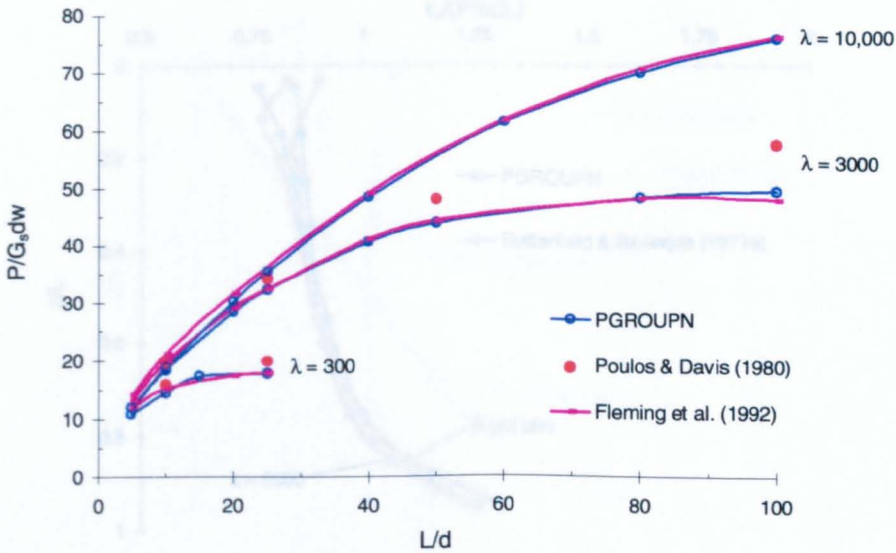


Fig. 4.4 Comparison of load settlement ratios calculated by PGROUPN with those of Fleming *et al.* (1992) and Poulos & Davis (1980) for single pile in homogeneous soil.

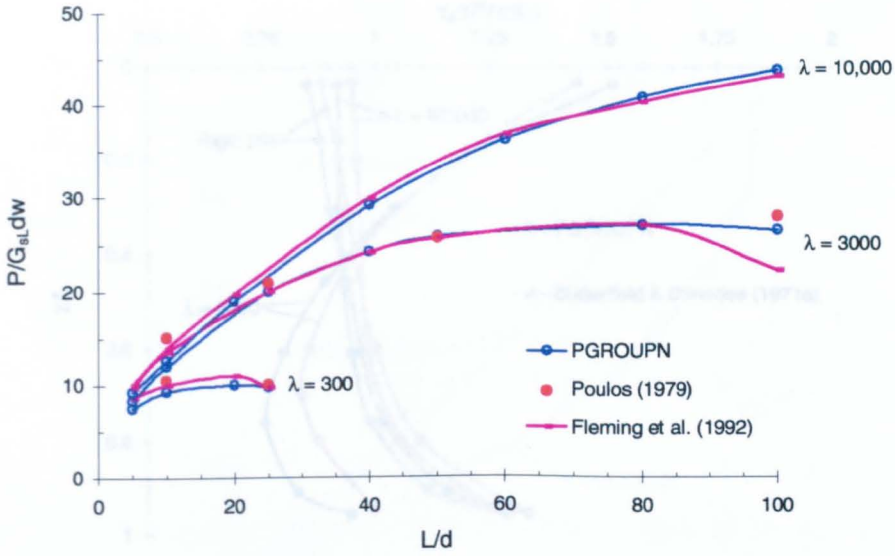


Fig. 4.5 Comparison of load settlement ratios calculated by PGROUPN with those of Fleming *et al.* (1992) and Poulos (1979) for single pile in Gibson soil.

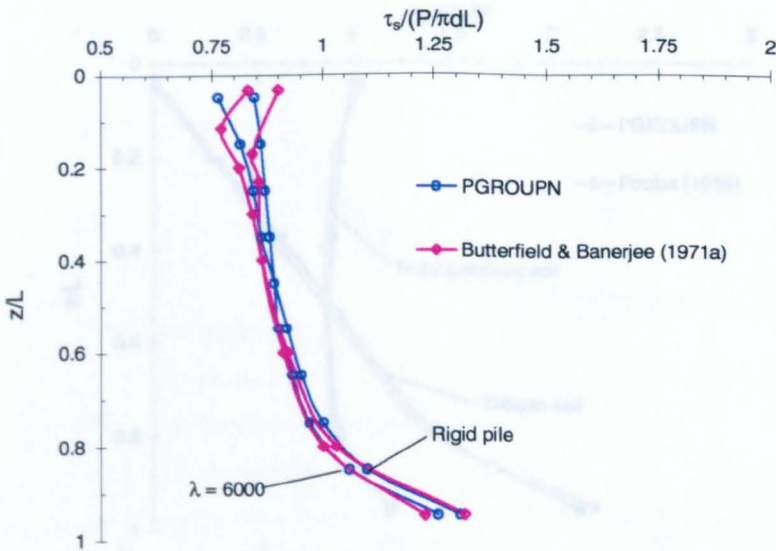


Fig. 4.6 Comparison of shaft shear stress distribution calculated by PGROUPN with that of Butterfield & Banerjee (1971a) for single pile ( $L/d = 20$ ) in homogeneous soil.

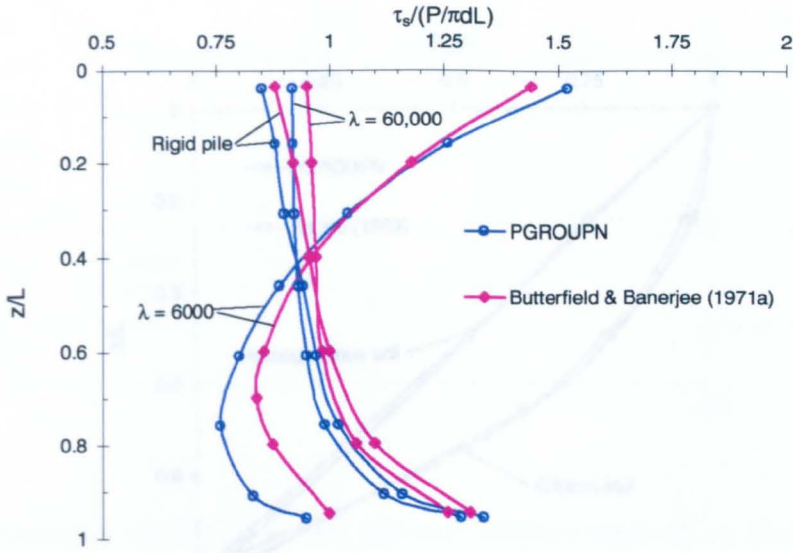


Fig. 4.7 Comparison of shaft shear stress distribution calculated by PGROUPN with that of Butterfield & Banerjee (1971a) for single pile ( $L/d = 80$ ) in homogeneous soil.

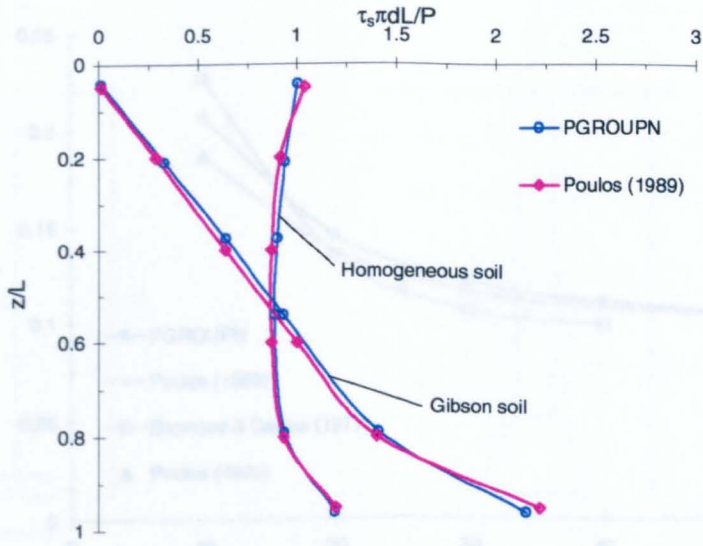


Fig. 4.8 Comparison of shaft shear stress distribution calculated by PGROUPN with that of Poulos (1989) for single pile ( $L/d = 25$ ) in homogeneous and Gibson soils.

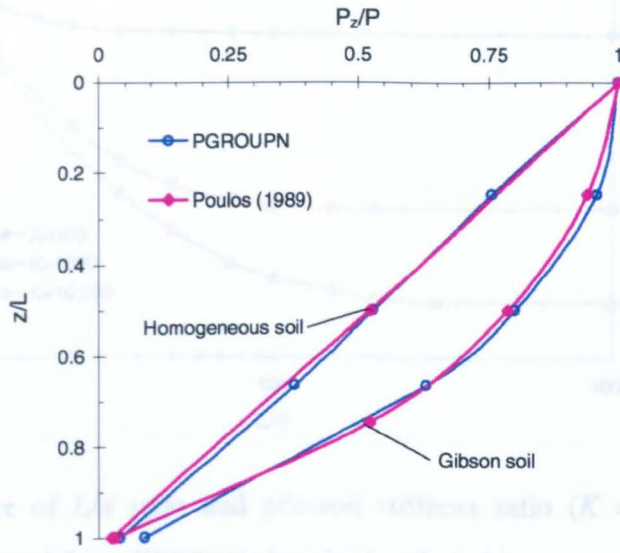


Fig. 4.11 Influence of  $L/d$  on axial load distribution (NOTE:  $v_{10}$  is the pile head settlement for  $L/d=10$ ).

Fig. 4.9 Comparison of axial load distribution calculated by PGROUPN with that of Poulos (1989) for single pile ( $L/d = 25$ ) in homogeneous and Gibson soil.

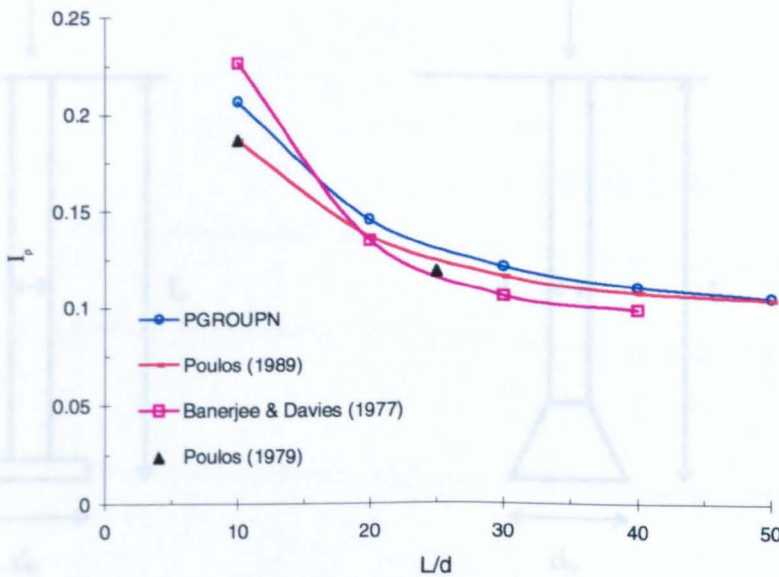


Fig. 4.10 Comparison between solutions for head settlement of single pile in Gibson soil layer of finite depth ( $H = 2L$ ).

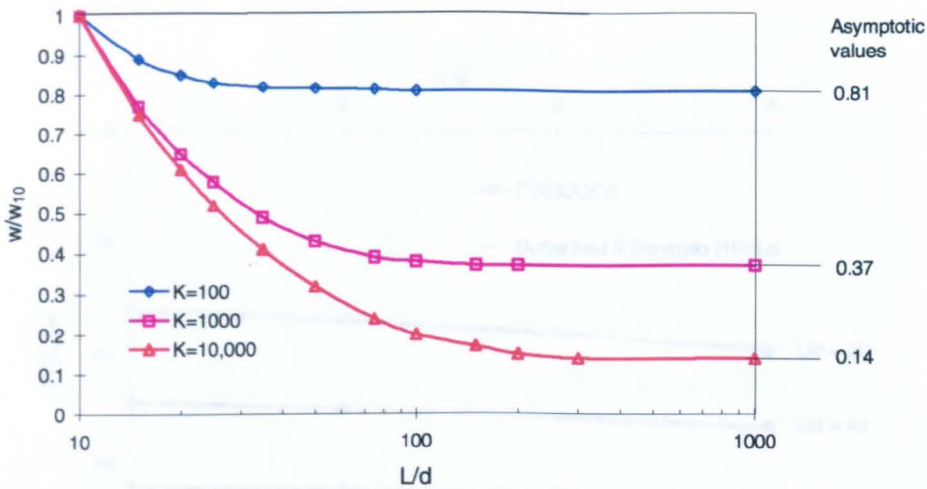


Fig. 4.11 Influence of  $L/d$  ratio and pile-soil stiffness ratio ( $K = E_p/E_s$ ) on pile head settlement ( $w$ ) calculated from PGROUPN for single pile in homogeneous soil (NOTE:  $w_{10}$  is the pile head settlement for  $L/d = 10$ ).

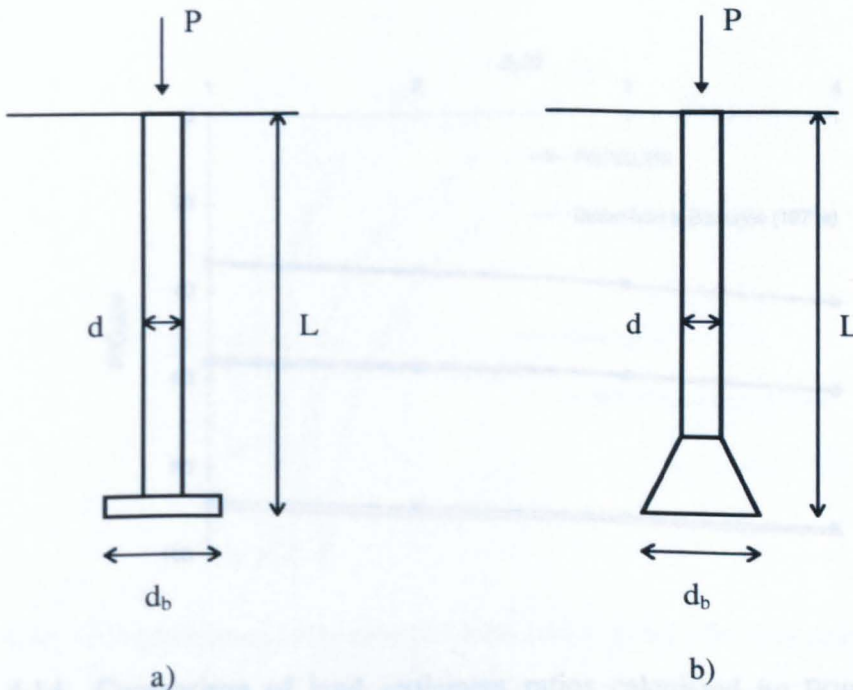


Fig. 4.12 a) PGROUPN idealisation of an under-reamed pile; b) typical under-reamed pile.

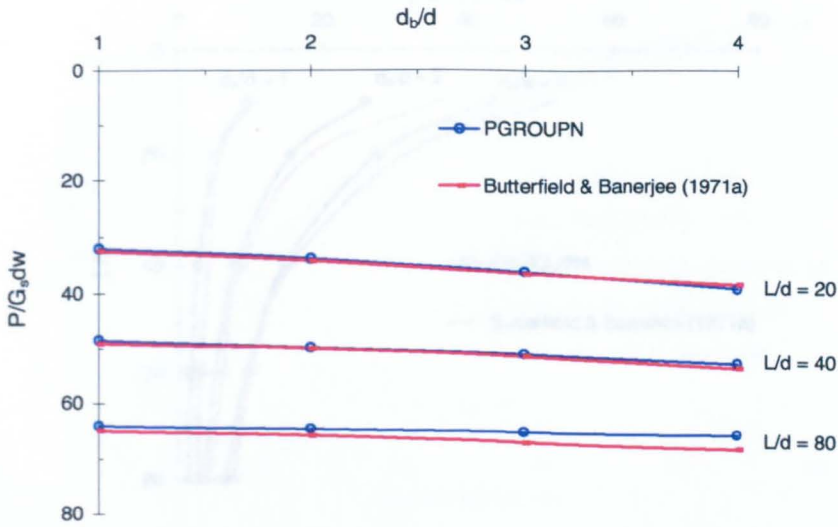


Fig. 4.13 Comparison of proportion of load taken up by pile base calculated by PGROUPN

Fig. 4.13 Comparison of load settlement ratios calculated by PGROUPN with that of Butterfield & Banerjee (1971a) for under-reamed piles ( $\lambda = 6000$ ) in homogeneous soil.

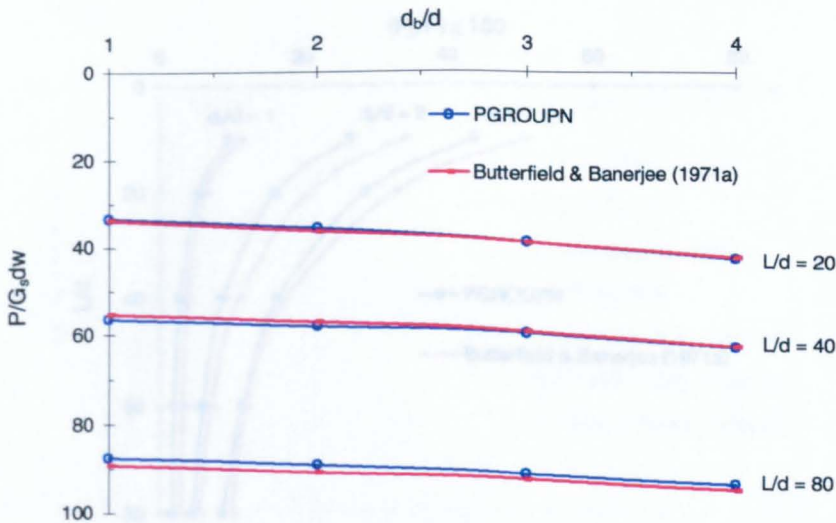


Fig. 4.14 Comparison of proportion of load taken up by pile base calculated by PGROUPN

Fig. 4.14 Comparison of load settlement ratios calculated by PGROUPN with that of Butterfield & Banerjee (1971a) for under-reamed piles ( $\lambda = 30,000$ ) in homogeneous soil.

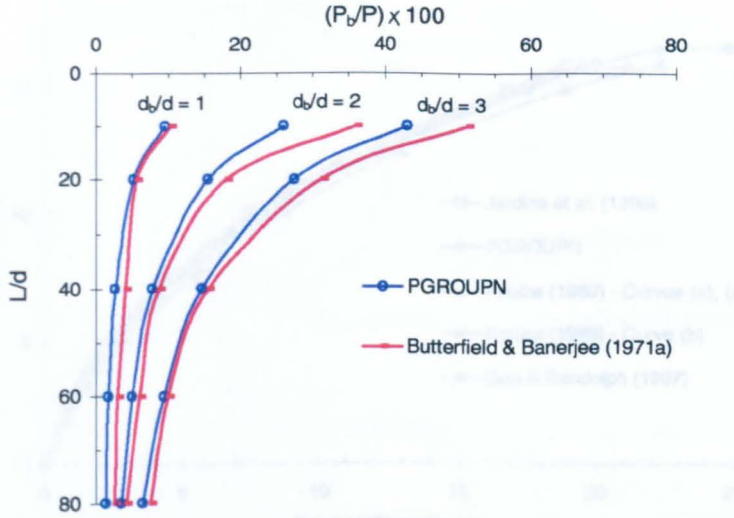


Fig. 4.15 Comparison of proportion of load taken up by pile base calculated by PGROUPN with that of Butterfield & Banerjee (1971a) for under-reamed piles ( $\lambda = 6000$ ) in homogeneous soil.

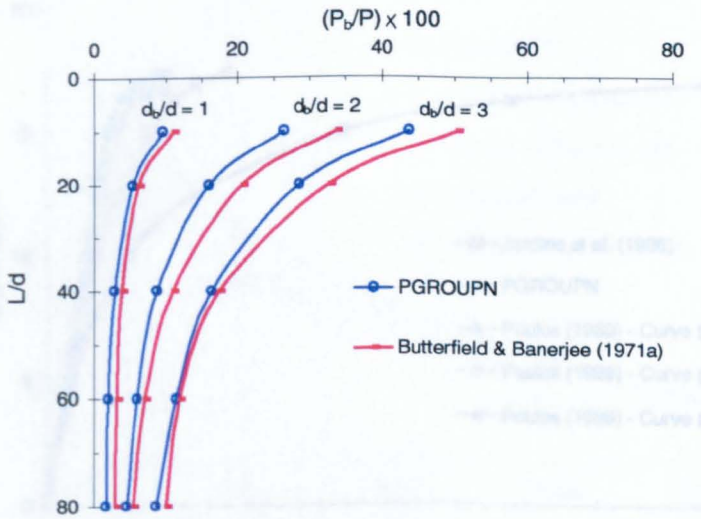


Fig. 4.16 Comparison of proportion of load taken up by pile base calculated by PGROUPN with that of Butterfield & Banerjee (1971a) for under-reamed piles ( $\lambda = 30,000$ ) in homogeneous soil.

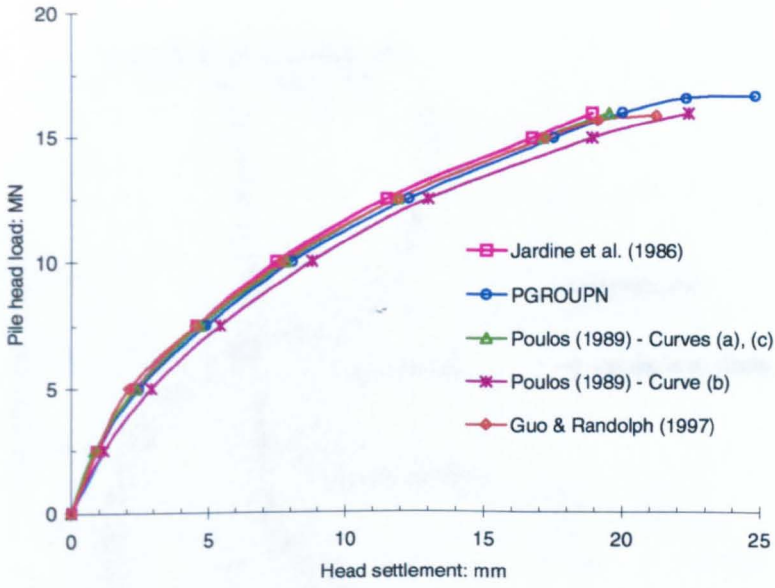


Fig. 4.17 Comparison of load-settlement response for single pile ( $E_p = 30$  GPa) in homogeneous soil.

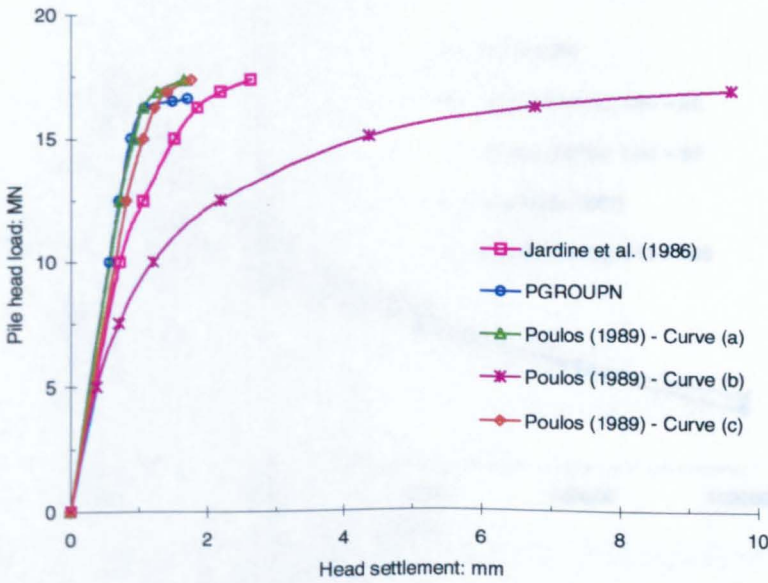


Fig. 4.18 Comparison of load-settlement response for single pile ( $E_p = 30,000$  GPa) in homogeneous soil.

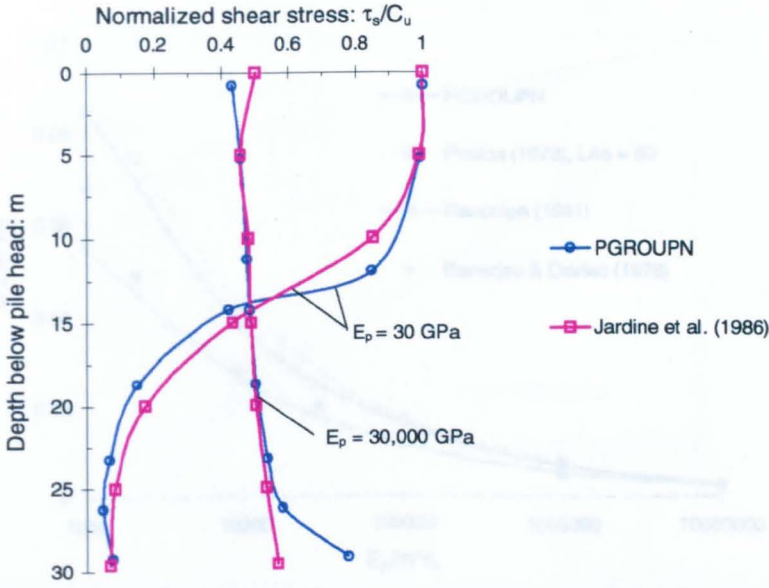


Fig. 4.19 Comparison of shaft shear stress distribution calculated by PGROUPN with that of Jardine *et al.* (1986) at a load level  $P/P_u = 0.5$  in homogeneous soil conditions.

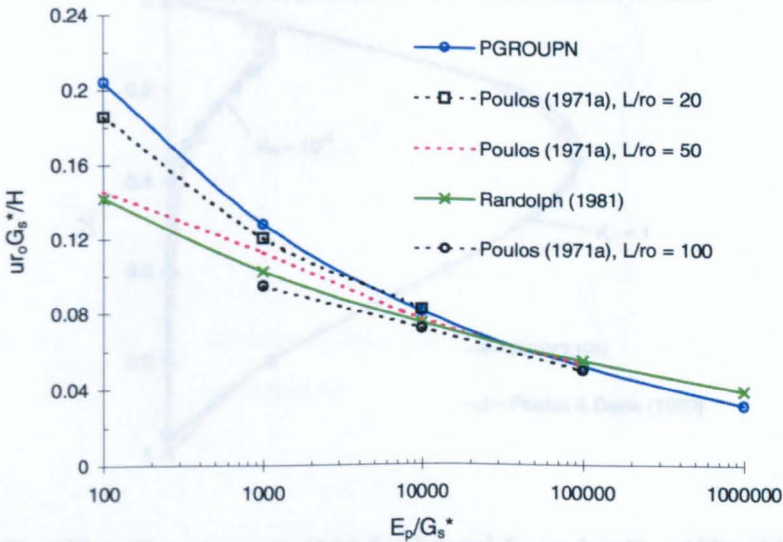


Fig. 4.21 Profile of bending moments  $(M_z)$  for lateral force loading  $(H)$  of free-head pile in

Fig. 4.20 Pile head deflection ( $u$ ) due to lateral force ( $H$ ) for homogeneous soil conditions.

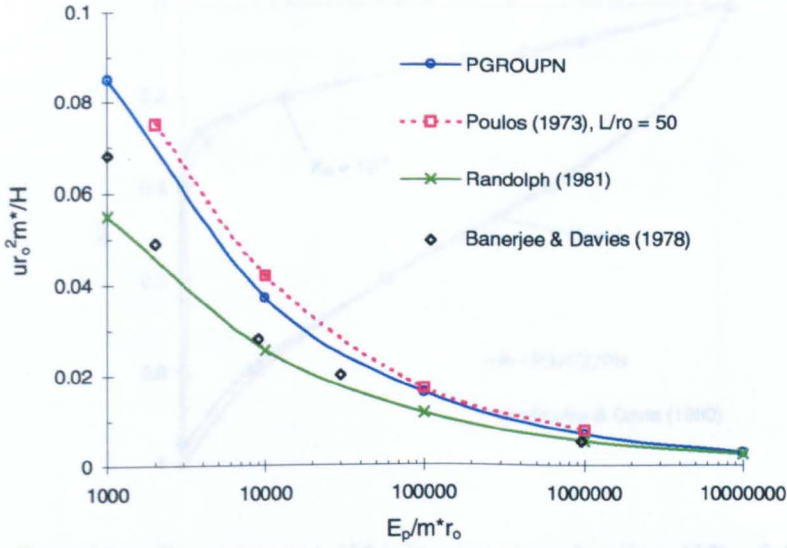


Fig. 4.21 Pile head deflection ( $u$ ) due to lateral force ( $H$ ) for Gibson soil conditions.

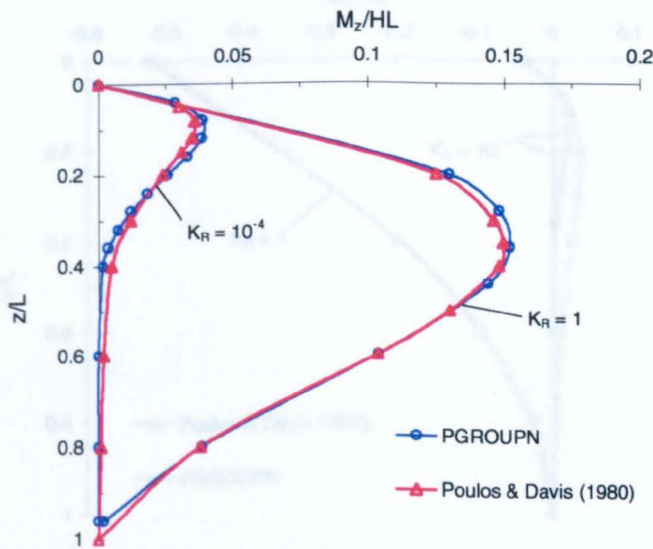


Fig. 4.22 Profile of bending moment ( $M_z$ ) for lateral force loading ( $H$ ) of free-head pile in homogeneous soil.

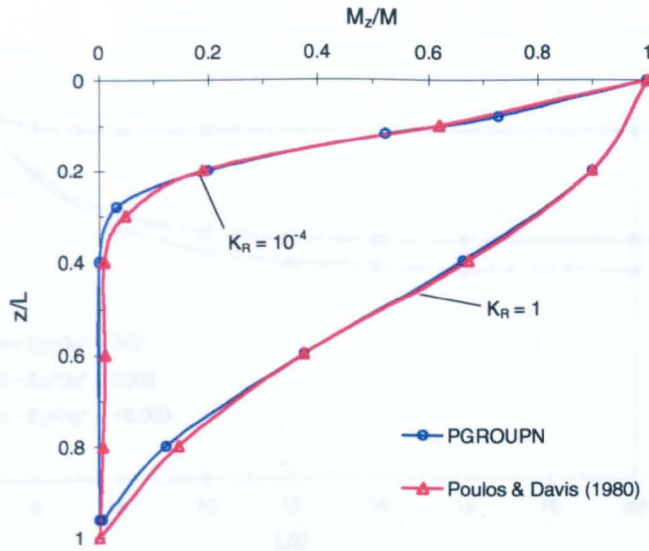


Fig. 4.23 Profile of bending moment ( $M_z$ ) for moment loading ( $M$ ) of free-head pile in homogeneous soil.

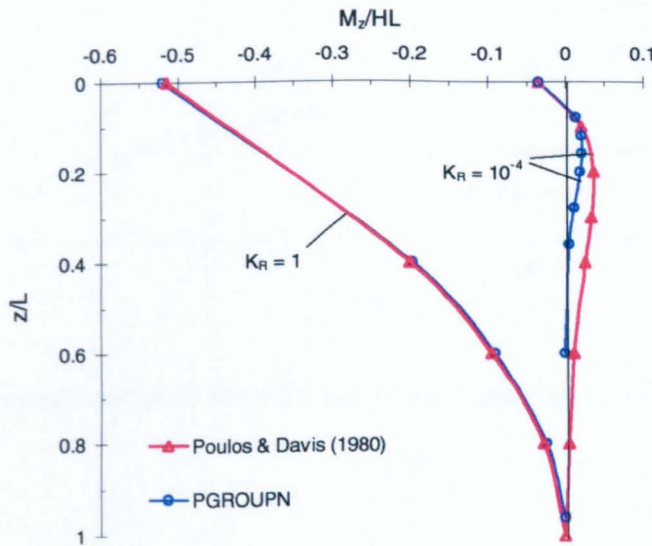


Fig. 4.24 Profile of bending moment ( $M_z$ ) for lateral force loading ( $H$ ) of fixed-head pile in homogeneous soil.

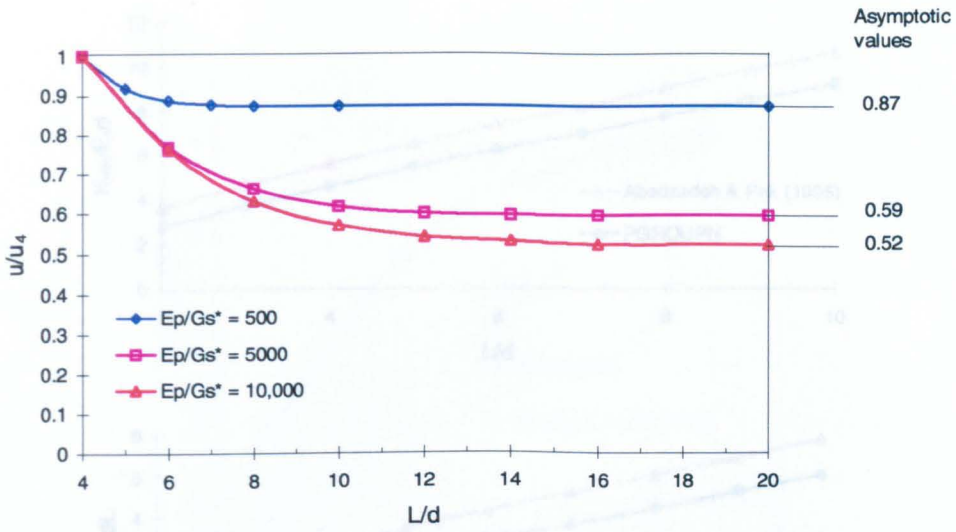


Fig. 4.25 Influence of  $L/d$  ratio and pile stiffness ratio ( $E_p/G_s^*$ ) on pile head deflection ( $u$ ) calculated from PGROUPN for single pile in homogeneous soil (NOTE:  $u_4$  is the pile head deflection for  $L/d = 4$ ).



Fig. 4.26 Stiffness coefficients of laterally loaded rigid piles ( $K = \infty$ ) in homogeneous soil.

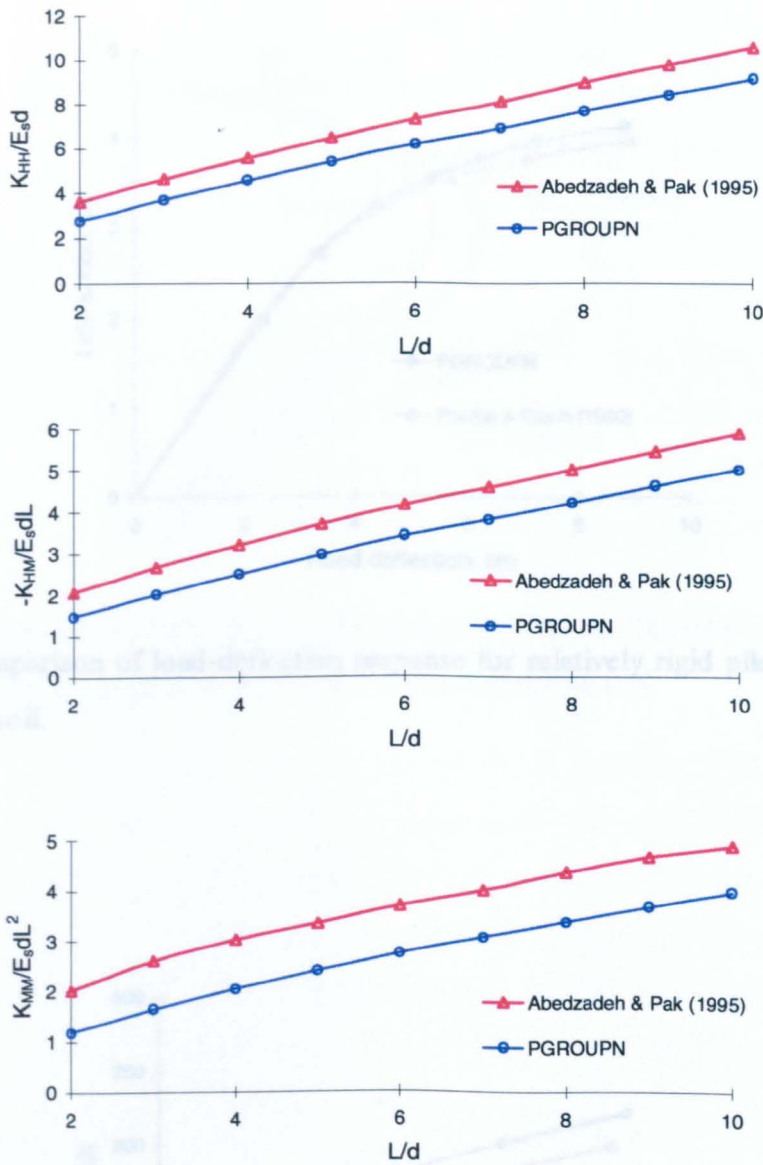


Fig. 4.26 Stiffness coefficients of laterally loaded rigid piles ( $K = \infty$ ) in homogeneous soil.

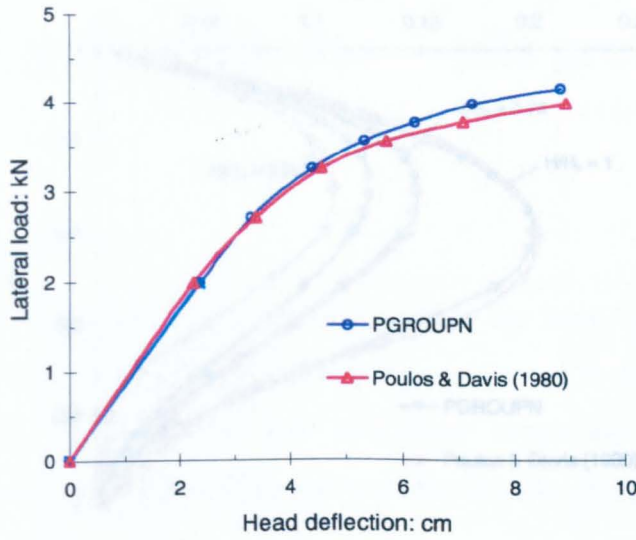


Fig. 4.27 Comparison of load-deflection response for relatively rigid pile ( $K_R = 10^{-2}$ ) in homogeneous soil.

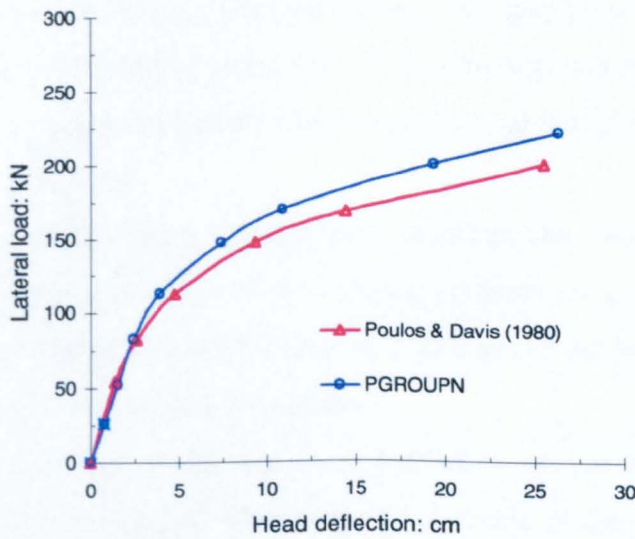


Fig. 4.28 Comparison of load-deflection response for relatively flexible pile ( $K_R = 10^{-4}$ ) in homogeneous soil.

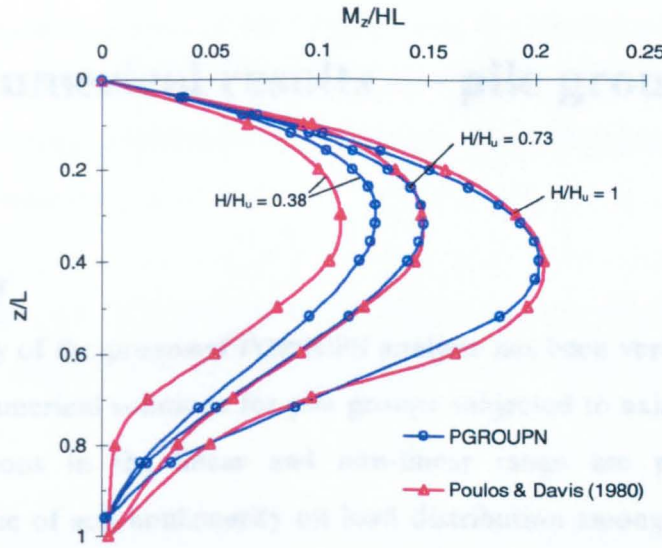


Fig. 4.29 Influence of local yield on bending moments of free-head pile ( $K_R = 10^{-2}$ ) subjected to lateral force ( $H$ ) and embedded in homogeneous soil.

The PGROUPN program has proved capable of matching the results of other methods of analysis for the problem of a single pile under axial or lateral loading. However, as the majority of pile foundations will consist not of a single pile but of a group of piles, it is essential to study the effects of interaction between neighbouring piles in a group. In fact, it has long been recognised that groups of piles tend to deform more than a proportionally loaded single pile. This is because neighbouring piles will be within each others' displacement fields and hence the load per pile to generate a given displacement will be reduced.

In the linear elastic range, this Chapter examines the validity of the proposed approach by comparison with some of the existing methods for pile groups under axial or lateral loading. In addition, the behaviour of a pile group subjected to simultaneous axial load, lateral load and moment is examined.

Very little numerical work has been published to show the effects of soil non-linearity on pile group response. Therefore, the accuracy of the proposed approach in the non-linear range may only be examined by comparison with well-documented case histories, for some of which alternative numerical analyses have been performed. This comparative study is presented in Chapter 6. However, some non-linear results, as

# CHAPTER 5

## Numerical results — pile groups

### 5.1 Summary

The validity of the proposed PGROUPN analysis has been verified by comparison with alternative numerical solutions for pile groups subjected to axial and lateral loads. Benchmark solutions in the linear and non-linear range are presented, and the significant influence of soil nonlinearity on load distribution among piles in a group is highlighted.

### 5.2 Introduction

The PGROUPN program has proved capable of matching the results of other methods of analysis for the problem of a single pile under axial or lateral loading. However, as the majority of piled foundations will consist not of a single pile but of a group of piles, it is essential to study the effects of interaction between neighbouring piles in a group. In fact, it has long been recognised that groups of piles tend to deform more than a proportionally loaded single pile. This is because neighbouring piles will be within each others' displacement fields and hence the load per pile to generate a given displacement will be reduced.

In the linear elastic range, this Chapter examines the validity of the proposed approach by comparison with some of the existing methods for pile groups under axial or lateral loading. In addition, the behaviour of a pile group subjected to simultaneous axial load, lateral load and moment is examined.

Very little numerical work has been published to show the effects of soil nonlinearity on pile group response. Therefore, the accuracy of the proposed approach in the non-linear range may only be examined by comparison with well-documented case histories, for some of which alternative numerical analyses have been performed. This comparative study is presented in Chapter 6. However, some non-linear results, as

predicted by PGROUPN, are now presented with the primary aim of highlighting the relevant influence of soil nonlinearity on load distribution among piles in a group.

Thus, the main objectives of this Chapter may be summarised as follows:

- a) Linear elastic range: validation of PGROUPN by comparison with alternative numerical solutions;
- b) Non-linear range: use of PGROUPN to investigate aspects of pile group behaviour not previously studied, with particular emphasis on the load distribution within the group of piles.

As regards pile discretization, for the axial response, the height-to-diameter ratio ( $h/d$ ) of the pile shaft element employed in the numerical simulations presented below has been selected according to the recommendations given in Section 4.3.1.1, ie a  $h/d$  ratio of 2. For the lateral response, the recommended value of  $h/d$  from the single pile analyses is 1 (refer to Section 4.4.1.1); however, for a laterally loaded pile group, piles at the edges of the group are loaded in tension and compression, ie the axial and lateral response are related; thus, in order to avoid the numerical instabilities mentioned in Section 4.3.1.1, a  $h/d$  ratio of 2 has been adopted throughout.

Furthermore, it must be remembered that the value of Poisson's ratio ( $\nu_r$ ) adopted in the numerical examples presented in this thesis is 0.5, unless otherwise stated. This is the appropriate value for fully saturated clay under undrained conditions.

### 5.3 Pile groups under axial loading

An examination of the accuracy of the PGROUPN solution against published numerical methods is presented. First the effect of two neighbouring piles is investigated, and then the analysis is extended to general pile group problems.

In order to present solutions in the non-linear range by means of the simple elastic-perfectly plastic soil model adopted in the PGROUPN analysis, it is convenient to introduce the parameter  $P_g/P_u$ , where  $P_g$  is the total axial load acting on the group and  $P_u$  is its ultimate axial-load capacity. The ratio  $P_g/P_u$  represents the applied load level

of the pile group, while its inverse is the overall safety factor against failure of the group.

### 5.3.1 Two-pile interaction analysis

The degree of interaction between two equally loaded, identical piles may be expressed as an interaction factor,  $\alpha$ , defined as the ratio of the additional settlement induced in the single pile due to load on an adjacent pile, to the settlement of the single pile under its own load.

Figures 5.1 to 5.7 show the linear elastic interaction factors ( $\alpha$ ) plotted against the normalized pile spacing ( $s/d$ ) for a variety of pile slenderness ratios ( $L/d$ ) and relative stiffnesses between pile and soil ( $K = E_p/E_s$ ). It has been found that the interaction effect is more significant for more rigid piles and for decreasing pile spacing. Moreover, it can be observed that the interaction factors for Gibson soil are significantly smaller than those obtained for homogeneous soil conditions; as pointed out by Randolph & Wroth (1979), this difference may be partially attributed to the higher proportion of load taken by the base of a pile in a Gibson soil compared to a homogeneous soil.

In particular, Figs. 5.1 and 5.2 show a comparison of the PGROUPN results (in homogeneous soil) with those predicted by the BEM analysis of Poulos & Davis (1980) for various pile slenderness ratios ( $L/d = 25, 50$ ) and pile-soil relative stiffnesses ( $K = 100, 1000$  and  $\infty$ , which corresponds to a perfectly rigid pile). The solutions are in good agreement except for long, very compressible piles (ie  $L/d = 50, K = 100$ ), where the present analysis gives slightly lower interaction factors than the Poulos & Davis analysis. In the evaluation of the two-pile interaction factors, the Poulos & Davis approach may be considered to have approximately the same degree of rigour as PGROUPN. However, it should be emphasised that in the PGROUPN analyses a  $h/d$  ratio of 2 has been adopted throughout (where  $h$  is the height of the pile shaft element); this discretization corresponds to 12 or 25 pile shaft elements for  $L/d = 25$  or 50, respectively. Instead, the Poulos & Davis solutions are obtained using a coarser pile discretization of 10 shaft elements, irrespective of pile length.

Figures 5.3 and 5.4 compare the interaction factors calculated by PGROUPN with those obtained by the semi-analytical approach of Randolph & Wroth (1979), based on the superposition of individual pile displacement fields, and the BEM analysis of Randolph (1977), which is similar to the PGROUPN approach. The piles are rigid (ie  $K = \infty$ ) and are embedded in an elastic soil mass with a Poisson's ratio ( $\nu_s$ ) of 0.4. Figure 5.3, which refers to piles in homogenous soil, shows that the semi-analytical model of Randolph & Wroth tends to underpredict the interaction between piles compared to the boundary element analyses of Randolph and PGROUPN, especially for piles of  $L/d > 20$ . Figure 5.4, which refers to piles ( $L/d = 20$ ) in homogeneous soil and Gibson soil (with zero stiffness at the ground surface), shows that PGROUPN gives lower interaction factors than Randolph & Wroth, especially at large spacings.

Figure 5.5 shows the interaction factors for rigid piles ( $L/d = 25$ ) embedded in a homogeneous soil stratum, with a finite-layer depth  $H = 2.5L$  (where  $L$  is the pile length). The results from PGROUPN compare favourably with the BEM analysis of Poulos (1968) and the hybrid approach by Chow (1987c), in which load-transfer curves are used to model the individual pile response and a FEM solution is adopted to evaluate the interaction between piles.

Figures 5.6 and 5.7 show the interaction factors for two piles embedded in a Gibson soil (with zero stiffness at the surface) for various pile slenderness ratios ( $L/d = 20, 40$ ) and pile-soil relative stiffnesses ( $E_p/E_{sL} = 100, 10000$ , where  $E_{sL}$  is the soil Young's modulus at the level of the pile base). The surrounding soil is characterised by a finite-layer depth of  $H = 2L$  and a Poisson's ratio of 0.3. It may be observed a generally good agreement with the BEM solution of Poulos (1979), in which the soil modulus is taken as the mean of the moduli at the influenced and influencing nodes in Mindlin's solution (such as in PGROUPN), and the more rigorous solutions of Banerjee (1978), which employs the solution of Chan *et al.* (1974) for a layered half space (refer to Section 1.4.3), and Chow (1987c) (described above).

It has been customary to examine the effects of interaction between piles for soil which may be assumed to be linear elastic. The author is not aware of the existence of published results which show the interaction effect between piles when the linear elastic assumption is no longer valid at high load levels. Therefore, the influence of soil

nonlinearity on the interaction factors ( $\alpha$ ) for two equally loaded identical piles (with  $d = 1$  m,  $E_p = 25$  GPa) embedded in a homogeneous soil is studied using the PGROUPN analysis. For this purpose, the following typical parameters are chosen:

Undrained shear strength ( $C_u$ )	= 50 kPa
Adhesion factor ( $\alpha$ )	= 0.5

Figures 5.8 to 5.11 show the interaction factors ( $\alpha$ ) as a function of the applied load level  $P_g/P_u$  (where  $P_g$  is the total axial load acting on the group of two piles and  $P_u$  is its ultimate axial-load capacity) for different values of the pile slenderness ratio ( $L/d = 25, 50$ ), the relative pile-soil stiffness ( $K = E_p/E_s = 100, 1000$  and  $\infty$ ) and the dimensionless pile spacing ( $s/d = 2.5, 5$ ).

It may be observed that, for the longer and more compressible pile (ie  $L/d = 50$  and  $K = 100$ ), the reduction in the interaction factor becomes significant at relatively low load levels. For instance, Fig. 5.10 shows that, at a normalized pile spacing ( $s/d$ ) of 2.5, the interaction factor ( $\alpha$ ) starts to decrease at a load level  $P_g/P_u = 0.2$ , reducing to about 50% of its elastic value at half the ultimate load. Instead, for the more rigid piles ( $K = 1000$  and  $\infty$ ), the values of  $\alpha$  are constant until a load level of about 0.9 is reached, and thereafter they reduce quite dramatically. This difference is a consequence of the fact that the load-settlement response of a relatively rigid pile is nearly linear until the ultimate load is reached; instead, for a relatively compressible pile, the load-settlement response is markedly non-linear, even at low load levels (refer to Section 3.6).

### 5.3.2 Pile group settlement

In order to analyse a general pile group, the majority of available numerical codes are based on the superposition of the two-pile interaction factors (see, for example, DEFPIG by Poulos, 1980a; PIGLET by Randolph, 1987; GRUPPALO by Mandolini & Viggiani, 1997 — for further details see Section 1.5). This procedure is obviously fairly approximate because, in calculating the interaction between two piles, it ignores the reinforcing effect of intervening piles in the group and hence produces an overestimation of the interaction

among piles. In contrast, in the complete BEM approach employed in PGROUP (Banerjee & Driscoll, 1976) and PGROUPN, pile-soil-pile interaction is evaluated by taking into account the simultaneous presence of all the piles in the group, thereby leading to a more realistic representation of pile group behaviour.

For a  $3 \times 3$  pile group in a homogeneous linear elastic soil, Table 5.1 compares the group settlement obtained by PGROUPN with those predicted from the numerical codes DEFPIG, PIGLET and PGROUP. The piles have a  $L/d$  ratio of 40, a  $s/d$  ratio of 3 and are embedded in a homogeneous elastic soil layer with a Poisson's ratio of 0.49. The group settlement ( $w$ ) is expressed in terms of the dimensionless parameter  $I_g$ :

$$I_g = \frac{wdE_s}{P_g} \quad (5.1)$$

where  $P_g$  is the total axial load acting on the group.

Very good agreement between the different solutions is observed, for both very compressible ( $K = E_p/E_s = 30$ ) and very stiff ( $K = 30,000$ ) piles in a semi-infinite and in a finite soil layer ( $H/L = 1.67$ , where  $H$  is the depth of soil layer and  $L$  is the pile length). An exception is the PIGLET analysis for the very compressible pile group, in which case the predicted settlement is significantly greater than the other three solutions.

Figures 5.12 and 5.13 show solutions for the settlement of square pile groups in a (linear elastic) Gibson soil with zero stiffness at the surface and a  $E_p/E_{sL}$  ratio of 1000 ( $E_{sL}$  is the soil Young's modulus at the level of the pile base); in this case, the value of  $E_s$  in Equation (5.1) refers to  $E_{sL}$ . Figure 5.12 considers a finite soil layer ( $H/L = 2$ ), while Fig. 5.13 considers a semi-infinite soil layer. The piles have a  $L/d$  ratio of 40 and a  $s/d$  ratio of 3.

The PGROUPN solution is compared with the results predicted from DEFPIG (which adopts the mean of the soil moduli at the influenced and influencing nodes in Mindlin's solution), the semi-analytical approach employed in PIGLET and the complete BEM solution of Banerjee & Davies (1977), which adopts a more rigorous, but computationally expensive, method to model soil inhomogeneity (refer to Section 1.4.3). Reasonable agreement between the four sets of solutions is observed.

Figure 5.14 shows the group settlement ratio  $R$ , (ie the ratio of the settlement of the group to that of an isolated single pile at the same average load — refer to Equation (1.3)) as a function of the  $L/d$  ratio and the number of piles in the group for typical pile and soil properties ( $s/d = 4$ ,  $H/L = 2$ , linear elastic Gibson soil with a Poisson's ratio of 0.3, zero stiffness at the surface and a  $E_p/E_{sL}$  ratio of 1000). It is observed that  $R$ , increases as both  $L/d$  and the number of piles increase. Also, the influence of  $L/d$  is small when  $L/d$  exceeds 25. Some differences in the calculated values of  $R$ , are evident as the group size increases; however, as already mentioned above, the code DEFPIG is based on the interaction factor approach and hence overevaluates the interaction among piles, especially for large groups (see, for example, Poulos, 1993; Randolph, 1994; Mandolini & Viggiani, 1997).

Figures 5.15 and 5.16 (after Randolph, 1994) show the computed overall pile group stiffness for square groups of piles embedded in a homogeneous elastic soil, with  $L/d = 25$ ,  $E_p/G_s = 1000$  (where  $G_s$  is the soil shear modulus) and  $s/d = 2.5$  and 5. The pile group stiffness is normalized as  $k_p/(sG_s\sqrt{n})$ , where  $k_p$  is the ratio of the total vertical load acting on the group to the average settlement of the group and  $n$  is the number of piles in the group. In the analyses of GRUPPALO and PIGLET, axial interaction effects between piles have been assumed to become insignificant for pile spacing ( $s$ ) greater than a limiting value  $s_{max}$ , as defined in Equation (1.2). Therefore, in the interests of consistency, the same approach has been applied to the PGROUPN analysis. It is worth noting that, due to the limited size of the pile groups examined, the value of  $s_{max}$  does not influence the PGROUP solution.

As already observed above, DEFPIG grossly underestimates the group stiffness, especially for the wider pile groups ( $s/d = 5$ ); this may be partially attributed to the fact that the code does not include a maximum interaction spacing ( $s_{max}$ ). Reasonable agreement between PGROUPN and GRUPPALO is evident. Also, it is worth noting that results from PGROUPN are in excellent agreement with PGROUP, but the latter is limited to groups of  $8 \times 8$  piles, due to the magnitude of computer resources required to analyse larger groups (Butterfield & Douglas, 1981; Randolph, 1994; Mandolini & Viggiani, 1997). In contrast, PGROUPN took about 150 CPU s for the  $20 \times 20$  pile group (considering the symmetry of the pile arrangement). This observation is of great significance because it demonstrates the

applicability of the complete BEM approach to large pile groups, whereas previous work (ie PGROUP) was restricted to small pile groups.

Further, it may be noted that, for very large pile groups, where the ratio of pile group width to pile length becomes much greater than unity, the group stiffness should approach that of a shallow foundation. This would correspond to a limiting stiffness of about 4.5 (Fraser & Wardle, 1976), as indicated in Figs. 5.15 and 5.16.

In the non-linear range, the main features of load-settlement behaviour of axially loaded pile groups are described in Section 3.6, and typical load-settlement curves are shown in Fig. 3.7. Comparisons with load-settlement curves obtained from alternative numerical analyses (and field test data) are described in Chapter 6.

### 5.3.3 Load distribution

A consequence of the interaction between piles is that, for piles loaded through a rigid pile cap, the piles near the edge of the group take a higher proportion of the applied load than the piles near the centre (refer to Section 1.3.2.1). However, an important drawback of the linear elastic methods of pile group analysis is that they result in a considerable overestimation of the load concentration at the outer piles and hence in an overconservative design. In fact, consideration of soil nonlinearity results in a reduction of the pile-soil system stiffness, the reduction being greater for piles at a greater load level, ie for the outer piles. Consequently, as the load level increases, the load distribution to the individual piles of the group becomes more uniform if compared with the one obtained by the linear elastic approach. This feature has been demonstrated both theoretically and experimentally (see, for example, Caputo & Viggiani, 1984; Chow, 1986a, 1986b, 1987c; Poulos, 1988, 1989, 1993; Randolph, 1994).

In order to analyse the distribution of load in an axially loaded group of piles in a homogeneous elastic soil, the following dimensionless parameters are of interest:  $P/(G_s dw)$ ,  $\lambda$ ,  $L/d$  and  $s/d$  — where  $P$  is the axial load acting on the individual pile head,  $G_s$  is the soil shear modulus,  $w$  is the group settlement and  $\lambda = E_p/G_s$  is the stiffness ratio. In Fig. 5.17, the load distribution predicted by the proposed computer program PGROUPN for a  $3 \times 3$  pile group is compared to the rigorous BEM solution by Butterfield & Banerjee (1971a), the semi-analytical approach by Randolph & Wroth (1979) and the hybrid approach by

Chow (1986a), in which the individual pile response is modelled using load-transfer curves and the group interaction is determined based on Mindlin's solution. The results are calculated for  $\lambda = 6000$  and a normalized pile spacing  $s/d = 2.5$ . Except for some discrepancy in the solution of Randolph & Wroth, reasonably good agreement is obtained between the solutions.

The significant effects of soil nonlinearity on the axial load distribution, as predicted by PGROUPN, are investigated in Figs. 5.18 to 5.22. Figure 5.18 shows the load distribution (where  $P$  is the axial load acting on the individual pile head and  $P_{av}$  is the average axial load acting on each pile head) between a group of  $3 \times 3$  piles, having a length ( $L$ ) of 25 m, a diameter ( $d$ ) of 1 m and a Young's modulus ( $E_p$ ) of 25 GPa. The piles are embedded in a homogeneous soil layer characterised by a Young's modulus ( $E_s$ ) of 25 MPa — this corresponds to a relative pile-soil stiffness ( $K = E_p/E_s$ ) of 1000.

In the linear elastic range, results from PGROUPN compare favourably with those predicted by the interaction factor approach of Poulos & Davis (1980). It is observed that, as the normalized pile spacing ( $s/d$ ) increases, the load distribution becomes more uniform, the load on the outer piles decreasing while the load on the centre piles increases. This is a consequence of the fact that the group interaction decreases for increasing pile spacing.

In order to examine the effects of soil nonlinearity (using PGROUPN) for the homogeneous soil profile (Figs. 5.18 to 5.21), typical values of  $E_p/C_u = 1000$  and  $\alpha = 0.5$  have been chosen. Figure 5.18 shows the predicted load distribution as a function of the load level  $P_g/P_u$ , where  $P_g$  is the total axial load acting on the group and  $P_u$  is its ultimate axial-load capacity (in this case, the predicted value of  $P_u$  is about 11 MN). It is evident that consideration of the non-linear response yields a reduction in the load concentration at the corner piles (pile 1) and a more even load distribution. Clearly, the higher the load level, the higher the reduction in the load concentration at the corner piles obtained by the non-linear analysis.

Figures 5.19 to 5.21 show the effect of varying the following parameters: the pile-soil relative stiffness ( $K = E_p/E_s$ ), the  $L/d$  ratio and the number of piles. Figure 5.19 shows the load distribution when  $K$  is increased from 1000 to  $\infty$  (this has been obtained by adopting a very large value of  $E_p$ ); Figure 5.20 has been obtained by considering  $K = 1000$  and increasing the pile length ( $L$ ) from 25 to 50 m (in this case the predicted value of  $P_u$  is

about 20 MN); Figure 5.21 has been obtained by increasing the number of piles from 9 to 25, while the values of  $K$  and  $L/d$  are 1000 and 25, respectively (in this case the predicted value of  $P_u$  is about 30 MN).

For the initial elastic response, good agreement is generally obtained with the (linear elastic) BEM solution of Poulos & Davis (1980), which is based on the interaction factor approach. The following characteristics of behaviour are observed:

- a) (Fig. 5.19) Nonuniformity of load distribution increases with increasing the pile-soil relative stiffness ( $K$ ); this is a consequence of the fact that interaction effects increase with increasing  $K$  (refer, for example, to Figs. 5.1 and 5.2). In this case, inclusion of non-linear soil response yields a significant reduction in the load concentration at the corner piles. It may be observed that a negative load is obtained for the centre pile (pile 3) at low values of  $s/d$  and low load factors; however, it is doubtful whether negative loads would occur in practical cases (Poulos & Davis, 1980);
- b) (Fig. 5.20) The load distribution becomes more uniform as  $L/d$  increases; this is a consequence of the fact that the interaction effect decreases with increasing  $L/d$  (as shown in Figs. 5.1 and 5.2). In this case, the effects of soil nonlinearity are less marked except for very high load levels ( $P_g/P_u = 0.9$ );
- c) (Fig. 5.21) The load distribution is considerably influenced by the number of piles in the group, the major influence being that the ratio of the load on the corner piles (pile 1) to the average pile load increases as the number of pile increases; inclusion of non-linear soil response yields a significant reduction in the load concentration at the corner piles, even at relatively low load levels. Clearly, in this case, a linear elastic solution would be inappropriate.

It is evident that these features reflect the characteristics of the two-pile interaction, ie the higher the degree of interaction between piles, the higher the load concentration at the outer piles and hence the nonuniformity of load distribution. As a consequence, the effects of nonlinearity, which result in a reduction of the load concentration at the outer piles and

hence in a more uniform load distribution, will be more significant for groups where the nonuniformity of load distribution is more evident.

Finally, Fig. 5.22 shows the load distribution between a group of  $3 \times 3$  piles embedded in a Gibson soil where the Young's modulus increases from zero (at the surface) to 50 MPa at the level of the pile base. The piles have a length ( $L$ ) of 25 m, a diameter ( $d$ ) of 1 m and a Young's modulus ( $E_p$ ) of 25 GPa. In order to examine the effects of soil nonlinearity, as predicted by PGROUPN, values of  $E_s/C_u = 1000$  (over pile depth) and an adhesion factor  $\alpha = 0.5$  have been assumed. The calculated value of  $P_u$  is about 13 MN.

It is worth noting that the predicted load distribution is more uniform than for the case of a homogeneous soil with the same average Young's modulus over pile depth (refer to Fig. 5.18). As already pointed out in Section 5.3.1, this is a consequence of the fact that the interaction factors for Gibson soil are significantly smaller than those obtained for homogeneous soil. Finally, it may be observed that the effects of soil nonlinearity become significant at very high load levels ( $P_g/P_u = 0.9$ ), especially for the central pile (pile 3).

## 5.4 Pile groups under lateral loading

The validity and accuracy of the PGROUPN analysis against alternative numerical solutions are presented. First the effect of two neighbouring piles is investigated, and then the analysis is extended to pile groups.

As the length of a pile is rarely a relevant parameter in calculating its response under lateral loading, only piles which are longer than their critical length (ie flexible piles) are considered (for further details refer to Section 4.4.1). In addition, it is essential to observe that the rotational stiffness of pile groups is usually high, due to the size and stiffness of the pile cap, and hence the interaction between so-called 'fixed-head' (ie zero rotation) piles is of most relevance in practice. Therefore, the numerical solutions presented below refer only to the analysis of fixed-head piles subjected to lateral load. However, the PGROUPN approach cannot be applied to groups of piles which are free to rotate, ie 'free-head' piles (only free-head single piles can be analysed).

Further, it should be emphasised that the presentation of the theoretical non-linear results in terms of the applied load level  $H_g/H_u$  (where  $H_g$  is the total lateral load acting on the group and  $H_u$  is its ultimate lateral-load capacity) is no longer

appropriate, since a (flexible) pile deflects excessively or fails by yielding of the pile section before this value of  $H_u$  can be developed.

#### 5.4.1 Two-pile interaction analysis

The interaction factor ( $\alpha$ ) is defined, in a similar manner to that for axially loaded piles, as the fractional increase in deflection of a pile due to the presence of a similarly loaded neighbouring pile. In the numerical solutions presented below, the interaction factors (for flexible, fixed-head piles) are calculated as a function of the pile and soil properties, the distance between the piles and, unlike for axially loaded piles, the direction of loading.

Figures 5.23 and 5.24 show the linear elastic interaction factors ( $\alpha$ ) plotted against the dimensionless pile spacing ( $s/d$ ) as a function of the direction of loading ( $\beta = 0, 90^\circ$ ) and the pile-soil relative stiffness ( $K = E_p/E_s = 80, 8000$ ) for homogeneous soil conditions. Figures 5.25 and 5.26 show similar solutions for piles in a (linear elastic) Gibson soil, with zero stiffness at the surface, for the cases  $E_p/E_{sL} = 20, 20000$ , where  $E_{sL}$  is the soil Young's modulus at the level of the pile base.

For the cases considered, a number of features are worthy of note: (a) the interaction for piles on a line normal to the direction of loading ( $\beta = 90^\circ$ ) (see inset to Fig. 5.23) at a given spacing is significantly less than that for piles along the line of loading ( $\beta = 0$ ); (b) the interaction effect is more significant for more rigid piles and for decreasing pile spacing; (c) the interaction for piles in a soil with stiffness proportional to depth is less than that for piles in homogeneous soil.

In the solutions presented above, results from the PGROUPN analysis are compared with the finite element fitted algebraic expressions of Randolph (1981), with subsequent modifications (Randolph, 1983b), and the hybrid approach by Chow (1987c), in which load-transfer curves are used to model the individual pile response and a FEM solution is adopted to evaluate the interaction between piles.

There is generally good agreement between the solutions, although the interaction factors calculated from PGROUPN at close spacings tend to be underpredicted compared with the FEM solutions. As already pointed out by Randolph (1981), one possible explanation of this divergence is the idealization of the pile as a

thin strip for the PGROUPN analysis. This has the effect of increasing the amount of soil between piles compared with the three-dimensional FEM analyses, thus leading to lower interaction factors at close spacings. Moreover, it may be noted that, at large spacings, the PGROUPN solution leads to slightly higher interaction factors than those calculated from the finite element analyses. This divergence between FEM and BEM analyses for large spacings has already been noted by Randolph (1977).

#### 5.4.2 Pile group deflection

As pointed out in Section 1.3.2.2, the analysis of laterally loaded pile groups is complicated by the interaction between rotational and lateral displacement of the group. Thus, only if rotation of the pile cap (and hence axial translation of the piles) is prevented, do the piles deflect purely horizontally. For this case ('fixed-head pile groups'), it is possible to define the group deflection ratio  $R_u$ , ie the ratio of the deflection of the group to that of an isolated single pile at the same average load (refer to Equation (1.5)).

Figures 5.27 and 5.28 show the group deflection ratio ( $R_u$ ) for square fixed-head groups of piles ( $s/d = 3$ ) embedded in linear elastic homogeneous soil and Gibson soil (with zero stiffness at the surface), respectively. The group deflection ratios ( $R_u$ ) are plotted over a range of pile stiffness ratios, represented by different values of the critical slenderness ratio ( $L_c/r_o = 10, 30$ ), as defined in Equations (4.12) and (4.13). It is observed that  $R_u$  increases as the number of piles increases. Moreover, values of  $R_u$  reflect the higher interaction between stiffer piles and for homogeneous soil conditions, as already observed for the two-pile interaction and for the axially loaded case.

Results from PGROUPN are compared with those obtained by Fleming *et al.* (1992) (based on the work of Randolph, 1981, 1983b), in which pile-soil-pile interaction is evaluated via superposition of interaction factors determined from expressions fitted to the results of FEM analyses. It is observed that the PGROUPN analysis predicts smaller values of the group deflection ratio ( $R_u$ ). A preliminary explanation may be found in the already observed differences between lateral interaction coefficients at close spacings (refer to Figs. 5.23 to 5.26). Another explanation may be found in the already discussed limitations of the interaction factor approach which does not take into account the reinforcing effects of all

the group piles and hence overevaluates the interaction among piles (refer to Section 5.3.2).

In the non-linear range, the main features of the load-deflection response of laterally loaded pile groups are described in Section 3.6, and typical load-deflection curves are shown in Fig. 3.8. Comparisons with the load-deflection behaviour obtained from alternative numerical approaches (and field test data) are presented in Chapter 6.

### 5.4.3 Load distribution

The computed lateral load distribution to the individual piles in fixed-head pile groups is examined by comparison with alternative methods in the linear elastic range, and the influence of soil nonlinearity, as predicted by PGROUPN, is discussed. It should be emphasised that the numerical simulations presented below take no account of possible failure by yielding of the pile section, ie the pile is assumed to remain elastic. Figures 5.29 to 5.33 show the lateral load distribution (where  $H$  is the lateral load acting on the individual pile head and  $H_{av}$  is the average lateral load acting on each pile head) as a function of the normalized pile spacing ( $s/d$ ) for square groups of piles, having a length ( $L$ ) of 25 m, a diameter ( $d$ ) of 1 m and a Young's modulus ( $E_p$ ) of 25 GPa. The charts are presented for constant values of the stiffness ratio  $K_R = E_p I_p / E_s L^4$ , where  $I_p$  is the second moment of area of pile section and  $E_s$  is the soil Young's modulus (refer to Equation (4.11)).

Figures 5.29 to 5.31 show typical lateral load distribution for different stiffness ratios ( $K_R = 10^{-5}$ ,  $10^{-2}$ ) and number of piles in the group. In order to examine the effect of soil nonlinearity, values of the undrained shear strength ( $C_u$ ) of 100, 10 and 100 kPa and total lateral load ( $H_g$ ) of 10, 8 and 18 MN are arbitrarily assumed for the PGROUPN analyses in Figs. 5.29, 5.30 and 5.31, respectively.

It is evident that the characteristics of behaviour are similar to those of axially loaded pile groups. In fact, as the pile spacing increases, the load distribution becomes more uniform, the load on the outer piles decreasing while the load on the centre piles increases. Further, nonuniformity of load distribution becomes more marked for less flexible groups and for increasing the number of piles in the group. Again, consideration of the non-linear response yields a reduction in the load concentration at the corner piles

and a more uniform load distribution to the individual piles of the group — such an uniformity of load distribution to the group piles becomes more marked with increasing the load level.

It is worth noting that the PGROUPN elastic solutions compare favourably with the complete BEM approach of Burghignoli & Desideri (1995), while the agreement with the hybrid method of Leung & Chow (1987), in which the individual pile response is modelled using load-transfer curves and the group interaction is determined based on Mindlin's solution, is reasonable except for closely spaced pile groups. Instead, some discrepancies are observed with the BEM solution of Poulos & Davis (1980), based on the interaction factor approach.

As already observed (refer to Section 1.4.3), the interaction factor approach solves the group problem by calculating the displacement influence coefficients for each pair of piles in the group and by merely overlapping the effects. Instead, the complete approach (such as that employed in PGROUPN), by considering the simultaneous presence of all the piles within the group, is able to account for the reinforcing effect of the piles. The resulting greater uniformity of load distribution to the individual piles of the group obtained by the latter approach may be explained with the following example (as demonstrated theoretically by Burghignoli & Desideri). Consider a group of, say, 9 identical, free piles arranged in a square configuration. If a lateral load is applied to one pile of the group and its head displacement is calculated, it is observed that the central pile (the most affected by the presence of the other piles) will be subjected to a significant reduction of the head displacement due to the greater stiffness of the surrounding soil, 'reinforced' by the presence of the other piles. This characteristic of behaviour is in agreement with the greater homogeneity of load distribution obtained by the complete approach in the case in which the same group of piles are connected by a rigid cap. In fact, the increased stiffness of the central pile results in a higher proportion of the applied load taken by the pile and hence in a more uniform load distribution when compared with the interaction factor approach. It is clear that this reinforcing effect of the piles becomes more significant for closely spaced pile groups.

Therefore, it may be concluded that each pile interacts with the surrounding soil with a twofold effect: on the one hand, the displacement of the other piles tends to increase

as a result of the stresses transferred to the surrounding soil (this increase can be expressed in terms of ‘interaction factors’); on the other, by stiffening the medium in which the piles are placed, the effects of interaction with the other piles are reduced. The latter aspect cannot be reproduced in the interaction factor method and it can only be accounted for by a complete BEM (or FEM) approach. Moreover, the results presented in this thesis show that these reinforcing effects are more significant in a laterally loaded pile group than in an axially loaded one.

The numerical examples described above refer to relatively stiff ( $K_R = 10^2$ ) and relatively flexible ( $K_R = 10^5$ ) piles. In order to analyse piles commonly encountered in practice, Fig. 5.32 adopts a stiffness ratio ( $K_R$ ) of  $10^4$ , which corresponds to a (constant) soil modulus ( $E_s$ ) of 31 MPa. For this case, typical values of  $C_u = 50$  kPa and  $H_g = 10$  MN are chosen to illustrate the influence of soil nonlinearity.

The idealization of the soil as a material with stiffness proportional to depth (and zero stiffness at ground level) is probably a better assumption than that of a homogeneous soil when considering lateral loading (see, for example, Poulos & Davis, 1980; Randolph, 1981). This is due to the fact that the large strains which occur in the soil close to the pile head will reduce the relevant soil modulus to a low value. Figure 5.33 shows the load distribution for fixed-head piles in a Gibson soil where the soil modulus and the undrained shear strength increase from zero (at the surface) to  $E_{sL} (= 2E_s) = 62$  MPa and  $C_{uL} (= 2C_u) = 100$  kPa at the level of the pile base (where  $E_s$  and  $C_u$  are the values adopted for the homogeneous soil profile described above). The non-linear results are calculated for a total lateral load acting on the group ( $H_g$ ) of 8 MN. As already observed for axially loaded pile groups, the predicted load distribution is more uniform than for the case of a homogeneous soil with the same average Young’s modulus over pile depth (refer to Fig. 5.32). This is a consequence of the fact that the interaction factors for Gibson soil are seen to be significantly smaller than those obtained for homogeneous soil conditions.

## 5.5 Pile groups under general loading conditions

The deformations and the load distribution of a 12-pile group under general loading conditions, ie a combination of axial load, lateral load and moment, are examined in the linear elastic range. Banerjee *et al.* (1981) provided some output of the PGROUP program

(version 3.0), which is the most rigorous of the numerical codes currently available (refer to Section 1.5). This offers an excellent opportunity to make an accurate comparison with the results obtained from PGROUPN. The details of the input parameters are (refer to Fig. 5.34):

Number of pile types ( $n$ )	= 7
Number of pile shaft elements per pile ( $N$ )	= 4
Length ( $L$ ) of raked piles (pile types labelled 1, 2, 3)	= 10 m
Length ( $L$ ) of vertical piles (pile types labelled 4, 5, 6, 7)	= 9 m
Angle of rake ( $\phi$ ) of pile types 1, 2, 3	= $14^\circ$
Pile diameter ( $d$ )	= 0.3 m
Pile spacing (centre-to-centre)	= 0.9 m
Pile Young's modulus ( $E_p$ )	= 24 GPa
Young's modulus of the homogeneous soil ( $E_s$ )	= 9 MPa
Vertical load on cap ( $V$ )	= 200 kN
Horizontal load on cap ( $H$ )	= 50 kN
Moment on cap ( $M$ )	= 20 kNm
Eccentricity of vertical load	= 0.3 m

It may be noted that, according to the recommendations given in Section 3.4.6, the central pile in the row of piles labelled 1 would be identified with a different pile type number, ie the ideal number of pile types ( $n$ ) would be 8. However, Banerjee and colleagues have adopted the pile numbering depicted in Fig. 5.34 in order to give an example of how the size of the problem may be reduced by making use of symmetries between piles which only carry approximately equal loads.

Table 5.2 compares the settlement ( $w$ ), deflection ( $u$ ) and rotation ( $\theta$ ) of the pile group calculated by the two computer programs, while Figs. 5.35, 5.36 and 5.37 compare the distribution with depth of axial load, transverse load and bending moment, respectively. Excellent agreement between the two solutions is evident, thereby confirming the accuracy of the proposed PGROUPN approach for linear elastic analysis.

## 5.6 Concluding remarks

The response of pile groups subjected to axial and lateral loads has been examined. A generally good agreement is observed when comparing the proposed PGROUPN solution with alternative numerical procedures for the computation of the response of pile groups embedded in a linear elastic half-space. In the non-linear range, benchmark solutions are not available in the literature and therefore a check of the overall accuracy of the present approach may only be obtained by comparison with well-documented field load tests, for some of which other numerical studies have been published. Nevertheless, some results from PGROUPN were presented in order to highlight the significant influence of soil nonlinearity on the load distribution to the individual piles of the group.

The results presented herein demonstrate that a complete BEM approach can be economically applied to large pile group systems, whereas previous work (ie PGROUP) was limited to problems of small dimensions because of enormous computational resources. One of the main advantages of a complete analysis method over the interaction factor approach (such as that employed in DEFPIG and PIGLET) is that it fully accounts for the simultaneous presence of all the group piles and hence considers their reinforcing effect. Instead the interaction factor approach solves the group problem by merely superposing the two-pile interaction factors. This results in an overestimation of the interaction effect between piles in a group, thereby leading to larger group deformations and a less uniform distribution of loads to the individual piles.

In addition, inclusion of soil nonlinearity demonstrates a further reduction of the load concentration at the outer piles and a more even load distribution to the group piles if compared with the one predicted by a linear elastic approach. These observations are of basic importance in practice because they offer the prospect of significant improvements in design procedures and potential saving of materials.

As regards computing costs, it has been observed that about 100 load increments are generally sufficient to achieve a converged solution of the PGROUPN analyses. The average CPU time for the non-linear numerical simulations presented above is about 15 s, thereby demonstrating the efficiency of the proposed approach for routine design problems.

## TABLES CHAPTER 5

Table 5.1 Comparison between solutions for settlement of  $3 \times 3$  pile group in homogeneous soil ( $L/d = 40$ ,  $s/d = 3$ ,  $\nu_s = 0.49$ ).

Method	Values of $I_G$			
	$H/L = 1.67$		Semi-infinite soil layer	
	$K = 30$	$K = 30,000$	$K = 30$	$K = 30,000$
PGROUPN	0.057	0.019	0.066	0.028
PGROUP	0.063	0.020	0.067	0.025
PIGLET	NA	NA	0.105	0.026
DEFPIG	0.058	0.021	0.069	0.029

Table 5.2 Comparison with PGROUP for 12-pile group in homogeneous soil under general loading conditions.

	$w$ (mm)	$u$ (mm)	$\theta$ (radians $\times 10^{-5}$ )
PGROUPN	2.04	-0.77	7.33
PGROUP	2.03	-0.78	7.20

### FIGURES CHAPTER 5

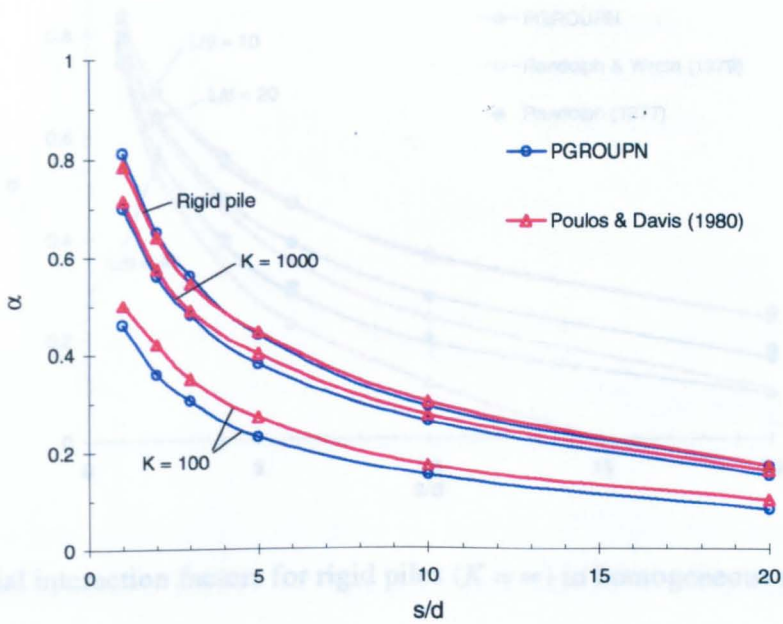


Fig. 5.1 Axial interaction factors for piles in homogeneous soil ( $L/d = 25$ ).

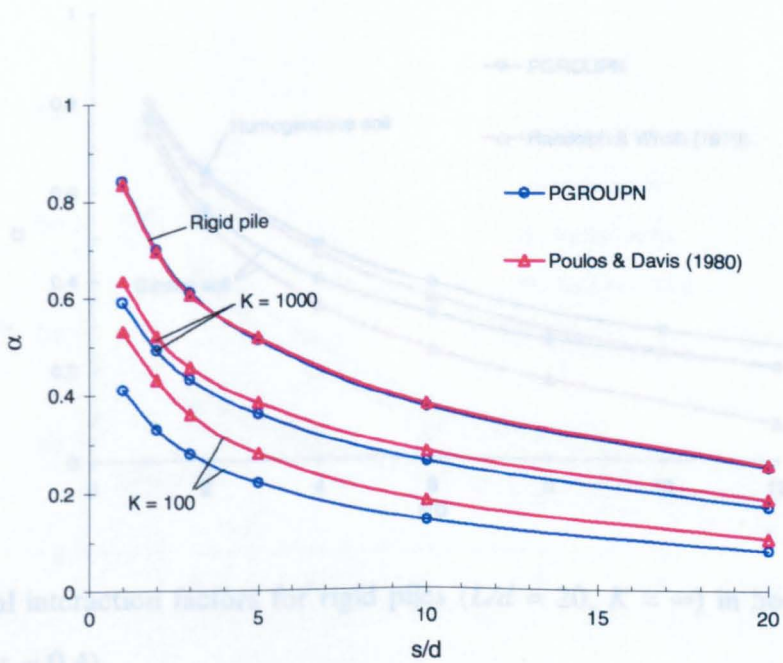


Fig. 5.2 Axial interaction factors for piles in homogeneous soil ( $L/d = 50$ ).

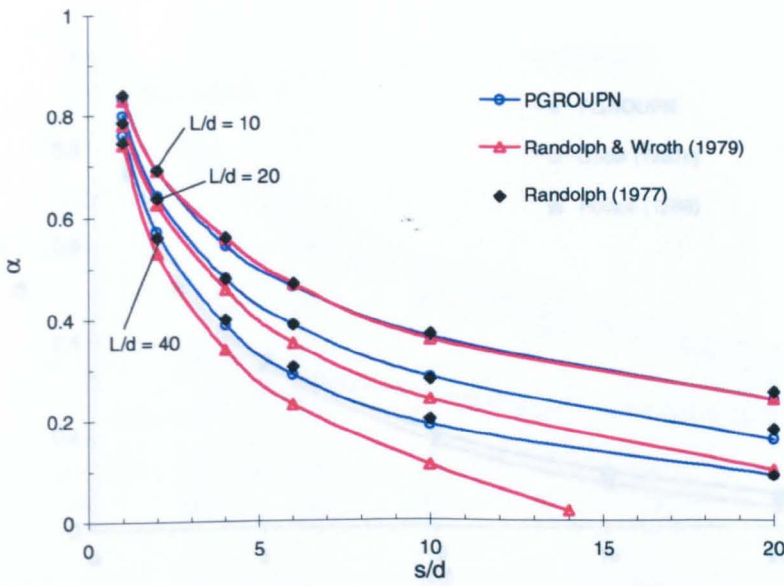


Fig. 5.3 Axial interaction factors for rigid piles ( $K = \infty$ ) in homogeneous soil ( $\nu_s = 0.4$ ).

layer of finite depth ( $H = 2.5L$ ).

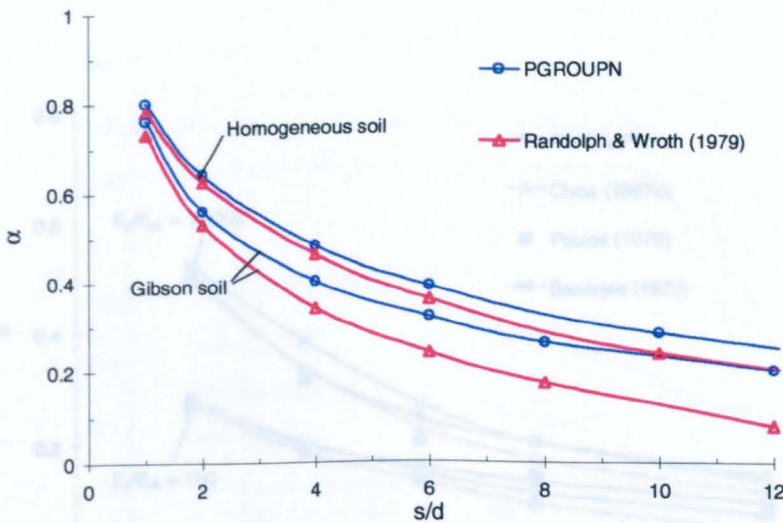


Fig. 5.4 Axial interaction factors for rigid piles ( $L/d = 20$ ,  $K = \infty$ ) in homogeneous and Gibson soils ( $\nu_s = 0.4$ ).

Fig. 5.6 Axial interaction factors for piles ( $L/d = 20$ ) in Gibson soil layer ( $\nu_s = 0.3$ ) of finite depth ( $H = 2L$ ).

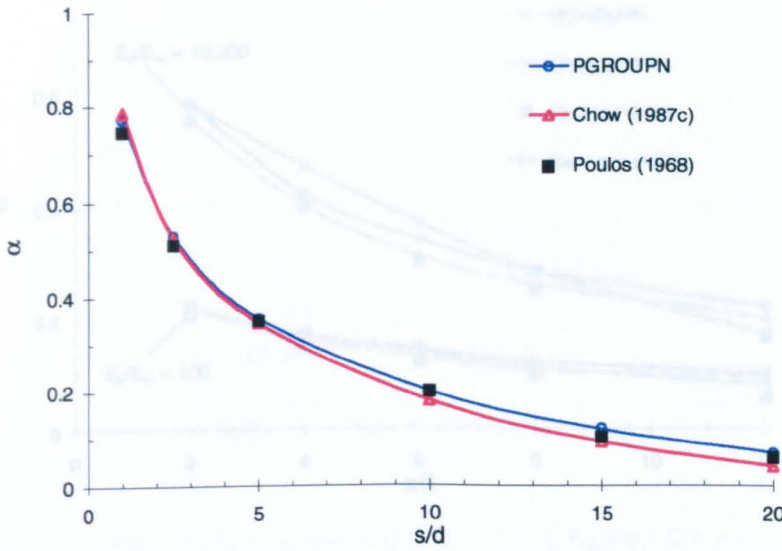


Fig. 5.5 Axial interaction factors for rigid piles ( $L/d = 25$ ,  $K = \infty$ ) in homogeneous soil layer of finite depth ( $H = 2.5L$ ).

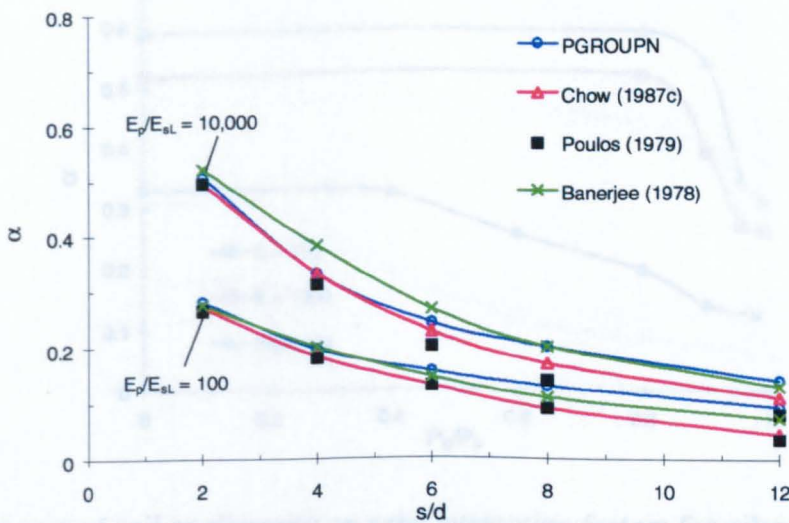


Fig. 5.6 Axial interaction factors for piles ( $L/d = 20$ ) in Gibson soil layer ( $\nu_s = 0.3$ ) of finite depth ( $H = 2L$ ).

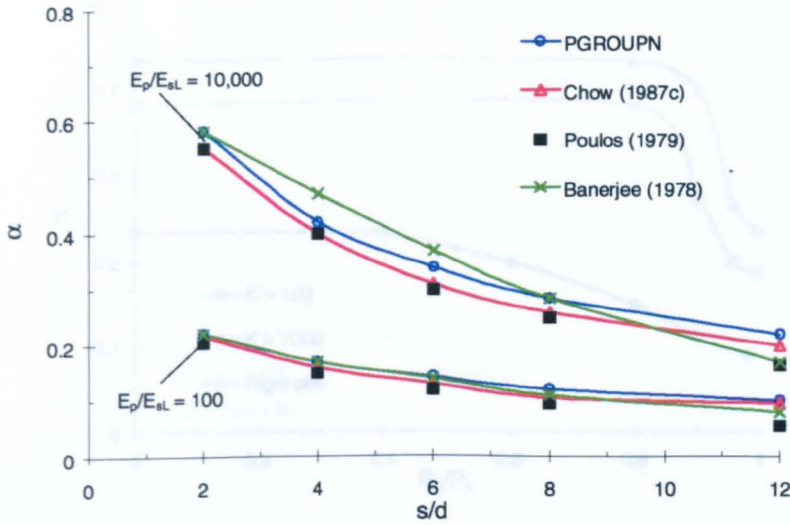


Fig. 5.7 Influence of soil nonlinearity on axial interaction factors for piles ( $L/d = 40$ ) in Gibson soil layer ( $\nu_s = 0.3$ ) of finite depth ( $H = 2L$ ).

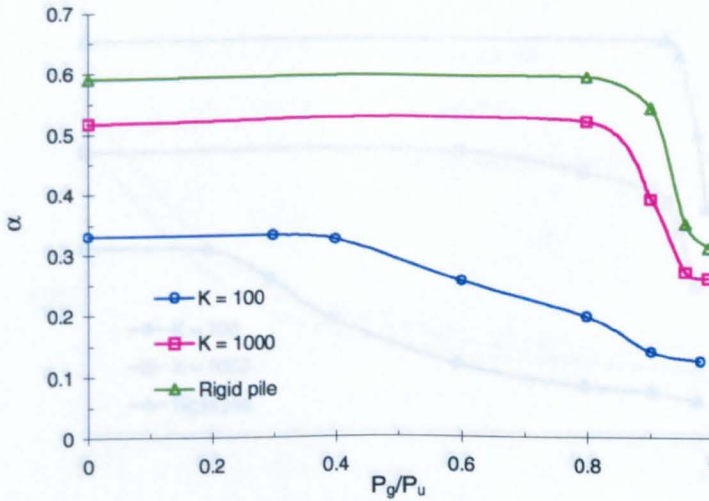


Fig. 5.8 Influence of soil nonlinearity on axial interaction factors for piles ( $L/d = 25$ ,  $s/d = 2.5$ ) in homogeneous soil.

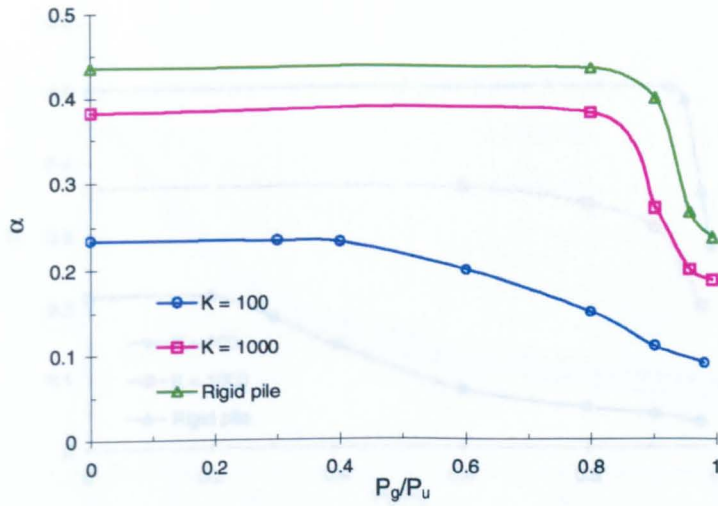


Fig. 5.9 Influence of soil nonlinearity on axial interaction factors for piles ( $L/d = 25$ ,  $s/d = 5$ ) in homogeneous soil.

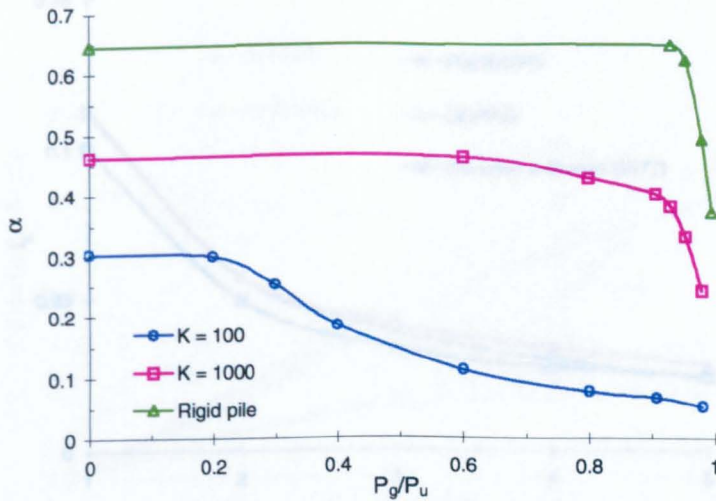


Fig. 5.10 Influence of soil nonlinearity on axial interaction factors for piles ( $L/d = 50$ ,  $s/d = 2.5$ ) in homogeneous soil.

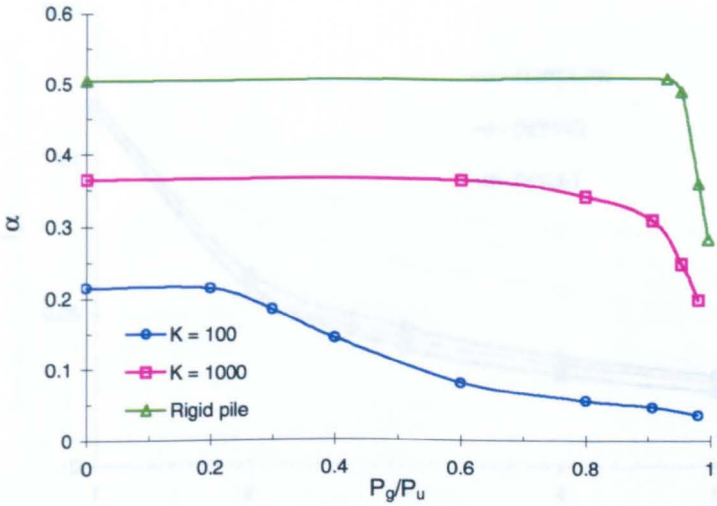


Fig. 5.11 Influence of soil nonlinearity on axial interaction factors for piles ( $L/d = 50$ ,  $s/d = 5$ ) in homogeneous soil.

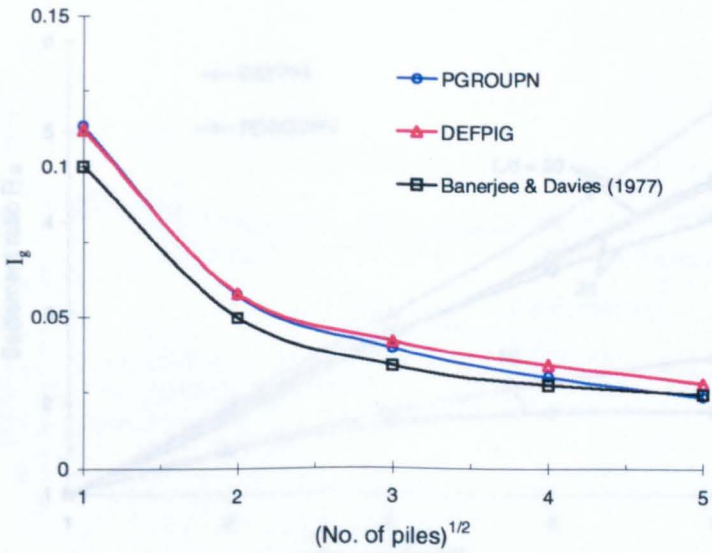


Fig. 5.12 Comparison between solutions for pile group settlement in Gibson soil layer of finite depth  $H = 2L$  ( $L/d = 40$ ,  $s/d = 3$ ,  $E_p/E_{sL} = 1000$ ).

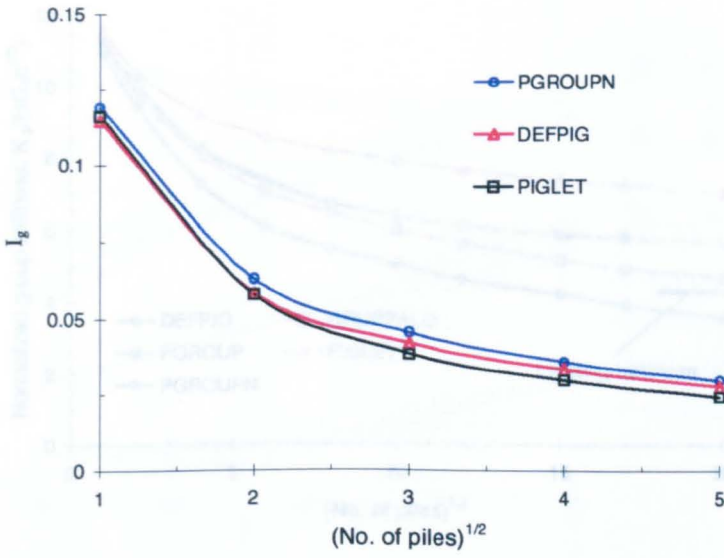


Fig. 5.13 Comparison between solutions for pile group settlement in Gibson soil layer of semi-infinite depth ( $L/d = 40$ ,  $s/d = 3$ ,  $E_p/E_{sL} = 1000$ ).

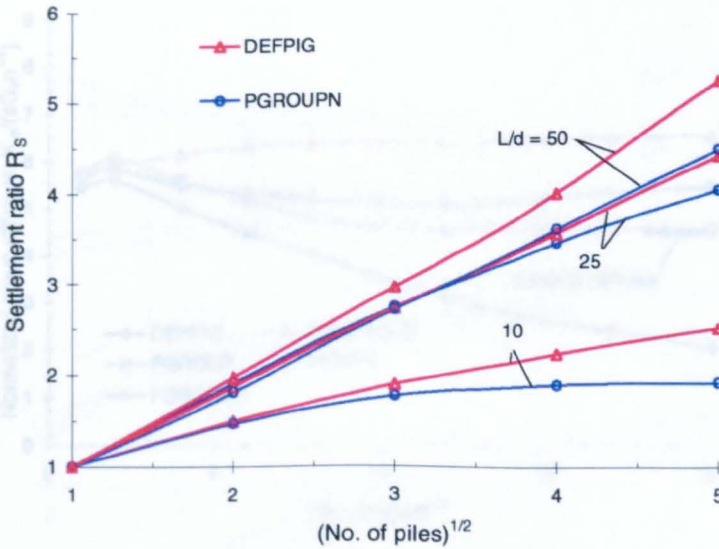


Fig. 5.14 Influence of geometric parameters on group settlement ratio in Gibson soil conditions ( $H = 2L$ ,  $s/d = 4$ ,  $E_p/E_{sL} = 1000$ ,  $\nu_s = 0.3$ ).

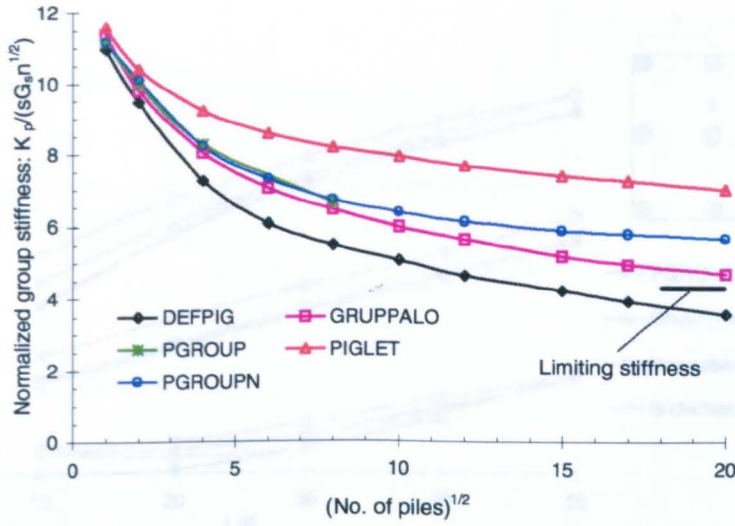


Fig. 5.15 Comparison between computer programs for pile group stiffness in homogeneous soil conditions ( $L/d = 25$ ,  $E_p/G_s = 1000$ ,  $s/d = 2.5$ ).

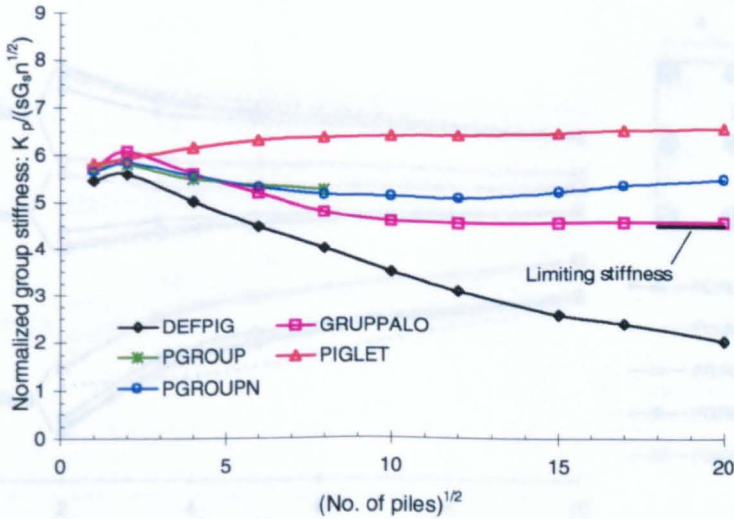


Fig. 5.16 Comparison between computer programs for pile group stiffness in homogeneous soil conditions ( $L/d = 25$ ,  $E_p/G_s = 1000$ ,  $s/d = 5$ ).

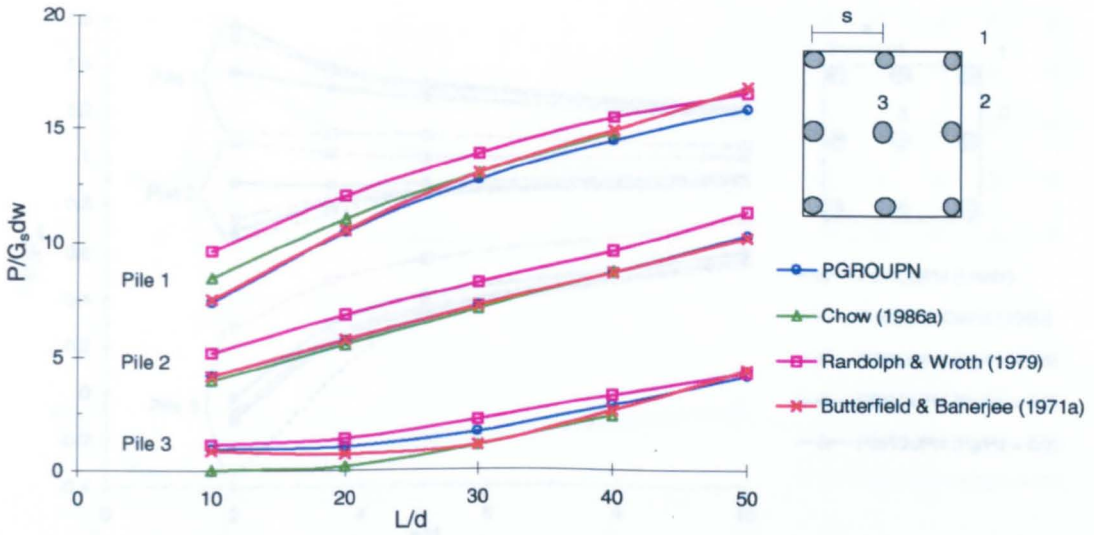


Fig. 5.17 Comparison of axial load distribution to individual piles in  $3 \times 3$  pile group in homogeneous soil ( $\lambda = 6000$ ,  $s/d = 2.5$ ).

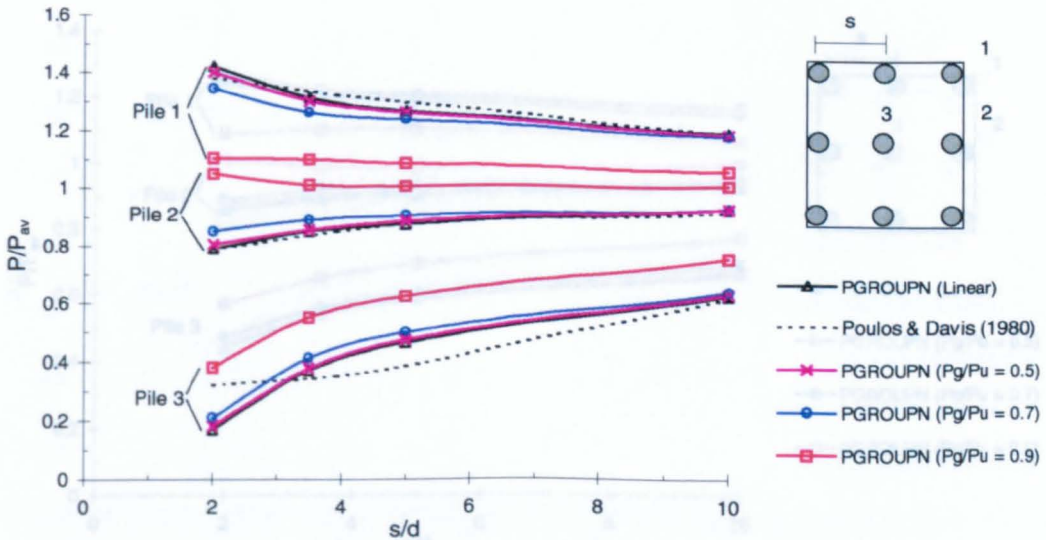


Fig. 5.18 Comparison of axial load distribution to individual piles in  $3 \times 3$  pile group in homogeneous soil ( $K = 1000$ ,  $L/d = 25$ ).

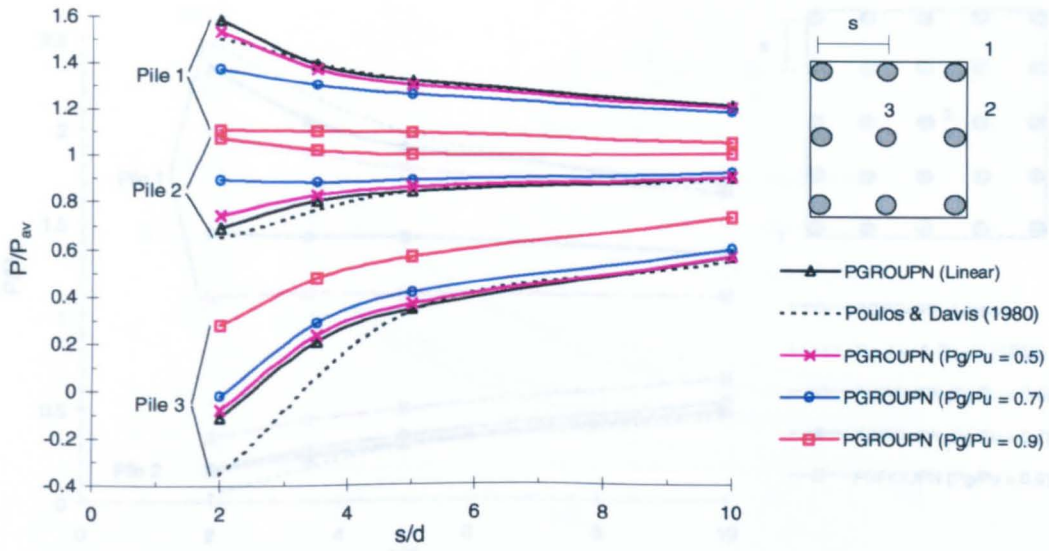


Fig. 5.19 Comparison of axial load distribution to individual piles in  $3 \times 3$  pile group in homogeneous soil ( $K = \infty$ ,  $L/d = 25$ ).

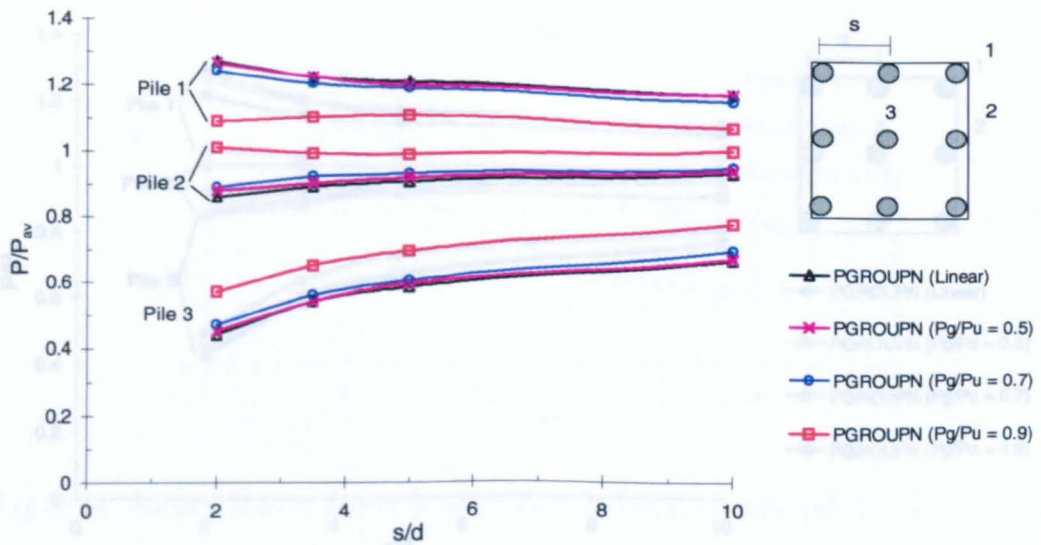


Fig. 5.20 Comparison of axial load distribution to individual piles in  $3 \times 3$  pile group in homogeneous soil ( $K = 1000$ ,  $L/d = 50$ ).

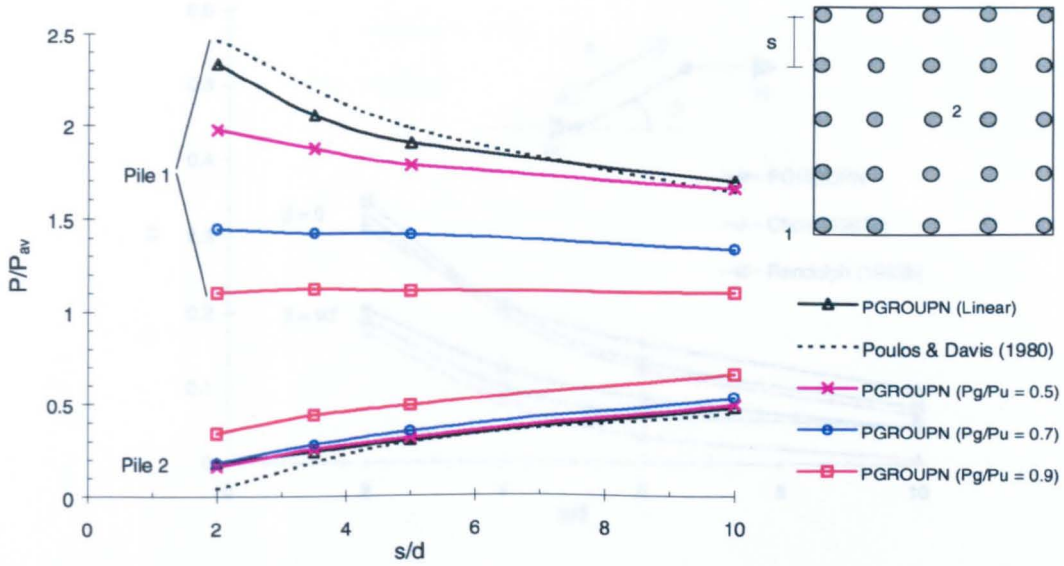


Fig. 5.21 Comparison of axial load distribution to individual piles in  $5 \times 5$  pile group in homogeneous soil ( $K = 1000, L/d = 25$ ).

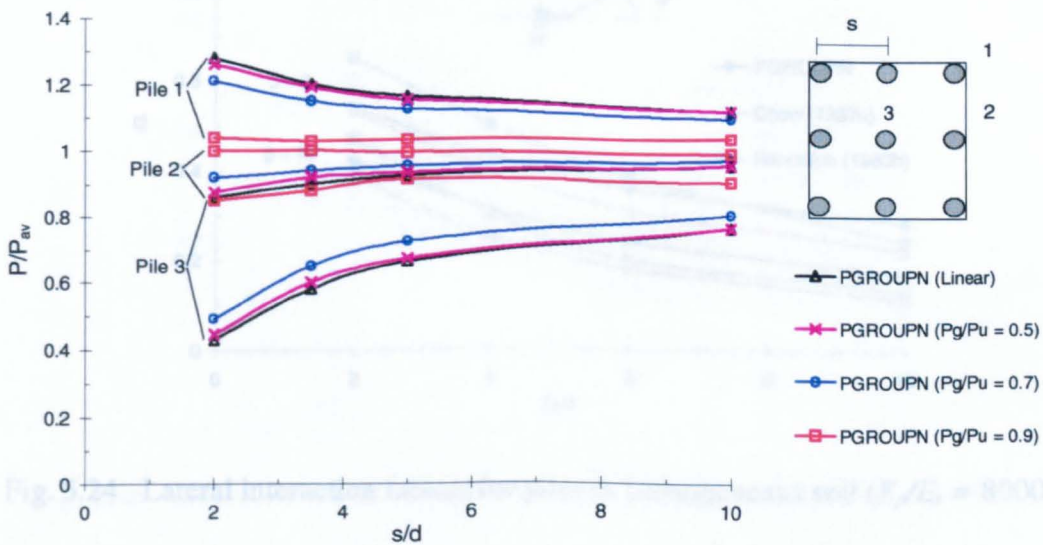


Fig. 5.22 Comparison of axial load distribution to individual piles in  $3 \times 3$  pile group in Gibson soil.

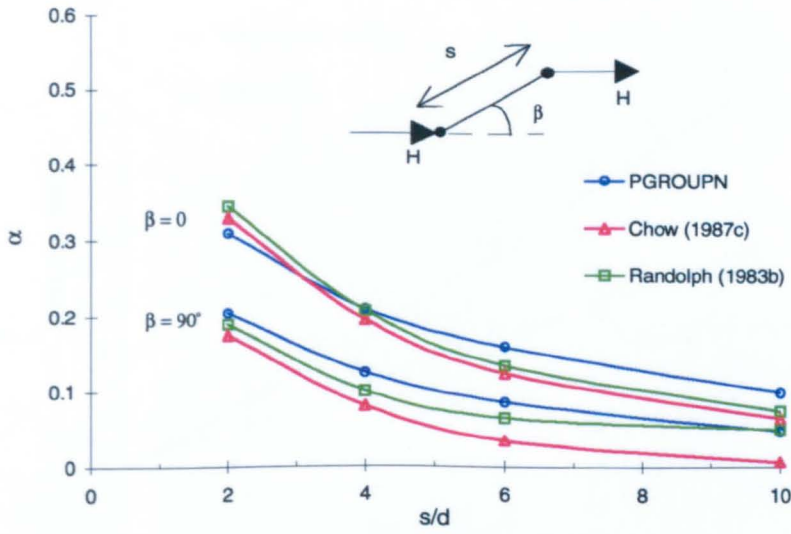


Fig. 5.23 Lateral interaction factors for piles in homogeneous soil ( $E_p/E_s = 80$ ).

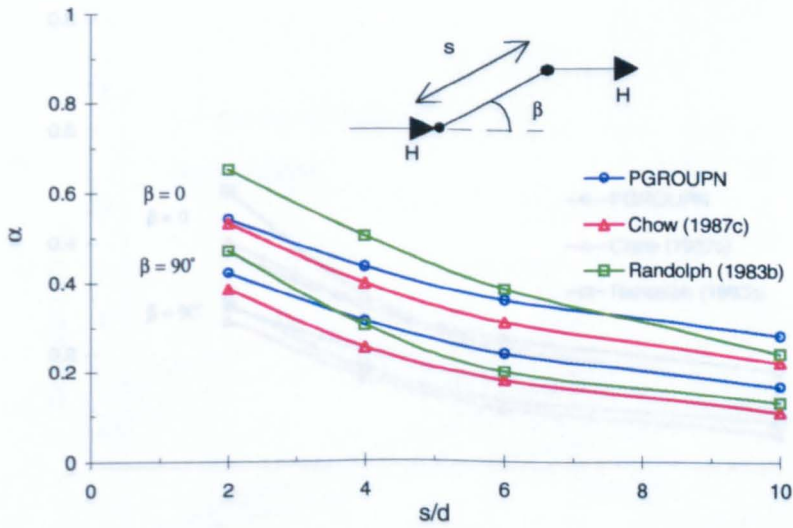


Fig. 5.24 Lateral interaction factors for piles in homogeneous soil ( $E_p/E_s = 8000$ ).

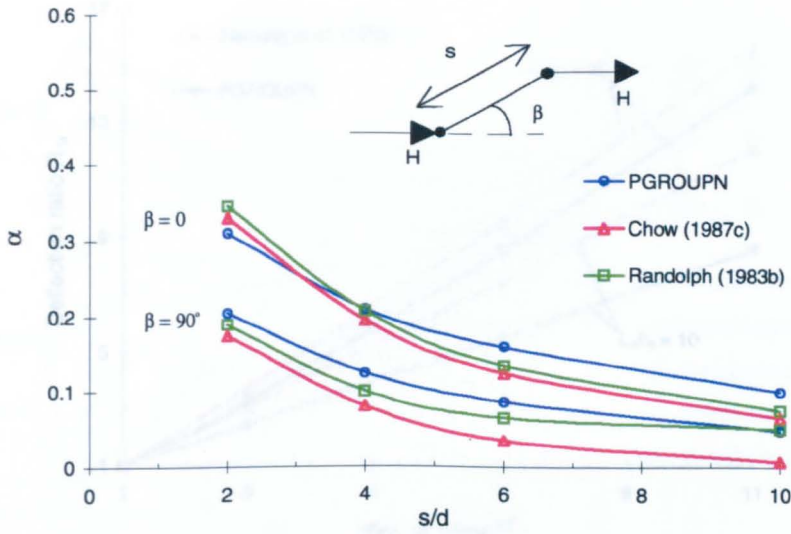


Fig. 5.25 Lateral interaction factors for piles in Gibson soil ( $E_p/E_{sL} = 20$ ).

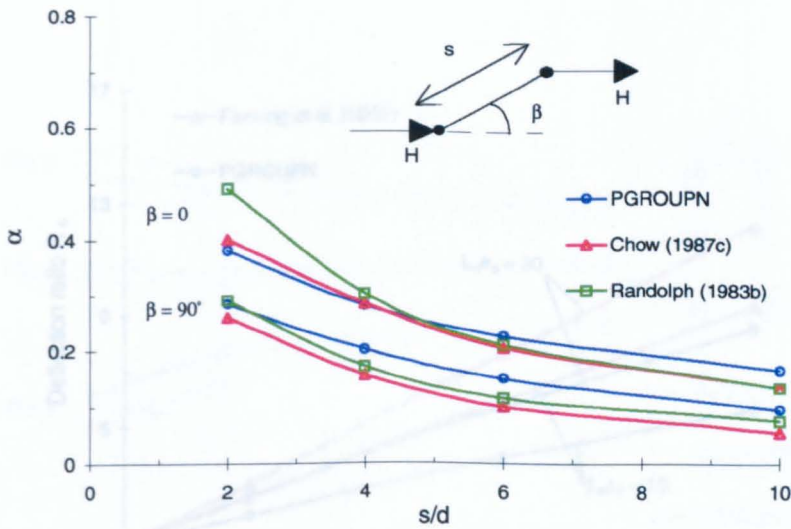


Fig. 5.26 Lateral interaction factors for piles in Gibson soil ( $E_p/E_{sL} = 20,000$ ).

Fig. 5.28 Deflection ratios for square fitted-pile pile groups ( $s/d = 3$ ) in Gibson soil.

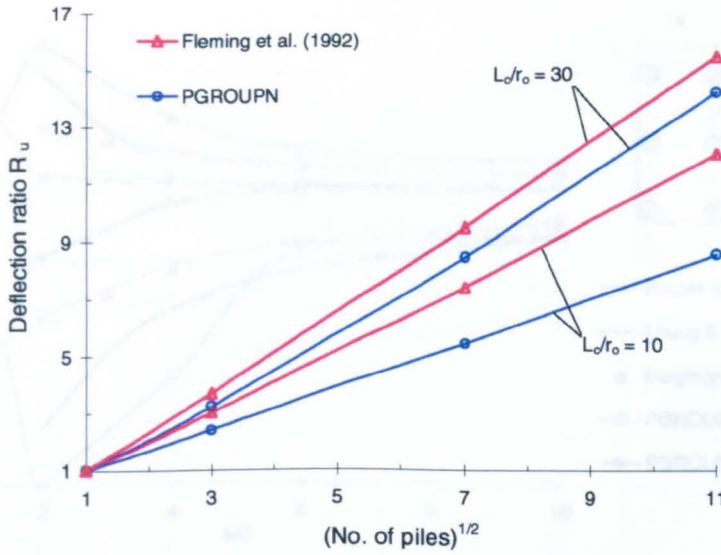


Fig. 5.27 Deflection ratios for square fixed-head pile groups ( $s/d = 3$ ) in homogeneous soil.

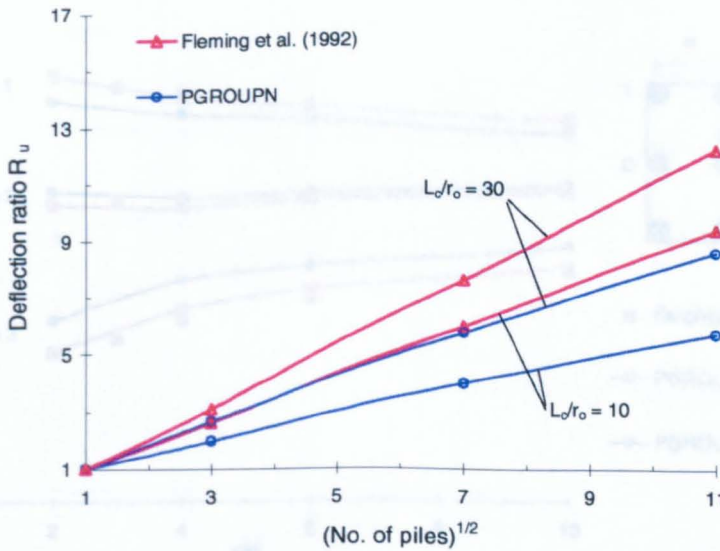


Fig. 5.28 Deflection ratios for square fixed-head pile groups ( $s/d = 3$ ) in Gibson soil.

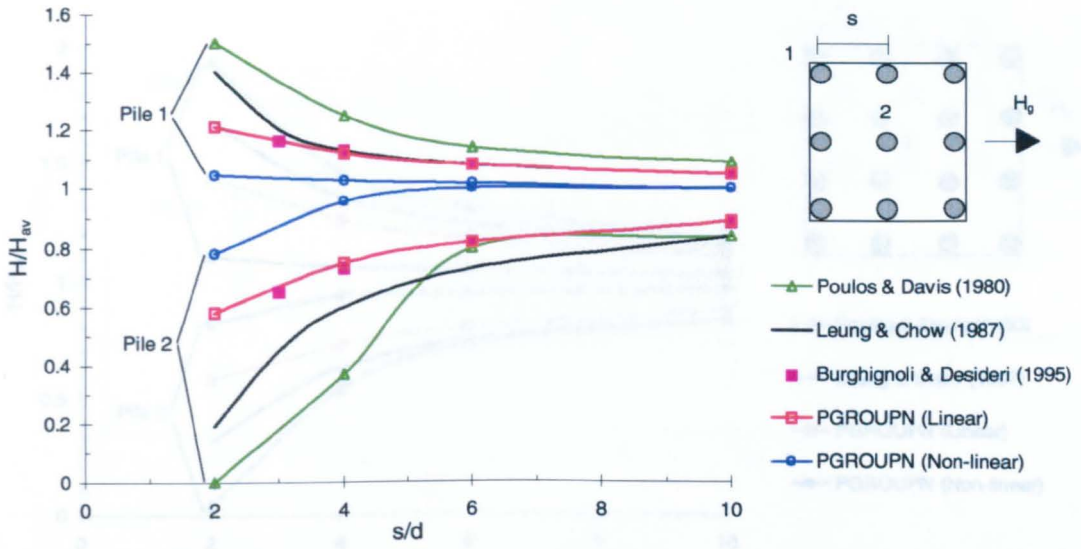


Fig. 5.29 Comparison of lateral load distribution to individual piles in fixed-head  $3 \times 3$  pile group in homogeneous soil ( $K_R = 10^5$ ).

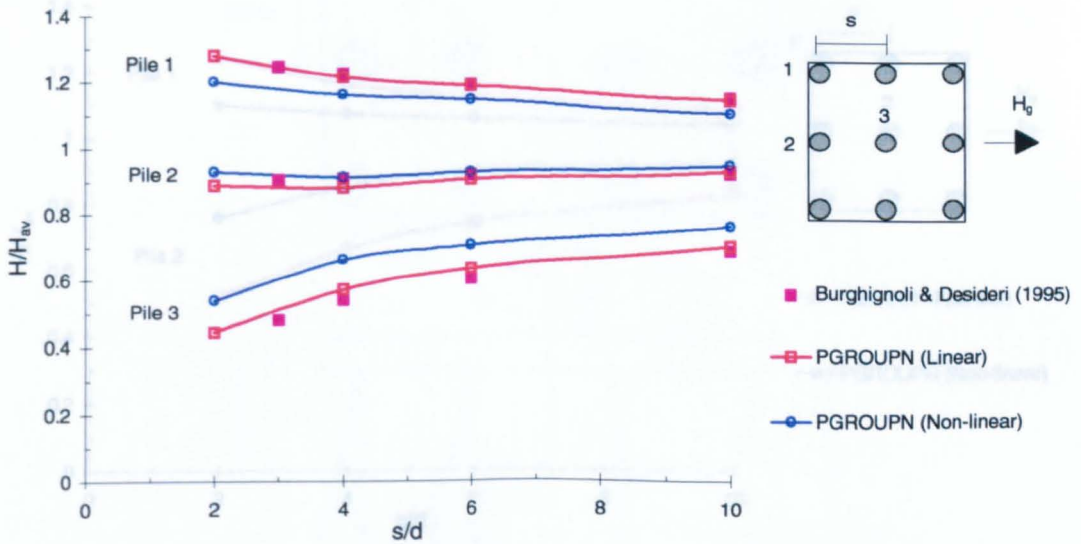


Fig. 5.30 Comparison of lateral load distribution to individual piles in fixed-head  $3 \times 3$  pile group in homogeneous soil ( $K_R = 10^2$ ).

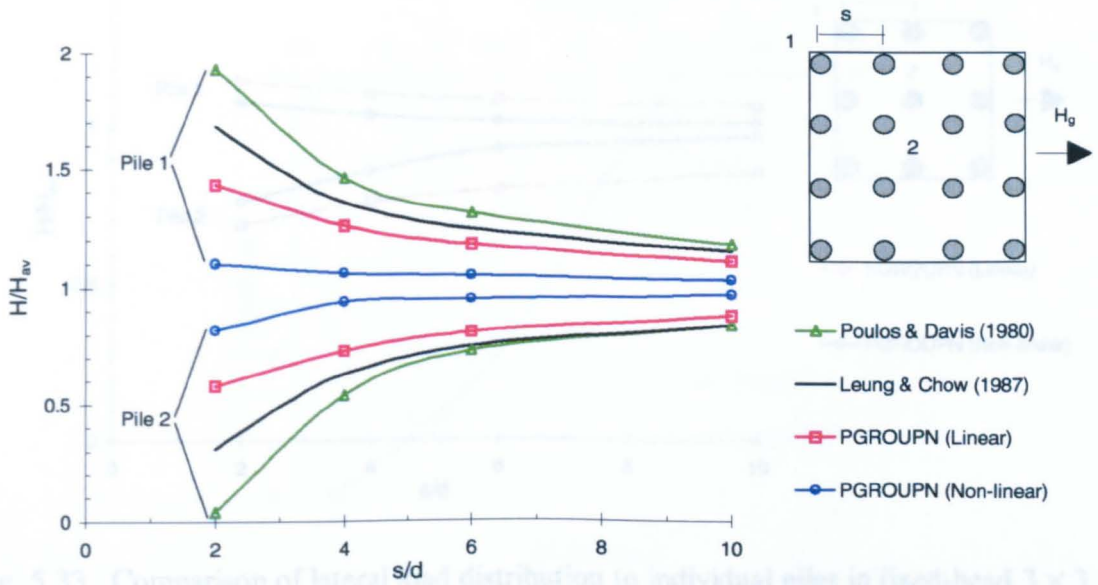


Fig. 5.31 Comparison of lateral load distribution to individual piles in fixed-head 4 × 4 pile group in homogeneous soil ( $K_R = 10^{-5}$ ).

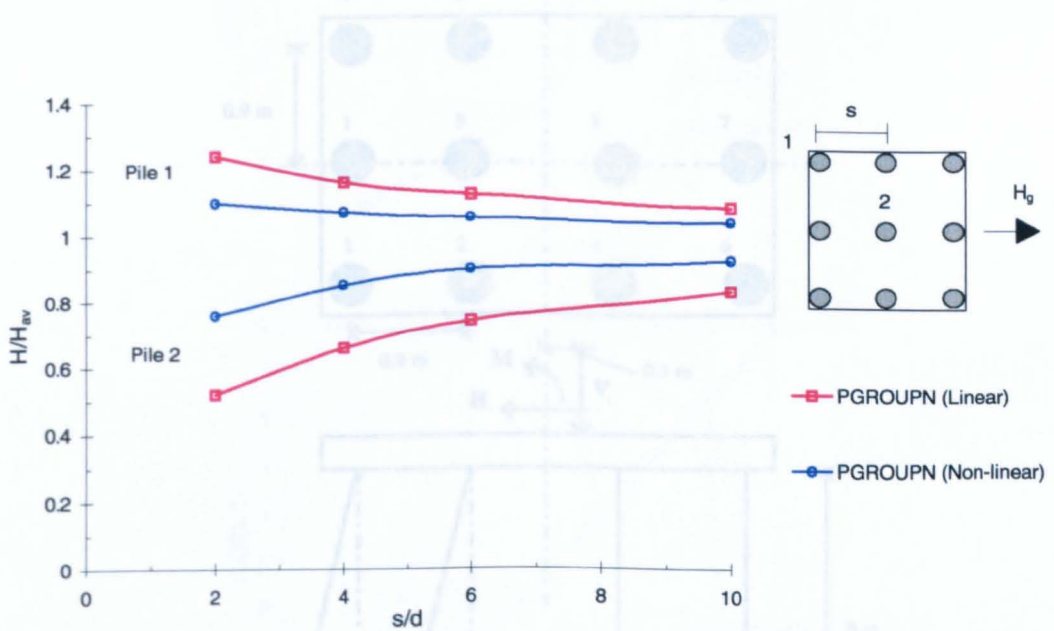


Fig. 5.34 Pile group geometry for comparison with PGROUPN.

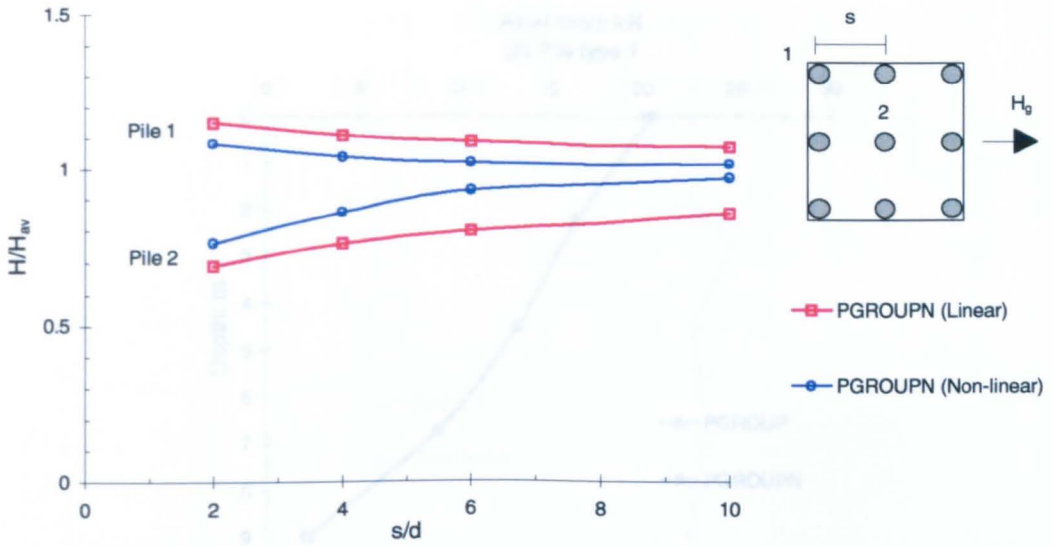


Fig. 5.33 Comparison of lateral load distribution to individual piles in fixed-head 3 × 3 pile group in Gibson soil.

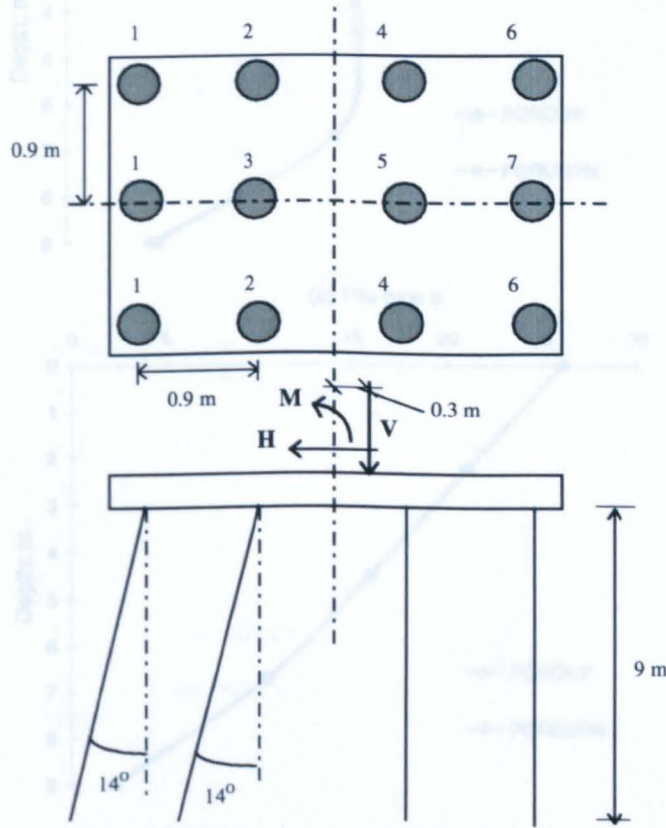


Fig. 5.34 Pile group geometry for comparison with PGROUP.

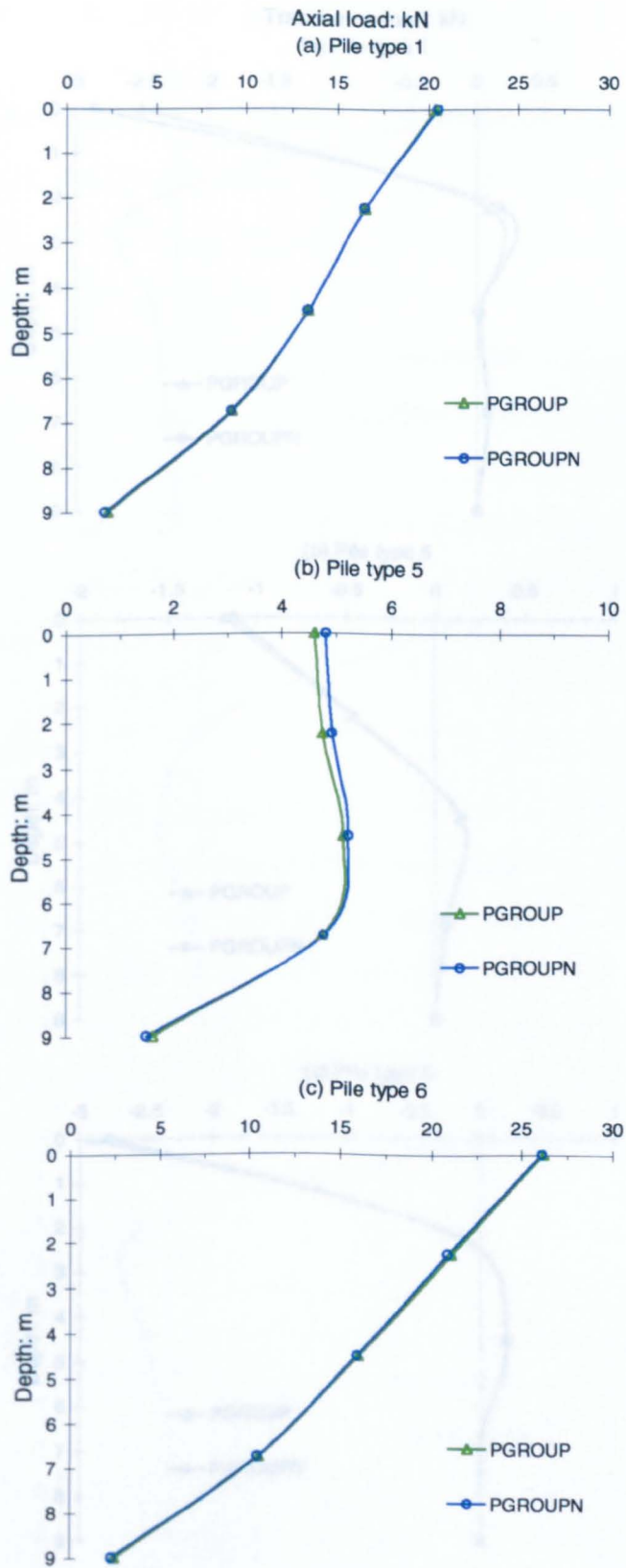


Fig. 5.35 Axial load distribution.

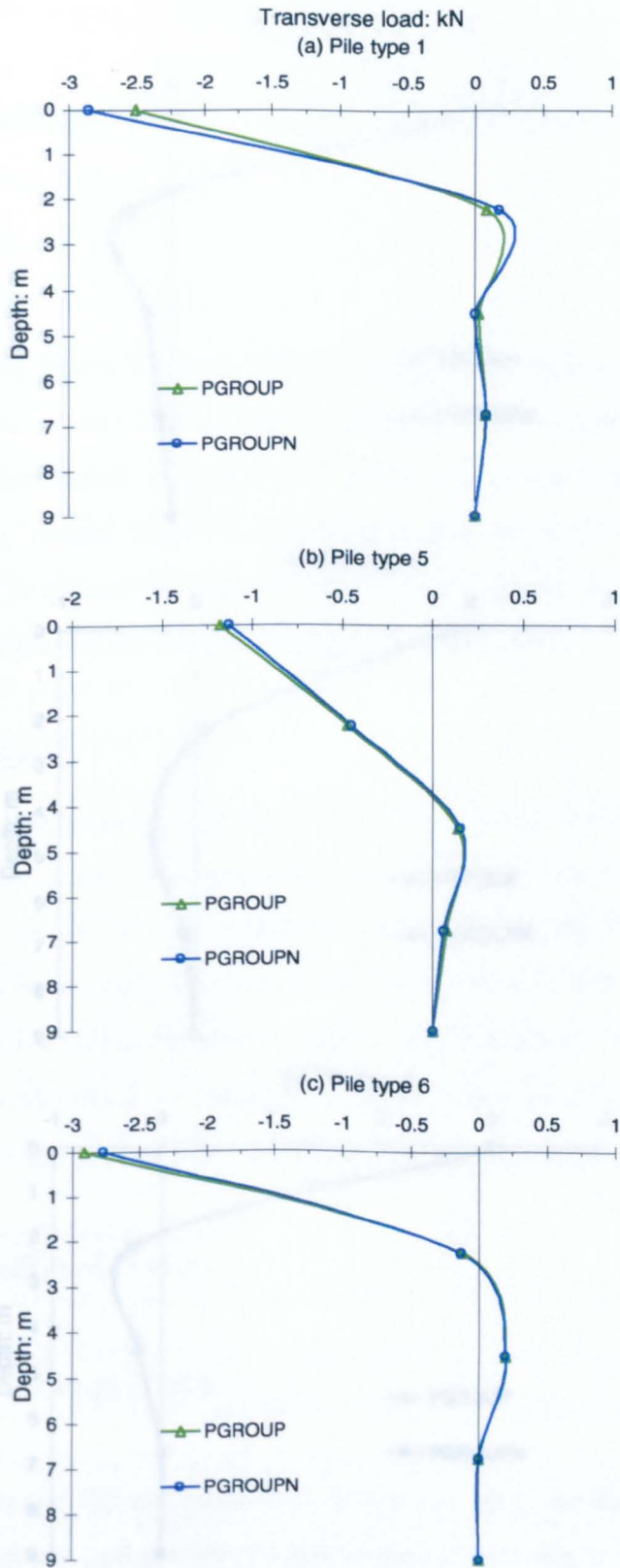


Fig. 5.36 Transverse load distribution.

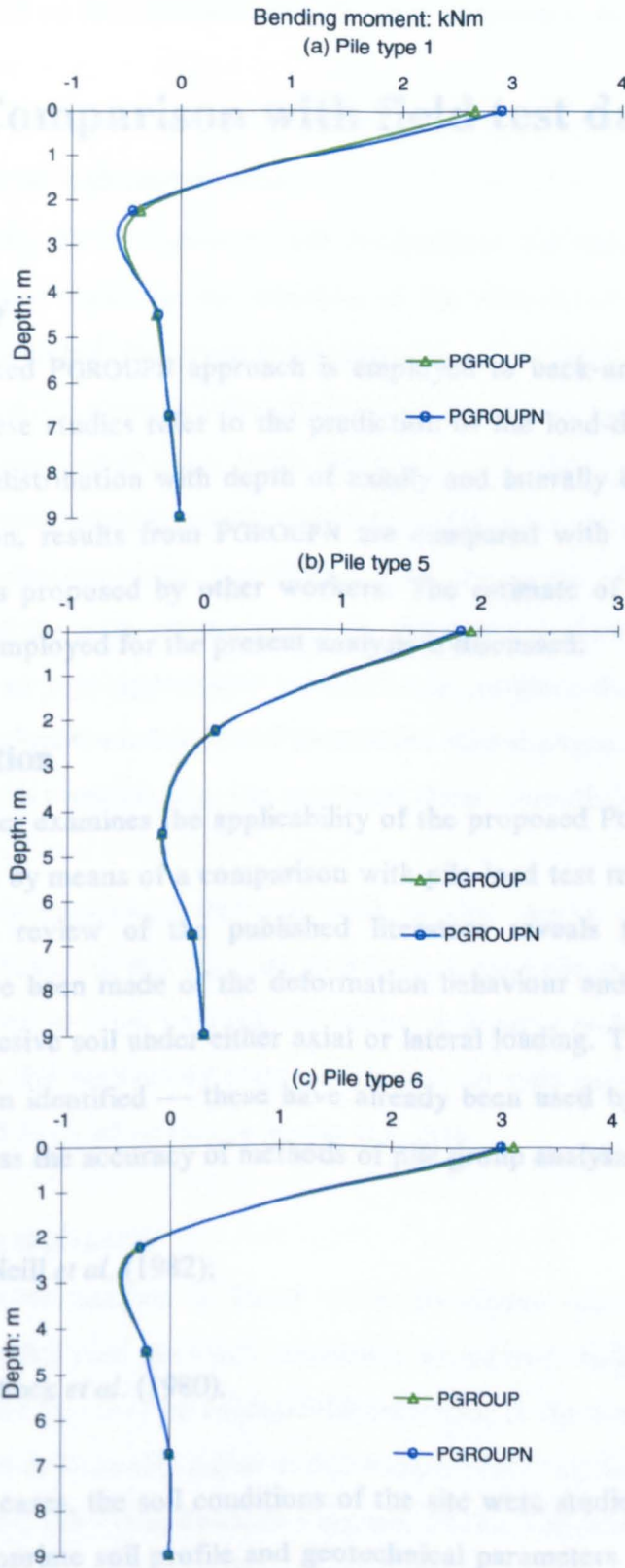


Fig. 5.37 Bending moment distribution.

## CHAPTER 6

### Comparison with field test data

#### 6.1 Summary

The proposed PGROUPN approach is employed to back-analyse two published case histories. These studies refer to the prediction of the load-deformation response and the pile load distribution with depth of axially and laterally loaded piles and pile groups. In addition, results from PGROUPN are compared with those obtained from numerical methods proposed by other workers. The estimate of the appropriate soil parameters to be employed for the present analysis is discussed.

#### 6.2 Introduction

This Chapter examines the applicability of the proposed PGROUPN approach to practical problems by means of a comparison with pile-load test results from published case histories. A review of the published literature reveals few cases in which measurements have been made of the deformation behaviour and load distribution of pile groups in cohesive soil under either axial or lateral loading. Two well known case histories have been identified — these have already been used by other authors as a benchmark to assess the accuracy of methods of pile group analysis:

- Field tests by O'Neill *et al.* (1982);
- Field tests by Matlock *et al.* (1980).

For each of these cases, the soil conditions of the site were studied carefully, in order to assess the appropriate soil profile and geotechnical parameters to be adopted in the present analysis. In addition, the predictions of other workers are discussed and compared with those obtained by the proposed approach.

The critical question of estimation of soil parameters is also addressed, and attention is focused on correlations between these parameters and commonly available in-situ test data.

### 6.3 Selection of soil parameters

In predicting the behaviour of pile foundations, the designer is faced with a number of decisions, including the selection of the method of analysis and the soil parameters to be adopted. However, it has long been recognised that the latter aspect is generally of greater importance than the method of analysis, provided that a soundly based method is employed (Poulos, 1989; Fleming *et al.*, 1992).

The proposed PGROUPN approach is intended for the non-linear analysis of pile foundations in cohesive soils, specifically fully saturated clay under undrained conditions. One of the main advantages of the PGROUPN analysis over more common load-transfer ( $t-z$  or  $p-y$ ) approaches is that it can simulate the essential non-linear features with a minimum number of soil parameters whose physical meanings are clear, ie the initial Young's modulus ( $E_s$ ), the undrained shear strength ( $C_u$ ) and the Poisson's ratio ( $\nu_s$ ).

It is widely recognised that the most reliable means of determining these parameters, in particular  $E_s$  and  $C_u$ , is by backfiguring from the results of full-scale pile load tests. However, in most practical situations, it is not possible to carry out such testing, at least in the preliminary stages of design. In such cases, resort is made to parameters derived from laboratory or in-situ test data.

#### 6.3.1 Young's modulus ( $E_s$ )

The PGROUPN analysis is based on a non-linear (elastic-perfectly plastic) interface model. In this case, previous experience shows that the initial (tangent) value of Young's modulus ( $E_s$ ) may be successfully employed in the prediction of the initial stiffness of the load-deformation curve of pile foundations (see, for example, Poulos & Davis, 1980; Poulos, 1989; Mandolini & Viggiani, 1997). The initial soil modulus  $E_s$  is also regarded as 'low strain' (ie less than about 0.001%) modulus (Jardine *et al.*, 1984, 1986; Randolph, 1994). The use of an initial value of  $E_s$  represents an advantage over a

purely linear elastic analysis which requires a secant value of  $E_s$ , relevant for normal working conditions. In fact, the choice of an appropriate secant value of  $E_s$  is by no means straightforward.

It is now well-understood that the values of  $E_s$  determined from conventional triaxial tests with external measurement of axial strain of the soil sample (which is highly inaccurate at strains less than about 0.1%) are usually much smaller (typically one-fourth to one-tenth) than the initial tangent modulus. The most reliable means of obtaining the low strain shear modulus ( $G_o$ ), which is connected with  $E_s$  by the formula  $E_s = 2G_o(1 + \nu_s)$ , is to carry out cross-hole shear wave measurements. Mandolini & Viggiani (1997) showed that there is a substantial agreement between low strain shear moduli derived from cross-hole data and those backfigured from pile loading tests, with a trend of the latter to fit the lower limit of the geophysical measurements.

If shear wave velocity measurements are not available, dynamic triaxial compression tests or resonant-column tests of undisturbed soil samples in laboratory are usually performed. Recent developments in the local measurement of small strains in the triaxial apparatus (Goto *et al.*, 1991; Cuccovillo & Coop, 1997) and in the bender element technique (Viggiani & Atkinson, 1995) have assisted in closing the gap between the static and dynamic measurement of shear moduli. In fact, it has been demonstrated that both static shear moduli and dynamic shear moduli are almost identical when precise measurements are made at very low shear strain levels of the order of  $10^{-5}$  (Abiss, 1981; Burland, 1989, Tatsuoka & Kohata, 1995; Lo Presti, 1995; Jamiolkowski *et al.*, 1995).

However, all of these means of measuring shear moduli are expensive and time-consuming, and require specialised techniques. Consequently, a number of empirical relationships have been proposed between low strain shear modulus (as determined from shear wave velocities) and parameters obtained from conventional in-situ and laboratory test results. Considering that the Poisson's ratio under undrained conditions is definite, i.e.  $\nu_s = 0.5$  (refer to Section 6.3.2), it is found convenient to express such correlations in terms of the initial Young's modulus ( $E_s$ ) rather than the initial shear modulus ( $G_o$ ).

Various correlations between  $E_s$  and SPT  $N$ -value have been proposed in Japan and the USA (Ohsaki & Iwasaki, 1973; Imai & Tonouchi, 1982; Sykora & Koester, 1986). Based on this work, Wroth *et al.* (1979) and Randolph (1994) proposed the following correlation:

$$E_s = 36N^{0.8} \quad [\text{MPa}] \quad (6.1)$$

However a linear correlation may be adopted for convenience, as suggested by Hirayama (1991, 1994) and Poulos (1993, 1994):

$$E_s = 14N \quad [\text{MPa}] \quad (6.2)$$

Alternatively, the initial soil modulus may be correlated with the results of the cone penetration test, as proposed by Randolph (1994):

$$E_s = 15(10q_c)^{0.6} \quad [\text{MPa}] \quad (6.3)$$

where  $q_c$  is the cone resistance (in MPa). This correlation is broadly consistent with recommendations by Imai & Tonouchi (1982).

However, it is often more convenient to correlate the initial soil modulus with the undrained shear strength ( $C_u$ ), and the following correlation is suggested by Hirayama (1991, 1994) and Poulos (1993, 1994):

$$E_s = 1500C_u \quad (6.4)$$

Several other correlations have been proposed, ie  $E_s = 1500\text{--}3000C_u$  (Jardine *et al.*, 1986),  $E_s = 1200\text{--}2700C_u$  (Kuwabara, 1991),  $E_s = 1900C_u$  (Kagawa, 1992). Thus, Equation (6.4) may give appropriate average values which are on the safe side.

However, it must be stated that such empirical correlations (Equations (6.1) to (6.4)) can only be expected to provide an approximate estimate of initial soil modulus

and hence their use may only be recommended in practice in some cases as follows (Gazetas, 1991):

- a) In feasibility studies and preliminary design calculations;
- b) For final design calculations in big projects as supplementary data or in small projects as main data;
- c) For initial data in back analyses;
- d) To provide an order-of-magnitude check against the experimentally determined values.

It should be emphasised that such correlations refer to the vertical response of pile foundations. More research is needed to define reliable correlations to determine the initial Young's modulus of the soil in the horizontal direction. This modulus is, in general, greater than the initial vertical modulus — for instance, in London Clay, the initial horizontal modulus is about twice the initial vertical modulus (Atkinson, 1975).

However, in order to take into account the higher strains associated with laterally loaded piles, the empirical correlations commonly adopted for non-linear analyses propose values of the horizontal modulus which are smaller (typically one-tenth) than the initial vertical moduli, ie:

$$E_h = 250-400C_u \quad (\text{Poulos \& Davis, 1980})$$

$$E_h = 50-200C_u \quad (\text{Reese \& Desai, 1977})$$

It is expected that high values of  $E_h/C_u$  are associated with highly plastic stiff clays.

Although the PGROUPN analysis is intended for pile groups embedded in an isotropic soil medium, it can be used for obtaining the approximate response to loading of pile groups in an anisotropic soil (ie the soil modulus in the horizontal direction is different from that in the vertical direction) by considering the horizontal and vertical behaviour separately and applying superposition (Banerjee & Driscoll, 1977).

### 6.3.2 Poisson's ratio ( $\nu_s$ )

Poisson's ratio of the soil is a necessary input parameter into analyses that involve elastic continuum theory, but its effect is generally quite minor when the solutions are expressed in terms of Young's modulus rather than shear modulus. It is widely recognised that the appropriate value of  $\nu_s$  for fully saturated clays under undrained conditions is 0.5 (see, for example, Ohsaki & Iwasaki, 1973; Poulos, 1989).

### 6.3.3 Undrained shear strength ( $C_u$ ) and adhesion factor ( $\alpha$ )

The limiting stresses defined in Section 2.4.4 are based on values of the undrained shear strength determined from conventional laboratory tests:

*limit bearing stress*

$$t_x = N_c C_u \quad (6.5) \quad (2.17 \text{ bis})$$

*limit shear stress (skin friction)*

$$t_s = \alpha C_u \quad (6.6) \quad (2.18 \text{ bis})$$

As regards driven piles, Fleming *et al.* (1992) observe that the value of  $\alpha$  deduced from pile load tests appears to reduce from unity or more for piles in clay of low strength, down to 0.5 or below for clay of strength above about 100 kPa. The American Petroleum Institute (API) Code RP 2A (1984) suggests a value of the adhesion factor ( $\alpha$ ) equal to 1 for  $C_u \leq 25$  kPa and to 0.5 for  $C_u \geq 70$  kPa, and a linear variation in between. Semple & Rigden (1984) observed that only a fraction of the pile load tests contained in the 1984 API data base refer to driven steel pipe piles in cohesive soil profiles. They therefore propose a value of the adhesion factor ( $\alpha$ ) equal to 1 for  $C_u \leq 35$  kPa and to 0.5 for  $C_u \geq 80$  kPa, and a linear variation in between. Based on published and unpublished records of pile loading tests, Tomlinson (1994) has compiled charts which establish a relationship between  $\alpha$  and  $C_u$  for different types of clay.

However, it has been recognised that the appropriate value of  $\alpha$  depends not strictly on the shear strength of the clay, but on its past stress history and overconsolidation ratio (OCR) (Randolph *et al.*, 1979; Randolph & Wroth, 1981; Kraft, 1982; Fleming *et al.*, 1992). This may conveniently be represented by the strength ratio ( $C_u / \sigma'_v$ ) of the soil, where  $\sigma'_v$  is the effective overburden stress (Randolph & Wroth, 1982). From the analysis of load tests on driven piles, Randolph & Murphy (1985) plotted the adhesion factor ( $\alpha$ ) against the average in-situ strength ratio ( $C_u / \sigma'_v$ ). From these plots, Fleming and colleagues derived a general expression for the value of  $\alpha$  (as a function of  $C_u / \sigma'_v$ ) in closed form. For normally consolidated clay located at great depth or overconsolidated clay, Semple (1980) proposed a diagram for evaluating the value of  $\alpha$  in terms of average OCR along the pile shaft.

Turning to bored piles, Fleming and colleagues propose that the average adhesion factor ( $\alpha$ ) may be approximately taken as 0.7 times the value for driven piles. For piles in stiff overconsolidated London Clay, it has been customary to assume an  $\alpha$  value of 0.45 (Skempton, 1959). This value is based on  $C_u$  determinations on unconsolidated-undrained triaxial tests performed on standard 38mm diameter specimens. However, a large number of pile loading tests carried out by Building Research Establishment (refer to Patel, 1989, 1992) has shown that 100mm samples are more likely to intersect the natural fissures in London Clay and hence they give a more reliable estimate of the strength of the clay mass. These tests demonstrate that values of  $C_u$  from the 100mm samples are about 23% lower than the 38mm samples, and hence it is concluded that higher adhesion factors ( $\alpha = 0.6$ ) may be employed.

It may be noted that effective stress approaches which relate the skin friction to the in-situ effective stress state have been proposed for both driven and bored piles (eg Chandler, 1968; Burland, 1973; Meyerhof, 1976; Fleming *et al.*, 1992). However, for piles in clay, a total stress approach is still commonly applied (Poulos, 1989; Fleming *et al.*, 1992). This is mainly due to the difficulties in estimating the radial effective stresses and interface angles of friction at the point of failure (Chow, 1997).

Some correlations between the skin friction and the results of standard penetration or cone penetration tests have been proposed (Shioi & Fukui, 1982;

Schmertmann, 1978; De Ruiter & Beringen, 1979; Bustamante & Gianceselli, 1982). However, it should be emphasised that wide variations exist between some of these correlations (Poulos, 1989; Fleming *et al.*, 1992).

#### 6.4 Comparison with O'Neill *et al.* (1982)

O'Neill *et al.* (1982) reported the results of axial loading tests on full-scale single piles and pile groups driven into stiff overconsolidated clay. Figure 6.1 summarises the geotechnical data at the test site which was located at the University of Houston (after Poulos, 1989). Geotechnical data are available from standard penetration tests, cone penetration tests, pressuremeter tests, unconsolidated-undrained triaxial tests, laboratory consolidation tests and seismic cross-hole tests (refer to Mahar & O'Neill, 1983).

All piles were closed-ended tubular steel pipes with an external radius of 137 mm, a wall thickness of 9.3 mm and a penetration depth of 13.1 m. Nine of the piles were installed in a  $3 \times 3$  configuration with centre-to-centre spacing  $s = 3d$  (where  $d$  is the external diameter of the piles). The piles were connected to a massive reinforced concrete block, thus enforcing a condition of equal displacements of the piles in the group. There was a clearance of 0.9 m between the pile cap and the ground surface. Each of the two single piles was installed at opposite sides of the 9-pile group at a distance of about 3.7 m from the group centre pile. The two single piles and the 9-pile group were loaded to failure in compression on three occasions, approximately 18, 80 and 108 days after installation. The results discussed below refer to the first of these tests. Within six days after the final 9-pile test, a 5-pile subgroup consisting of the centre edge piles (piles 2 in Fig. 6.3) plus the centre pile (pile 3), and a 4-pile subgroup consisting of the centre edge piles only were tested to failure. The details of the pile parameters and the group configuration are as follows:

Embedded length of piles ( $L$ )	= 13.1 m
Pile external diameter ( $d$ )	= 0.2740 m
Pile internal diameter ( $d_i$ )	= 0.2554 m
Centre-to-centre pile spacing ( $s$ )	= 0.8220 m
Depth of overhang of the pile cap ( $g$ )	= 0.9 m

Young's modulus of steel piles ( $E_p$ ) = 210 GPa

For all the PGROUPN analyses, the number of pile shaft elements per pile ( $N$ ) has been selected according to the recommendations given in Section 4.3.1.1, ie  $N = 24$ . It has been found that about 200 load increments ( $NINC$ ) are generally sufficient to achieve convergence of the PGROUPN solution process. The resulting (average) computing time for the numerical simulations on the 9-pile group is about 120 s (using a Pentium 133 MHz with 16 Mb RAM).

#### 6.4.1 Current analysis

A prediction of the load-settlement response and the load distribution for the reference single piles and the pile groups described above is proposed. The profiles of  $E_s$  and  $C_u$  employed in the present study are based on the geotechnical data reported by Poulos (1989) in his Rankine Lecture (refer to Fig. 6.1):

- a) The seismic cross-hole data are used to estimate a profile of the initial soil modulus ( $E_s$ ), which has been assumed to vary linearly with depth from 100 MPa at the surface to 400 MPa at the pile base;
- b) The Poisson's ratio is taken as 0.5 (relevant for fully saturated clay under undrained conditions);
- c) The undrained shear strength profiles deduced from unconsolidated-undrained triaxial tests in the laboratory and from pressuremeter tests showed quite different trends. In the current analysis, the interpreted shear strength profile is based primarily on unconsolidated-undrained tests as the method used to predict pile capacity is based on this kind of strength tests (Kraft *et al.*, 1981). Thus, the assumed undrained shear strength profile is  $C_u = 40.3$  kPa at the surface, increasing linearly to  $C_u = 174.4$  kPa at the level of the pile base, as deduced from a regression analysis over pile depth. It may be noted that such a profile, which is very similar to that suggested by Poulos (ie  $C_u =$

53 kPa at the surface, increasing linearly to  $C_u = 147$  kPa at the pile base), represents a crude approximation of the actual scattered profile;

- d) The average value of the adhesion factor ( $\alpha$ ) is taken as 0.5. This is based on a correlation of  $\alpha$  with  $C_u$  (rather than with  $C_u / \sigma'_v$ ), as discussed in Section 6.3.3 (API Code RP 2A, 1984; Semple & Rigden, 1984; Fleming *et al.*, 1992).

Thus, the soil parameters to be used in the present study may be summarised as follows:

Young's modulus at ground level ( $E_{so}$ )	= 100 MPa
Rate of increase of Young's modulus with depth ( $m$ )	= 23 MPa per metre
Poisson's ratio ( $\nu_s$ )	= 0.5
Undrained shear strength at ground level ( $C_{u0}$ )	= 40.3 kPa
Rate of increase of undrained shear strength with depth ( $c$ )	= 10.2 kPa per metre
Adhesion factor ( $\alpha$ )	= 0.5

Figures 6.2 and 6.3 show a generally good agreement between the computed and measured load-settlement behaviour of the average of the two reference single piles and the pile groups. It is worth noting that the response of the pile group is more linear than that of the single pile, and this feature of behaviour becomes more marked with increasing the number of piles in the group. This trend has already been observed by Randolph (1994).

The axial load distribution between the piles in the 9-pile group at a working load of 2.58 MN and at a load nearing failure of 5.66 MN are presented in Figs. 6.4 and 6.5, showing a fair agreement between the computed and measured values. It is worth noting that, at a working load level, the largest loads occurred in the corner piles and the smallest in the centre pile. Closer to the failure load of the pile group, the load distribution amongst the piles is fairly even. Of course, at this load level, the degree of accuracy of the analysis would to a large extent depend on the agreement between the assumed ultimate pile capacities and the actual values in the field. For instance, O'Neill and colleagues observe that the centre pile carried the highest load at failure, as contrasted to the lowest at working

load, due to a slightly higher end-bearing load that may have resulted from higher effective confining stresses in the soil in the interior of the group.

It should be emphasised that Poulos (1989) does not present numerical results in the non-linear range. However, the next section shows a comparison of the PGROUPN results with those predicted by alternative non-linear analyses.

#### 6.4.2 Prediction by previous workers

Further application of the PGROUPN approach is examined by comparison with the results obtained from alternative numerical analyses. The test reported by O'Neill and colleagues was analysed by Chow (1986a) by means of a hybrid method in which the response of the individual piles is modelled using the load-transfer method and the interaction between the piles is effected using Mindlin's solution. The test was also analysed by the same author (Chow, 1987c) using a hybrid approach in which load-transfer curves are used to model the individual pile response and a FEM solution is adopted to evaluate the interaction between piles.

In order to ensure consistency between analyses, the set of soil properties employed by Chow (1986a) and Chow (1987c) is used in this study, as described below. The soil Young's modulus at the surface is 144 MPa, increasing linearly at the rate of 23.6 MPa per metre, as deduced from the cross-hole data interpreted by Kraft *et al.* (1981). The soil Poisson's ratio is taken as 0.5. The undrained shear strength is  $C_u = 47.9$  kPa at the surface, increasing linearly to  $C_u = 239$  kPa at the pile base. An end-bearing pressure of 2.15 MPa ( $= 9C_u$ ) has been adopted. Back analysis of the average of the two reference single pile tests gave an average  $\alpha = 0.34$  for the shaft resistance. Thus:

Young's modulus at ground level ( $E_{s0}$ )	= 144 MPa
Rate of increase of Young's modulus with depth ( $m$ )	= 23.6 MPa per metre
Poisson's ratio ( $\nu_s$ )	= 0.5
Undrained shear strength at ground level ( $C_{u0}$ )	= 47.9 kPa
Rate of increase of undrained shear strength with depth ( $c$ )	= 14.6 kPa per metre
Adhesion factor ( $\alpha$ )	= 0.34

Figures 6.6 and 6.7 show a generally good agreement between the computed and measured load-settlement behaviour of the reference single pile, the 4-pile subgroup (piles 2) and the 9-pile group. If these results are compared with those obtained in the previous section (refer to Figs. 6.2 and 6.3), it is observed that an equally good fit of load-settlement curves for both single piles and pile groups can be obtained using two different combinations of  $E_s$  and  $C_u$ . In particular, the profile of undrained shear strength proposed by Chow (1986a, 1987c), which is based on back-analysis of the reference single pile tests, predicts an ultimate capacity of the single piles and the pile groups which is similar to the prediction described in Section 6.4.1.

Figures 6.8 and 6.9 report the computed and measured axial load distribution with depth among the piles in the 9-pile group at a working load of 2.58 MN and at a load nearing failure of 5.66 MN, respectively. In addition, Tables 6.1 and 6.2 show the computed and measured axial loads taken by the individual pile heads in the linear and non-linear range. It is worth noting that, even at a working load level of 2.58 MN, the mild nonlinearity in the computed solution has a relevant influence on the load distribution, and improves on the agreement between the computed and the measured values. Closer to the failure load of the pile group, the effect of nonlinearity is to cause a redistribution of the loads in the individual piles of the group, leading to a more uniform distribution. At this load level, the linear elastic solutions are not strictly applicable, but the actual trend is well reflected in the non-linear solutions.

The test reported by O'Neill and colleagues was analysed by Hirayama (1991) by means of a method which considers the effect of induced non-homogeneity due to pile settlements on pile-soil and pile-soil-pile interactions. The calculated soil moduli are introduced in a non-linear BEM analysis based on a hyperbolic interface model.

The set of soil properties adopted by Hirayama is as follows: the assumed undrained shear strength profile is  $C_u = 53$  kPa at the surface, increasing linearly to  $C_u = 147$  kPa at the level of the pile base (as suggested by Poulos, 1989); the end-bearing pressure is equal to  $9C_u$ ; the adhesion factor is evaluated in terms of average OCR, as proposed by Semple (1980), i.e.  $\alpha = 0.5$ ; the initial soil modulus is evaluated on the basis of the empirical correlation  $E_s = 1500C_u$  (refer to Equation (6.4)). The Poisson's ratio is taken as 0.5. Thus:

Young's modulus at ground level ( $E_{so}$ )	= 79.5 MPa
Rate of increase of Young's modulus with depth ( $m$ )	= 10.8 MPa per metre
Poisson's ratio ( $\nu_s$ )	= 0.5
Undrained shear strength at ground level ( $C_{uo}$ )	= 53 kPa
Rate of increase of undrained shear strength with depth ( $c$ )	= 7.2 kPa per metre
Adhesion factor ( $\alpha$ )	= 0.5

Figures 6.10 and 6.11 compare the computed and measured load-settlement response of the single pile and the 9-pile group. It is worth noting that the two numerical solutions compare favourably. However, for the 9-pile group, the measured initial response is stiffer than the response computed by Hirayama and PGROUPN.

#### 6.4.3 Application of empirical correlations for determining $E_s$

The influence of the method of determination of the soil Young's modulus has been investigated by using the correlations described in Section 6.3.1 (Equations (6.1)–(6.4)), and employing the PGROUPN analysis.

For all analyses, the assumed undrained shear strength profile is  $C_u = 53$  kPa at the surface, increasing linearly to  $C_u = 147$  kPa at the level of the pile base (as suggested by Poulos, 1989), while the assumed adhesion factor ( $\alpha$ ) is 0.5 (refer to Section 6.4.1). The Poisson's ratio is taken as 0.5. Four different distributions of soil modulus with depth are deduced from Equations (6.1)–(6.4) as follows:

- a) (Equation 6.1) The interpreted values of  $N$  are 5 at the surface and 25 at the pile base, as deduced from the SPT profile shown in Fig. 6.1; this yields a profile of  $E_s$  which varies linearly with depth from 130.5 MPa at the surface to 472.8 MPa at the level of the pile base;
- b) (Equation 6.2) A profile of  $E_s$  which varies linearly with depth from 70 MPa at the surface to 350 MPa at the level of the pile base (with  $N = 5$  at the surface,  $N = 25$  at the pile base);

- c) (Equation 6.3) The interpreted values of cone resistance are  $q_c = 1.6$  MPa at the surface and  $q_c = 4.2$  MPa at the level of the pile base, as deduced from the CPT profile shown in Fig. 6.1; this yields a profile of  $E_s$  which varies linearly with depth from 79 MPa at the surface to 141 MPa at the level of the pile base;
- d) (Equation 6.4) Based on the profile of  $C_u$  described above, the assumed soil modulus profile is  $E_s = 79.5$  MPa at the surface, increasing linearly to 221 MPa at the pile base.

Figures 6.12 and 6.13 show the computed load-settlement behaviour of the single pile and the 9-pile group. It is immediately apparent that the closest predictions are given by the correlation  $E_s = 36N^{0.8}$  [MPa]. In general, the measured initial response is stiffer than that calculated by means of the empirical correlations. Such differences are more evident for the 9-pile group than for the single pile. This suggests that an accurate evaluation of  $E_s$  is crucial in predicting the behaviour of large pile groups. As already observed in Section 6.3, the most satisfactory procedure for assessing the soil modulus is by backfiguring from the results of full-scale pile load tests. However, the present study suggests that the value of  $E_s$ , as derived from seismic cross-hole data, may be successfully employed in the prediction of the pile settlement, thereby confirming the findings of Mandolini & Viggiani (1997).

It is worth noting that the observed discrepancies between the measured values and those calculated by means of the empirical correlations tend to be on the conservative side, ie the predicted settlements are larger than the actual settlements. Finally, it may be observed that the numerically predicted curves in Fig. 6.13 are almost linear up to the failure load, whereas the measured response attains more curvature.

## 6.5 Comparison with Matlock *et al.* (1980)

Because of the high cost and logistical difficulty of conducting lateral load tests on pile groups, relatively few full-scale load test results are available in the literature to

show the deformation behaviour and load distribution within a pile group embedded in cohesive soil. In addition, the majority of these tests refer to piles which are loaded under free-head conditions (ie zero moment), whereas the PGROUPN analysis applies to piles which are rigidly connected to the cap. The choice is therefore restricted to a comparison with the field tests conducted by Matlock *et al.* (1980), although these experiments refer to closely spaced pile groups in which shadowing effects are significant. Such effects, which consist of overlapping of failure zones and a consequent increase of group deflections, cannot be readily reproduced in the PGROUPN model (for further details refer to Section 1.3.2.2).

The lateral load tests reported by Matlock and colleagues refer to a single pile, 5-pile and 10-pile circular groups embedded in soft clay. Figures 6.14 and 6.15 summarise the geotechnical data at the test site which was located at Harvey, Louisiana. To avoid organic material, the soil around the piles was excavated and the 'mudline' established at 2.4 m (8 ft in Fig. 6.14) below the ground surface.

All piles were tubular steel pipes with an external radius of 84 mm, a wall thickness of 7.1 mm and a penetration depth of 11.6 m. The centre-to-centre spacing was 3.4 and 1.8 pile diameters for the 5-pile and 10-pile groups, respectively. Pile-head deflections were enforced at two elevations (one at 0.23 m above the groundline, ie at the level of the lower support, and the other near the pile top) by a special loading device to simulate pile-head restraints typical of offshore structures, as described in Figs. 6.16 and 6.17. In order to simulate the above-mentioned restraint imposed by the experimental setup, an applied moment  $M$  has been considered at the level of the lower support for the single pile. The assumed value of  $M$  is such that  $M/H = -0.8125$  m (where  $H$  is the applied lateral load), as deduced by the measurement of  $M = -26$  kNm by Matlock and colleagues for  $H = 32$  kN. As observed by Poulos & Randolph (1983), the loading support system may be assumed to apply the same relative restraint to the group piles (between the free-head and fixed-head cases) as to the single piles. Thus, the pile cap loading conditions consist of a lateral load and associated restraining moment of  $H = 140$  kN,  $M = -114$  kNm for the 5-pile group, and  $H = 250$  kN,  $M = -203$  kNm, for the 10-pile group.

In this study, the set of soil parameters used follows that reported by Bogard & Matlock (1983) and employed by Leung & Chow (1987), as shown below: an approximate

linearly increasing profile of the undrained shear strength is deduced from an in-situ vane-shear device, while an empirical correlation factor of  $E/C_u = 150$  is adopted for the Young's modulus of soft clay. A Poisson's ratio of 0.5 and an adhesion factor ( $\alpha$ ) of 0.5 have been adopted. Thus, the input parameters for the PGROUPN analysis are:

Embedded length of piles ( $L$ )	= 11.6 m
Pile external diameter ( $d$ )	= 0.1680 m
Pile internal diameter ( $d_i$ )	= 0.1538 m
Depth of overhang of the pile cap ( $g$ )	= 0.23 m
Young's modulus of steel piles ( $E_p$ )	= 210 GPa
Young's modulus at ground level ( $E_{s0}$ )	= 1575 kPa
Rate of increase of Young's modulus with depth ( $m$ )	= 390 kPa per metre
Poisson's ratio ( $\nu_s$ )	= 0.5
Undrained shear strength at ground level ( $C_{u0}$ )	= 10.5 kPa
Rate of increase of undrained shear strength with depth ( $c$ )	= 2.6 kPa per metre
Adhesion factor ( $\alpha$ )	= 0.5

For all the PGROUPN analyses, the number of pile shaft elements per pile ( $N$ ) has been selected according to the recommendations given in Section 5.2, ie  $N = 34$ . It has been found that about 100 load increments ( $NINC$ ) are sufficient to achieve a converged solution of the PGROUPN analyses. The resulting CPU time for the numerical simulations on the 10-pile group is about 200 s (using a Pentium 133 MHz with 16 Mb RAM).

Figures 6.18, 6.19 and 6.20 compare the measured average pile head load-deflection curves for the single pile, the 5-pile and 10-pile groups, respectively, with those predicted by PGROUPN and the hybrid approach of Leung & Chow, in which the individual pile response is modelled using load-transfer ( $p$ - $y$ ) curves and the group interaction is determined based on Mindlin's solution. It is worth noting that, due to the effect of pile-soil-pile interaction, the computed response of the pile group becomes more linear with increasing the number of piles in the group. This trend has already been observed in axially loaded pile groups. Reasonably good agreement with the measured values is achieved for

the single pile, while the PGROUPN response for the 5-pile and 10-pile groups is too stiff at high load levels. Such discrepancies (also noted in the solution of Leung & Chow) may be partially attributed to shadowing effects, which lead to increased group deflections. In addition, the nonlinearity of the group results from the experiments as compared with the near linear PGROUPN curves may also be related to soil disturbance caused by installation.

Figures (6.21) to (6.23) compare the computed and measured profile of bending moments along the piles under the loading conditions described above. For the pile groups, the profiles of bending moment refer to pile 1 (see Fig. 6.17). However, Matlock and colleagues observed that the variations of shear and bending moment among the piles of the groups were found to be very small. This feature of behaviour is well reflected in the PGROUPN solutions. The diagrams show that PGROUPN underestimates the maximum positive bending moment by about 50% for the pile groups, while a close agreement between computed and measured values is obtained for the single pile. As pointed out by Rollins *et al.* (1998), who performed similar load tests on closely spaced pile groups, this divergence may in part be attributed to group effects that become more significant as displacements increase and failure zones begin to overlap. The group effects cause the soil to behave as a softer material, leading to higher moments particularly at larger depths below the ground level. Finally, it should be emphasised that the experimental method of controlling moments to the pile head is fraught with difficulty and the moments are also strongly influenced by lateral movement as well as rotation. Therefore, the single-pile predictions are probably the most reliable results provided by Matlock and colleagues.

## 6.6 Concluding remarks

Application of the PGROUPN analysis to two well documented published case histories has shown that the suggested method is capable of giving reasonable estimates of the load-deformation response and load distribution of pile groups in cohesive soil under either axial or lateral loading. It has been shown that the PGROUPN solution avoids exaggeration of pile loads at group extremities which is common with linear elastic models, and predicts a more realistic load distribution to the individual piles of the group.

The proposed code is numerically efficient and exploits the capacity of modern desk top computers to provide a full continuum solution to large group problems in short time. One of the main features of the PGROUPN analysis is that it can simulate the essential non-linear features with a minimum number of soil parameters whose physical meaning is clear. By comparison with a purely linear elastic analysis, the present method requires only one additional soil parameter to be completely defined, ie the undrained shear-strength ( $C_u$ ) distribution with depth. This parameter is routinely measured in soils investigation. In addition, it should be emphasised that, in a linear elastic model, the selection of appropriate secant soil moduli is difficult. Instead, the proposed non-linear solution requires specification of the initial tangent soil modulus ( $E_s$ ). The present study suggests that the value of  $E_s$ , as derived from seismic cross-hole data, may be successfully employed in the prediction of the pile group settlement. Alternatively, approximate values of  $E_s$  may be deduced from empirical correlations with conventional in-situ and laboratory test results.

These features of PGROUPN represent an advantage over more common load-transfer (hybrid) approaches (eg those proposed by Chow and his co-workers), which are limited by the questionable assessment of the value of the modulus of subgrade reaction from intrinsic soil properties and the computational effort required to analyse large groups.

## TABLES CHAPTER 6

Table 6.1 Comparison of axial load distribution to individual pile heads in 9-pile group at a working group load of 2.58 MN.

Method	Average pile loads (kN)		
	Corner pile	Edge pile	Centre pile
Measured (O'Neill <i>et al.</i> , 1982)	294	285	267
Chow (1986a): Non-linear	295	284	269
PGROUPN (Non-linear)	295	283	266
Chow (1986a): Linear	315	274	229
PGROUPN (Linear)	311	275	237

Table 6.2 Comparison of axial load distribution to individual pile heads in 9-pile group at a group load nearing failure of 5.66 MN.

Method	Average pile loads (kN)		
	Corner pile	Edge pile	Centre pile
Measured (O'Neill <i>et al.</i> , 1982)	635	608	696
Chow (1986a): Non-linear	631	629	626
PGROUPN (Non-linear)	633	627	622
Chow (1986a): Linear	690	600	502
PGROUPN (Linear)	681	603	520

FIGURES CHAPTER 6

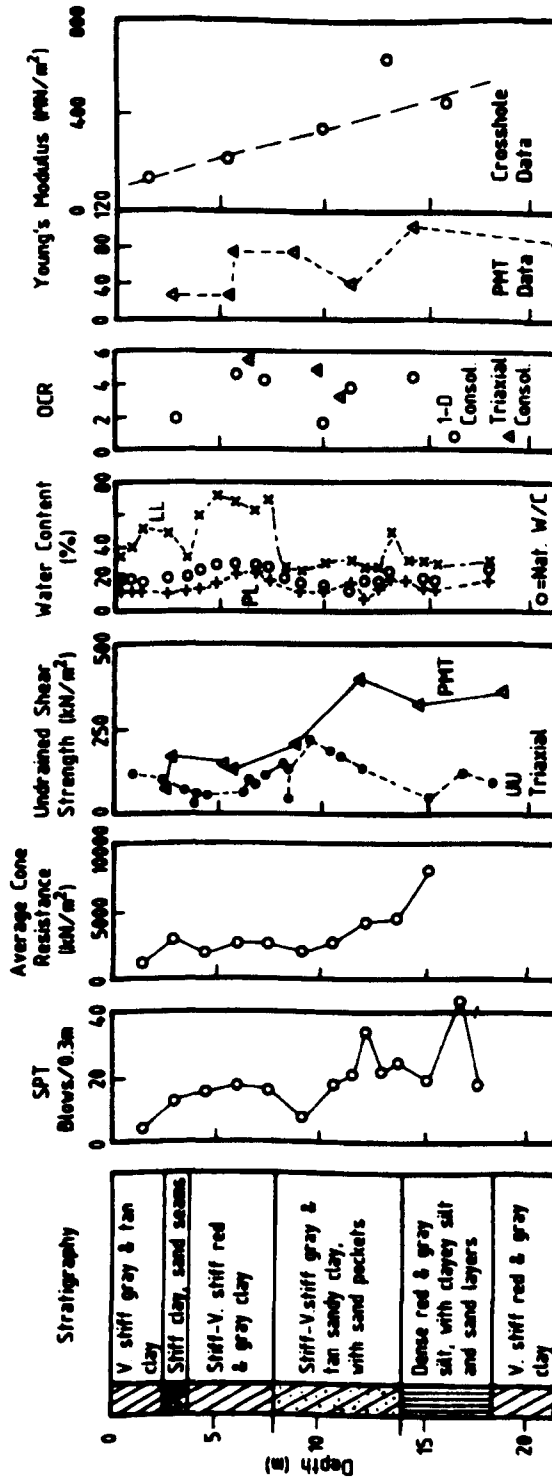


Fig. 6.1 Summary of geotechnical data at University of Houston test site (after Poulos, 1989).

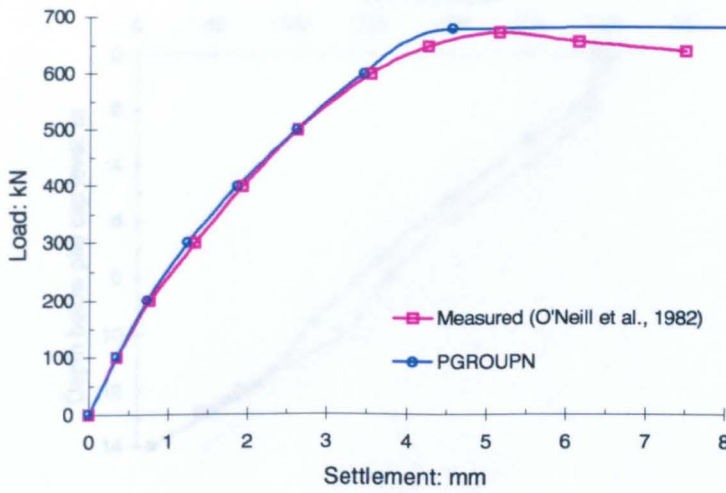


Fig. 6.2 Comparison between predicted and measured load-settlement behaviour of single pile.

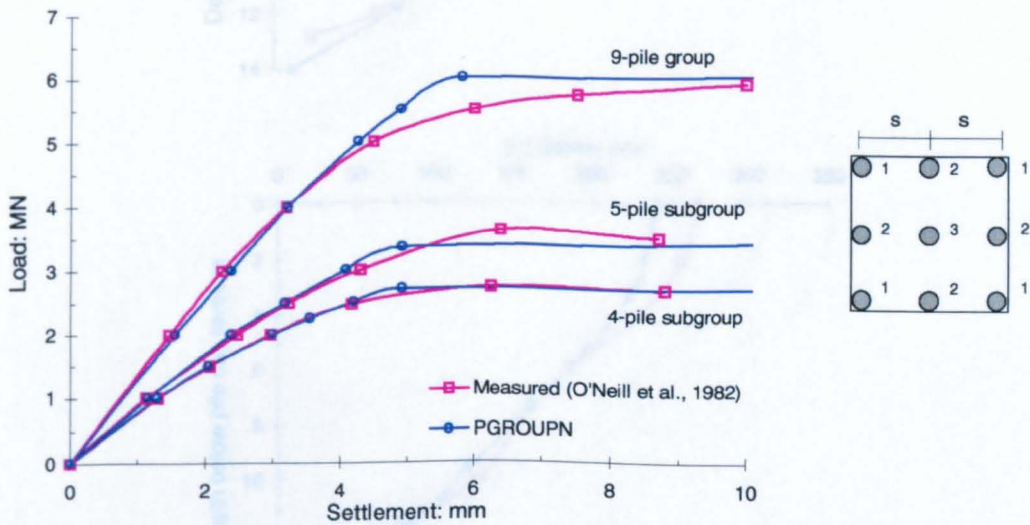


Fig. 6.3 Comparison between predicted and measured load-settlement behaviour of pile groups.

Fig. 6.4 Comparison between predicted and measured axial load distribution in 9-pile group at a working group load of 2.58 MN

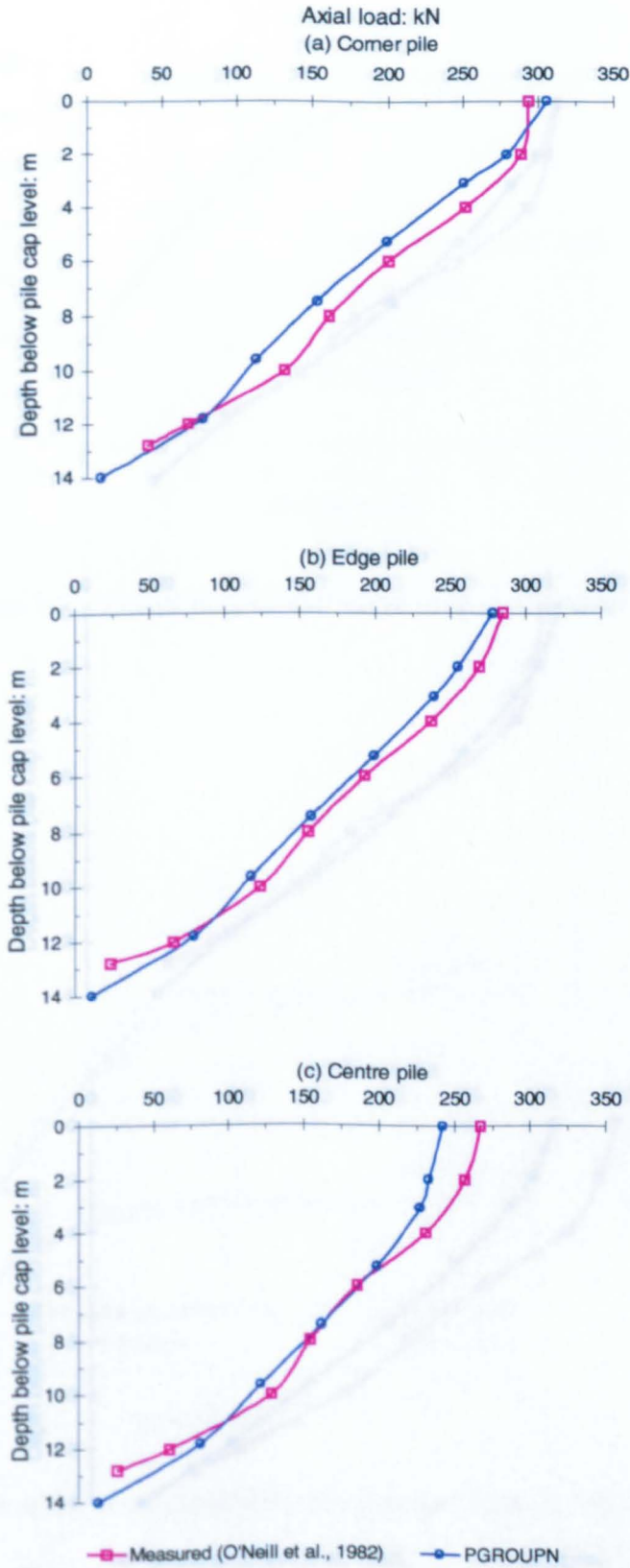


Fig. 6.4 Comparison between predicted and measured axial load distribution in 9-pile group at a working group load of 2.58 MN.

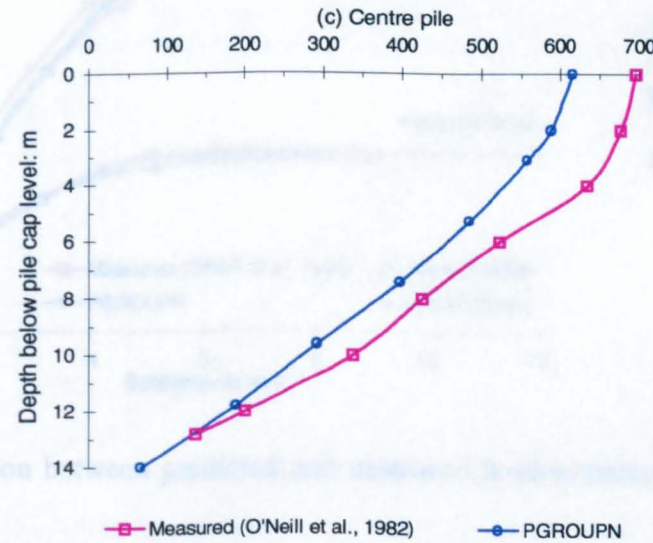
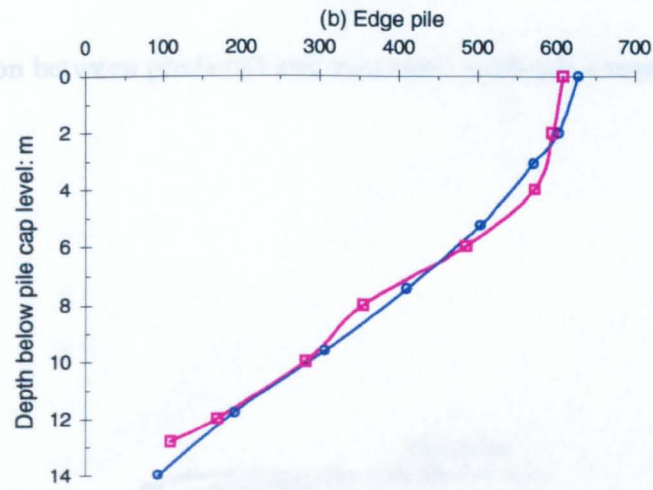
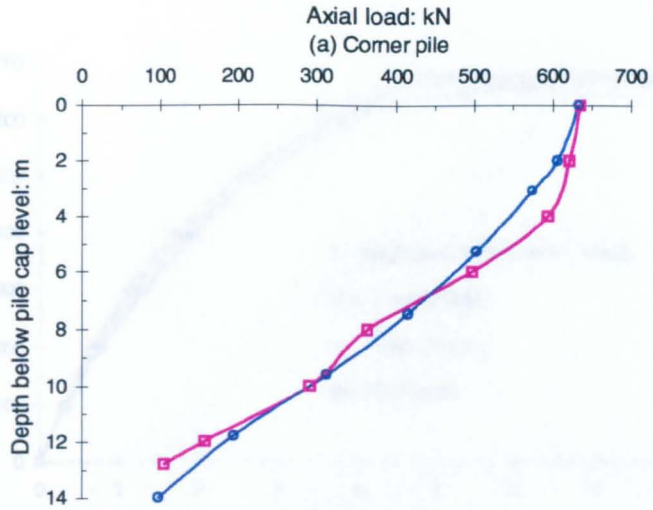


Fig. 6.6 Comparison between predicted and measured axial load distribution in 9-pile group at a group load nearing failure of 5.66 MN.

Fig. 6.7 Comparison between predicted and measured axial load distribution in 9-pile group at a group load nearing failure of 5.66 MN.

Fig. 6.5 Comparison between predicted and measured axial load distribution in 9-pile group at a group load nearing failure of 5.66 MN.

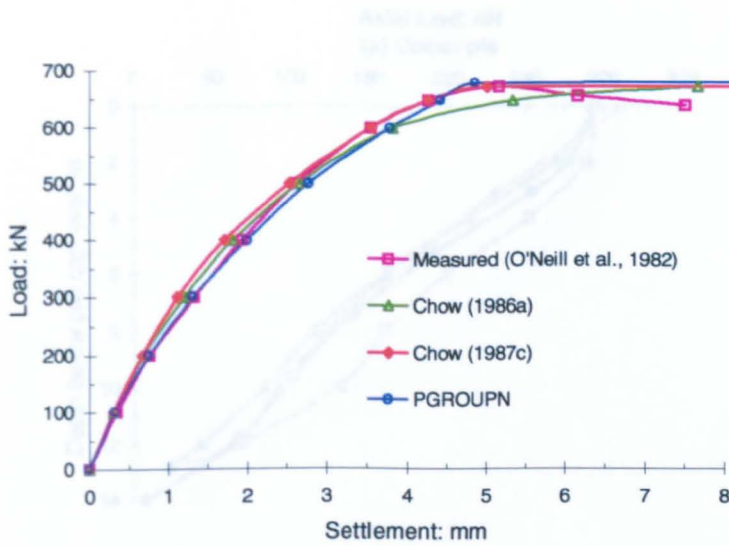


Fig. 6.6 Comparison between predicted and measured load-settlement behaviour of single pile.

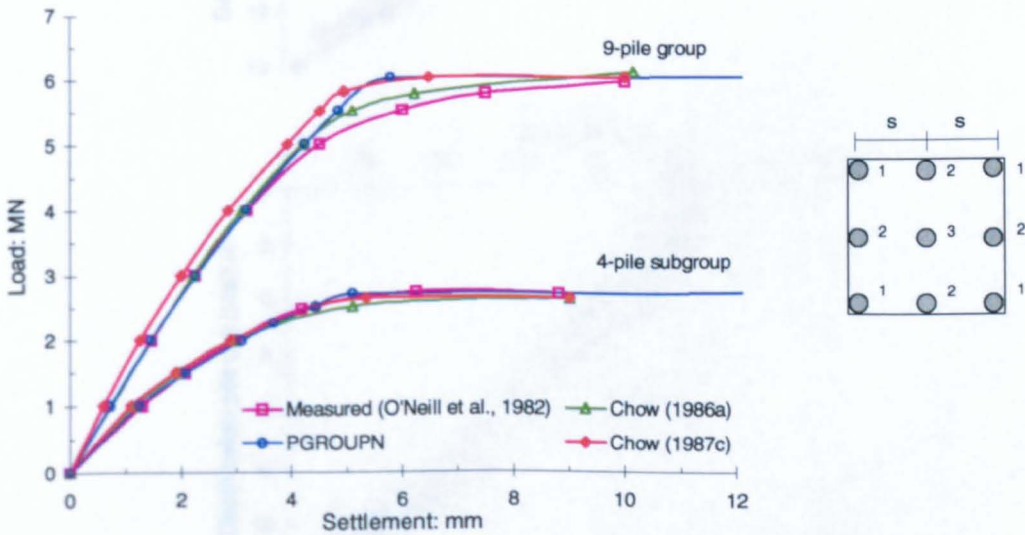


Fig. 6.7 Comparison between predicted and measured load-settlement behaviour of pile groups.

Fig. 6.8 Comparison between predicted and measured load-settlement behaviour of pile group at a working group load of 1000 kN.

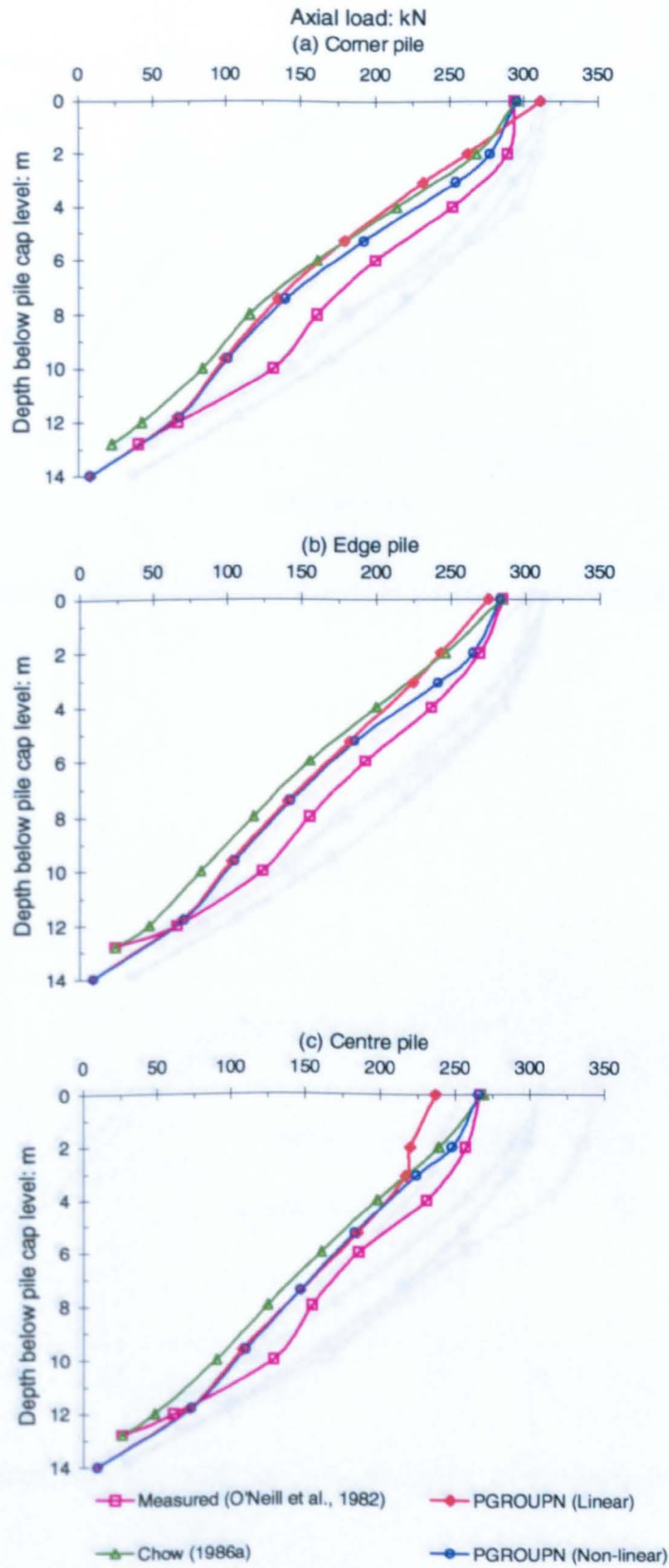


Fig. 6.8 Comparison between predicted and measured axial load distribution in 9-pile group at a working group load of 2.58 MN.

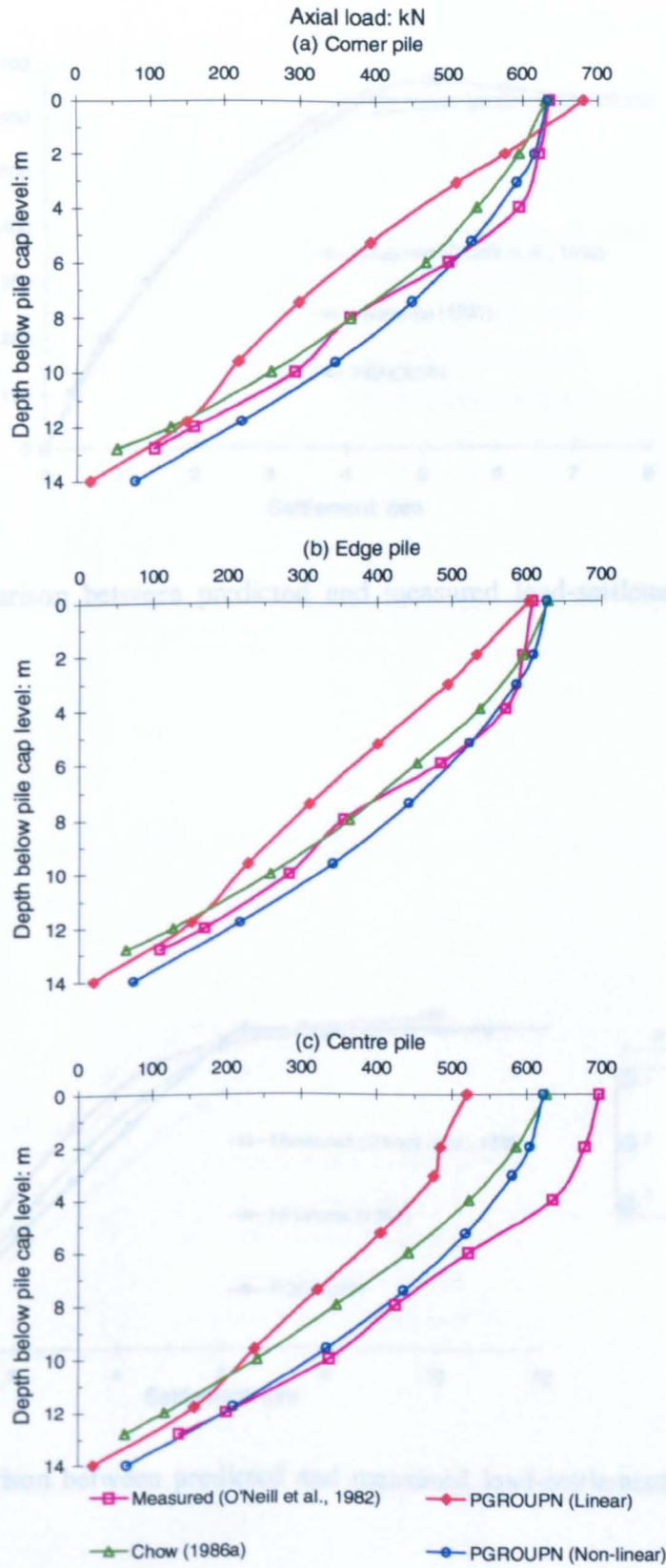


Fig. 6.9 Comparison between predicted and measured axial load distribution in 9-pile group at a group load nearing failure of 5.66 MN.

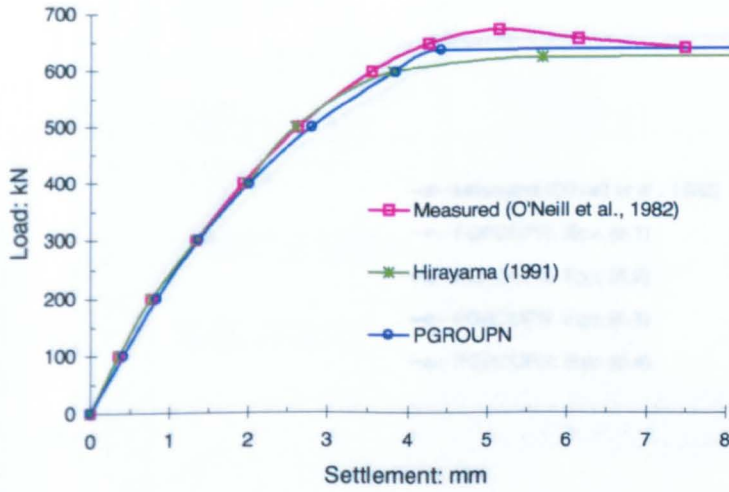


Fig. 6.10 Comparison between predicted and measured load-settlement behaviour of single pile.

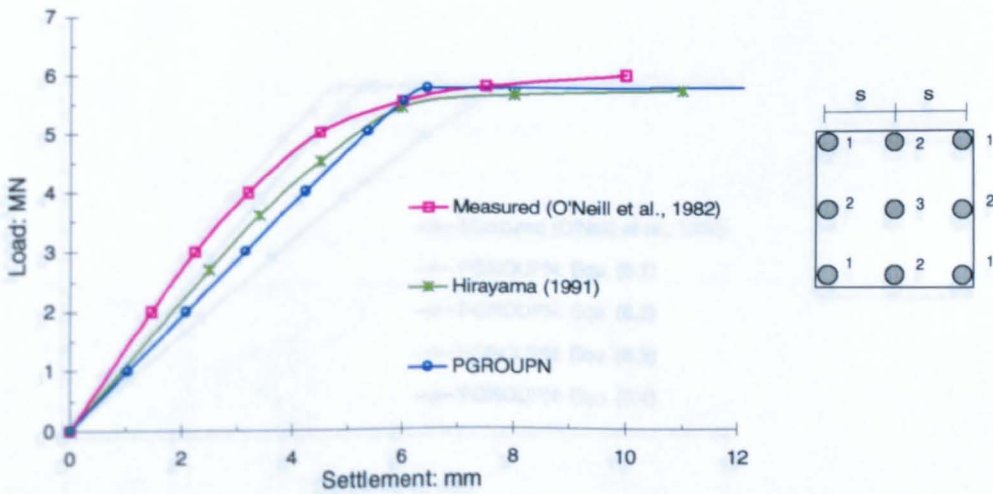


Fig. 6.11 Comparison between predicted and measured load-settlement behaviour of 9-pile group.

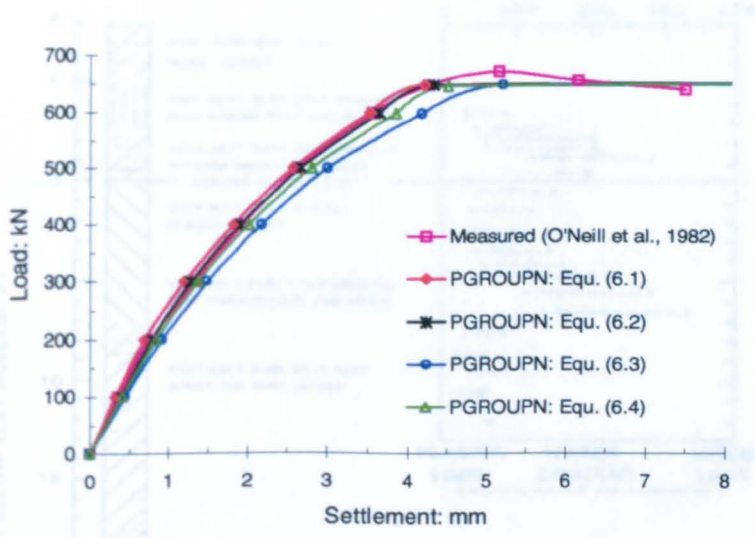


Fig. 6.12 Load-settlement behaviour of single pile: application of empirical correlations for determining  $E_p$ .

Fig. 6.14 Soil conditions at Harvey test site, as described by Mallock et al. (1980) (NOTE: 1 ft = 0.3048 m).

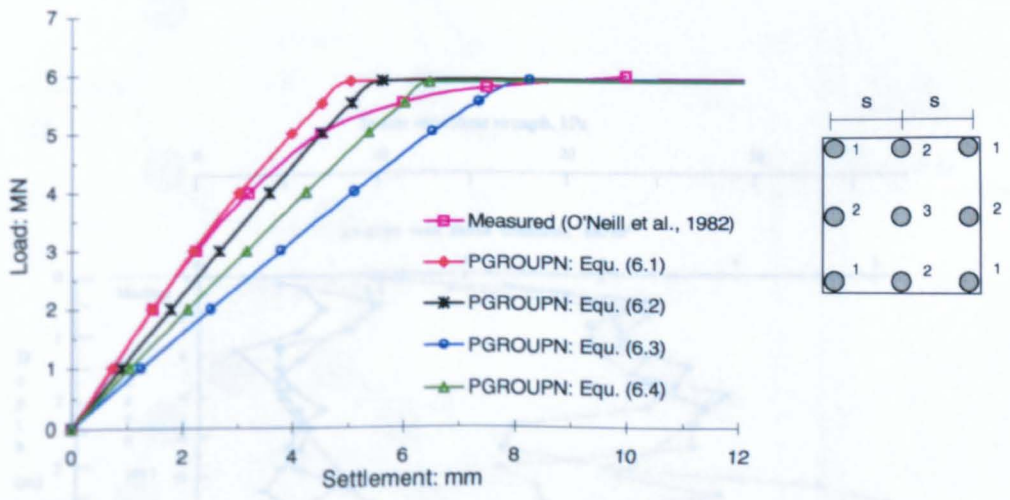


Fig. 6.13 Load-settlement behaviour of 9-pile group: application of empirical correlations for determining  $E_p$ .

Fig. 6.15 In-situ vane shear strength profile at Harvey test site, as described by Mallock et al. (1980) (NOTE: 1 ft = 0.3048 m;  $1 \text{ MN/m}^2 = 0.1458 \text{ MN/m}^2$ ).

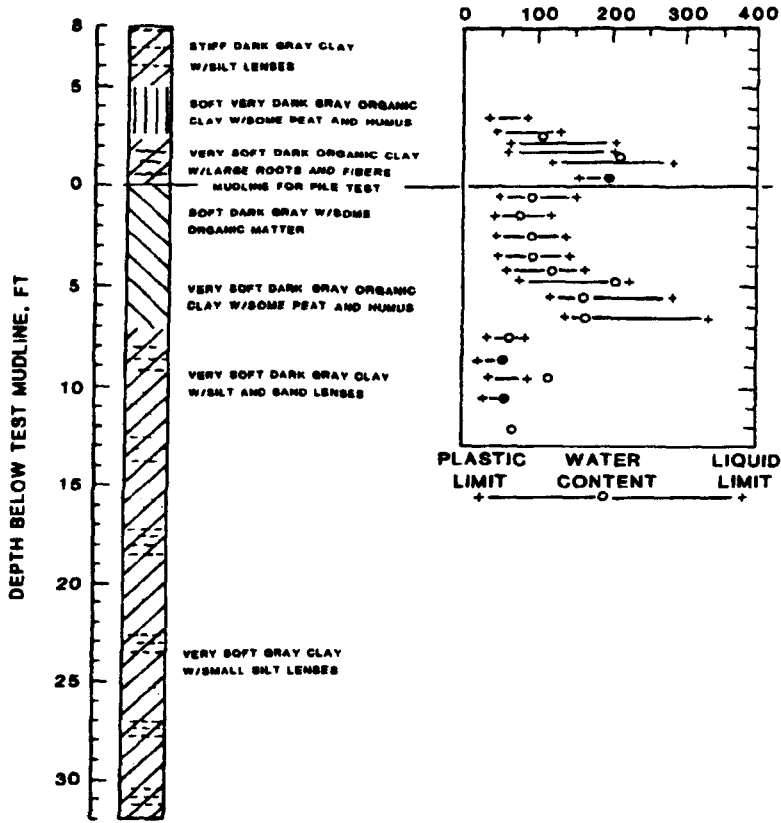


Fig. 6.14 Soil conditions at Harvey test site, as described by Matlock *et al.* (1980) (NOTE: 1 ft = 0.3048 m).

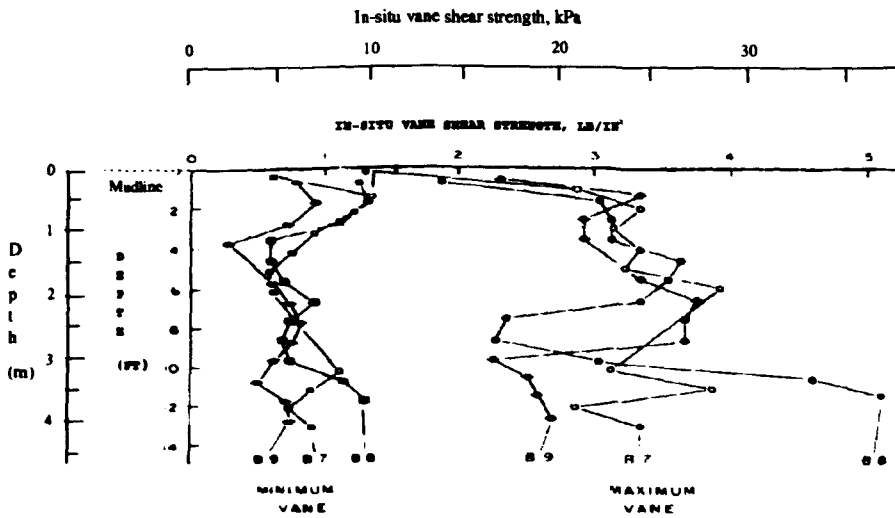


Fig. 6.15 In-situ vane shear strength profile at Harvey test site, as described by Matlock *et al.* (1980) (NOTE: 1 ft = 0.3048 m; 1 lb/in<sup>2</sup> = 6.895 kPa).

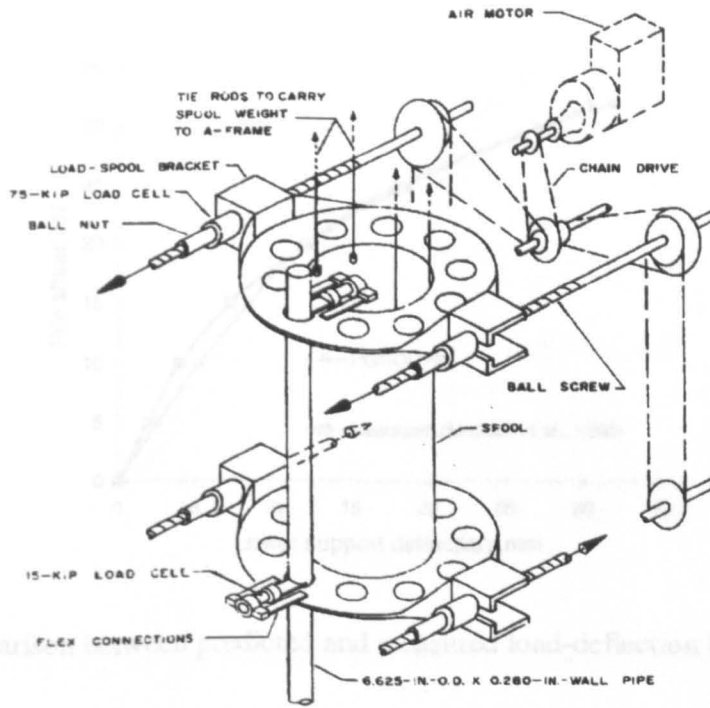


Fig. 6.16 Pile test setup at Harvey test site, as described by Matlock *et al.* (1980).

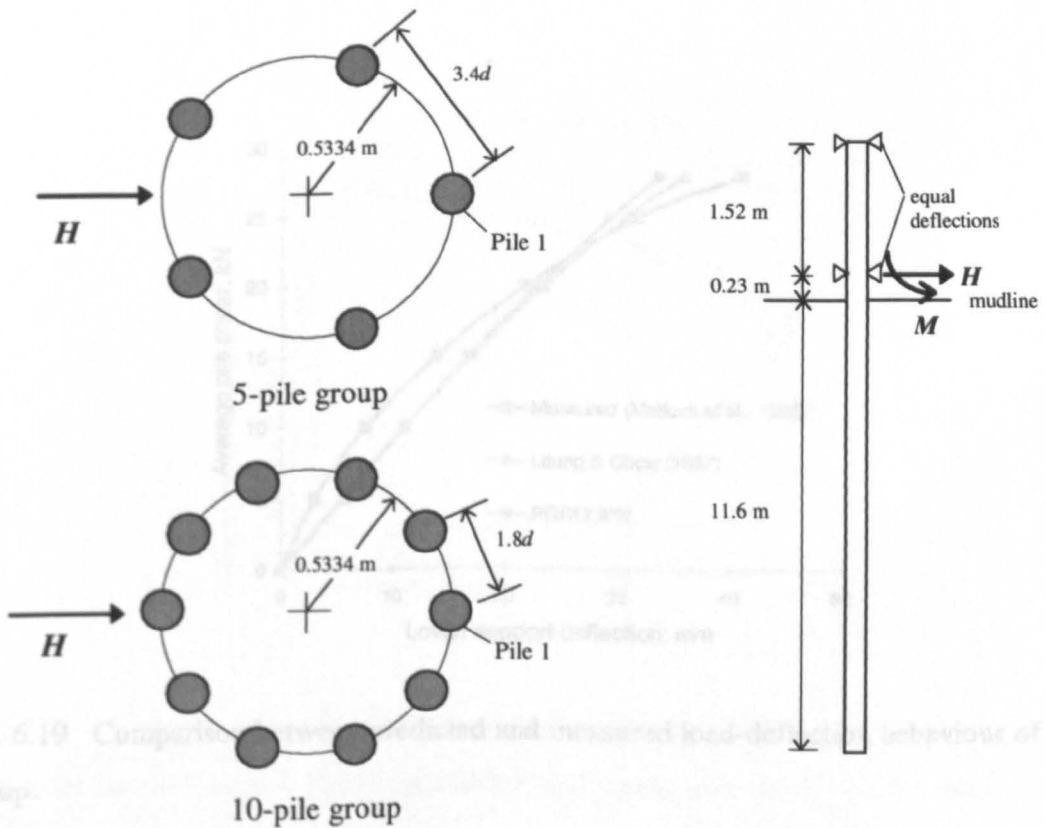


Fig. 6.17 Pile group geometry and loading arrangement (after Poulos & Randolph, 1983).

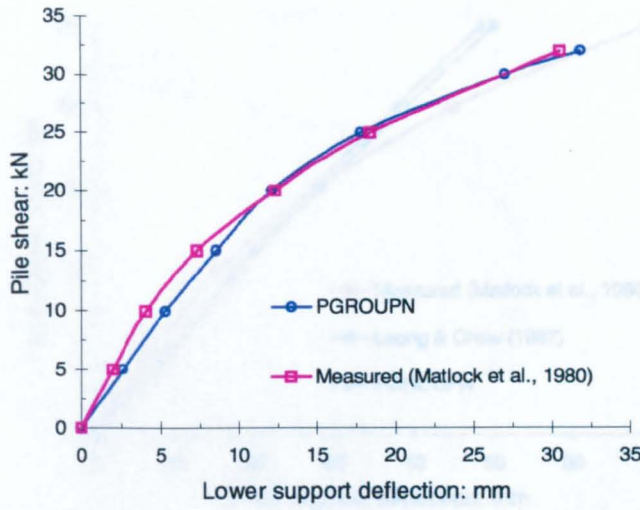


Fig. 6.18 Comparison between predicted and measured load-deflection behaviour of single pile.

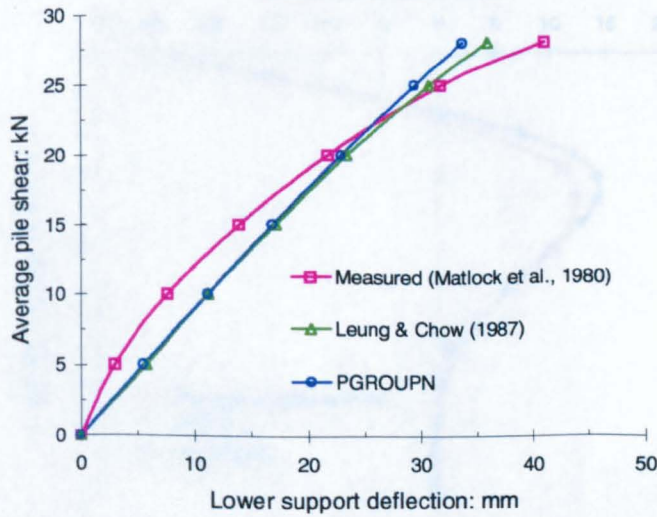


Fig. 6.19 Comparison between predicted and measured load-deflection behaviour of 5-pile group.

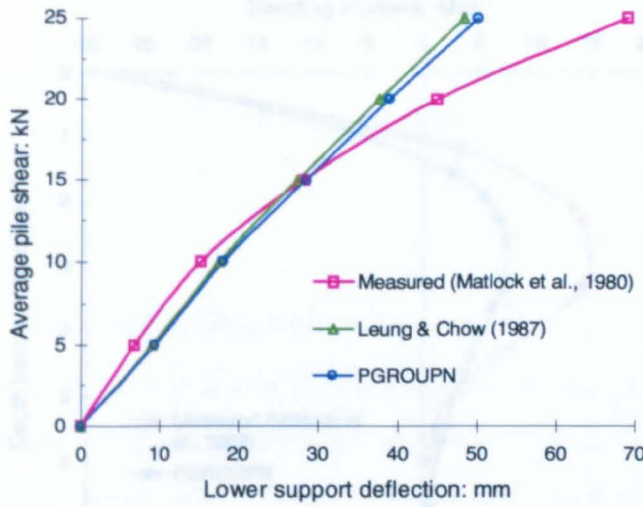


Fig. 6.20 Comparison between predicted and measured load-deflection behaviour of 10-pile group.

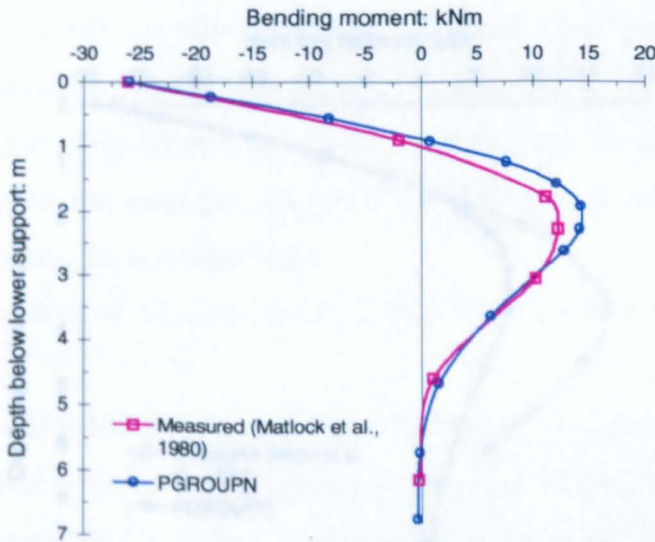


Fig. 6.21 Comparison between predicted and measured bending moment profile of single pile under lateral load  $H = 32$  kN (associated restraining moment  $M = -26$  kNm).

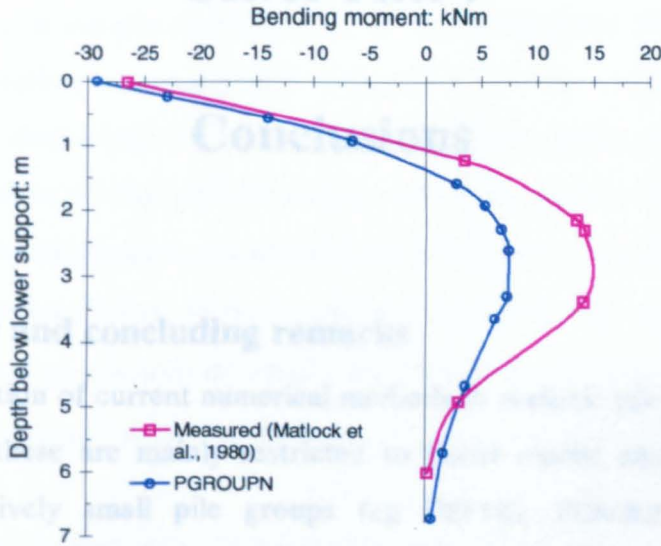


Fig. 6.22 Comparison between predicted and measured bending moment profile for pile 1 from lateral load test ( $H = 140 \text{ kN}$ ,  $M = -114 \text{ kNm}$ ) of 5-pile group.

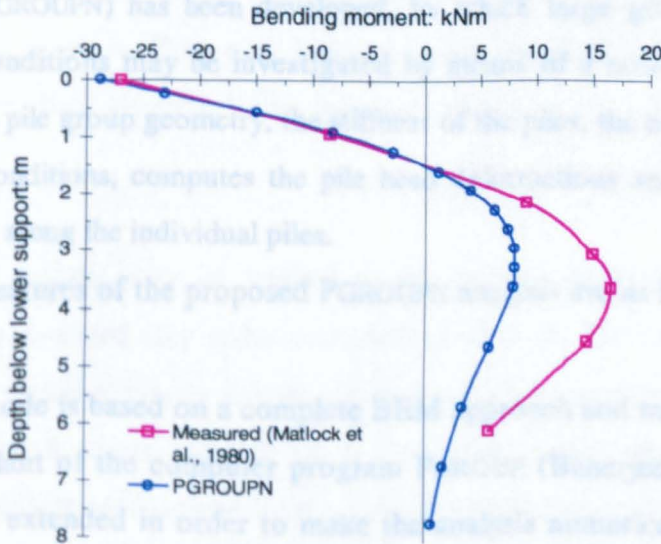


Fig. 6.23 Comparison between predicted and measured bending moment profile for pile 1 from lateral load test ( $H = 250 \text{ kN}$ ,  $M = -203 \text{ kNm}$ ) of 10-pile group.

# CHAPTER 7

## Conclusions

### 7.1 Summary and concluding remarks

The application of current numerical methods to realistic pile group problems is deficient because these are mainly restricted to linear elastic analyses (eg PIGLET, PGROUP) or relatively small pile groups (eg DEFPIG, PGROUP). Several hybrid approaches have recently been proposed, in which load-transfer (non-linear) functions are used to model the individual pile response and a continuum solution is adopted to determine the group interaction. The main drawback to these approaches is the problematic evaluation of the modulus of subgrade reaction from intrinsic soil properties — this modulus may only be obtained by using empirical parameters or by backfiguring from the results of pile load tests.

In this thesis, an attempt at removing these limitations has been made. A computer program (called PGROUPN) has been developed, by which large groups of piles under general loading conditions may be investigated by means of a non-linear analysis. The program, given the pile group geometry, the stiffness of the piles, the external loads and the surrounding soil conditions, computes the pile head deformations and the distribution of loads and moments along the individual piles.

The main features of the proposed PGROUPN analysis are as follows:

- a) The numerical code is based on a complete BEM approach and may be regarded as a generic descendant of the computer program PGROUP (Banerjee & Driscoll, 1976) which has been extended in order to make the analysis numerically efficient and to include the effects of soil nonlinearity. The strategies adopted for achieving efficiency gains are as follows: (1) the pile base is represented by one (circular) element only; (2) the diagonal soil flexibility terms are calculated via analytical integration of the singular Mindlin functions; (3) the off-diagonal soil flexibility

terms are evaluated by approximating the continuously distributed loads by equivalent point loads acting at the pile nodes; (4) use of Bernoulli-Euler beam theory for pile domain discretization and analytical integration of the singular functions; (5) exploitation of similarities in forming single-pile flexibility matrices; (6) more efficient calculation of the unit boundary condition vector; (7) pile-soil system solved via LU decomposition. As regards the inclusion of non-linear soil response, this has been accomplished, in an approximate manner, by means of a stepwise linear incremental procedure in which the global flexibility matrix  $[G_p + G_s]$  is modified as one or more elements at the pile-soil interface reach the yield conditions;

- b) Any combination of vertical loads, horizontal loads and moments may be applied to the pile cap. This makes the program particularly suitable for the design of road bridges (with adjacent embankments) and similar work on railways — in these circumstances, horizontal loads can be large and associated with a range of vertical loading conditions;
- c) The piles are assumed to be rigidly connected by a rigid free-standing cap (a reasonable assumption in most cases) which imposes the same head displacements and prevents differential head rotation. Piles may have different geometries (length, external and internal diameter, base diameter) and may be inclined in the direction of horizontal loading;
- d) The non-linear analysis may be applied to pile groups embedded in cohesive soil, specifically fully saturated clay under undrained conditions. The soil at the interface is modelled as an elastic-perfectly plastic material, which is assumed to behave linearly elastic at small strain levels, but fails when the stresses at the pile-soil interface reach certain limiting values (determined from a limit equilibrium analysis). The analysis only requires the definition of three soil parameters whose physical meanings are clear, i.e. the (initial tangent) Young's modulus  $E_s$ , the Poisson's ratio  $\nu_s$ , and the undrained shear strength  $C_u$ . This represents a significant advantage over more common load-transfer

approaches which are based on either empirical parameters or the results of full-scale pile load tests;

- e) PGROUPN exploits the capacity of modern desk top computers to provide a full continuum solution in short time, whereas previous work (ie PGROUP) was restricted to problems of small dimensions because of enormous computational resources;
- f) A 'complete' approach, ie a simultaneous consideration of all elements of all the piles within the group, avoids the superposition problems which occur with interaction factors (eg in PIGLET and DEFPIG), permitting the stiffening effect of piles within the soil mass to be taken into account; such an approach has the desirable effect of avoiding exaggeration of corner loads in large groups in both the horizontal and vertical senses. In addition, inclusion of nonlinearity effects further reduces the load concentration at the outer piles and predicts a more uniform load distribution to the individual piles of the group. These observations are of basic importance in practice because they offer the prospect of tangible improvements in design procedures and potential saving of materials;
- g) Application of the PGROUPN analysis to two well documented published case histories has shown that the suggested method is capable of giving reasonable estimates of the load-deformation response and load distribution of pile groups in cohesive soil under either axial or lateral loading. This lends some confidence in using the analysis in practice.

## **7.2 Recommendations for future work**

The research in this thesis has been exclusively theoretical, relying on either alternative numerical analyses or published data from pile tests in order to substantiate the proposed model of pile group behaviour. It is clear that the most important aspect of any future work must be to achieve a full validation and calibration of the PGROUPN analysis by identifying, instrumenting and monitoring real structures. For this purpose,

arrangements are being proposed in conjunction with the Transport Research Laboratory and Kvaerner Cementation Foundations Ltd.

Additional technical features which might be added to the program are:

- a) Development of a graphical user interface for input data and the presentation of results;
- b) Extension of the non-linear analysis to deal with frictional soil (sands or drained analysis in clays) by introducing revised expressions of the limiting bearing stress and skin friction;
- c) Extension of the model to handle multi-layered soils, for instance by using the analytical solution for a layered half space formulated by Chan *et al.* (1974) or the approximate procedure proposed by Lee & Poulos (1990);
- d) Treatment of end-bearing piles by adopting the mirror-image technique (eg Poulos & Davis, 1980);
- e) Inclusion of soil-raft interaction effects: in the linear elastic range, this may easily be accomplished by using a BEM approach (Banerjee & Driscoll, 1976); in the non-linear range, the BEM algorithm of PGROUPN may be coupled with a FEM approach (Hain & Lee, 1978; Griffiths *et al.*, 1991; El-Mossallamy & Franke, 1997; Viggiani, 1998);
- f) Incorporation of shadowing effects for closely spaced pile groups under lateral loading by using empirical parameters to simulate the loss of soil resistance in piles within trailing rows (Brown *et al.*, 1987);
- g) Inclusion of cyclic loading effects (refer, for instance, to a similar work developed for single piles by Lee, 1997).

## References

- Abbiss, C. P. (1981). Shear wave measurements of the elasticity of the ground. *Géotechnique* **31**, No. 1, 91-104.
- Abdrabbo, C. M. (1976). *A model scale study of axially loaded pile foundations*. PhD thesis, University of Southampton.
- Abedzadeh, F. & Pak, R. Y. S. (1995). Horizontal translation and rocking rotation of a rigid tubular foundation. *Géotechnique* **45**, No. 1, 83-94.
- Ahmad, S., Davies, T. G. & Manolis, G. D. (1985). Viscoelastic analysis of piles and pile groups. *Int. J. Numer. Anal. Meth. Geomechs.* **9**, 237-252.
- API Code RP 2A (1984). *Recommended practice for planning, designing, and constructing fixed offshore platforms*. American Petroleum Institute, Dallas, Texas.
- Atkinson, J. H. (1975). Anisotropic elastic deformations in laboratory tests on undisturbed London Clay. *Géotechnique* **25**, No. 2, 357-374.
- Baguelin, F., Bustamante, M., Frank, R. & Jezequel, J. F. (1975). La capacité portante des pieux. *Annales de l'Institut du Batiment et des Travaux Publics*. Suppl. 330, Série SF/116, 1-22.
- Banerjee, P. K. (1976). Integral equation methods for analysis of piece-wise non-homogeneous, three-dimensional elastic solids of arbitrary shape. *Int. J. Mech. Sciences* **18**, 293-303.
- Banerjee, P. K. (1978). Analysis of axially and laterally loaded pile groups. *Developments in soil mechanics*, Applied Science Publishers, London, 317-346.
- Banerjee, P. K. & Davies, T. G. (1977). Analysis of pile groups embedded in Gibson soil. *Proc. 9th Int. Conf. Soil Mech. Fdn Engng, Tokyo* **1**, 381-386.
- Banerjee, P. K. & Davies, T. G. (1978). The behaviour of axially and laterally loaded single piles embedded in nonhomogeneous soils. *Géotechnique* **28**, No. 3, 309-326.
- Banerjee, P. K. & Driscoll, R. M. (1974). *Analysis of pile groups subjected to any loading conditions*. Highway Directorate Publications, Department of the Environment, London.
- Banerjee, P. K. & Driscoll, R. M. (1975). *A program for the analysis of pile groups of any geometry subjected to any loading conditions*. HECB/B/7, Department of the Environment, London.
- Banerjee, P. K. & Driscoll, R. M. (1976). Three-dimensional analysis of raked pile groups. *Proc. Instn Civ. Engrs, Part 2*, Vol. 61, Dec., 653-671.

- Banerjee, P. K. & Driscoll, R. M. (1977). *Program for the analysis of pile groups of any geometry subjected to horizontal and vertical loads and moments, PGROUP (2.0)*. HECB/B/7, Department of Transport, HECB, London.
- Banerjee, P. K., Driscoll, R. M. & Davies, T. G. (1981). *Program for the analysis of pile groups of any geometry subjected to horizontal and vertical loads and moments, PGROUP (3.0)*. HECB/B/7, Department of Transport, HECB, London.
- Barton, Y. O. (1982). *Laterally loaded model piles in sand: centrifuge tests and finite element analyses*. PhD thesis, University of Cambridge.
- Bjerrum, L., Johnson, W. & Ostenfeld, C. (1957). The settlement of a bridge abutment on friction piles. *Proc. 4th Int. Conf. Soil Mech. Fdn Engng, London 2*, 14-19.
- Bogard, D. & Matlock, H. (1983). Procedures for analysis of laterally loaded pile groups in soft clay. *Proc. Conf. on Geotech. Practice in Offshore Engineering, Austin*, 499-535.
- Boussinesq, M. J. (1885). *Applications des potentiels a l'étude de l'équilibre et du mouvement des solides élastiques*. Paris: Gautier Villars.
- Broms, B. B. (1964). Lateral resistance of piles in cohesive soils. *J. Soil Mechs Fdn Division, Am. Soc. Civ. Engrs* **90**, No. SM2, 27-63.
- Brown, D. A. & Shie, C. F. (1990a). Three dimensional finite element model of laterally loaded piles. *Computers and Geotechnics* **10**, No. 1, 59-79.
- Brown, D. A. & Shie, C. F. (1990b). Numerical experiments into group effects on the response of piles to lateral loading. *Computers and Geotechnics* **10**, No. 4, 211-230.
- Brown, D. A., Reese, L. C. & O'Neill, M. W. (1987). Cyclic lateral loading on a large scale pile group. *J. Geotech. Engng, Am. Soc. Civ. Engrs* **113**, No. 11, 1326-1343.
- Burghignoli, A. & Desideri, A. (1995). Analisi di un gruppo di pali sollecitati da forze orizzontali. *Rivista Italiana di Geotecnica*, No. 3, 163-178.
- Burland, J. B. (1973). Shaft friction of piles in clay — a simple fundamental approach. *Ground Engng* **6**, No. 3, 30-42.
- Burland, J. B. (1989). 'Small is beautiful' — the stiffness of soils at small strains. *9th Bjerrum Mem. Lecture, Can. Geotech. J.* **26**, No. 4, 499-516.
- Burland, J. B., Broms, B. B. & de Mello, V. F. B. (1977). Behaviour of foundations and structures. *Proc. 9th Int. Conf. Soil Mech. Fdn Engng, Tokyo 2*, 495-546.
- Bustamante, M. & Gianceselli, L. (1982). Pile bearing capacity prediction by means of static penetrometer CPT. *Proc. 2nd Eur. Symp. on Penetration Testing, Amsterdam 2*, 493-500.
- Butterfield, R. & Banerjee, P. K. (1970). A note on the problem of a pile reinforced half-space. *Géotechnique* **20**, No. 1, 100-103.

- Butterfield, R. & Banerjee, P. K. (1971a). The elastic analysis of compressible piles and pile groups. *Géotechnique* **21**, No. 1, 43-60.
- Butterfield, R. & Banerjee, P. K. (1971b). The problem of pile group-pile cap interaction. *Géotechnique* **21**, No. 2, 135-142.
- Butterfield, R. & Douglas, R. A. (1981). *Flexibility coefficients for the design of piles and pile groups*. CIRIA Technical Note 108, London.
- Caputo, V. & Viggiani, C. (1984). Pile foundation analysis: a simple approach to nonlinearity effects. *Rivista Italiana di Geotecnica*, No. 2, 32-51.
- Castelli, F., Maugeri, M. & Motta (1992). Analisi non lineare del cedimento di un palo singolo. *Rivista Italiana di Geotecnica*, No. 2, 115-135
- Chan, K. S., Karasudhi, P. & Lee, S. L. (1974). Force at a point in the interior of a layered elastic half space. *Int. J. Solids Struct.* **10**, 1179-1199.
- Chandler, R. J. (1968). The shaft friction of piles in cohesive soils in terms of effective stresses. *Civ. Eng. Public Wks. Rev.* **63**, 48-51.
- Chin, F. K. (1970). Estimation of the ultimate load of piles not carried to failure. *Proc. 2nd South East Asian Conf. on Soil Eng.*, 81-90.
- Chin, J. T. (1988). *Analysis of piles and pile groups embedded in a layered half space*. MEng thesis, National University of Singapore.
- Chin, J. T. & Poulos, H. G. (1991). Axially loaded vertical piles and pile groups in layered soil. *Int. J. Numer. Anal. Meth. Geomechs* **15**, No. 7, 497-511.
- Chow, F. (1997). Talking point. *Ground Engng* **30**, No. 10, 3.
- Chow, Y. K. (1986a). Analysis of vertically loaded pile groups. *Int. J. Numer. Anal. Meth. Geomechs* **10**, No. 1, 59-72.
- Chow, Y. K. (1986b). Discrete element analysis of settlement of pile groups. *Computers & Structures* **24**, 1, 157-166.
- Chow, Y. K. (1986c). Behaviour of pile groups under axial loads. *Proc. 3rd Int. Conf. Numer. Meths. in Offshore Piling, Nantes*, 237-251.
- Chow, Y. K. (1987a). Iterative analysis of pile-soil-pile interaction. *Géotechnique* **37**, No. 3, 321-333.
- Chow, Y. K. (1987b). Three-dimensional analysis of pile groups. *J. Geotech. Engng, Am. Soc. Civ. Engrs* **113**, No. 6, 637-651.
- Chow, Y. K. (1987c). Axial and lateral response of pile groups embedded in nonhomogeneous soils. *Int. J. Numer. Anal. Meth. Geomechs* **11**, 621-638.

- Chow, Y. K. (1991). Pile-soil-pile interaction considering weakened zone of soil around piles. *Computers and Geotechnics* **12**, No. 2, 163-174
- Chow, Y. K., Chin, J. T., Kog, Y. C. & Lee, S. L. (1990). Settlement analysis of socketed pile groups. *J. Geotech. Engng, Am. Soc. Civ. Engrs* **116**, No. 8, 1171-1184.
- Clancy, P. & Randolph, M. F. (1996). Simple design tools for piled raft foundations. *Géotechnique* **46**, No. 2, 313-328.
- Cooke, R. W. (1974). The settlement of friction pile foundations. *Proc. Conf. on Tall Buildings, Kuala Lumpur, Dec.*, No. 3, 7-19.
- Cooke, R. W., Bryden-Smith, D. W., Gooch, M. N. & Sillett, D. F. (1981). Some observations of the foundation loading and settlement of a multi-storey building on a piled raft foundation in London Clay. *Proc. Instn Civ. Engrs, Part 1, Vol. 70, Aug.*, 433-460.
- Cooke, R. W., Price, G. & Tarr, K. W. (1980). Jacked piles in London Clay: interaction and group behaviour under working conditions. *Géotechnique* **30**, No. 2, 97-136.
- Cox, W. R., Dixon, D. A. & Murphy, B. S. (1984). Lateral load tests on 25.4-mm (1-in.) diameter piles in very soft clay in side-by-side and in-line groups. *Laterally loaded deep foundations: analysis and performance*, ASTM STP 835, J. A. Langer, E. T. Mosley, and C. D. Thompson (ed), American Society for Testing and Materials, 122-139.
- Coyle, H. M. & Reese, L. C. (1966). Load transfer for axially loaded piles in clay. *J. Soil Mechs Fdn Division, Am. Soc. Civ. Engrs* **92**, No. SM2, 1-26.
- Cruse, T. A. (1969). Numerical solutions in three-dimensional elastostatics. *Int. J. Solids Struct.* **5**, 1259-1274.
- Cruse, T. A. (1973). Application of the boundary-integral equation method for three-dimensional stress analysis. *Computers & Structures* **3**, 509-527.
- Cruse, T. A. (1974). An improved boundary-integral equation method to three-dimensional elastic stress analysis. *Computers & Structures* **4**, 741-754.
- Cuccovillo, T. & Coop, M. R. (1997). The measurements of local axial strains in triaxial tests using LVDTs. *Géotechnique* **47**, No. 1, 167-171.
- D'Appolonia, E. & Romualdi, J. P. (1963). Load transfer in end-bearing steel H-piles. *J. Soil Mechs Fdn Division, Am. Soc. Civ. Engrs* **89**, No. SM2, 1-25.
- Davies, T. G. & Budhu, M. (1986). Non-linear analysis of laterally loaded piles in heavily overconsolidated clays. *Géotechnique* **36**, No. 4, 527-538.
- De Ruiter, J. & Beringen, F. L. (1979). Pile foundations for large North Sea structures. *Marine Geotechnol.* **3**, No. 3, 267-314.

- El-Mossallamy, Y. & Franke, E. (1997). *Piled rafts; numerical modelling to simulate the behaviour of piled raft foundations*. Published by the Authors, Darmstadt.
- England, M. (1993). A method of analysis of stress induced displacement in soils with respect to time. *Proc. 2nd Int. Geot. Sem. on Deep Foundations on Bored and Auger Piles, BAP II, Ghent*, 241-246.
- Evangelista, A. & Viggiani, C. (1976). Accuracy of numerical solutions for laterally loaded piles in elastic half-space. *Proc. 2nd Int. Conf. on Num. Methods in Geom., Blacksburg 3*, 1367-1370.
- Fathallah, R. C. (1978). *Theoretical and experimental investigation of the behaviour of axially loaded single piles driven in saturated clays*. PhD thesis, University College, Cardiff.
- Fleming, W. G. K. (1992). A new method for single pile settlement prediction and analysis. *Géotechnique 42*, No. 3, 411-425.
- Fleming, W. G. K. (1997). Execution and interpretation of pile loading tests. *XVI Ciclo di Conferenze di Geotecnica di Torino, Politecnico di Torino*, pp 21.
- Fleming, W. G. K., Weltman, A. J., Randolph, M. F. & Elson, W. K. (1992). *Piling Engineering (2nd edn)*. Blackie Academic & Professional, Glasgow.
- Focht, J. A., Jr. & Koch, K. J. (1973). Rational analysis of the lateral performance of offshore pile groups. *Proc. 5th Offshore Technology Conf., Houston*, Paper 1896, 701-708.
- Frank, R. (1974). *Etude théorique du comportement des pieux sous charge verticale, introduction de la dilatance*. Dr-Eng. thesis, University Paris VI (Pierre et Marie Curie University).
- Fraser, R. A. & Wardle, L. J. (1976). Numerical analysis of rectangular rafts on layered foundations. *Géotechnique 26*, No. 4, 613-630.
- Gazetas, G. (1991). Foundation vibrations. In H.-Y. Fang (ed.), *Foundation Engineering handbook*, New York: Van Nostrand Reinhold, 553-593.
- Ghosh, N. (1975). *A model scale investigation of the working load stiffness of single piles and groups of piles in clay under centric and eccentric vertical loads*. PhD thesis, University of Southampton.
- Gibson, R. E. (1974). The analytical method in soil mechanics. *Géotechnique 24*, No. 2, 115-140.
- Goto, S., Tatsuoka, F., Shibuya, S., Kim, Y. S. & Sato, T. (1991). A simple gauge for local small strain measurements in laboratory. *Soils and Fdns 31*, No. 1, 169-180.
- Griffiths, D. V., Clancy, P. & Randolph, M. F. (1991). Piled raft foundations analysis by finite elements. *Proc. 7th Int. Conf. on Num. Methods in Geom., Cairns 2*, 1153-1157.
- Guo, W. D. & Randolph, M. F. (1997). Vertically loaded piles in non-homogeneous media. *Int. J. Numer. Anal. Meth. Geomechs 21*, 507-532.

- Ha, H. B. & O'Neill, M. W. (1983). Discussion on 'Theoretical  $t$ - $z$  curves'. *J. Geotech. Engng, Am. Soc. Civ. Engrs* **109**, No. GT10, 1353-1355.
- Hain, S. J. & Lee, I. K. (1978). The analysis of flexible pile-raft systems. *Géotechnique* **28**, No. 1, 65-83.
- Hirayama, H. (1991). Pile-group settlement interaction considering soil non-linearity. *Computer methods and advances in geomechanics*, (eds Beer, Booker & Carter), Balkema, 139-144.
- Hirayama, H. (1994). Secant Young's modulus from  $N$ -value or  $C_u$  considering strain levels. *Proc. 1st Int. Conf. on Pre-failure Deformation of Geomaterials, Sapporo* **1**, 247-252.
- Hull, T. S. (1987). *The static behaviour of laterally loaded piles*. PhD thesis, University of Sidney.
- Imai, T. & Tonouchi, K. (1982). Correlation of  $N$  value with  $S$ -wave velocity. *Proc. 2nd Eur. Symp. on Penetration Testing, Amsterdam*, 67-72.
- Jamiolkowski, M., Lancellotta, R., & Lo Presti, D. C. F. (1995). Remarks on the stiffness at small strains of six Italian clays. *Keynote Lecture, Proc. 1st Int. Conf. on Pre-failure deformation of Geomaterials*, (eds Shibuya, Mitachi & Miura), Balkema, Vol. 2, 817-836.
- Jardine, R. J., Potts, D. M., Fourie, A. B. & Burland, J. B. (1986). Studies of the influence of non-linear stress-strain characteristics in soil-structure interaction. *Géotechnique* **36**, No. 3, 377-396.
- Jardine, R. J., Symes, M. J. & Burland, J. B. (1984). The measurements of soil stiffness in the triaxial apparatus. *Géotechnique* **34**, No. 3, 323-340.
- Kagawa, T. (1992). Moduli and damping factors of soft marine clays. *J. Geotech. Engng, Am. Soc. Civ. Engrs* **118**, No. 9, 1360-1375.
- Kelvin (Lord) (1848). Note on the integration of the equations of equilibrium of an elastic solid. *Cambridge & Dublin Math. J.*
- Koizumi, Y. & Ito, K. (1967). Field tests with regard to pile driving and bearing capacity of piled foundations. *Soils and Fdns* **7**, No. 3, 30-53.
- Kraft, L. M. (1982). Effective stress capacity model for piles in clay. *J. Geotech. Engng, Am. Soc. Civ. Engrs* **10**, No. GT11, 1387-1404.
- Kraft, L. M., Ray, R. P. & Kagawa, T. (1981). Theoretical  $t$ - $z$  curves. *J. Geotech. Engng, Am. Soc. Civ. Engrs* **107**, No. GT11, 1543-1561.
- Kuwabara, F. (1991). Settlement behaviour of non-linear soil around single piles subjected to vertical loads. *Soils and Fdns* **31**, No. 1, 39-46.
- Lachat, J. C. & Watson, J. O. (1976). Effective numerical treatment of boundary integral equations: a formulation for three-dimensional elastostatics. *Int. J. Num. Meth. Engng* **10**, 991-1005.
- Lambe, T. W. (1973). Predictions in soil engineering. *Géotechnique* **23**, No. 2, 149-202.

- Lee, C. Y. (1993). Pile group settlement analysis by hybrid layer approach. *J. Geotech. Engng, Am. Soc. Civ. Engrs* **119**, No. 6, 984-997.
- Lee, I. K. (1977). Application of finite element method in Geotechnical Engineering, I: linear analysis. *Finite element techniques: A short course of fundamentals and applications*, Chapter 17, University of South Wales.
- Lee, Y. P. (1997). *Cyclic analysis of laterally loaded pile foundations*. PhD thesis, University of Glasgow.
- Lee, C. Y. & Poulos (1990). Axial response analysis of piles in vertically and horizontally non-homogeneous soils. *Computers and Geotechnics* **9**, No. 3, 133-148.
- Leung, C. F. & Chow, Y. K. (1987). Response of pile groups subjected to lateral loads. *Int. J. Numer. Anal. Meth. Geomechs* **11**, No. 3, 307-314.
- Lo Presti, D. C. F. (1995). General report: measurements of shear deformation of geomaterials in the laboratory. *Keynote Lecture, Proc. 1st Int. Conf. on Pre-failure deformation of Geomaterials*, (eds Shibuya, Mitachi & Miura), Balkema, Vol. 2, 1067-1088.
- Mahar, L. J. & O'Neill, M. W. (1983). Geotechnical characterisation of desiccated clay. *J. Geotech. Engng, Am. Soc. Civ. Engrs* **109**, No. 1, 57-71.
- Mandolini, A. (1994). Modelling settlement behaviour of piled foundations. *Pile foundations — Experimental investigations, analysis and design*. Naples: Cuen, 361-406.
- Mandolini, A. & Viggiani, C. (1997). Settlement of piled foundations. *Géotechnique* **47**, No. 4, 791-816.
- Massonet, C. E. (1965). Numerical use of integral procedures. *Stress analysis*, ed. Zienkiewicz, O. C. & Hollister, G. S., Chapter 10.
- Matlock, H. (1970). Correlation for design of laterally loaded piles in soft clay. *Proc. 2nd Offshore Technology Conf., Houston*, Vol. 1, 577-594.
- Matlock, H. & Haliburton, T. A. (1964). *BMCOL-28 — A program for numerical analysis of beam columns on non-linear supports*. Report to the Shell Group, Austin.
- Matlock, H., Ingram, W. B., Kelley, A. E. & Bogard, D. (1980). Field tests of the lateral-load behaviour of pile groups in soft clay. *Proc. 12th Offshore Technology Conf., Houston*, 163-174.
- Mattes, N. S. (1969). The influence of radial displacement compatibility on pile settlements. *Géotechnique* **19**, No. 1, 157-159.
- Mattes, N. S. (1972). *The analysis of settlement of piles and pile groups in clay soils*. PhD thesis, University of Canterbury, Christchurch, New Zealand.

- Mattes, N. S. & Poulos, H. G. (1969). Settlement of a single compressible pile. *J. Soil Mechs Fdn Division, Am. Soc. Civ. Engrs* **95**, No. SM1, 189-207.
- Meyer, P. L., Holmquist, D. V. & Matlock, H. (1975). Computer predictions for axially loaded piles with non-linear supports. *Proc. 7th Annual Offshore Technology Conf., Houston*, Paper 2186.
- Meyerhof, G. G. (1959). Compaction of sands and bearing capacity of piles. *J. Soil Mechs Fdn Division, Am. Soc. Civ. Engrs* **85**, No. SM6, 1-29.
- Meyerhof, G. G. (1976). Bearing capacity and settlement of pile foundations. *J. Geotech. Engng, Am. Soc. Civ. Engrs* **102**, No. GT3, 197-228.
- Mindlin, R. D. (1936). Force at a point in the interior of a semi-infinite solid. *Physics* **7**, 195-202.
- Naylor, D. J. & Hooper, J. A. (1974). An effective stress finite element analysis to predict the short and long term behaviour of a piled raft foundation on London Clay. *Proc. Conf. Settlements of Structures, Cambridge*, 394-402.
- Nystrom, G. A. (1984). Finite-strain axial analysis of piles in clay. *Anal. Design Pile Fdns, Am. Soc. Civ. Engrs*, 1-20.
- Ohsaki, Y. & Iwasaki, R. (1973). On dynamic shear moduli and Poisson's ratios of soil deposits. *Soils and Fdns* **13**, No. 4, 61-73.
- O'Neill, M. W., Ghazzaly, O. I. & Ha, H. B. (1977). Analysis of three-dimensional pile groups with non-linear soil response and pile-soil-pile interaction. *Proc. 9th Annual Offshore Technology Conf., Houston*, Paper 2838, 245-256.
- O'Neill, M. W., Hawkins, R. A. & Mahar, L. J. (1982). Load transfer mechanism in piles and pile groups. *J. Geotech. Engng, Am. Soc. Civ. Engrs* **108**, No. GT12, 1605-1623.
- Ottaviani, M. (1972). Un esempio di applicazione del metodo degli elementi finiti allo studio di pali di fondazione in terreni stratificati. *Rivista Italiana di Geotecnica* **6**, No. 3, 1-13.
- Ottaviani, M. (1975). Three-dimensional finite element analysis of vertically loaded pile groups. *Géotechnique* **25**, No. 2, 159-174.
- Patel, D. C. (1989). *A case study of shaft friction of bored piles in London Clay in terms of total and effective stress*. MSc thesis, University of London.
- Patel, D. C. (1992). Interpretation of results of pile tests in London Clay. *Proc. Conf. on Piling, European Practice and world-wide trends*, Instn Civ. Engrs, London, 100-110.
- Poulos, H. G. (1968). Analysis of the settlement of pile groups. *Géotechnique* **18**, No. 4, 449-471.
- Poulos, H. G. (1971a). Behaviour of laterally loaded piles: I — Single piles. *J. Soil Mechs Fdn Division, Am. Soc. Civ. Engrs* **97**, No. SM5, 711-731.

- Poulos, H. G. (1971b). Behaviour of laterally loaded piles: II — Pile groups. *J. Soil Mechs Fdn Division, Am. Soc. Civ. Engrs* **97**, No. SM5, 733-751.
- Poulos, H. G. (1973). Load-deflection prediction for laterally loaded piles. *Aust. Geomech. J.* **G3**, No. 1, 1-8.
- Poulos, H. G. (1974). Analysis of pile groups subjected to vertical and horizontal loads. *Aust. Geomech. J.* **G4**, No. 1, 26-32.
- Poulos, H. G. (1975). Lateral load-deflection prediction for pile groups. *J. Soil Mechs Fdn Division, Am. Soc. Civ. Engrs* **101**, No. GT1, 19-34.
- Poulos, H. G. (1976). Discussion to Three-dimensional analysis of vertically loaded pile groups, M. Ottaviani. *Géotechnique* **26**, No. 1, 238-239.
- Poulos, H. G. (1977). Settlement of pile foundations. In *Numerical methods in geotechnical engineering*, McGraw Hill, New York, Chapter 10.
- Poulos, H. G. (1979). Settlement of single piles in nonhomogeneous soil. *J. Geotech. Engng, Am. Soc. Civ. Engrs* **105**, No. GT5, 627-641.
- Poulos, H. G. (1980a). *User's guide to program DEFPIG — Deformation Analysis of Pile Groups*. School of Civil Engineering, University of Sidney.
- Poulos, H. G. (1980b). An approach for the analysis of offshore pile groups. *Proc. Numerical Methods in Offshore Piling*, Instn. Civ. Engrs, London, 119-126.
- Poulos, H. G. (1982). Single pile response to cyclic lateral load. *J. Geotech. Engng, Am. Soc. Civ. Engrs* **108**, No. GT3, 355-375.
- Poulos, H. G. (1988). Modified calculation of pile group settlement interaction. *J. Geotech. Engng, Am. Soc. Civ. Engrs* **114**, No. 6, 697-706.
- Poulos, H. G. (1989). Pile behaviour — theory and application. *29th Rankine Lecture, Géotechnique* **39**, No. 3, 365-415.
- Poulos, H. G. (1990). *DEFPIG — Deformation analysis of pile groups. User's guide*. Centre for Geotechnical Research, University of Sidney.
- Poulos, H. G. (1993). Settlement prediction for bored pile groups. *Proc. 2nd Int. Geot. Sem. on Deep Foundations on Bored and Auger Piles, BAP II, Ghent*, 103-117.
- Poulos, H. G. (1994). Settlement prediction for driven piles and pile groups. *Proc. Conf. on vertical and horizontal deformations of foundations and embankments*, College Station, Texas, Geotechnical Special Publication, Vol. 2, No. 40, 1629-1649.
- Poulos, H. G. & Davis, E. H. (1968). The settlement behaviour of single axially loaded incompressible piles and piers. *Géotechnique* **18**, No. 3, 351-371.

- Poulos, H. G. & Davis, E. H. (1974). *Elastic solutions for soil and rock mechanics*. New York: Wiley.
- Poulos, H. G. & Davis, E. H. (1980). *Pile foundation analysis and design*. New York: Wiley.
- Poulos, H. G. & Hewitt, C. M. (1986). Axial interaction between dissimilar piles in a group. *Proc. 3rd Int. Conf. Num. Methods in Offshore Piling, Nantes*, 253-270.
- Poulos, H. G. & Mattes, N. S. (1969). The behaviour of axially loaded end-bearing piles. *Géotechnique* **19**, No. 2, 285-300.
- Poulos, H. G. & Mattes, N. S. (1971). Settlement and load distribution analysis of pile groups. *Aust. Geomech. J.* **G1**, No. 1, 18-28.
- Poulos, H. G. & Randolph, M. F. (1983). Pile group analysis: a study of two methods. *J. Geotech. Engng, Am. Soc. Civ. Engrs* **109**, No. 3, 355-372.
- Randolph, M. F. (1977). *A theoretical study of the performance of piles*. PhD thesis, University of Cambridge.
- Randolph, M. F. (1981). The response of flexible piles to lateral loading. *Géotechnique* **31**, No. 2, 247-259.
- Randolph, M. F. (1983a). Design of piled raft foundations. *Proc. Symp. on Recent Developments in Laboratory and Field Tests and Analysis of Geotechnical Engineering Problems, Bangkok*, 523-537.
- Randolph, M. F. (1983b). PIGLET — a computer program for the analysis and design of pile groups under general loading conditions. *Proc. Symp. on Recent Developments in Laboratory and Field Tests and Analysis of Geotechnical Engineering Problems, Bangkok*, 1-67.
- Randolph, M. F. (1987). PIGLET, a computer program for the analysis and design of pile groups. *Report GEO 87036, Perth, University of Western Australia*.
- Randolph, M. F. (1994). Design methods for pile groups and piled rafts. *Proc. 13th Int. Conf. Soil Mech. Fdn Engng, New Delhi* **5**, 61-82.
- Randolph, M. F. & Clancy, P. (1993). Efficient design of piled rafts. *Proc. 2nd Int. Geot. Sem. on Deep Foundations on Bored and Auger Piles, BAP II, Ghent*, 119-130.
- Randolph, M. F. & Houlsby, G. T. (1984). The limiting pressure on a circular pile loaded laterally in cohesive soil. *Géotechnique* **34**, No. 4, 613-623.
- Randolph, M. F. & Murphy, B. S. (1985). Shaft capacity of driven piles in clay. *Proc. 17th Annual Offshore Technology Conf., Houston*, Paper 4883, 371-378.
- Randolph, M. F. & Wroth, C. P. (1978). Analyses of deformation of vertically loaded piles. *J. Geotech. Engng, Am. Soc. Civ. Engrs* **104**, No. GT12, 1465-1488.

- Randolph, M. F. & Wroth, C. P. (1979). An analysis of the vertical deformation of pile groups. *Géotechnique* **29**, No. 4, 423-439.
- Randolph, M. F. & Wroth, C. P. (1981). Application of the failure state in undrained simple shear to the shaft capacity of driven piles. *Géotechnique* **31**, No. 1, 143-157.
- Randolph, M. F. & Wroth, C. P. (1982). Recent developments in understanding the axial capacity of piles in clay. *Ground Engng* **15**, No. 7, 17-25.
- Randolph, M. F., Carter, J. P. & Wroth, C. P. (1979). Driven piles in clay — the effects of installation and subsequent consolidation. *Géotechnique* **29**, No. 4, 361-393.
- Reese, L. C. & Desai, C. S. (1977). Laterally loaded piles. In *Numerical methods in geotechnical engineering*, McGraw Hill, New York, Chapter 9.
- Reese, L. C. & Matlock, H. (1960). Numerical analysis of laterally loaded piles. *Proc. 2nd Conf. on electronic computation, Am. Soc. Civ. Engrs, Pittsburgh*.
- Reese, L. C., Cox, W. R. & Koop, F. D. (1974). Analysis of laterally loaded piles in sand. *Proc. 6th Annual Offshore Technology Conf., Houston*, 473-483.
- Rizzo, F. J. (1967). An integral equation approach to boundary value problems of classical elastostatics. *Quarterly of Applied Mathematics* **25**, 83-95.
- Rollins, K. M., Peterson, K. T. & Weaver, T. J. (1998). Lateral load behaviour of full-scale pile group in clay. *J. Geotech. and Geoenv. Engng, Am. Soc. Civ. Engrs* **124**, No. 6, 468-478.
- Schmertmann, J. H. (1978). *Guidelines for cone penetration test — in performance and design*. US Dept. of Transportation, Federal Highways Administration, Washington.
- Semple, R. M. (1980). Discussion of Session 8. *Proc. Conf. Recent Developments in the Design and Construction of Piles, Instn Civ. Engrs, London*, 397-399.
- Semple, R. M. & Rigden, W. J. (1984). Shaft capacity of driven pipe piles in clay. *Proc. Symp. on analysis and design of pile foundation*, San Francisco, Am. Soc. Civ. Engrs, 59-79.
- Shioi, Y. & Fukui, J. (1982). Application of N-value to design of foundations in Japan. *Proc. 2nd Eur. Symp. on Penetration Testing, Amsterdam* **1**, 159-164.
- Skempton, A. W. (1953). Discussion: Piles and pile foundations, Settlement of pile foundations. *Proc. 3rd Int. Conf. Soil Mech. Fdn Engng, Zurich* **3**, 72.
- Skempton, A. W. (1959). Cast-in-situ bored piles in London Clay. *Géotechnique* **9**, 153-173.
- Smith, I. M. (1982). *Programming the finite element method with application to geomechanics*. New York: Wiley.
- Steinbrenner, W. (1934). Tafeln zur Setzungberechnung. *Strasse* **1**, 221.

- Sullivan, W. R., Reese, L. C. & Fenske, C. W. (1979). Unified method for analysis of laterally loaded piles in clay. *Proc. Conf. on Numerical Methods in Offshore Piling*, Instn. Civ. Engrs, London, 135-146.
- Sykora, D. W. & Koester, J. P. (1986). Review of existing correlations between dynamic shear resistance and standard penetration resistance in soils. *Proc. 2nd Conf. Earthquake Engineering and Soil Dynamics*, Am. Soc. Civ. Engrs, Geotechnical Special Technical Publication No. 20, 389-404.
- Tatsuoka, F. & Kohata, Y. (1995). Stiffness of hard soils and soft rocks in engineering applications. *Keynote Lecture, Proc. 1st Int. Conf. on Pre-failure deformation of Geomaterials*, (eds Shibuya, Mitachi & Miura), Balkema, Vol. 2, 947-1063.
- Terzaghi, K. & Peck, R. B. (1967). *Soil mechanics in engineering practice (2nd edn)*. New York: Wiley.
- Tomlinson, S. J. (1994). *Pile design and construction practice (4th edn)*. E & FN Spon, London.
- Van Impe, W. F. (1991). Deformations of deep foundations. *Proc. 10th Europ. Conf. on Soil Mech. and Found. Eng., Florence 3*, 1031-1062.
- Van Weele, A. F. (1993). Quality assessment foundation piles after installation. *Proc. 2nd Int. Geot. Sem. on Deep Foundations on Bored and Auger Piles, BAP II, Ghent*, 459-467.
- Vesic, A. S. (1969). Experiments with instrumented pile groups in sand. *Performance of Deep Foundations*, ASTM STP 444, 177-222.
- Viggiani, C. (1998). Pile groups and piled raft behaviour. *Proc. 3rd Int. Geot. Sem. on Deep Foundations on Bored and Auger Piles, BAP III, Ghent*, 77-91.
- Viggiani, G. & Atkinson, J. H. (1995). Interpretation of bender element tests. *Géotechnique* **45**, No. 1, 149-154.
- Vijayvergiya, V. N. (1977). Load-movement characteristics of piles. *Proc. 4th Symp. Waterway, Port, Coastal and Ocean Div., Am. Soc. Civ. Engrs, Long Beach, California*, Vol. 2, 269-284.
- Whitaker, T. (1957). Experiments with model piles in groups. *Géotechnique* **7**, 147-167.
- Winkler, E. (1867). *Die lehre von der elastizitat und festigkeit*. Prague: Dominicus.
- Wood, L. A. (1978). A note on the settlement of piled structures. *Ground Engng* **11**, No. 4, 38-42.
- Wroth, W. P., Randolph, M. F., Houlsby, G. T. & Fahey, M. (1979). A review of the engineering properties of soils, with particular reference to the shear modulus. *Cambridge University Research Report, CUED/D-Soils TR75*.
- Yamashita, K., Tomono, M. & Kakurai, M. (1987). A method for estimating immediate settlement of piles and pile groups. *Soils and Fdns* **27**, No. 1, 61-76.

Zienkiewicz, O. C. (1971). *The finite element method in engineering science*. London: McGraw Hill.

# Appendix A

## Published papers

- Basile, F. (1999). Non-linear analysis of pile groups. *Proceedings of the Institution of Civil Engineers, Geotechnical Engineering*, in press.
- Basile, F. (1998). Non-linear analysis of vertically loaded pile groups. *Proc. 3rd Int. Geotech. Seminar on Deep Foundations on Bored and Auger Piles, BAP III*, Ghent, 425-431.
- Basile, F. (1997). PGROUPN, a computer program for the non-linear analysis of pile groups under general loading conditions. *Proc. XVI Ciclo di Conferenze di Geotecnica di Torino, I pali e le fondazioni su pali, Politecnico di Torino, Torino*, pp 11.
- Basile, F. & Davies, T. G. (1997a). The boundary element method for non-linear analysis of piled foundations. *Proc. 1st UK Conf. on Boundary Integral Methods, Leeds*, 29-37.
- Basile, F. & Davies, T. G. (1997b). Linear and non-linear analysis of laterally loaded pile groups. *Proc. 5th ACME Conf. on Computational Mechanics in the UK, London*, 84-87.
- Basile, F. (1996). Non-linear analysis of pile groups under general loading conditions. *Proc. 4th BGS Conf. of Young Geotechnical Engineers, Oxford*, 21-22.

